BASIC NUTRIENT CATION CHEMISTRY OF TWO ECUADORIAN ANDISOLS

THESIS

A thesis submitted in partial fulfillment of the requirements for the degree of Master of Science in the College of Agriculture at the University of Kentucky

By

Soraya Patricia Alvarado Ochoa

Lexington, Kentucky

Director: Dr. John Grove, Assoc. Professor of Agronomy

Lexington, Kentucky

2004

ABSTRACT OF THESIS

BASIC NUTRIENT CATION CHEMISTRY OF TWO ECUADORIAN ANDISOLS

Andisols are noted as soils with constant surface-potential colloids dominated by amorphous aluminosilicates. A combination of routinely performed analyses was used to evaluate nutrient status, clay mineralogy, and the charge and cation sorption properties of two acidic Ecuadorian Andisols from experimental fields under crop production. Additionally, a highly weathered soil of south-central Kentucky was studied to contrast the constant surface-potential behavior coming from a mineralogical source lacking in amorphous aluminosilicates. Mineralogical analyses indicated that the clay fraction in those Andisols was dominated by amorphous material but enough crystalline minerals were present to be quantified. Surface charge characterization confirmed that those soils were dominated by constant surface-potential colloids and required an unbuffered approach to assess cation exchange properties. Also, the magnitude of the effects of pH on the negative charge was different among the three studied soils, which confirms the presence of different kinds of major ion-exchange materials, and the predominant role of soil organic matter as a constant surface-potential colloid. Additionally, the marked increase in cation exchange capacity and consequent enhancement in the retention of exchangeable “bases” with increasing pH observed for the Haplustand, Melanudand, and surface Typic Paleudalf was more marked for Ca than for K. In contrast, K was more preferred than Ca in the subsurface Typic Paleudalf, whose clay fraction was dominated by kaolinite. Finally, K/Ca+Mg quantity-intensity relationships for both Andisols showed that the release of K to the soil solution was influenced by the presence of competing cations such as Ca and Mg, and their close relationship with changes in soil pH that were directly affected by soil fertilizer and/or amendment applications.

KEYWORDS: Andisols, constant surface potential minerals, quantity-intensity relationships.

_____

_____

BASIC NUTRIENT CATION CHEMISTRY OF TWO ECUADORIAN ANDISOLS

By

Soraya Patricia Alvarado Ochoa

_____
Director of Thesis

_____
Director of Graduate Studies

_____

RULES FOR THE USE OF THESIS

Unpublished theses submitted for the Master's degree and deposited in the University of Kentucky Library are as a rule open for inspection, but are to be used only with due regard to the rights of the authors. Bibliographical references may be noted, but quotations or summaries of parts may be published only with the permission of the authors, and with the usual scholarly acknowledgments.

Extensive coping or publication of the thesis in whole or in part also requires the consent of the Dean of the Graduate School of the University of Kentucky.

A library that borrows this thesis for use by its patrons is expected to secure the signature of each user.

Name	Date

THESIS

Soraya Patricia Alvarado Ochoa

The Graduate School

University of Kentucky

2004

MASTER'S THESIS RELEASE

I authorize the University of Kentucky Libraries to reproduce this thesis in whole or in part for purposes of research.

Signed: _____

Date: _____

To my parents, Beatríz and Jorge, who inspire me to greater achievements; my husband, Thomás, who has given me constant love and invaluable support throughout this program; and my brothers, David, Jorge, and Carlos, who have always believed in me, with love.

ACKNOWLEDGEMENTS

Gratitude is expressed to my major advisor, Dr. John Grove, for his unfailing support, guidance, and encouragement during this program. In addition, I wish to thank the other members of my advisory committee, Dr. A. D. Karathanasis and Dr. Christopher J. Matocha, for their invaluable insights that guided achievement of this research. The author is also deeply indebted to the entire faculty and staff of the Agronomy Department for their professional counsel and technical and instrumental assistance.

In addition, I would like to extend my sincere gratefulness to INIAP, the Instituto Nacional de Investigaciones Agropecuarias, and PROMSA, the Programa de Modernización de los Servicios Agropecuarios, which are the Ecuadorian government agencies that supported my scholarship. The same appreciation is expressed to Dr. José Espinosa, the director of the PPI-Northern Latin America Office, for his continuous help and support. I also express my gratitude to Ing. Francisco Mite, and Ing. Franklin Valverde for kindly providing soil samples from the Haplustand and Melanudand field experiments, respectively.

TABLE OF CONTENTS

LIST OF TABLES

LIST OF FIGURES

INTRODUCTION

Andisols are soils derived from volcanic ash and pumice. They were first recognized as a great group and tentatively named as Ando soils by Thorp and Smith in 1949. *Ando* means dark soil in Japanese; An, "dark" or "black", and do "soil" (Wada, 1985). Andisols are not abundant in nature. They make up only 0.76 % of the world's soil resources (Uehara and Gillman, 1981). At first believed to occur mainly in Japan (Kanno, 1956); and New Zealand (Taylor and Cox, 1956), Andisols were found to be more widespread than expected. Those soils are located throughout a wide range of climatic conditions, from subalpine regions to the humid tropics. Regardless of the differences in climate in which they have been formed, Andisols constitute a group of soils with similar morphological, physical, and mineralogical characteristics. The most conspicuous features that Andisols have in common are a thick black surface horizon and a soil mineralogy dominated by active amorphous weathering products, such as allophane, imogolite, and Al-humus complexes (Shoji et al., 1993). That highly reactive soil colloidal fraction is believed responsible for the unique physical and chemical properties of Andisols, such as low bulk density, high water retention, constant surface potential characteristics, and strong phosphate sorption. However, the extent to which these properties are expressed in an Andisol depends on its stage of soil development.

Volcanic ash soils have been extensively studied in Japan and New Zealand; however, very little is known about weathering, soil formation, and soil chemistry on the slopes of volcanic peaks in the Andes. Wright (1964) classified the South American Andisols into two groups, the high-latitude group of Chile and Argentina and the low-latitude group of Ecuador and Colombia, and stressed the importance of moisture regime,

which correlates with minor variations in soil morphology and with land use properties. Nevertheless, soils formed on volcanic ash parent materials and classified as Andisols are widespread in Ecuador, from the cold highlands to warm and humid areas of the coastal plain. Consequently, the stage of soil development and the physical and chemical properties of these soils are expected to be different. Andisols represent 24.6 per cent of the total area of Ecuadorian soils, and are utilized for food crop production. Despite their extensive use, they have significant fertility problems that are accentuated by intensive agricultural utilization. An understanding of the basic nutrient cation behavior governing soil fertility is prerequisite to determining the feasibility of increasing soil productivity, considering that there is relatively little information on the cation selectivity of Andisols, particularly those with well-characterized ion-exchange materials (Wada, 1985).

Since interpretation of data for soil management purposes depends on knowledge of surface charge characteristics of soil colloids, it is desirable to partition the effects of the permanent and variable charge components on soil behavior. Variable charge characteristics in Andisols are primarily due to no crystalline materials and soil organic matter. Those were first observed in the variation of cation exchange capacity (CEC) as determined by different methods (Birrel and Gradwell, 1956; Egawa et al., 1959). The amount of variable charge is determined by measuring cation and anion retention at varying pH and electrolyte concentrations (Wada and Okamura, 1980). Realizing, however, that most Andisols also contain crystalline minerals such as halloysite and 2:1-type phyllosilicates with and without hydroxyl-Al interlayering, these soils would contain a mixture of variable and permanent charge colloids. Consequently, the Uehara and Gillman (1980) model, which treats the net surface charge density of mixed systems as

the sum of the two types of charge, could be applied and the amount of permanent charge in the soil could be estimated. In essence, the pH value where the variable charge components have equal amounts of negative and positive charge, pHo, is identified and the total amount of negative and positive charge at this pH are then determined. An excess of negative charge at pHo is assumed to be permanent negative charge, while an excess of positive charge is permanent positive charge. This approach will not be successful when both permanent positive and permanent negative occur in the same soil; only the net permanent charge can be estimated in this case. Applying the model, those authors found small amounts of net permanent charge (either positive or negative) in some soils, and thus explained the relative positions of measured pHo and PZNC, the latter being the pH where the net charge of the whole system is zero.

On the other hand, determining the macronutrient cation status of soils, including both soil solution and exchangeable fractions, is of primary importance to understanding how these nutrients become readily available to plants or how readily they are subject to leaching and chemical transformations. Matthews and Beckett (1962) presented a technique for describing the relationship between exchangeable and soil solution K which they called the quantity-intensity (Q/I) relationship for K in a soil. The quantity factor represents the change in exchangeable K of the soil, while the intensity factor is the ratio of the activity of K to the square root of the activity of Ca plus Mg in the soil solution. When the activity ratios are determined for several solution K concentrations and plotted against the change in exchangeable K, a curve is obtained which describes the K Q/I relationship for the given soil.

In an effort for a better understanding of the basic nutrient cation chemistry in Ecuadorian Andisols, this study determined some chemical and mineralogical characteristics of two Andisols. In addition, to contrast with the surface charge behavior of the distinctive constant surface potential colloids, such as amorphous aluminosilicate minerals, present in Andisols a Typic Paleudalf from Kentucky, whose mineralogy shows mainly crystalline aluminosilicate minerals was characterized as well. The objectives were:

a) To characterize soil colloid fractions;

b) To determine surface charge characteristics;

c) To study soil cation and anion adsorption phenomena as a function of pH;

d) To define the buffer capacity of these soils for K, Ca and Mg through quantity-intensity relationships.

LITERATURE REVIEW

Colloidal Composition of Andisols

Clay Mineralogy of Andisols

Andisols have been defined as soils developing in volcanic ash, pumice, cinders, and other volcanic ejecta with an exchange complex that is dominated by X-ray amorphous compounds of aluminum (Al), silica (Si), and humus, or a matrix dominated by glass (Wada, 1985). Most scientists agree that the dominating presence of allophane coincides with maximum development of an Andisol's characteristics. The occurrence of allophane and allophanelike material is usually connected with areas of recent volcanic activity, but in a few instances allophane has also been detected in soils formed from basaltic rock (Wada, 1977). Although several other clay minerals have been found in Andisols, the majority opinion is that it is the allophane that gives the soil its distinctive properties: high organic matter content, high water-holding capacity, high porosity, low bulk density, and high phosphate fixation capacity (Tan, 1984).

Formation of opaline silica, allophanelike constituents, allophane, imogolite, poorly ordered iron oxides, occurs during the early stage of soil formation from volcanic ash under humid, temperate climatic conditions (Wada, 1980). However, embryonic halloysites were also found under certain climatic conditions (Wada and Kakuto, 1985b). At the early stage of weathering, smectite, vermiculite, and mica are also present in Andisols, and hydroxy-Al interlayering occurs in the former two minerals with advanced weathering (Wada, 1985).

Allophane was described as an amorphous material having little or no structural organization, but high-resolution electron microscopy has indicated that allophane

consists of “hollow spherules” with diameters of 3.5 to 5 nm. The variability in allophane’s shape and size results from aggregation of these spherules with themselves and with other clay constituents. Data on allophane chemical composition indicates SiO_2/Al_2O_3 molar ratios of 1.0 to 2.0; and H_2O (+)/Al_2O_3 molar ratios of 2.5 to 3.0. The calculated and measured specific surface values for allophane are 1050 m^2g^{-1} and 700 to 1100 m^2g^{-1}, respectively (Wada, 1985). Even though the surface area values are high, some of this surface is not accessible to large molecules. This is not equivalent to the internal and external surfaces of swelling clays, but is due to the small size of voids and small necks leading to voids (Maeda, et al., 1984). The heats of adsorption indicate that physical adsorption rather than chemical adsorption is dominant in allophane (Fieldes and Claridge, 1975). Allophane is dissolved by treatment with hot 0.5 M NaOH or 0.15 to 0.20 M oxalate-oxalic acid (pH 3.0 to 3.5).

Allophanelike constituents have a SiO_2/Al_2O_3 molar ratio lower than that of allophane and show a higher Al reactivity. Unlike allophane, allophanelike constituents are dissolved by treatment with dithionite-citrate and 2 % Na_2CO_3 solution. On the other hand, imogolite is said to be paracrystalline, because some randomness is involved in the alignment of the tube units. The calculated and measured specific surface areas are 1050 m^2g^{-1} and 900 to1000 m^2g^{-1} respectively. Imogolite is dissolved by treatment with hot 0.5 M NaOH or oxalate-oxalic acid. Imogolite coexists with allophane in many Andisols. Opaline silica appears as laminar particles, and is also soluble in hot 0.5 M NaOH, though not in oxalate-oxalic acid (Wada, 1985). Iron oxides, mostly non-crystalline species, are also common constituents of Andisols. Unlike Al, the stability of iron (Fe) in oxides is greater than that in humus complexes (Wada and Higashi, 1976). In tropical

regions of high rainfall (>2500 mm), non-crystalline Al and Fe hydroxides, rather than allophane and imogolite, appear as major clay constituents. A fibrous form of poorly crystalline goethite was also reported in some Andisols (Nakai and Yoshinaga, 1980).

Dixon and McKee (1974) found poorly organized and very small spherical particles in a volcanic soil from Mexico, which showed weak x-ray diffraction (XRD) and infrared (IR) features characteristic of halloysite. According to Wada (1985), the relative short life of allophane in a leaching environment under warm, humid climates is indicated by its transformation to halloysite in old and buried Andisols.

The more poorly ordered halloysite is unique as an exchange complex. It is X-ray amorphous, or nearly so, and has properties similar to those of allophane, depending on its Si/Al molar ratio (Wada and Kakuto, 1985b). The formation of halloysite is usually favored by a thick depositional overburden of volcanic ejecta that produces a silica-rich environment (Wada, 1980), such as in Japanese Andisols used for paddy rice (Wada et al., 1982). The age of the ash deposits containing halloysite ranges from about 10,000 to 250,000 yr (Wada, 1980).

Regarding the effects of parent ash, climate and base status, embryonic halloysites were not major clay components in Hawaiian soils derived from andesitic to basalt andesitic ashes under subhumid conditions (Wada et al., 1986), whereas they were found in the Ecuadorian soils derived from andesitic ash under more humid conditions (Wada and Kakuto, 1985b). The base saturation was, however; generally lower in the former (22-67%) than in the latter (57-91%) soils.

The effect of rainfall on the formation of halloysite from volcanic ash in tropical regions, (the Antilles, Ecuador, and Nicaragua) was noted by Colmet-Daage (1969).

Halloysite was not found in regions of high rainfall (>2500 mm), but was found in various forms and proportions in moderate rainfall regions (1500 to 2500 mm) with a pronounced dry season. In some intermediate regions, incipient forms of halloysite with amorphous substances appeared in young, sandy soils (Wada, 1985).

Wielemarker and Wakatsuki (1984) reported the presence of x-ray amorphous clay constituents in three little weathered Kenyan soils derived from peralkaline volcanic ashes. They inferred that these amorphous constituents consisted mainly of poorly ordered Fe-siliceous oxides. All soils were virtually free from allophane and exhibited low pH_{NaF} and low phosphate retention. However, those soils contained embryonic halloysites. Wakatsuki and Wielemaker (1985) pointed out that the unique clay mineralogy of the Kenyan soils was attributable to the peralkaline nature of parent ash and later to drier moisture regimes.

In contrast, Wada and Kakuto (1985b) found another unique mineral association that represents embryonic stages of halloysite formation in weathering of andesitic volcanic ash in three Ecuadorian soils, which did not contain allophane. This mineral association consisted of more or less poorly ordered halloysites and a "1.0 nm mineral". All the studied soils were found under an udic moisture regime, but the differences in annual precipitation and/or temperature regime resulted in differences in the base status and the pH_{CaCl2} between the soils containing halloysites and those containing allophane and imogolite. Colmet-Daage (1969) classified volcanic ash soils in Ecuador into three groups, soils with allophane, soils with halloysites, and soils of the allophane-halloysite transition or with embryonic stages of halloysite. The third group of soils was young and

sandy and occurred in the transition regions from high rainfall towards lesser rainfall or in those regions with a dry season.

In summary, mineralogical and chemical analyses of Andisols have indicated that their clay mineral composition varies depending on the stage of soil formation, the horizon, the petrological nature of the parent volcanic ash, the thickness of the overburden ash deposits, and probably other factors; and the formation and transformation of clay minerals by weathering of volcanic ash and pumices was very much affected by the accumulation of humus, which forms complexes with Al and Fe and with some clay minerals (Wada, 1980).

Soil Organic Matter of Andisols

The black color of Andisols is attributed to accumulation of high amounts of organic matter in the surface horizon. Andisols are geographically distributed in a wide variety of climatic conditions, from the artic and temperate regions to the warm humid tropics, where soil moisture regimes are expected to be quite different. Even under tropical conditions, Andisols can occur in areas with large differences in climate-for example, in the cool regions of the mountains and in the hot, humid lowlands, where the climate favors rapid decomposition of soil organic matter (Tan, 1984). However, soils with similar properties occur under drastically different climates. One of those properties is the accumulation of high amounts of soil organic matter. Organic carbon (C) contents of 6 to 7 percent are common in lowland Andisols in Indonesia (Tan and Van Schuylenborgh, 1961), while in Japan some Andisols may even contain 15 to 20 percent organic carbon (Wada and Aomine, 1973).

Humus accumulation constitutes one of the striking features of Andisols. The C content of each soil profile indicates its residence time at or near the surface, where the soil received a supply of organic matter from plant residue, which has often been greater under grass than under forest. The differences in the C content and its variation with depth among profiles reflect the geographical variation in the deposition of volcanic ash. Additionally, the predominating influence of moisture over temperature regime on the difference in the content of humus in virgin Japanese Andisols has been reported. However, humus has been decreased by cultivation, and this decline is more marked in both higher temperature and moisture regimes (Wada, 1985).

The mechanism of humus accumulation in Andisols has attracted the attention of many investigators. As reviewed by Wada and Higashi (1976), clay-humus interaction, specifically the allophane-humus interaction, was thought important in view of the probable protection of humus against the attack of microorganisms. The formation of allophane and related minerals in Andisols is implicitly assumed when their importance to the accumulation of humus is inferred. The absence or near absence of allophane and related minerals in some Andisol A1 and buried A1 horizons in which considerable amounts of humus accumulated was, however, found by Tokashiki and Wada (1975).

Wada (1985) pointed out that organic matter inhibits the formation of allophane and imogolite by lowering the activity of Al through formation of metal-ligand bonds. Those authors also suggested that the youngest humus, which has very low complexing ability for Al and Fe, evolves with time or soil formation into forms that complex Al and Fe. When the supply of organic matter is limited by burial of the soil, the humus evolves further into forms that have reacted with additional Al and Fe released by continued

weathering of volcanic ash. Some such Al and Fe may be present as hydrous oxides and allophanelike constituents and some as allophane and imogolite. On the other hand, Kato (1970) reported that sesquioxides made soluble by hydrogen peroxide (H_2O_2) and dithionite-citrate treatment, rather than allophane, were important to the accumulation of humus in some soils derived from volcanic ash.

According to Wada (1985), the fractions of Al and Fe most likely to complex with humus in Andisols were the polymer hydroxyions. The correlation between phosphate adsorption and humus content has been interpreted in terms of the reaction of such polymer hydroxy-Al, Fe ions with phosphate. A blocking of ionized carboxyl groups of humus by hydroxy-Al and Fe ions was also related to phosphate adsorption by Wada and Okamura (1980) in a study on the charge characteristics of Andisol A1 horizons.

Higashi and Wada (1977) found that the reactions between the inorganic constituents and humus result in the formation of clay-, silt-, and sand-sized aggregates in Andisols that are stable against sonic disruption. Both the C content of the clay-sized separate and the difference in the C content between the clay and silt or sand-sized separates were higher in the younger soils (< 2500 yrs) than in the older soils. This demonstrated the important role of Al- and Fe-humus complexes in aggregate formation and the growth of these aggregates with soil formation (Wada, 1985).

Basis of the Electrochemical Properties of Constant Surface-Potential Minerals

In constant surface-potential minerals, surface charge is created by the adsorption of ions onto the surface, the net charge being determined by that ion which is adsorbed in excess. The charging process requires the presence of these ions, called potential-determining ions, in the ambient solution in quantities sufficient for adsorption. In the

past, constant surface-potential minerals have often been called pH-dependent charge minerals, because the surface charge is dependent upon solution pH (H^+ and OH^- are potential-determining ions), but in this constant potential system, the magnitude of the surface charge is influenced by other conditions, so that the more general term, variable charge minerals, is preferred (Uehara and Gillman, 1981).

The potential of a soil system to change the magnitude and nature (positive or negative) of its surface charge is dependent on the soil's ability to specifically react with the potential-determining ions. This ability is subject to the mineral components of the soil and the chemical interactions among these components (Lumbanraja and Evangelou, 1991). Even though those components have been associated with inorganic minerals such as oxides, it should be remembered that organic matter is a very important constituent of soil colloidal material. The functional groups of organic matter, such as carboxyl and amino groups, are able to sorb and desorb potential-determining ions in a manner similar to the mineral oxides, so organic matter is also a good example of a constant potential or variable charge system (Uehara and Gillman, 1981). Gillman et al. (1982) pointed out that the presence of about 6% organic matter in some non-calcareous, non-saline soils from Queensland was apparently sufficient to give those samples significant variable charge characteristics. Additionally, Gillman (1985) reported that the point of zero charge of the variable charge components (pHo) is reduced by about one pH unit for each 1% increase in organic carbon or for each 100 μg/g increase in extractable phosphorus in oxidic soils from Queensland.

The relationship between pH and surface charge of soils is rather difficult to predict. This is especially true in soil systems where the clay minerals represent a mixture

of constant and variable charge. The net surface charge density of soil colloid mixtures is treated as the sum of the two types of surface charge. The permanent charge is assumed to be constant in magnitude, and negative, zero, or positive in sign, while the variable charge will vary in magnitude and sign with pH and electrolyte concentration. Based on these assumptions, relationships are developed which show that there are two zero points of charge. The zero point of charge of the mixture as a whole is designated the ZPNC. The ZPNC can be determined by ion adsorption measurements and pHo by potentiometric titration (Uehara and Gillman, 1980). When the soil solution pH is adjusted to a value equal to the pHo, the total net charge equals the permanent charge. At this pH a small but equal amount of cation and anion is adsorbed on the variable charge component so that the permanent charge is obtained by subtracting the anions adsorbed from the total cations adsorbed, as van Raij and Peech (1972) suggested after working with a number of highly weathered soils from Brazil. However, since specifically adsorbed ions will influence the position of pHo and since the zero point of titration depends on soil pH, it is difficult to envisage that the difference between these points represents permanent charge. Espinoza et al. (1975) measured permanent charge in excess of 40 meq/100 g in soils developed from volcanic ash using the van Raij and Peech (1972) approach. Consequently, according to the model presented by Uehara and Gillman (1980), the permanent charge of a mixed system is the difference between cation and anion adsorption at a pHo determined in the absence on specific adsorption. Furthermore, ZPNC is lower than pHo when the permanent charge is negative and higher than pHo when the permanent charge is positive.

Surface charge generation on variably charged colloid surfaces is not limited by specific adsorption or inner-sphere complex formation of H^+ or OH^- (Evangelou, 1998). Other ions, such as HPO_4^{2-}, Fe^{3+}, and Al^{3+}, may specifically or strongly adsorb and thereby influence the surface charge of soils (Sposito, 1984; Singh and Uehara, 1986; Uehara and Gillman, 1981). Wann and Uehara (1978) and Singh and Uehara (1986) presented evidence that weak specific adsorption also has an influence on variable charge surfaces. Wann and Uehara (1978) reported that the use of $CaCl_2$ as background electrolyte with an iron-rich soil shifted the pHo to lower pH values than when the background electrolyte was NaCl. They attributed this shift to the ability of Ca^{2+} to undergo low-affinity specific adsorption or form outer-sphere complexes, thus increasing the negative charge of the mineral's surface by displacing protons. The same authors also reported a decrease in the pHo of an oxisol from pH 4.7 to 3.5 in the presence of 1500 ppm P as PO_4^{3-} with $CaCl_2$ as the background electrolyte, which reveals that the potential of the soil to adsorb cations increases as a function of pH, phosphate added, and cation valence. The higher the valence, the greater the potential of the charged mineral surface to adsorb cations. Singh and Uehara (1986) concluded that ions forming outer-sphere complexes differ with respect to their potential to influence surface charge of variably charged minerals, when compared to ions forming inner-sphere complexes. Generally, cations forming outer-sphere complexes (e.g. Ca^{2+}) shift the pHo to lower pH values. Anions forming outer-sphere complexes (e.g. SO_4^{2-}) shift the pHo to higher pH values, whereas anions forming inner-sphere complexes (e.g., HPO_4^{2-}) shift the pHo to lower pH values.

Many researchers have reported that Ca^{2+} participates in outer-sphere complex reactions. However, Charlet and Sposito (1989) suggested that although three bivalent ions, Ca^{2+}, Mg^{2+}, and SO_4^{2-} might form both outer-sphere and inner-sphere surface complexes on a Brazilian Oxisol, the latter were more important for Ca^{2+} than for Mg^{2+} or SO_4^{2-}.

Electric Charge Characteristics of Andisols

The chemistry of Andisols reflects the influence of high amounts of variable charge and the lack of permanent charge (Wada, 1985). Many researchers are of the opinion that this variable charge finds its origin mainly in the clay fraction. Although organic matter may contribute to some degree to increasing the negative charge in Andisols, it has usually been given less credit than amorphous minerals like allophane (Tan, 1984). Taylor (1964) reported that Andisols in New Zealand had base saturation values that were inconsistent with their pH values because of the presence of a strong buffer capacity dominated by allophane. Generally these soils were considered to have high phosphate fixation capacities and a tendency to become rapidly deficient in potassium.

Some studies have shown that Andisols in which allophane and imogolite predominate have a small amount of negative charge under the conditions in which they occur in the field (Okamura and Wada, 1983) and that large organic cations such as tetramethyl- or tetraethyl-ammonium ion are excluded from those few negatively charged sites (Wada and Tange, 1984). On the basis of these observations, the toluidine blue (TB) test has been used for the assessment of allophane and imogolite, due to the fact that TB is adsorbed on negative charged colloids and exhibits a characteristic color change from

blue to purplish (metachromasis). The absence of TB metachromasis is not a reaction specific to allophane and imogolite. It indicates that negative charges are absent or present in very small amounts in a soil as it occurs in the field or that negative charge sites have no access to large cations such as TB in the solution. These are features common to Andisols with high active aluminum contents. Wada and Kakuto (1985a) applied the TB test to Chile and Ecuadorian soil samples derived from volcanic ash, and they pointed out that the absence of TB metachromasis could be used as a test assessing the predominance of allophane and imogolite with low SiO_2/Al_2O_3 ratios in B horizon samples. This test cannot be applied to allophanes with high SiO_2/Al_2O_3 ratios (>1.5) as well as "embryonic halloysites", which exhibit the metachromasis with TB. A1 or Ap horizon samples containing a large amount of Al- and Fe-humus complexes do not react with TB even in the absence of allophane and imogolite.

Independently of the origin of the negative charge in Andisols, some authors (Yoshida, 1953; and Harada and Kutsuna, 1955) reported that the CEC, which implies the amount of negative surface charge, increased with increasing pH and electrolyte concentration, and interpreted it in terms of the effects of these factors on ionization of carboxyl and phenol groups in humus and of hydroxyl groups in non-crystalline clay minerals. Espinoza et al. (1975) found that two Andisols (surface soils) retained a significant amount of NO_3^- below pH 6 and that the magnitude of net negative charge above pH 4.5 was very dependent on pH and electrolyte concentration. They suggested a complex mixture of pH dependent and permanent charge surfaces, the latter being attributed to ion substitutions and "site vacancies" in X-ray amorphous oxides and hydrous oxides. However, they did not discuss the effect of organic matter on the charge

characteristics. Wada (1985) pointed out that the degree of the development of negative and positive charges at different pH values and electrolyte concentrations for Andisols and weathered pumices depended on the kind of major ion-exchange materials. From his analysis using NH_4^+ and Cl^-, the author suggested functional relationships derived from regression analysis:

$$\log \sigma^- = a\ pH + b \log C + c$$

$$\log \sigma^+ = a'\ pH + b' \log C + c'$$

where σ^- is the amount of negative charge (meq/100 g soil), σ^+ is the amount of positive charge (meq/100 g soil), and C is the NH_4Cl concentration of the equilibrium solution. The a, b, c, a', b', and c' are constants for each soil, and values are different for the major ion-exchange materials. Wada (1985) indicated that the magnitude of the effects of pH and electrolyte concentration on the amount of negative charge decreases in the order: allophane and imogolite with a SiO_2/Al_2O_3 ratio close to 1.0, Al-humus complexes, 2:1and 2:1:1 layer silicate intergrades > allophane with a SiO_2/Al_2O_3 ratio of about 2.0 > mica, chlorite, and vermiculite > kaolinite and vermiculite-chlorite intergrades > smectite. Additionally, he indicated that the pH effect on negative charge was marked for Andisols containing Al-humus complexes and less marked for Andisols containing Al- and Ca-humus complexes and halloysite.

Regarding the development of positive surface charge in Andisols, Wada (1985) pointed out that only Andisols containing allophane and imogolite with a SiO_2/Al_2O_3 ratio of about 1 exhibited positive charge comparable with negative charge at field pH values. The soils containing iron oxides, gibbsite, and 2:1 and 2:1:1 layer silicate intergrades. The weathered pumice containing halloysite exhibited positive charge only at

and below pH 5.0. Positive charge was not evident in soils containing Al-humus complexes unless the soils contained allophane and imogolite. Ranst et al. (2002) reported that soils from Java, in Indonesia, that were rich in allophane exhibiting relatively high PZNC and pHo values. The relatively high pHo values for those soils indicated development of net positive variable charge at field pH values less than pHo. Those observations have an important bearing on the retention of non-specifically adsorbing anions such as NO_3^- in A1 or Ap horizons of these Andisols.

Base Status and Cation Exchange in Andisols

The content of exchangeable "bases" is generally low in Andisols developed in humid, temperate regions, such as Japan, New Zealand, and the northwestern U.S. This is a feature common to soils formerly called Dystrandepts, which have a "base" saturation of less than 50 % in their subsoils. Andisols formerly called Hydrandepts and developed in humid to perhumid tropical regions, e.g., Hawaii, show a similar feature. Though it is difficult to measure and define "base" saturation for soils with variable charge, the low "base" content of these soils is expected from the fact that their negative charge is smaller with decreasing pH and electrolyte concentration, which implies that their cation-exchange sites show a very high selectivity for H^+. Therefore, the soils show no strong acidity, despite their low to very low base saturation (Wada, 1985).

On the other hand, Andisols at an early stage of development, even in humid, temperate regions, show a relatively high "base" saturation. Soils called Haplustands, developed in relatively arid regions, also show a high "base" saturation. This is due to the reduced leaching of "bases" but also to the negative charge characteristics of halloysite and possibly of related poorly crystalline minerals (Wada, 1985).

Kobo and Ohba (1964) related the reaction and base status of 36 soils of the ando group to the degree of weathering. Their findings showed that as the pH in 1 N potassium chloride (KCl) solution decreased, the exchange acidity increased, and the content of exchangeable Ca and Mg decreased with increasing weathering of the soils. They pointed out that the mineralogical nature of the parent volcanic ash influenced the pH, exchange acidity, and exchangeable Ca and Mg. Similar results were reported by Ranst et al. (2002), and his work indicated that soil pH and exchangeable Ca decreased from East to West on Java, in Indonesia, which was attributed to the fact that the parent ash become more acid from east to west.

Research on the charge characteristics of some of the amorphous materials found that the CEC value of imogolite was 20 to 30 meq/100g , which was obtained in 10^{-2} to 10^{-1} M salt solution and at pH 7.0 (Wada,1977; Theng et al., 1982). Almost all its negative charge was pH dependent and probably arises from H^+ dissociation from the Si-OH groups. The CEC values varied from 10 to 50 meq/100 g for allophanes with an SiO_2/Al_2O_3 ratio between 1 and 2 (Wada, 1980; Gonzales-Batista et al., 1982; Theng et al., 1982). The difference in the negative charge characteristics between two allophanes with individual SiO_2/Al_2O_3 ratios of either 1 or 2 suggested a difference in the origin of negative charge. In both the allophanes, negative charge arise from the Si-OH group in the Si-O tetrahedral sheet, but additional negative charge possibly arises from the substitution of Si with Al in the Si-O sheet in the allophane with the SiO_2/Al_2O_3 ratio of 2 (Wada,1985).

The “base” holding capacity of Andisols varies greatly with pH and electrolyte concentration of the solution. Conventional CEC methods use buffered solutions for

saturation with the index cation, where the excess salt is removed by washing with water and/or alcohol. It is evident that the conventionally measured CEC of Andisols has no precise meaning and has little use in assessing the ability of the soils to retain "bases" in the field (Wada, 1985). The recognition that cation-exchange materials in soils carry variable, as well as constant, charge indicates the necessity for determining their CEC at a specified pH and electrolyte concentration and depends on the purpose of the CEC measurement. Moreover, in a study of the surface charge characteristics of soils from humid tropical Queensland, Gillman and Sumpter (1986b) found that it was necessary to distinguish between two types of CEC. When pH was lowered below about pH 5, a certain proportion of the exchange complex was occupied by Al^{3+}, despite efforts to saturate the soil with Ca^{2+}. Thus, total cation exchange capacity (CEC_T) was estimated as the adsorbed $Ca^{2+} + Al^{3+}$, where as basic cation exchange capacity (CEC_b) referred to the amount of adsorbed Ca^{2+}. The latter is of greater agronomic interest, as it gives information on the capacity of soil to retain those cations which are important plant nutrients.

Gillman (1979) proposed a method for determining the CEC of acid soils. In the Gillman method, a soil is initially equilibrated with unbuffered 0.002 M $BaCl_2$, for which the ionic strength approximates that of the soil solution in highly weathered soils near field capacity. Then, the retained Ba on the exchange complex is compulsively replaced with Mg using $MgSO_4$, causing the precipitation of $BaSO_4$. Magnesium becomes the index cation, and a sufficient amount of $MgSO_4$ is added to achieve the appropriate ionic strength. The use of unbuffered solutions throughout ensures that soil pH is maintained. It is not necessary to remove the magnesium once the correct equilibrium has been

established, because the amount of $MgSO_4$ added is known, then it is necessary only to measure the magnesium in the equilibrium solution to determine the adsorbed amount and consequently the CEC. Nevertheless, Matsue and Wada (1985) found that the Gillman method for CEC measurement could not be applied to soils showing specific adsorption of SO_4^{2-}. Those authors pointed out that SO_4^{2-} was specifically adsorbed on allophane and imogolite, replacing OH^- groups bonded with Al. This specific adsorption will compete with Ba precipitation for SO_4^{2-} in the solution and with the exchange of Cl^- retained on the positive charge sites. The adsorbed SO_4^{2-} and the associated increase in pH can also create new negative charge sites. Therefore, those authors proposed a new method, equilibrating the soil with 0.01 M $SrCl_2$, and replaced the retained Sr with 0.5 M HCl. This method would be suitable for the measurement of CEC in leached soils carrying both variable and constant negative charges, under conditions similar to those found in the field.

Another complication in CEC measurement emerges, as CEC is the product of specific surface and surface charge density, such that a reduction in specific surface must be accompanied by a reduction in CEC. Although fine-grained solids may be characterized by a well-defined specific surface value, non-crystalline substances-which can flow, coalesce, and form contact angles with other materials-vary in specific surface with deformation or dehydration. Amorphous materials in Hydrandepts, which irreversibly dehydrate into aggregates of silt, sand, and gravel size, lose specific surface with dehydration (Uehara and Gillman, 1981). Kanehiro and Sherman (1956), demonstrated that the CEC of Hydrandepts decreased measurably with dehydration, and that some of the CEC lost through dehydration could be recovered by re-hydration. They

also showed that the greatest percentage loss in CEC occurred in soils with low silica-sesquioxide ratios and the greatest recovery of CEC lost through dehydration occurred in younger, less-weathered soils with high silica-sesquioxide ratios. Gillman and Murtha (1983) examined the effects of drying, storing in an air-dry condition, and collecting samples at different times of year for two soils from coastal north Queensland. The properties measured were independent of sampling time, but both air-drying and storage reduced the capacity of these soils to sorb phosphorus, especially in the soil with high clay and oxide contents. Those authors concluded that the effect might be the result of a decrease in specific surface.

On the other hand, besides soil CEC, the selectivity with which the soil prefers a cation over other cations on the exchange site is important to an assessment of the fate of added cations. Evangelou et al. (1986) pointed out that changes in exchangeable K^+ and NH_4^+ in a Maury silt loam soil were more dependent on the ion affinity constant, as modified by the CEC, than on the CEC alone, often implied by many other researchers. Additionally, they reported that the affinity constants for K^+ and NH_4^+ were also altered disproportionally by differences in organic matter content. Unfortunately, there is relatively little information on the cation selectivity of Andisols, particularly those with well-characterized ion-exchange materials (Wada, 1985). Yoshida (1961) showed that Japanese soils of the Ando group adsorbed Ca preferentially over NH_4 and K, whereas other soils and clays showed the reverse. Hunsaker and Pratt (1971) reported a preference for Ca in Ca-Mg exchange with an allophane and a Dystrandept. Galindo and Bingham (1977) reported that K and Ca were preferentially adsorbed in K-Na exchange and Ca-

Mg exchange, respectively, in Chilean Dystrandepts. In contrast, Wada (1985) found little difference in the selectivity between Ca and Mg in an Andisol B horizon.

In K-Ca exchange on Chilean Andisols, Schalscha et al. (1975) found that an increase in pH produced an increase in negative charge that was largely balanced by an increase in the amount of Ca adsorbed. Wada (1985) pointed out that Andisols with variable charge show a marked reduction in retention of exchangeable "bases" with decreasing pH and electrolyte concentration, and this was more marked for K and NH_4 than for Ca. These two characteristics can act together and result in weaker retention of K and NH_4 under leaching conditions. The weak NH_4 retention could also be related to the low production potential of some Andisols used for paddy rice, where seasonal flooding reduces the surface soil and NH_4 is the main form of available nitrogen. Paddy rice growing on an allophanic soil also showed a high nitrogen absorption/dry matter production ratio at early stages of growth, as compared with other soils, which was related to a high NH_4 concentration in the soil solution.

Soil Potassium, Calcium and Magnesium Supply and Their Interaction

Knowledge of the composition of the soil solution, or any nutrient solution, is essential for predicting plant nutrient uptake. The uptake of a given ion depends not only on its activity in solution, but also on the activity of other ions and the relationship that exists between solution ions and exchangeable or solid-phase ions (Khasawneh, 1971). For instance, high rates of K fertilizers are known to reduce Mg concentrations in plants (Birch et al., 1966), but the reverse effect of Mg on K was either slight or nonexistent (Carolus, 1938; Omar and Kobbia, 1966; Smith et al., 1954). Walsh and O'Donohoe (1945) observed Mg deficiency in soils that had ample exchangeable Mg but too high

levels of available K. The literature is replete with similar reports on a variety of ions and their interactions. Ionic ratios have been used to explain such interactions on the process of ion uptake from both soils and nutrient solutions.

One of the most extensive uses of ionic ratios has been in the study of K nutrition derived from soils. There is evidence that the uptake of K^+ from soil and/or solution culture is dependent on the concentration of Ca^{2+} and/or Mg^{2+} (Elzam and Hodges, 1967; Maas, 1969; Zandstra and MacKenzie, 1968: Stout and Baker, 1981). Furthermore, there is evidence indicating that, for the range of Ca concentrations encountered in the soil solution (Adams, 1971; Curtin and Smillie, 1983), the uptake of K^+ and Ca^{2+} by excised roots appears to be competitive (Maas, 1969). In other words, K^+ uptake is inhibited in the presence of increasing concentrations of Ca^{2+}. Similar competitive effects have been demonstrated with increasing solution proton activity (Schofield, 1949). As a result, the activity ratio (AR_e^k)

$$\frac{\text{activity of } K^+}{(\text{activity of } Ca^{2+} \text{ and } Mg^{2+})^{1/2}} \quad \text{or} \quad \frac{a_K}{(a_{Ca+Mg})^{1/2}}$$

of a solution in equilibrium with a soil provides a satisfactory estimate of the availability of K. This ratio is a measure of the "intensity" of labile K in the soil and represents the K that is immediately available to crop roots (Havlin et al., 1999).

The equilibrium value for this ratio, AR_e^k, is determined in a rather tedious way from a curve of AR^k versus adsorbed potassium, but Le Roux and Sumner (1967) and Gillman and Bell (1978) showed that this value could be more easily obtained by actually measuring the potassium, calcium, and magnesium concentrations in the soil solution.

The values they obtained were well correlated with those determined by the conventional ionic equilibria procedure.

Soils with similar AR_e^k values may have quite different capacities for maintaining AR_e^k while K^+ is being depleted by plant uptake or leaching. Thus, to describe the K status of soils, it is necessary to specify not only solution K (intensity) but also the way in which the intensity depends on the quantity of labile K present. The quantity-intensity relationships (Q/I) are directed related with "exchangeable K", since this fraction has the principal role in replenishing solution K (Havlin et al., 1999).

It is very difficult for one to separate plant nutrient availability effects due to soil K chemistry from plant nutrient physiological effects (Haynes, 1980). The Q/I concept does not deal with physiological effects, but it appears to be influenced by them. Nevertheless, even if nutritional effects are assumed to play a limited role in K uptake under a given set of experimental conditions, the ability of a soil to replenish K^+ in the soil solution is highly complex process and definitely not solely dependent on K-(Ca-Mg) exchange alone. Additional factors controlling K availability include hysteresis or exchange irreversibility effects, anion effects, multi-cation effects, potential-determining ion effects, and kinetic effects (Evangelou et al., 1994).

On the other hand, Ca nutrition studies reported that mole ratios of Ca/(Ca+Mg) of less than 0.1 or of Al/Ca of more than 0.02 resulted in reduced root growth of soybeans (*Glycine max L.*) (Lund, 1970). Further calcium-magnesium interactions were also investigated by Key et al. (1962), and Martin and Page (1969). Key et al. (1962) reported poor growth whenever the Ca/Mg ratio was less than one. Howard and Adams (1965) attempted to determine a critical Ca/Mg ratio below which cotton taproot

elongation was reduced. They found that the critical Ca/Mg ratio in their experiments was 0.12, which was higher than the 0.091 value reported by Walker et al. (1955), but lower than 0.25 or 1, the values reported by Vlamis (1949) and Key et al. (1962), respectively. By reasoning that "ion antagonistic effects on Ca are the result of the total cation concentration in solution and are not restricted to the Mg concentration", they returned to the ratio of Ca to total cations in solution. They found that this ratio was very consistent for predicting Ca deficiency in their experiments with nutrient solutions as well as with soil. They reported that when Ca/total cationic ratio was less than 0.15-0.20, the elongation of cotton taproots was severely retarded in nutrient solutions as well as in soil. Later, Adams (1966) and Bennett and Adams (1970) demonstrated that if the ratio of the calcium activity to the sum of cationic activities in the soil solution was less than 0.15, calcium deficiency (even in a limed soil) could be expected. The results of Gillman and Bell (1978) showed that calcium deficiency might be a real problem in weathered tropical North Queensland soils according to the Bennett and Adams' criteria. Even though the chemistry of macrocations (K-Ca-Mg) in Andisols has not been extensively studied, Kamata (1978) recommended that the proportions of exchangeable Ca, Mg, and K in Japanese Andisols should be 50, 20, and 10 percent (molar charge basis), respectively, in order to have a balanced supply of these elements for most crops.

MATERIALS AND METHODS

Description of the Study Soils

The present study involved three soils characterized by a predominance of constant surface-potential constituents in their mineralogy. Those soils are currently under field production, two of them from Ecuador-South America (Figure 1), and one from south-central Kentucky, US (Figure 2). The location, parent material, soil series, and classification of each site are given in Table 1.

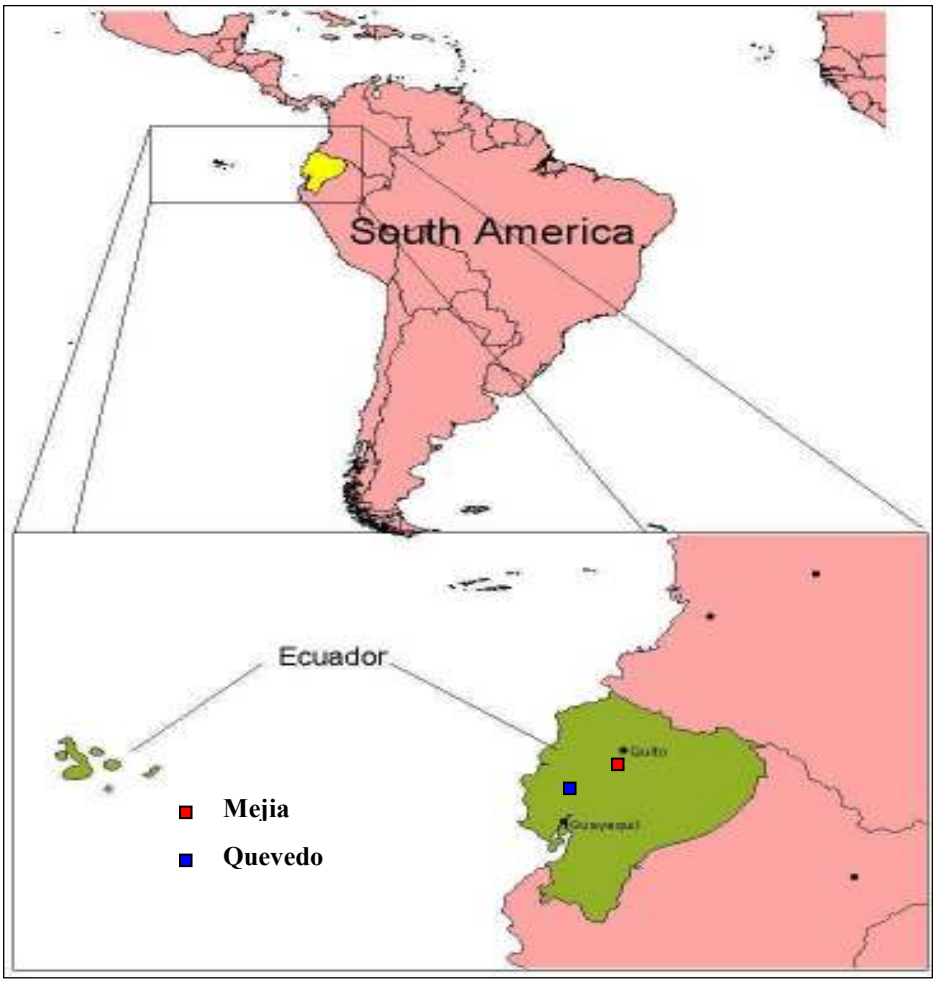

Figure 1: Site Location of Ecuadorian Andisols.

Figure 2: Site Location of the Typic Paleudalf.

Table 1: Location, Parent Material, and Classification of the Studied Soils

Soil	Soil Series	Location	Parent Material	Classification
1	NSD*	Metcalfe Co., KY, US	Residuum from St. Louis limestone	Fine, mixed, thermic Typic Paleudalf
2	NSD*	1°06' S Lat 79 °21' W Long; el., 120 m INIAP Exp. Stn, at Quevedo, Ecuador	Andesitic volcanic ash	Isohyperthermic (24 °C), Ustic (2,021 mm), Haplustand
3	NSD*	0°20'15'' S Lat 78°33'45''W Long; el., 3,050 m INIAP Exp. Stn, at Mejia, Ecuador	Andesitic volcanic ash	Isomesic (11 °C), Udic (1,200 mm), Melanudand

* No series designated

Characteristics of the Field Sites in Ecuador

Oil Palm Fertilization Experiment

The Haplustand is under an oil palm fertilization experiment that has been conducted at the "Pichilingue" Experimental Station of the National Institute of Agronomic Research (INIAP) in Ecuador since 1991. The effect of irrigation on fruit

bunch yield at five levels of mineral fertilizer has been measured since the onset of harvesting in 1993. The plots were arranged in a split plot design with the irrigation treatment as the main plot and fertilizer treatments as sub-plots. Nutrients in the fertilizer treatments included nitrogen (N), phosphorus (P), potassium (K), magnesium (Mg), sulfur (S), and calcium (Ca). These treatments consist of an un-fertilized control, +N, +NPK, +NPKMgS, and +NPKMgSCa. Table 2 lists sources and rate of nutrients applied since 1992.

Table 2: Nutrient Rates Applied to the Different Fertilizer Treatments from 1992 to 2002

Year	N*	P_2O_5	K_2O	MgO	S	$CaCO_3$
	kg/ha/year					
1992-93	57	23	21	11	10	279
1994	70	25	25	14	12	353
1995	140	72	200	36	32	980
1996	143	72	200	50	44	980
1997	229	72	286	50	44	980
1998-02	229	92	300	54	44	1001

***** Fertilizer sources were urea, triple super phosphate (TSP), potassium chloride (KCl), magnesium sulfate ($MgSO_4$) and calcium carbonate ($CaCO_3$).

Liming Experiment

The Melanudand is under a liming experiment that has been conducted at the "Santa Catalina" Experimental Station of INIAP in Ecuador. The effect of liming on crop yield has been measured since 1986. It has been cultivated to a crop rotation including corn, peas, beans, and barley. No-tillage cultivation has been used since 2000 at this experimental site. The plots were arranged in a split plot design with the liming rate as the main plot and liming frequency as sub-plots. The liming rate treatments

include 0, 1.5, 3.0, 4.5, 6.0, 9.0, 12.0, 15.0, and 18.0 tons of calcitic lime/ha. The site has been limed in 1986, 1992 and 1999.

Characteristics of the Typic Paleudalf

A Typic Paleudalf from Metcalfe County, south-central Kentucky was sampled. The soils in this county are formed under a humid, temperate climate. In these climatic conditions the soils are moist and subject to leaching most of the year, except for occasional dry periods in summer. As a result, practically all of the soils are strongly acid (Soil Conservation Service, 1967). Detailed information about the mineralogical and P-sorption characteristics of the studied soil is given in Mubiru (1992). The physical-chemical and mineralogical characteristics of the soil horizons sampled for the present study are given in appendix A (Source of data: Mubiru, 1992).

Soil Sample Collection and Preparation

The Haplustand was sampled at two different depths (0-10 and 10-30 cm) for every irrigated fertilizer treatment level, i.e., control, +N, +NPK, +NPKMgS, and +NPKMgSCa. Each fertilizer treatment has four replications, and the samples were collected in every replication at the two different depths. Ten cores per plot were sampled and composited. Preliminary chemical characterization was performed on each replication, while further mineralogical and chemical analyses used replicated composited samples. A detailed pedon description of this soil is given in appendix B.

Each treatment of the Melanudand was sampled at two different depths (0-20 and 20-40 cm). A detailed pedon description of this soil is given in appendix B. The sampled treatments included the following lime rates: 0, 3.0, 6.0, 12.0 and 18 ton/ha. All of those sampled have received the highest liming frequency, i.e., successive lime applications in

1986, 1992 and 1999. Each treatment has three replications, and the samples were collected in every replication at the two different depths. Ten cores per plot were sampled and composited. Preliminary chemical characterization was performed on each replication, while further mineralogical and chemical analyses used replicated composited samples.

The Typic Paleudalf was sampled at two different depths (0-18 cm, and 100-138 cm). A detailed pedon description of this soil is given in Mubiru (1992).

All soil samples were collected at prevailing field moisture and stored in polyethylene bags. Moist samples were used for mineralogical analyses and surface charge characterization. Sub-samples were air-dried, ground, and screened through a 2 mm sieve in preparation for additional physical and chemical analyses.

Mineralogical Methods

The mineralogy of both subsurface Andisols, using samples taken from the unamended control plots in each field trial, was characterized by selective dissolution analysis with 0.5 M NaOH, in combination with X-ray diffraction (XRD) and thermogravimetry (TG). Quantitative interpretations were based on procedures outlined by Karathanasis and Hajek (1982). The subsurface soils were selected to avoid the influence of the higher soil organic matter contents in surface horizons. Additionally, the effects of soil mineral dispersion procedures, i.e., organic matter and free-Fe oxide removal, on amorphous materials and XRD and TG analyses were evaluated through sequential analysis of individual samples. This included: XRD and TG analyses before soil mineral dispersion, after soil mineral dispersion, and after amorphous material dissolution.

Soil Mineral Dispersion

Organic Carbon Oxidation

A moist soil sample (sieved past 2 mm) containing approximately 10 g was dispersed using a Na-acetate buffer solution (1 N, pH 5), and heated. When the suspension temperature stabilized at 80 ^{o}C, the first addition of hydrogen peroxide (30 % H_2O_2) was made to begin the organic carbon oxidation. After the effervescence subsided, more H_2O_2 was added until the reaction stopped.

Free Fe-Oxide Removal

The soil sample, free of organic matter, was quantitatively transferred into a bottle with Na-acetate, centrifuged at 2000 rpm for 5 min to remove the released bases and the supernatant solution was decanted. To the sediment a Na-citrate/Na-bicarbonate buffer (pH 7) solution was added, shaken well and placed in a hot water bath (80 ^{o} C) for 15 min. After that, Na-dithionite was added three times, allowing the effervescence to subside after each addition. Na-dithionite and Na-citrate are the iron reducing and chelating agents, respectively; bicarbonate buffers the suspension at pH 7, and Na favors dispersion, which causes the free iron oxides to be in suspension/solution. After centrifugation at 2000 rpm for 5 min., the supernatant was collected. The sediment was washed twice using a mixture of Na-citrate/Na-bicarbonate and NaCl, while collecting each time the supernatant solution to determine the dissolved Fe by atomic absorption spectroscopy (AAS), in order to estimate the amount of free Fe-oxides (Mehra and Jackson, 1960).

Clay Fractionation

Deionized water was added to the iron oxide-treated sediment, shaken for 15 min, and centrifuged at 750 rpm for 3.5 min. The dispersed fraction was decanted carefully. The step was repeated three times until the supernatant was relatively clear. The clay suspension was flocculated by addition of solid NaCl. The clear supernatant was siphoned and discarded, keeping the clay fraction undisturbed in the bottom of the beaker. The clay fraction was dried in an oven at 100 ^{o}C for 2 days and then ground to powder.

Selective Dissolution Analysis with 0.5 M NaOH

A 0.200-g aliquot of clay was transferred to a stainless steel beaker and dispersed in 2 ml of 0.5 N NaOH. The beaker with the sample was placed on an electric hot plate and 200 ml of boiling 0.5 N NaOH was added. The boiling was maintained for 2.5 min at 250 ^{o}C. The suspension was rapidly cooled in a cold water bath and the supernatant liquid removed by centrifugation at 2000 rpm for 10 min. The dissolved Si and Al were immediately determined by AAS. The fraction of poorly crystalline aluminosilicates soluble in 0.5 N NaOH in each soil were then estimated from the amount of dissolved SiO_2, and Al_2O_3 contained in this extract (Jackson et al., 1986).

X-Ray Diffraction Analysis

Two clay suspension sub samples, taken after the dissolution analysis with 0.5 M NaOH, were saturated with Mg and K using $MgCl_2$ (1 N) and KCl (1 N) solution, respectively, and filtered. The clay from the membrane filter was transferred to glass-slides by inverting and applying gentle pressure. Magnesium- and potassium- saturated clay slides were stored in a desiccator equilibrated at 52 % relative humidity using a

saturated $MgNO_3$ solution. A Phillips 1840 diffractometer, operated at 40 kV and 30 mA, and equipped with a long, fine-focused copper-tube, was used for XRD analysis of the Mg- and K-saturated clays at 25 ^oC, as well as for the potassium-saturated clay slides heated to 110, 300, and 500 ^oC. The samples were scanned at a rate of 0.02^o 2θ per second through a range of 2^o to 40^o 2θ. Magnesium-saturated clays were glycerolated with a 30 % glycerol-ethanol solution and left to equilibrate for at least 4 hr before analysis.

Quantitative estimates of kaolinite, quartz, feldspars, mica, hydroxy-interlayer vermiculite (HIV), and smectite were made from the relative intensity of their characteristics peaks at 0.7, 0.425, 0.32, 1.0, 1.4, and 1.4 nm, respectively, which was found by taking the product of the peak height and the width at half peak height. (Karathanasis and Hajek, 1982).

Thermal Analysis

Magnesium-saturated clays maintained at 52 % relative humidity were analyzed by TG for quantification of kaolinite, gibbsite, and HIV (Karathanasis and Hajek, 1982). A Dupont 990 thermal analyzer equipped with a 951 module was used for TG analysis. Temperature was sensed with chromel-alumel and platinel thermocouples. Clay samples of about 12 mg, placed in Al pans, were heated from ambient temperature to 1,000 ^oC in a dinitrogen gas atmosphere at a rate of 10 ^oC/min. Quantitative mineralogical determinations were based on weight losses as compared to values for standard smectite + vermiculite, kaolinite, gibbsite, and goethite (Karathanasis and Hajek, 1982).

Physical Methods

For particle-size analysis, pretreatments to remove organic matter, iron oxides, carbonates, and soluble salts were omitted. Fifty grams of air-dry soil were dispersed in a 0.1 N sodium hydroxide solution for 24 hr. Soil texture was determined by the Bouyoucos method (Bouyoucos, 1962).

Chemical Methods

Preliminary Soil Fertility Evaluation

The following analyses were made on air-dry 2 mm sieved Ecuadorian soil samples; organic carbon content was determined by wet oxidation using the Walkley-Black method (Walkley and Black, 1934). The soil pH in H_2O was measured with a glass electrode at a ratio of 10 ml/25 ml, and the pH in NaF was determined using 1 M NaF solution at a ratio of 1g/50 ml. The latter pH was read after 2 min. Exchangeable cations and CEC were determined using the barium chloride method, i.e., 0.1 M $BaCl_2$-0.01 M $MgSO_4$ solution (Hendershot and Duquette, 1986), and the ammonium acetate pH 7 method, i.e., 1 N $NH_4C_2H_3O_2$ at pH 7-19 % NaCl solution (Chapman, 1965). Exchangeable Ca, Mg, and K were extracted by three methods ($BaCl_2$, $NH_4C_2H_3O_2$, and Olsen) and were analyzed by AAS. The Olsen extraction solution consists of 0.5 M $NaHCO_3$ and 0.005 M EDTA (ethylenediaminetetraacetic acid, disodium salt), at pH 8.5. A 2.5 ml aliquot of soil sample is extracted with 25 ml of Olsen reagent by shaking for 10 minutes (Olsen et al., 1954). The suspension is then filtered through Whatman no. 42 filter paper and analyzed. Exchangeable Al and H were extracted with a 1 M KCl solution and determined by titration (McLean, 1965). Extractable Zn, Cu, Fe, and Mn were extracted with an Olsen solution and determined by AAS. Extractable P was also

extracted with an Olsen solution and determined colorimetrically at 680 nm using the ascorbic acid method (Olsen et al., 1954; and Watanabe and Olsen, 1965). Extractable S was determined with calcium phosphate [$CaH_4(PO_4)_2.H_2O$] extraction and determined turbidimetrically at 420 nm (Sheen, et al., 1935; Reisenauer et al., 1973; and Bettany and Halstead, 1972). Total nitrogen was determined by semimicro-Kjeldahl method (Nelson and Sommers, 1972; Bremner, 1960; and Bremner and Breitenbeck, 1983). The saturated paste extract method (U.S. Salinity Laboratory Staff, 1954) was used to measure electrical conductivity, and Ca, Mg, K, Na, Cl^-, HCO_3^-, CO_3^{-2}, and SO_4^{-2} in soil solution.

Statistics were performed using SAS Version 8 (SAS Institute, 1999). The GLM model procedure was used for analysis of variance, and significant differences among means were determined by LSD means separation. The 0.05 probability level was used to define statistical significance.

Specific Surface

Surface and subsurface samples of selected treatments were analyzed to determined specific surface by the ethylene glycol monoethyl ether (EGME) procedure (Carter et al., 1986; and Cihacek and Bremner, 1979). In order to assess the effect of drying on specific surface area determination, moist and dry (at 45 ^oC and 110^oC) samples were analyzed. All the soil samples were passed through a 60-mesh sieve. Approximately 1.1 g of each sample was weighed into a tared aluminum can, and wetted with approximately 3 ml of reagent-grade ethylene glycol monoethyl ether (EGME) to form soil-absorbate slurry. The can containing the sample-EGME slurry was placed in a chamber desiccator containing $CaCl_2$-EGME solvate. The entire chamber dessicator was placed in a vacuum desiccator containing $CaCl_2$. After giving 30 min for the sample-

solvate slurry to equilibrate, the dessicator was evacuated with a vacuum pump. The dessicator stood for about 7 days and was periodically evacuated. The samples were weighed at 1-day intervals, until constant weight was attained. The specific surface was calculated by the equation

$$A = W_g/(W_s \times 0.000286)$$

where A = specific surface in m^2/g, W_g = weight of EGME retained by the sample in g, W_s = weight of dried sample in g, and 0.000286 is the weight of EGME required to form a monomolecular layer on a square meter of surface.

Electrochemical Properties

Charge fingerprints, which are curves of total cation-exchange capacity (CEC), and anion-exchange capacity (AEC) across the pH range 3.0 to 8.0, were determined on selected samples using the method introduced by Gillman and Sumpter (1986b) and described in detail by Gillman and Abel (1986). Briefly, the moist soil samples were Ca saturated and brought into equilibrium with a 0.002 M $CaCl_2$ solution. The pH was adjusted to values in the range of 3.0 to 8.0 using HCl and $Ca(OH)_2$ solutions, respectively. Then 1 M NH_4NO_3 solution was used to extract Ca^{2+}, Al^{3+}, and Cl^- from the soil. Looking for the appropriate equilibration time for the exchange reactions, both two- and twenty four-hour periods were tested. Additionally, 1 M $Mg(NO_3)_2$ solution was used to extract Ca^{2+}, Al^{3+}, and Cl^- from the Ca saturated soil. Ca^{2+} and Al^{3+} were quantified by AAS, and Cl^- was determined colorimetrically at 480 nm using an adaptation of the automated ferricyanide method (Zall, et al., 1956; and Standard Methods for Examination of Water and Wastewater, 1989). Amounts adsorbed were calculated, allowing for entrained solutes. The CEC was defined as the $Ca^{2+} + Al^{3+}$ adsorbed, and AEC as the Cl^-

adsorbed. During use of this method, $pH_{0.002}$ (defined as an estimate of soil solution pH) is measured as the pH of a 1:10 soil/0.002 M $CaCl_2$ (g/ml) suspension following Ca saturation.

Additionally, as described by Gillman (1984), additional information was used for the determination of (i) the variation in negative (σ^-) and positive (σ^+) charge over a range of adjusted pH values defined by CEC and AEC, respectively; (ii) the point of zero charge of the variable charge components (pH_o); and (iii) the relative amount of permanent charge (σ_p). The permanent charge refers to the difference between σ^- and σ^+ at pH_o. The pH value where σ^- and σ^+ were equal is the point of zero net charge (PZNC). The pHo determination was based on the change in the adjusted pH value of the 0.002 M $CaCl_2$ suspension after Ca saturation following addition of 0.5 ml of 2 M $CaCl_2$ and 3 hrs shaking (pH 0.05). ΔpH was calculated as $pH_{0.05} - pH_{0.002}$, and a plot of ΔpH versus $pH_{0.002}$ revealed the point where ΔpH is zero. This is the pH where there are equal amounts of negative and positive charge on the variable charge surfaces (pHo).

The effect of divalent versus monovalent cation for measuring charge characteristics was examined by repeating the method described above on the same samples using KCl as the electrolyte.

Quantity-Intensity Relationships

Quantity-intensity relationships of the surface and subsurface samples of the Ecuadorian Andisols were determined by a procedure similar to that used by Beckett (1964b) and Rasnake and Thomas (1976). Solutions for individual soils were made up in a 0.002 M $CaCl_2$ matrix to contain different K (from KCl) concentrations, as shown in Table 3. Potassium concentration varied with soil, according to the initial Q/I response.

Two-gram moist samples of each soil were placed in 20 ml of each of those solutions. The samples were shaken for 24 hours on a reciprocating shaker. The supernatant solutions were analyzed for K, Ca, and Mg using AAS. The change in exchangeable K (ΔK ex) was calculated using the formula:

$$\Delta K\ ex = [K]\ original - [K]\ equilibrium,$$

where square brackets [ ] represent concentrations.

The activity ratio (AR^K) was calculated as:

$$AR^K = (K^+)/\ [(Ca^{2+}) + (Mg^{2+})]^{1/2}$$

where all activities are expressed as moles/liter in the equilibrium solution. The single-ion activity was estimated by

$$\alpha_j = \delta_j m_j ,$$

where α_j = single-ion activity, δ_j = single-ion activity coefficient of ionic species j, and m_j = molar concentration of species j (Sposito, 1981). The single-ion activity coefficient was estimated by the equations show below.

$$I = 0.0127\ EC,$$

where I = ionic strength and EC = electrical conductivity in dS/m at 25 ^oC (Griffin and Jurinak, 1973). The single-ion activity coefficient was then calculated by the Davies equation

$$Log\ \delta_j = -AZ_j^2\ \{[I^{1/2} / (1 + I^{1/2})] - 0.3\ I\}$$

where A = 0.512 at 25 ^oC.

The activity ratio was then plotted against ΔK ex to obtain Q/I curves.

Table 3: Potassium Concentrations Used in Q/I Curve Determinations

Soil	Field Experiment Treatment	K (from KCl) Concentration
Melanudand (0-20 cm)	0 ton lime/ha	0, 17, and 34 ppm
	3 ton lime/ha	0, 17, and 34 ppm
	6 ton lime/ha	0, 17, and 34 ppm
	12 ton lime/ha	0, 17, and 34 ppm
	18 ton lime/ha	0, 17, and 34 ppm
Melanudand (20-40 cm)	0 ton lime/ha	0, 13, and 26 ppm
	3 ton lime/ha	0, 13, and 26 ppm
	6 ton lime/ha	0, 13, and 26 ppm
	12 ton lime/ha	0, 13, and 26 ppm
	18 ton lime/ha	0, 13, and 26 ppm
Haplustand (0-10 cm)	Control	0, 12, and 24 ppm
	N	0, 18, and 36 ppm
	NPK	0, 33, and 66 ppm
	NPKSMg	0, 33, and 66 ppm
	NPKSMgCa	0, 33, and 66 ppm
Haplustand (10-30 cm)	Control	0, 14, and 28 ppm
	N	0, 15, and 30 ppm
	NPK	0, 49, and 98 ppm
	NPKSMg	0, 43, and 86 ppm
	NPKSMgCa	0, 27, and 54 ppm

RESULTS AND DISCUSSION

Mineralogical Analysis

The mineralogical composition of the clay fraction from the subsurface Melanudand and Subsurface Haplustand is presented in Table 4. The overall weathering index associated with the Melanudand was greater than that for the Haplustand, which is supported by the Udic regime of the former Andisol. In contrast to what the overall weathering index suggests, the poorly crystalline aluminosilicates removed from the Melanudand gave a SiO_2/Al_2O_3 of 3.8, and a $SiO_2/Al_2O_3 + Fe_2O_3$ ratio of 1.9. While, the Haplustand possessed lower SiO_2/Al_2O_3 and $SiO_2/Al_2O_3 + Fe_2O_3$ ratios, 2.5 and 1.5 respectively. These results clearly show that the amorphous fraction of the Haplustand has lost relatively more of its silica, which suggests that fraction has been more affected by the wetting and drying cycles that favor weathering and are associated with the Ecuadorian Coastal Plain climate, even though its moisture regime has been categorized as Ustic. Nevertheless, some of the differences in mineralogy between these Andisols could be explained by diversity in parent materials considering the multiple ash depositions events involved in these Andisols' formation, as well as their geographical variation.

Table 4: Mineralogical Composition of the Clay Fraction from the Subsurface Haplustand and Subsurface Melanudand

Mineral	**Haplustand (10-30 cm depth)**	**Melanudand (20-40 cm depth)**
HIV (%)	-	49
Smectite (%)	19	-
Vermiculite-Mica (%)	7	-
Mica (%)	7	4
Kaolinite + Metahalloysite (%)	11	11
Quartz (%)	7	3
Feldspars (%)	16	10
Free-Fe oxides (%)	5	4
Amorphous SiO_2 (%)	20	15
Amorphous Al_2O_3 (%)	8	4

Crystalline minerals contained in the clay fraction of each Andisol, before organic matter or free-Fe oxide dispersion could not be clearly resolved from their XRD patterns (Figures 3 to 8). All of those patterns lacked well defined peaks. This was expected due to the high levels of organic matter and amorphous materials that were present. Despite the low resolution of those patterns, some crystalline minerals were evidenced. Characteristic peaks for 1.4 nm minerals, mica, feldspars, and quartz were observed in both the Melanudand and the Haplustand patterns.

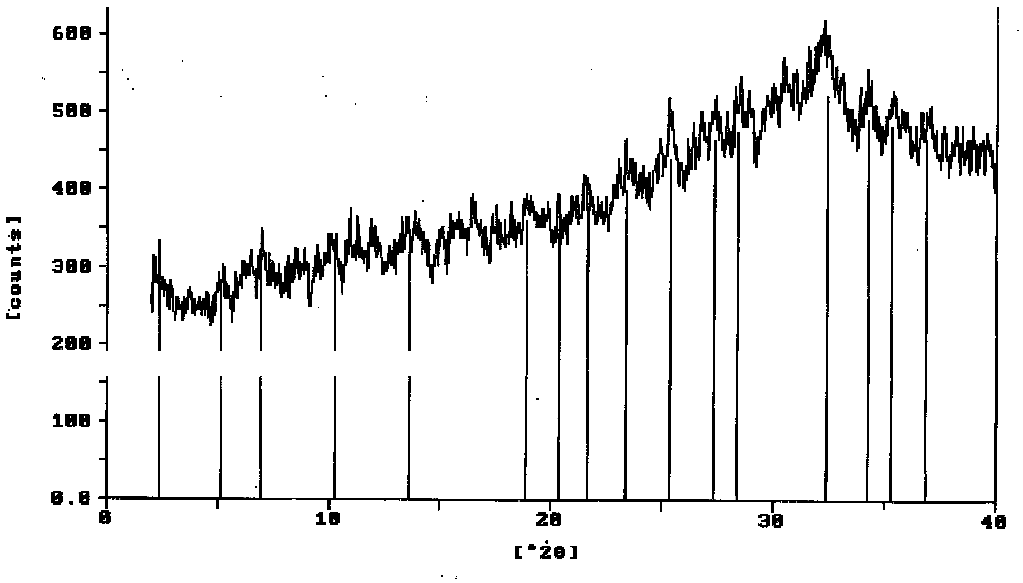

Figure 3: X-ray Diffraction Pattern of Mg-Saturated Clay Fraction (<2µm) Specimen from the Melanudand (20-40 cm) before Soil Mineral Dispersion.

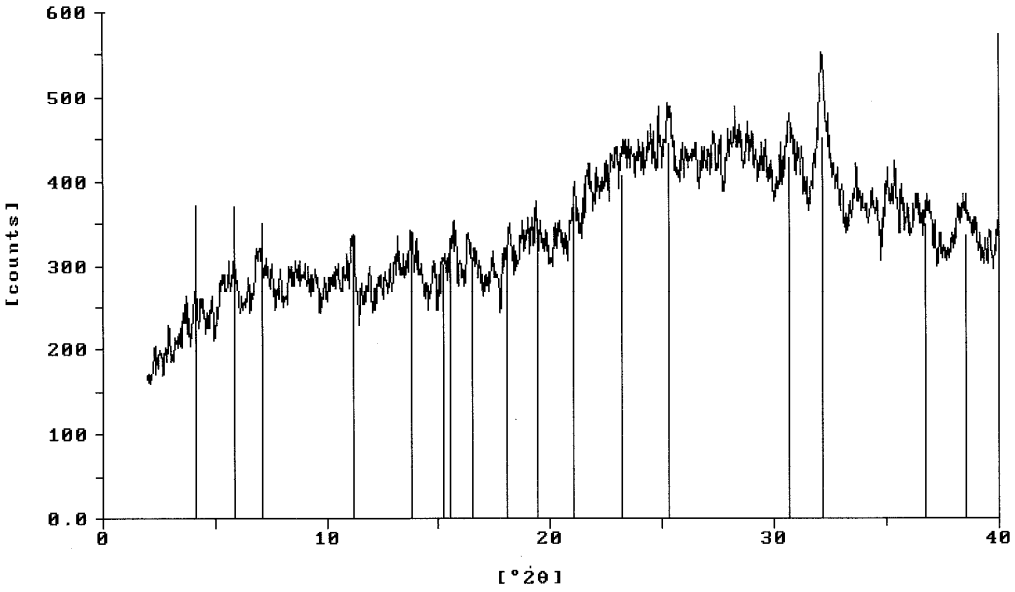

Figure 4: X-ray Diffraction Pattern of Mg-Saturated, Glycerol Solvated Clay Fraction (<2µm) Specimen from the Melanudand (20-40 cm) before Soil Mineral Dispersion.

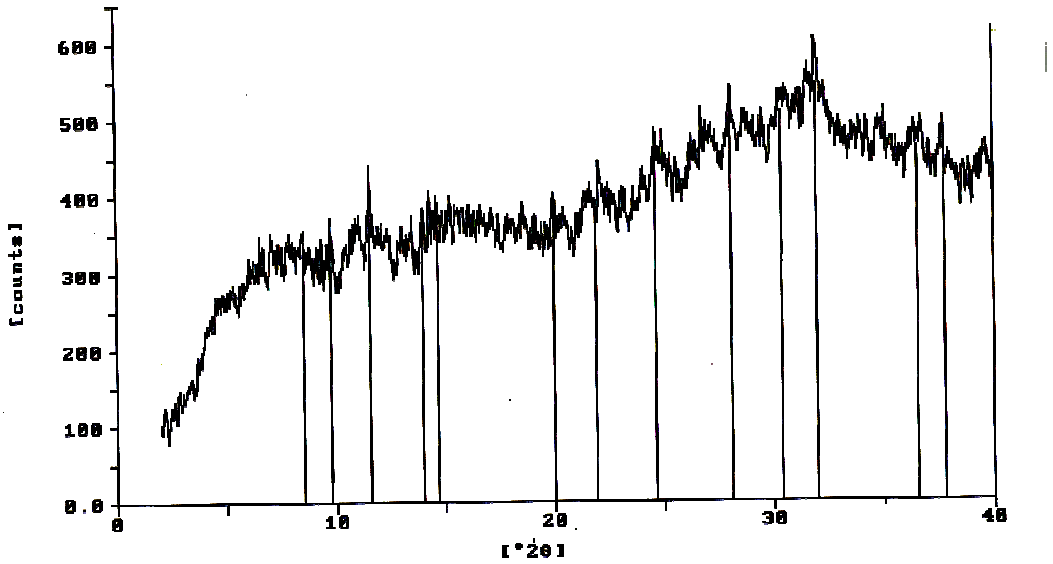

Figure 5: X-ray Diffraction Pattern of K-Saturated Clay Fraction (<2µm) Specimen from the Melanudand (20-40 cm) before Soil Mineral Dispersion.

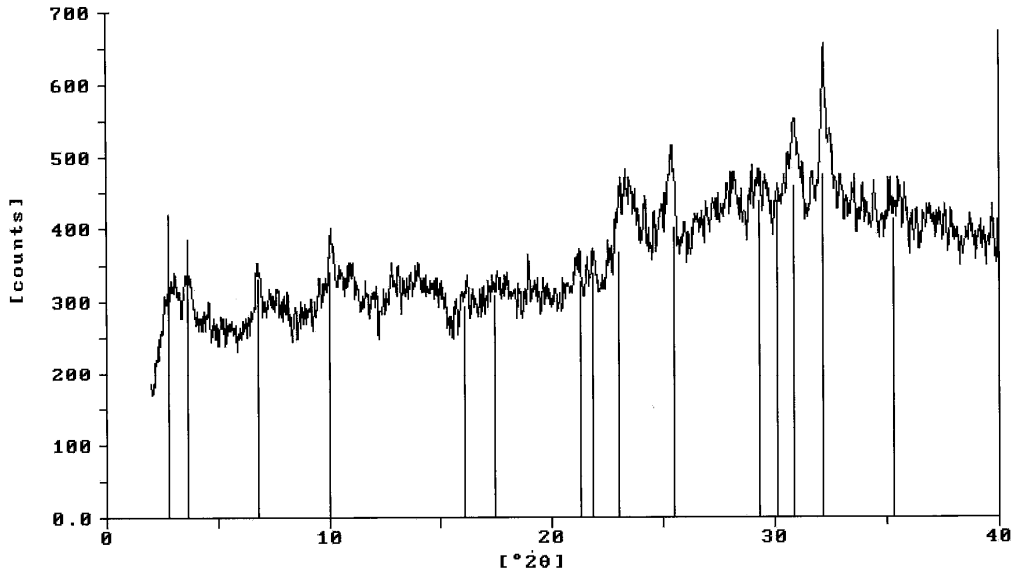

Figure 6: X-ray Diffraction Pattern of Mg-Saturated Clay Fraction (<2µm) Specimen from the Haplustand (10-30 cm) before Soil Mineral Dispersion.

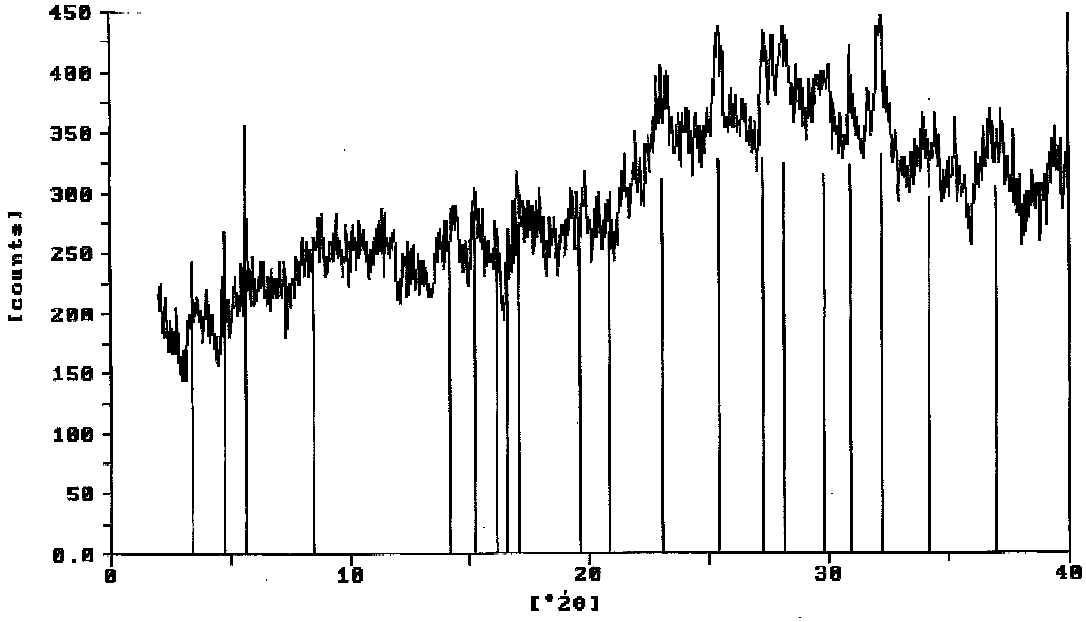

Figure 7: X-ray Diffraction Pattern of Mg-Saturated, Glycerol Solvated Clay Fraction (<2µm) Specimen from the Haplustand (10-30 cm) before Soil Mineral Dispersion.

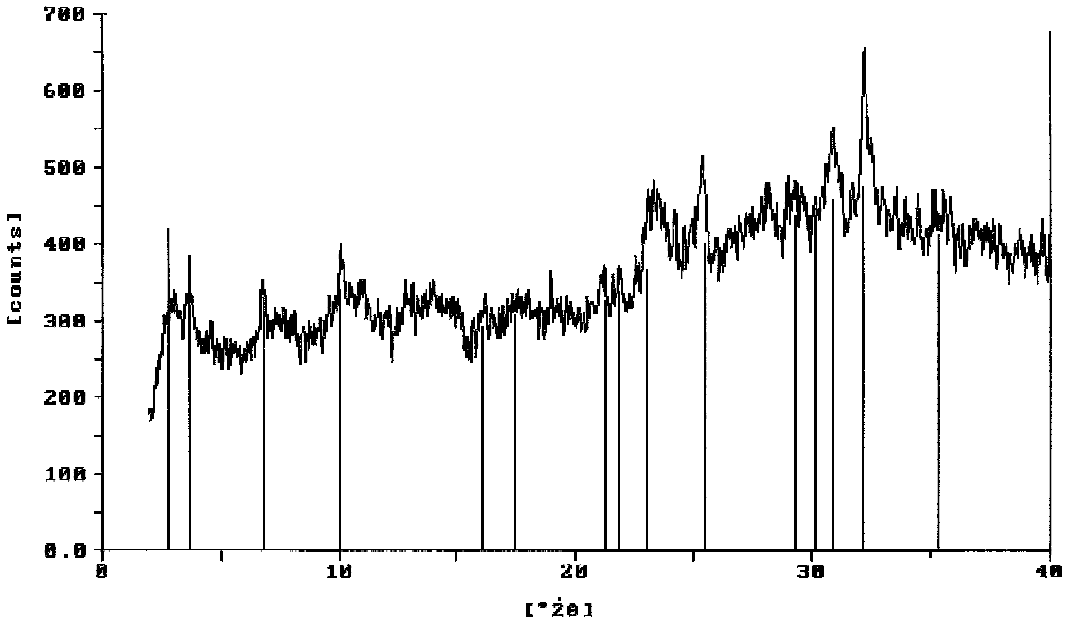

Figure 8: X-ray Diffraction Pattern of K-Saturated Clay Fraction (<2µm) Specimen from the Haplustand (10-30 cm) before Soil Mineral Dispersion.

After soil mineral dispersion i.e., organic matter oxidation and free-Fe removal, crystalline minerals contained in the clay fraction of both Andisols were identified from their XRD patterns (Figures 9 to 20). All of the quantitative interpretations were based on those patterns. The Mg-saturated clay XRD pattern for the Melanudand (Figure 9) indicated the presence of 1.4, 1.0, 0.74, 0.73, 0.425, and 0.32 nm components in significant amounts, which are associated with smectite, vermiculite, and/or chlorite, mica and/or halloysite, metahalloysite, kaolinite, quartz and feldspars respectively. The pattern from Mg-glycerol treatment (Figure 10) showed that this soil does not contain expanding clay minerals (smectites), since there was no characteristic 1.8 nm peak (Borchardt, 1989). The K-saturated clay, when heated successively from ambient temperature to 100, 300, and 550 ^{o}C (Figures 11 through 14), displayed the usual shift from 1.4 nm to 1.0 nm at 300 ^{o}C, culminating at 550 ^{o}C. Those treatments confirmed the presence of hydroxy-interlayered vermiculite (HIV) as the 1.4 nm mineral (Barnhisel and Bertsch, 1989), which would be associated with the high Al activity present in this soil**.** There was no decrease in the 1.0 nm peak, nor increase in the 0.7 nm peak intensity of the K-saturated clay when heated to 100 ^{o}C, so halloysite was not present. However, the disappearance of both 0.7 nm peaks at 550 ^{o}C (Figure 14) confirmed that those reflections are due to kaolinite and metahalloysite. The presence of the last mineral is supported by Wada and Kakuto (1985b), who reported embryonic stages of halloysite formation in three Ecuadorian soils. On the other hand, the Mg-saturated clay XRD pattern for the Haplustand (Figure 15) showed the presence of 1.4, 1.2, 1.0, 0.7, 0.50, 0.44, and 0.32 nm components in significant amounts, which are related to smectite, vermiculite, and/or chlorite, interstratified mineral, mica and/or halloysite,

metahalloysite, kaolinite, quartz and feldspars, respectively. The pattern from Mg-glycerol treatment (Figure 16) indicated that this soil contains expanding clay minerals (smectites), since the characteristic 1.8 nm peak was observed. The pattern for the K-saturated clay at 25^{o}C (Figure 17) again showed a shift from 1.4 nm to 1.0 nm, whose peak intensity decreased when heated at 100 ^{o}C. Those treatments confirmed the presence of vermiculite as part of the interstratified mineral. The disappearance of the 0.7 nm peak at 550 ^{o}C (Figure 20) confirmed that those reflections are due to kaolinite and metahalloysite.

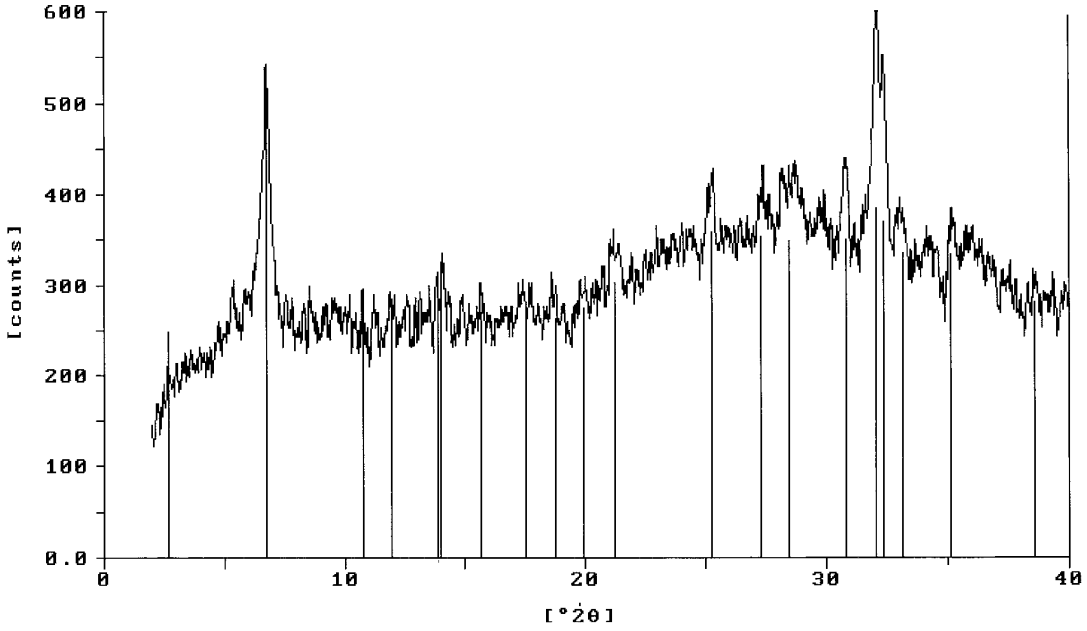

Figure 9: X-ray Diffraction Pattern of Mg-Saturated Clay Fraction (<2µm) Specimen from the Melanudand (20-40 cm) after Soil Mineral Dispersion.

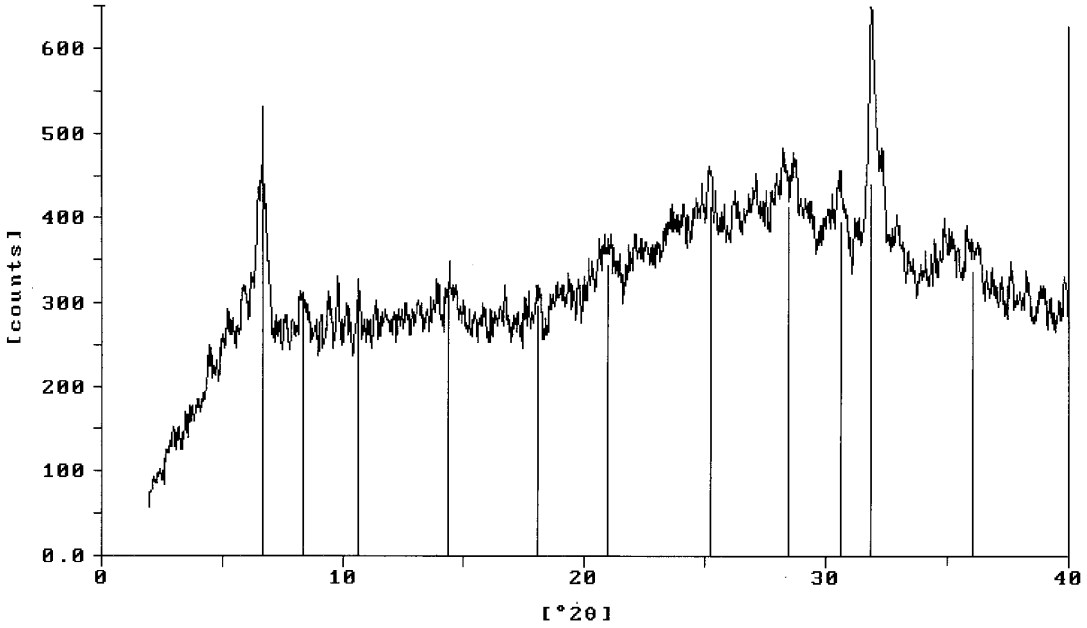

Figure 10: X-ray Diffraction Pattern of Mg-Saturated, Glycerol Solvated Clay Fraction (<2μm) Specimen from the Melanudand (20-40 cm) after Soil Mineral Dispersion.

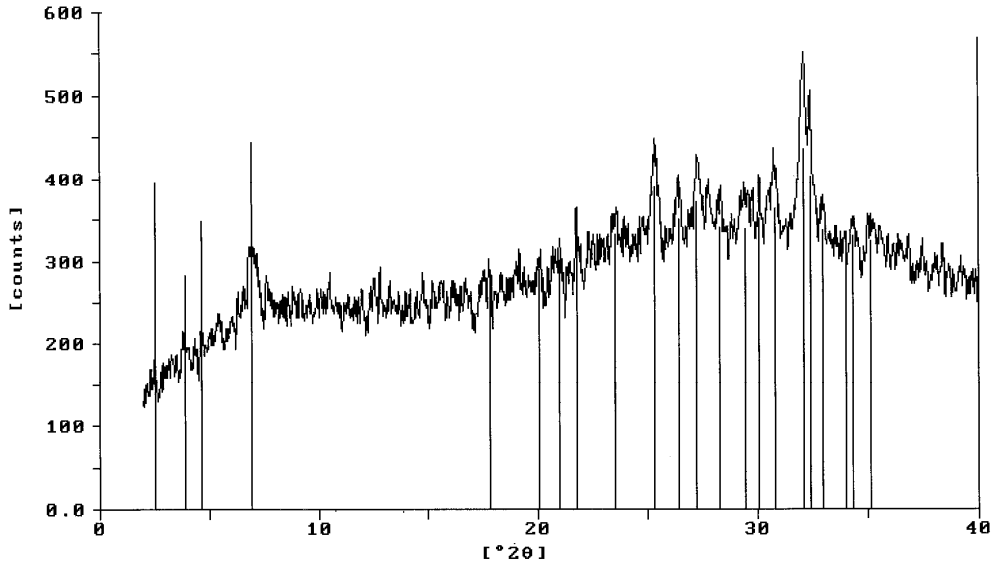

Figure 11: X-ray Diffraction Pattern of K-Saturated Clay Fraction (<2μm) Specimen from the Melanudand (20-40 cm) after Soil Mineral Dispersion.

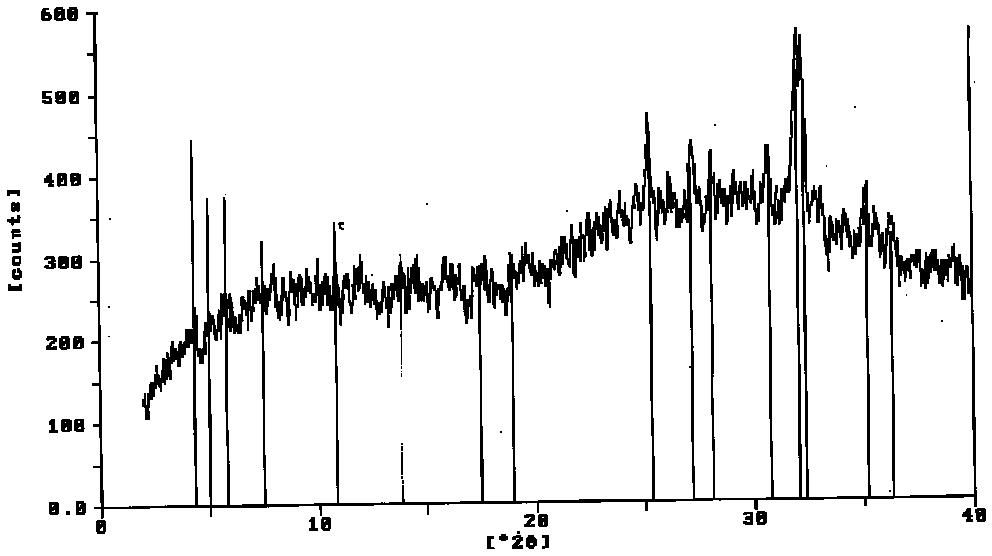

Figure 12: X-ray Diffraction Pattern of K-Saturated Clay Fraction (<2µm) Specimen Heated at 100 ^{o}C from the Melanudand (20-40 cm) after Soil Mineral Dispersion.

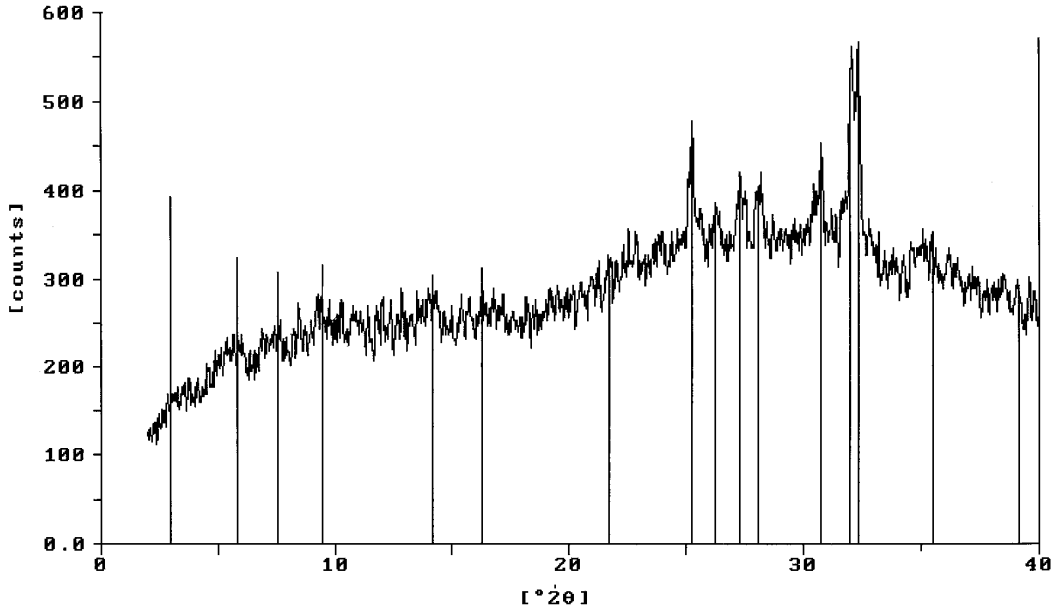

Figure 13: X-ray Diffraction Pattern of K-Saturated Clay Fraction (<2µm) Specimen Heated at 300 ^{o}C from the Melanudand (20-40 cm) after Soil Mineral Dispersion.

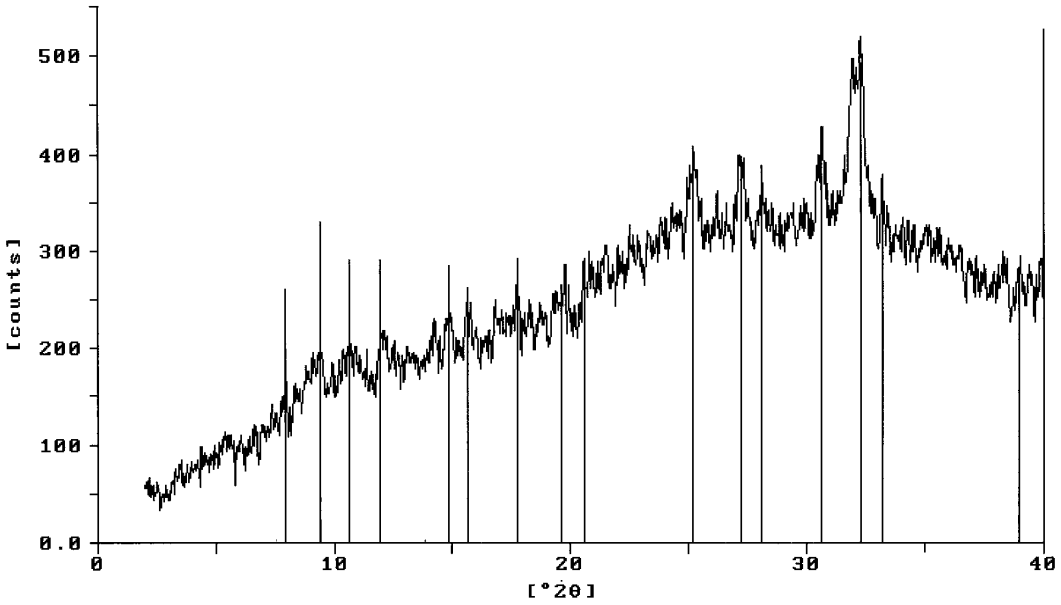

Figure 14: X-ray Diffraction Pattern of K-Saturated Clay Fraction (<2μm) Specimen Heated at 550 ^{o}C from the Melanudand (20-40 cm) after Soil Mineral Dispersion.

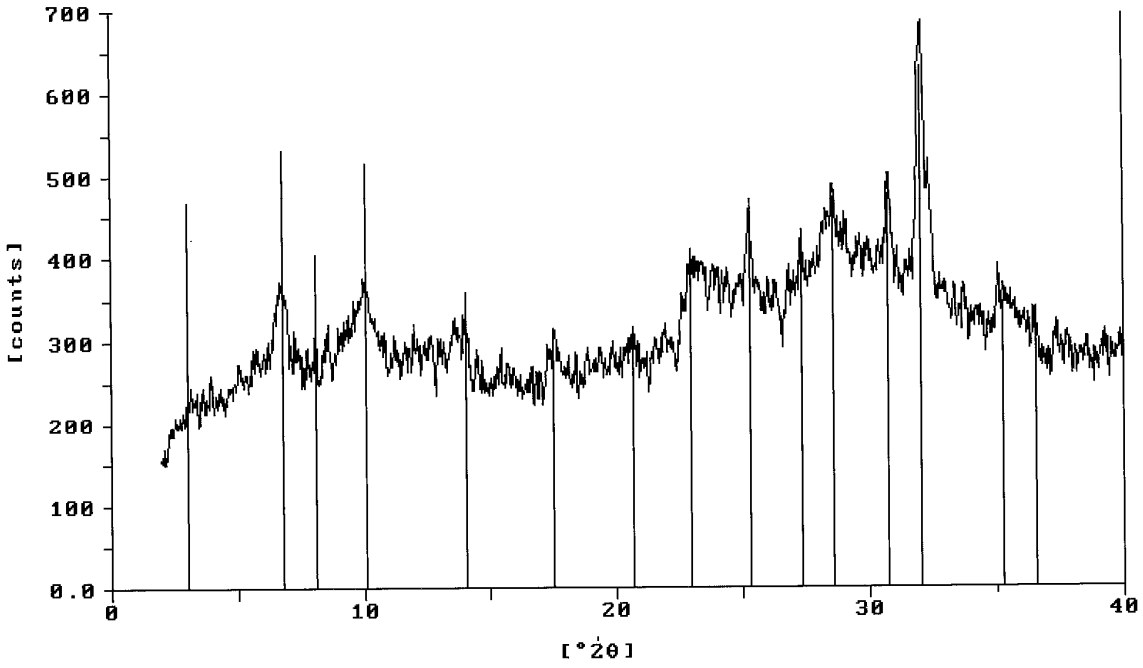

Figure 15: X-ray Diffraction Pattern of Mg-Saturated Clay Fraction (<2μm) Specimen from the Haplustand (10-30 cm) after Soil Mineral Dispersion.

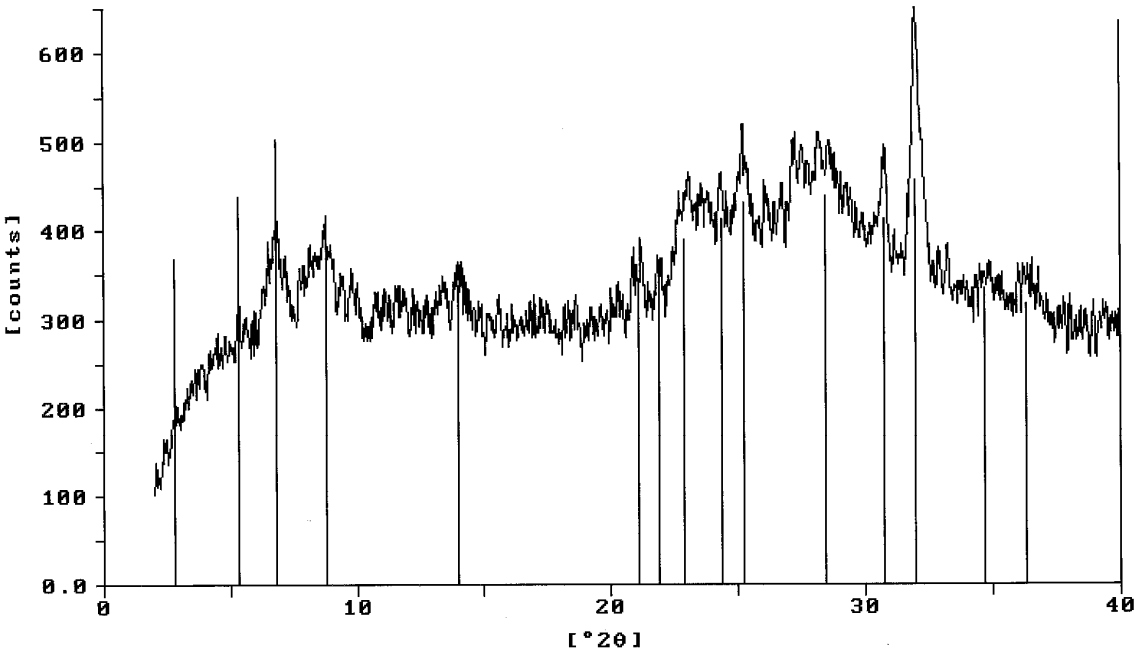

Figure 16: X-ray Diffraction Pattern of Mg-Saturated, Glycerol Solvated Clay Fraction (<2µm) Specimen from the Haplustand (10-30 cm) after Soil Mineral Dispersion.

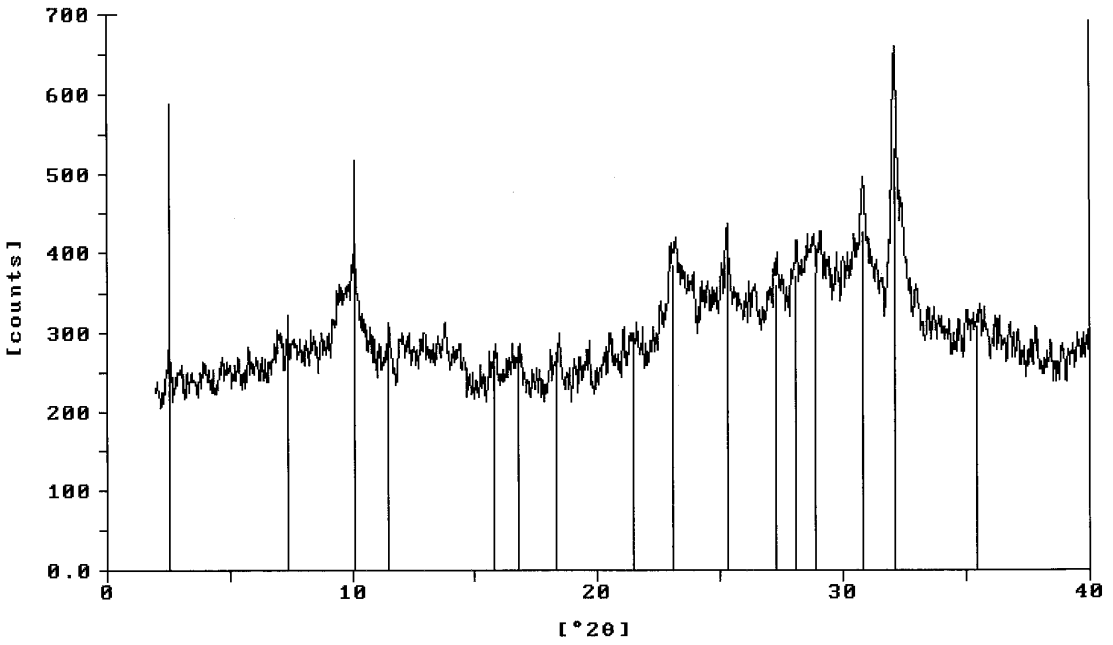

Figure 17: X-ray Diffraction Pattern of K-Saturated Clay Fraction (<2µm) Specimen from the Haplustand (10-30 cm) after Soil Mineral Dispersion.

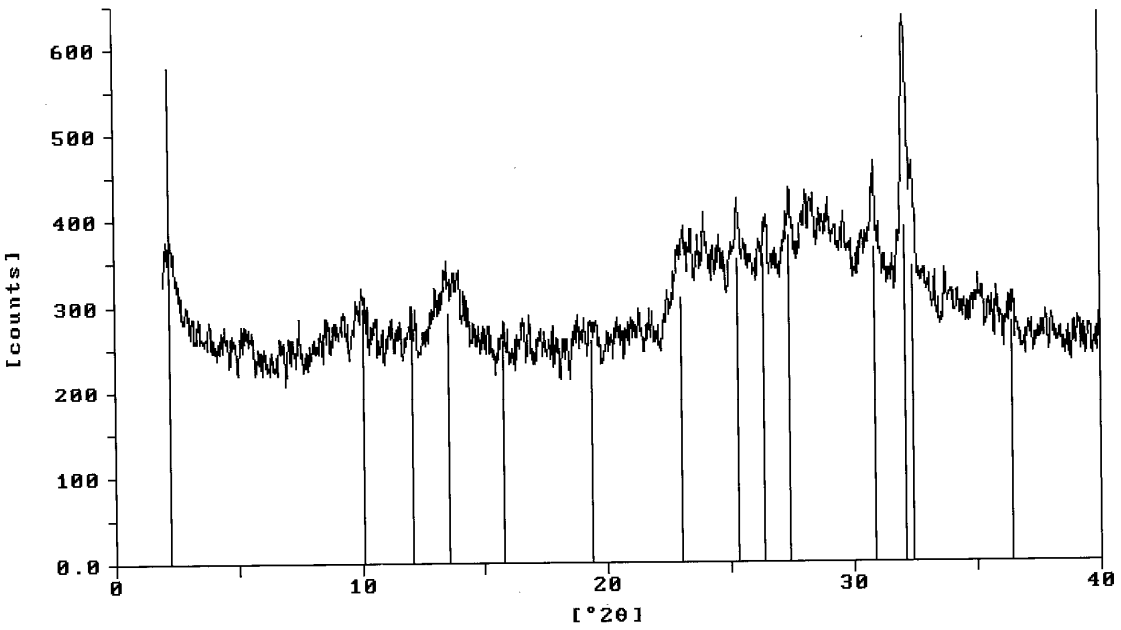

Figure 18: X-ray Diffraction Pattern of K-Saturated Clay Fraction (<2µm) Specimen Heated at 100 °C from the Haplustand (10-30 cm) after Soil Mineral Dispersion.

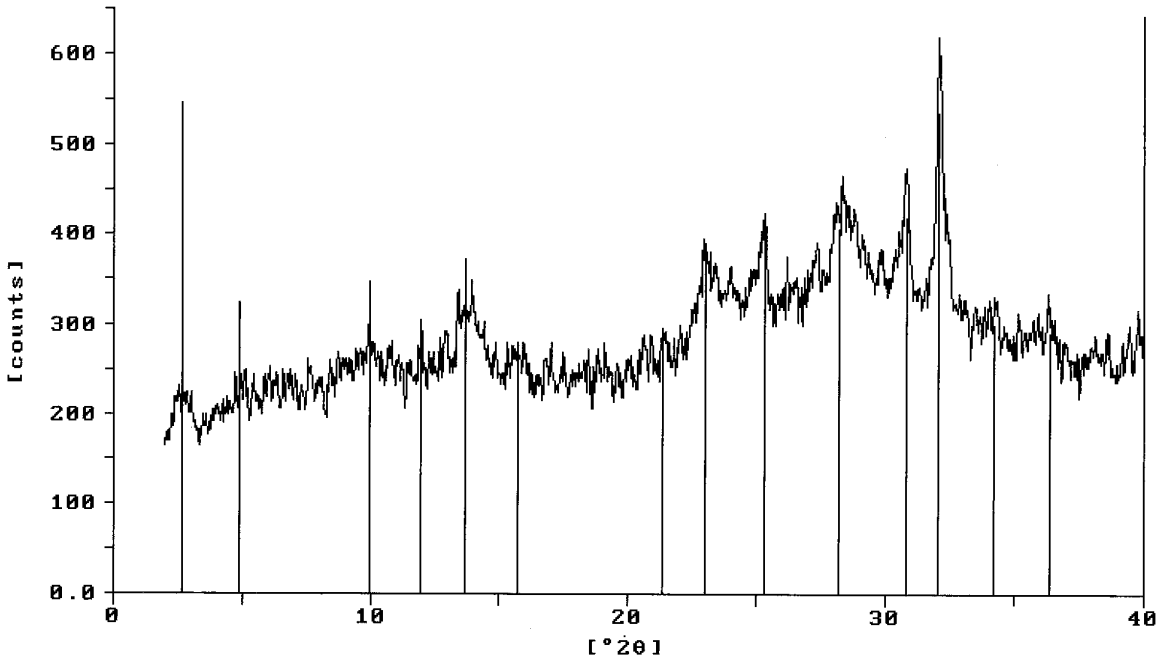

Figure 19: X-ray Diffraction Pattern of K-Saturated Clay Fraction (<2µm) Specimen Heated at 300 °C from the Haplustand (10-30 cm) after Soil Mineral Dispersion.

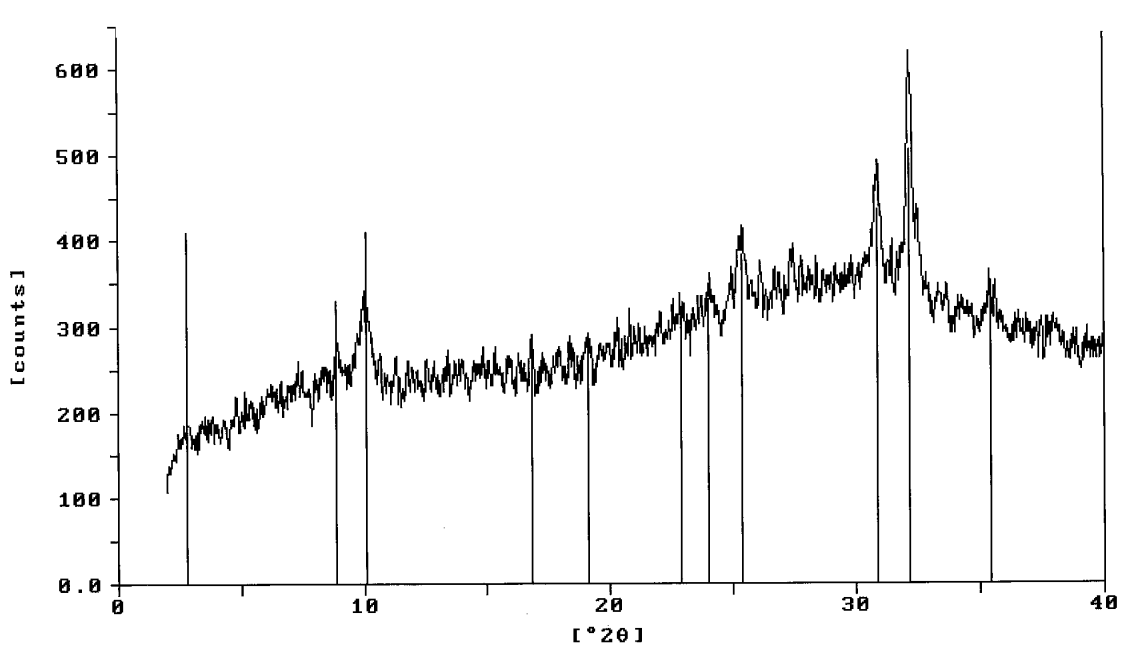

Figure 20: X-ray Diffraction Pattern of K-Saturated Clay Fraction (<2μm) Specimen Heated at 550 ^{o}C from the Haplustand (10-30 cm) after Soil Mineral Dispersion.

The XRD patterns for the clay fractions of both Andisols, after amorphous mineral removal, completely lost their definition (Figures 21 to 31). Those results would indicate that the hot 0.5 M NaOH treatment dissolved not only the poorly crystalline aluminosilicate components, but also some of the crystalline minerals present in those soils.

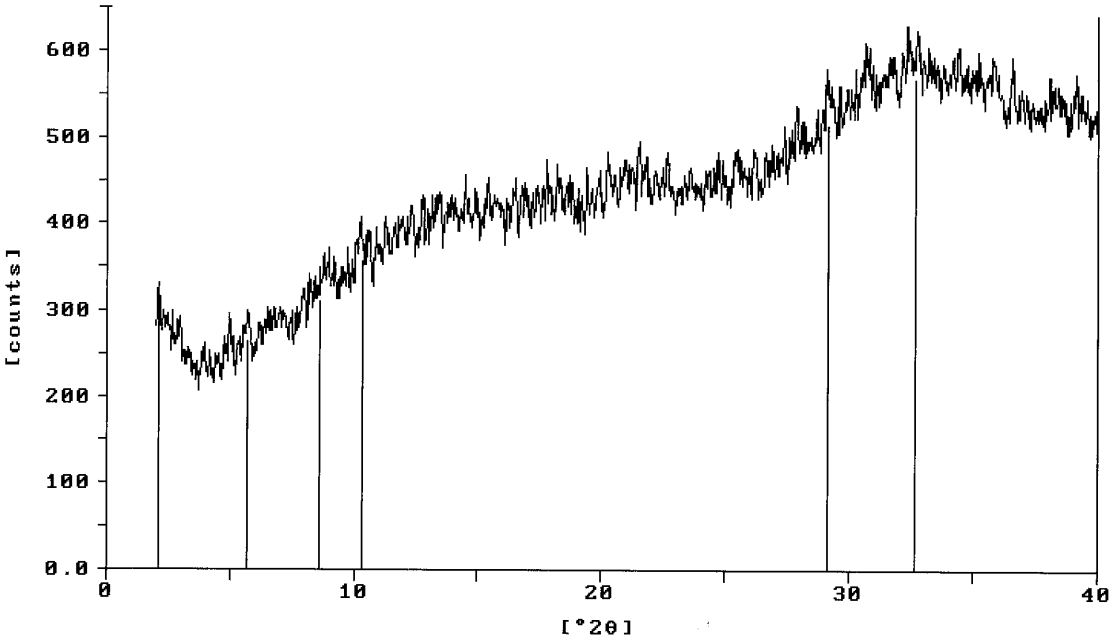

Figure 21: X-ray Diffraction Pattern of Mg-Saturated Clay Fraction (<2µm) Specimen from the Melanudand (20-40 cm) after Amorphous Material Dissolution.

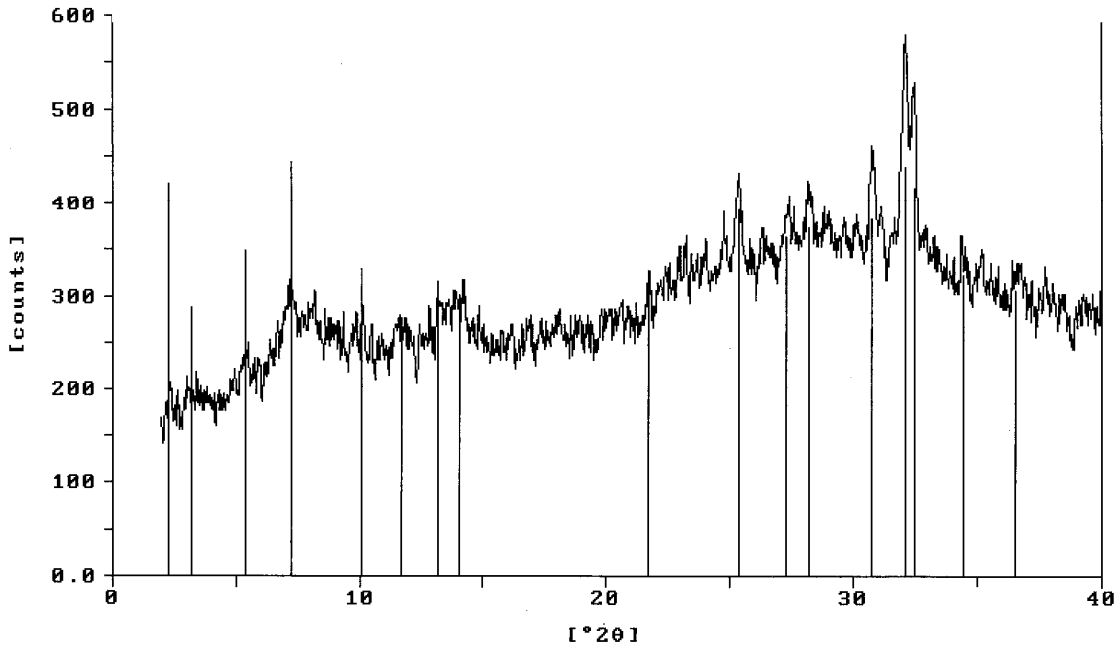

Figure 22: X-ray Diffraction Pattern of K-Saturated Clay Fraction (<2µm) Specimen from the Melanudand (20-40 cm) after Amorphous Material Dissolution.

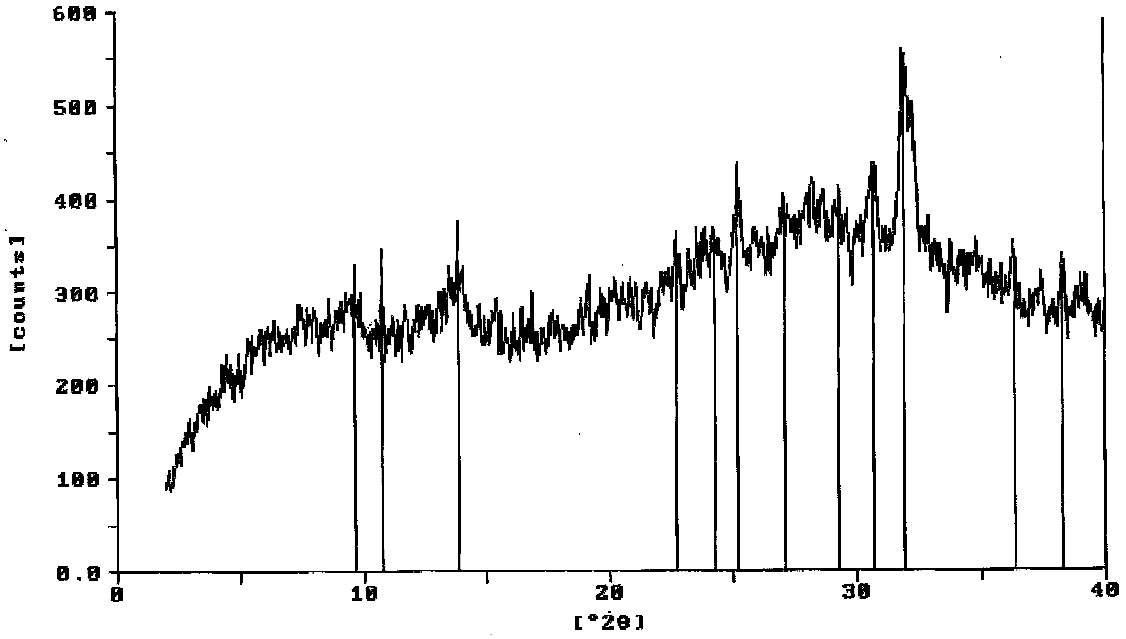

Figure 23: X-ray Diffraction Pattern of K-Saturated Clay Fraction (<2µm) Specimen Heated at 100 °C from the Melanudand (20-40 cm) after Amorphous Material Dissolution.

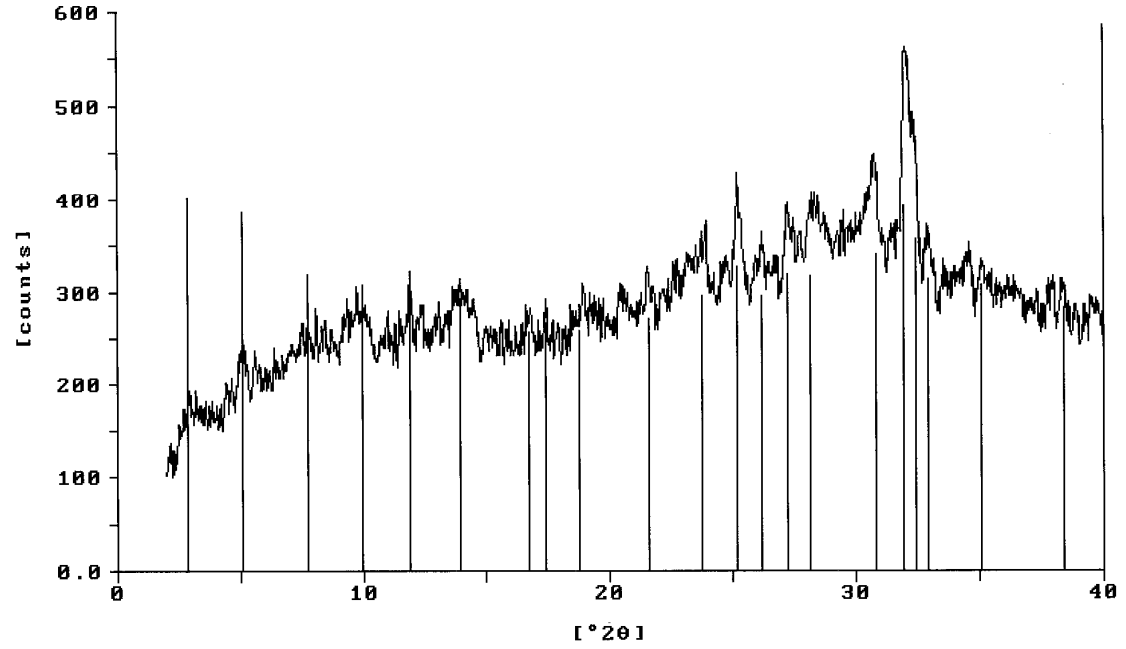

Figure 24: X-ray Diffraction Pattern of K-Saturated Clay Fraction (<2µm) Specimen Heated at 300 °C from the Melanudand (20-40 cm) after Amorphous Material Dissolution.

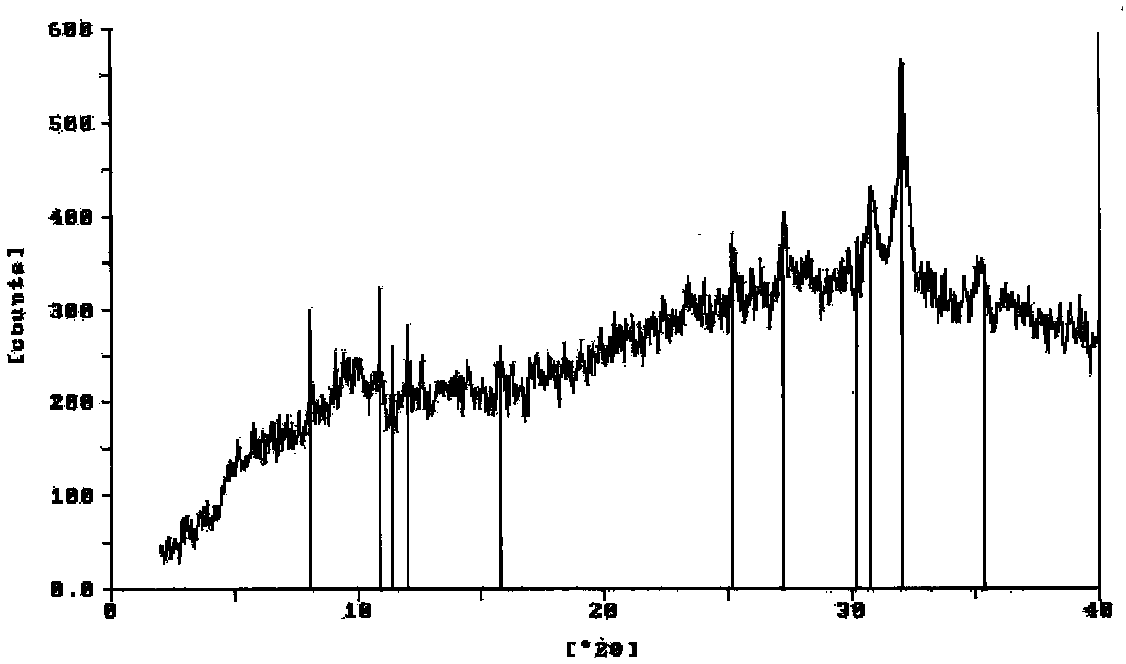

Figure 25: X-ray Diffraction Pattern of K-Saturated Clay Fraction (<2µm) Specimen Heated at 550 ^{o}C from the Melanudand (20-40 cm) after Amorphous Material Dissolution.

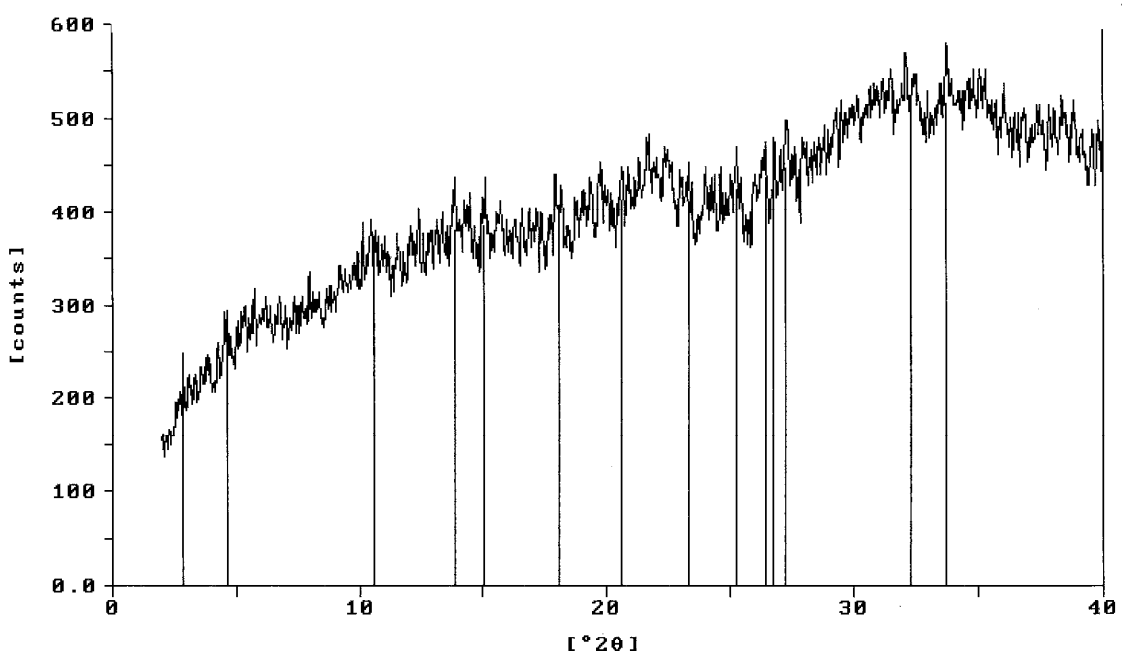

Figure 26: X-ray Diffraction Pattern of Mg-Saturated Clay Fraction (<2µm) Specimen from the Haplustand (10-30 cm) after Amorphous Material Dissolution.

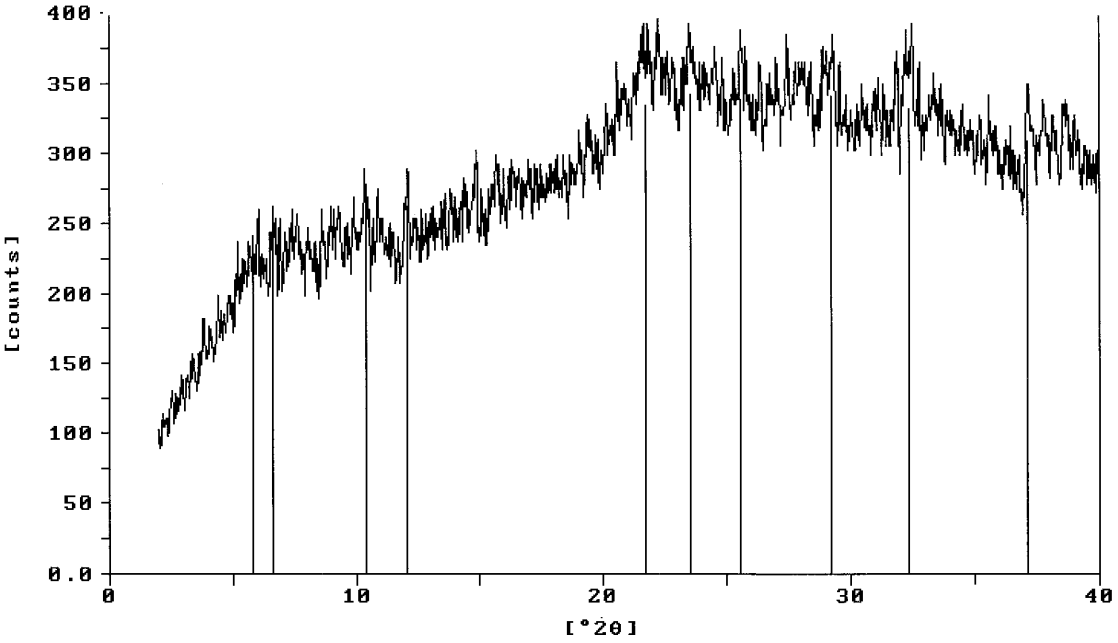

Figure 27: X-ray Diffraction Pattern of Mg-Saturated, Glycerol Solvated Clay Fraction (<2μm) Specimen from the Haplustand (10-30 cm) after Amorphous Material Dissolution.

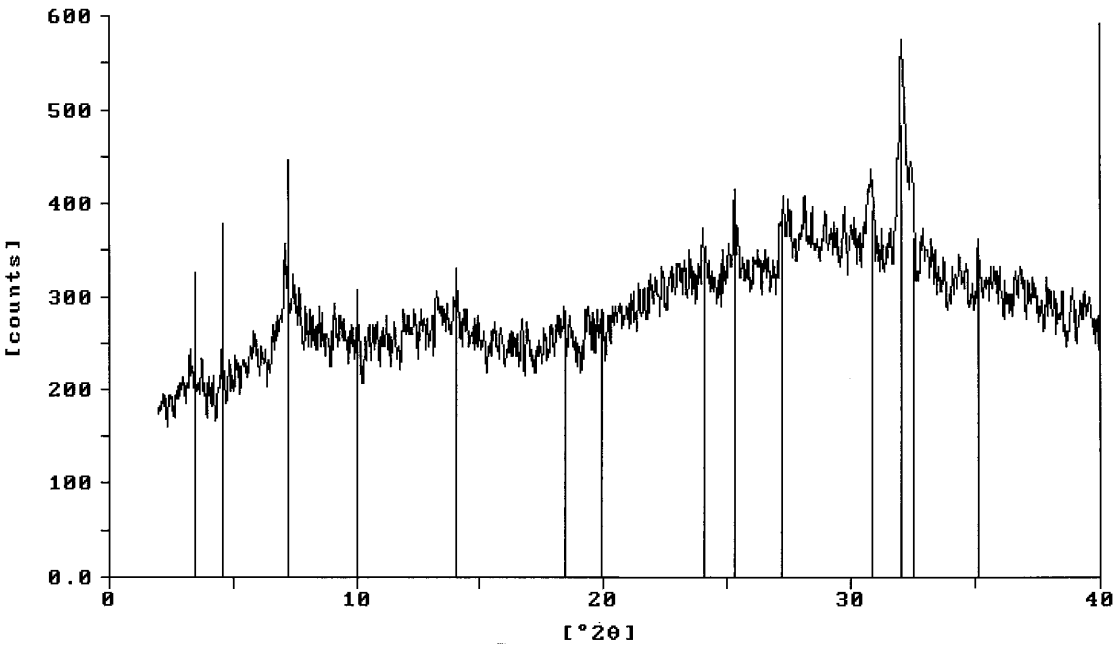

Figure 28: X-ray Diffraction Pattern of K-Saturated Clay Fraction (<2μm) Specimen from the Haplustand (10-30 cm) after Amorphous Material Dissolution.

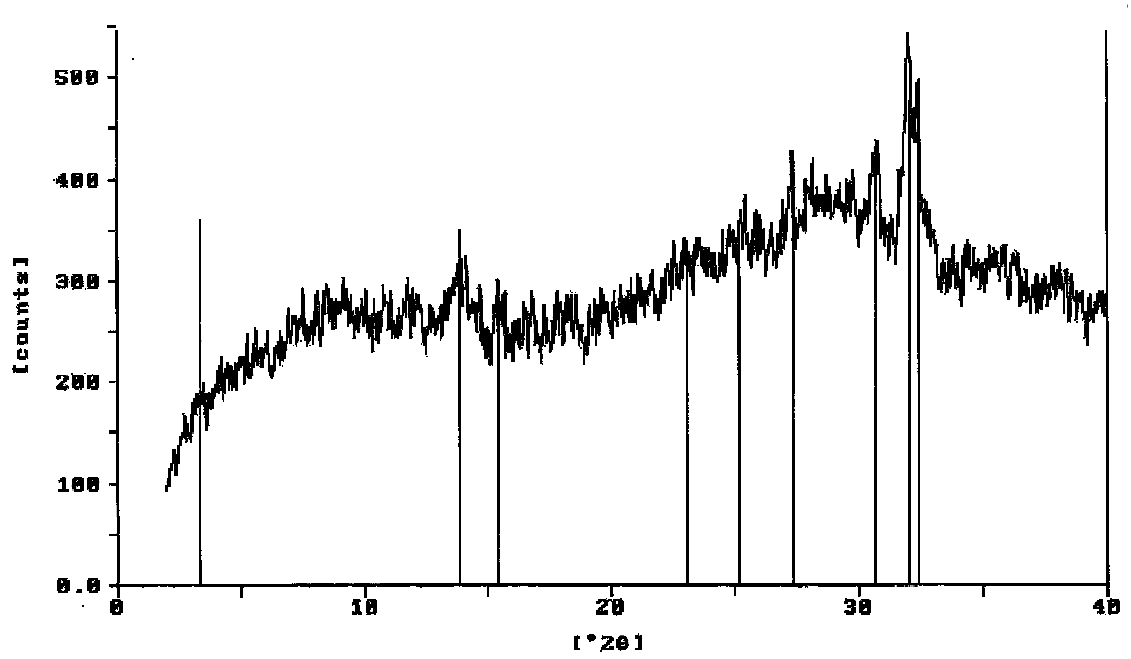

Figure 29: X-ray Diffraction Pattern of K-Saturated Clay Fraction (<2µm) Specimen Heated at 100 ^{o}C from the Haplustand (10-30 cm) after Amorphous Material Dissolution.

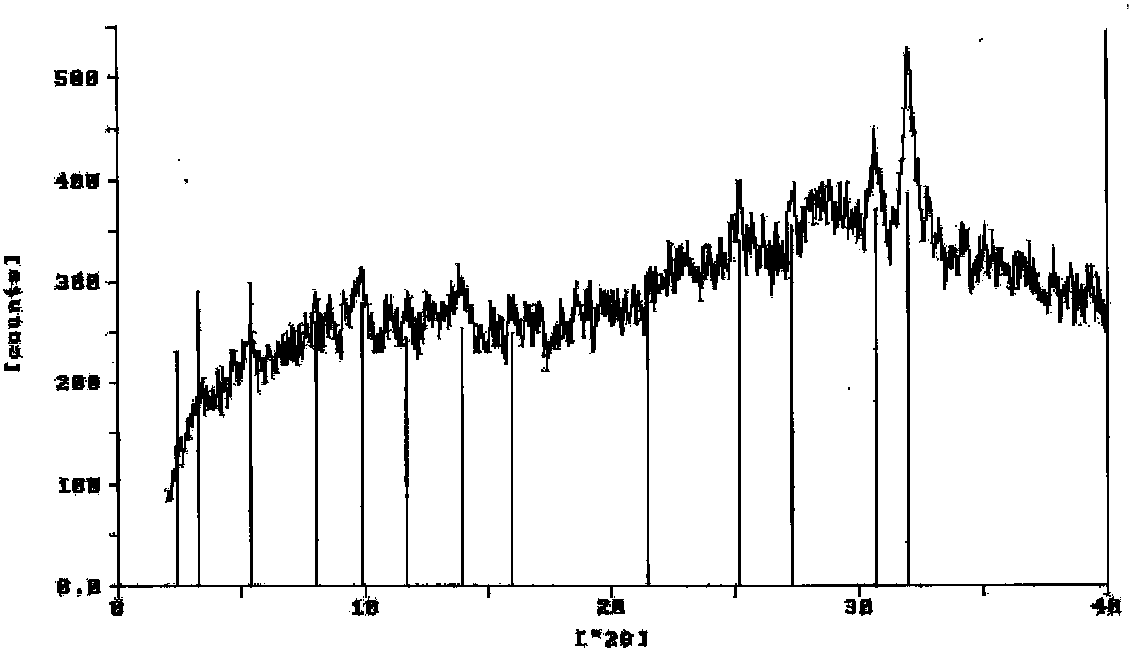

Figure 30: X-ray Diffraction Pattern of K-Saturated Clay Fraction (<2µm) Specimen Heated at 300 ^{o}C from the Haplustand (10-30 cm) after Amorphous Material Dissolution.

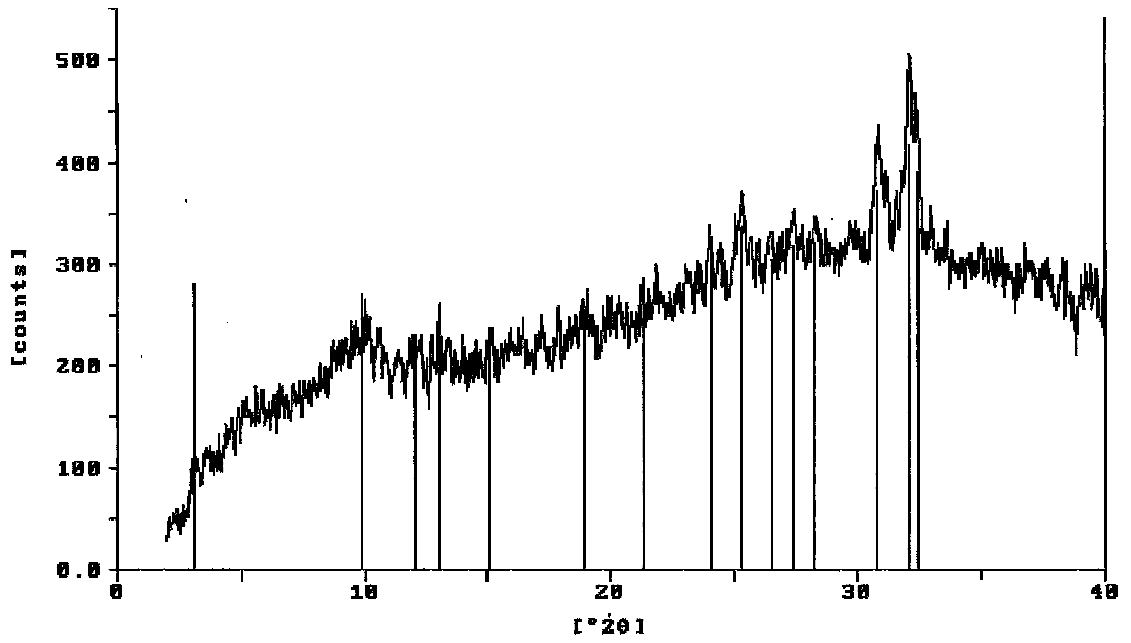

Figure 31: X-ray Diffraction Pattern of K-Saturated Clay Fraction (<2µm) Specimen Heated at 550 ^{o}C from the Haplustand (10-30 cm) after Amorphous Material Dissolution.

Thermogravimetric patterns for both Andisols before mineral dispersion i.e., organic matter oxidation and free-Fe removal, (Figures 32 and 33) presented much more definition as compared to their XRD patterns. The TG pattern for the Melanudand (Figure 32) showed three weight losses, two of them clearly defined (at 100 and 300 ^{o}C, respectively) and the other one between 400 and 600 ^{o}C. In a similar way, the TG pattern for the Haplustand (Figure 33) showed three weight losses. However, the clearly defined peaks were at 100 and 500 ^{o}C, while the third one was between 200 and 400 ^{o}C. All of the weight losses during thermal analysis could be attributed to dehydration of organic matter, amorphous materials, some oxides/hydroxides, or even 1:1 and 2:1 layer silicates. Nevertheless, the feature at 300 ^{o}C was lost after soil mineral dispersion in both soils (Figures 34 and 35), which clearly suggest that weight loss should be attributed to dehydration of free Fe-oxides.

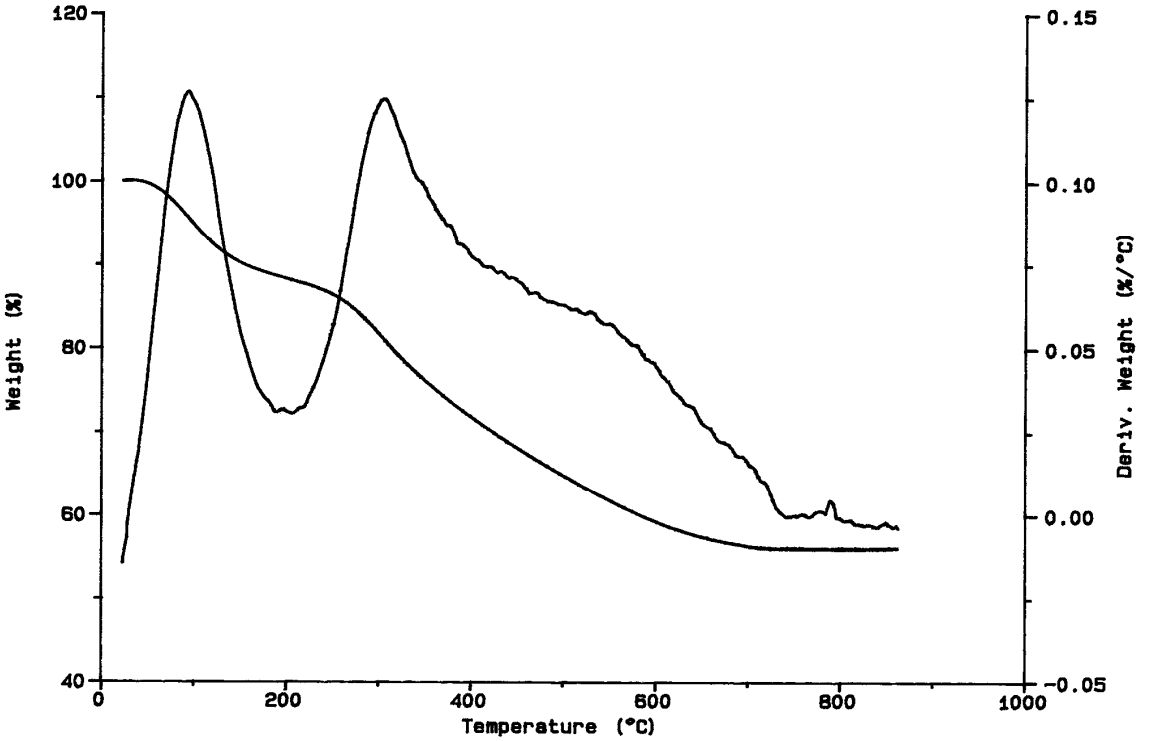

Figure 32: TGA Pattern of Mg-Saturated Clay Fraction (<2µm) Specimen from the Melanudand (20-40 cm) before Soil Mineral Dispersion.

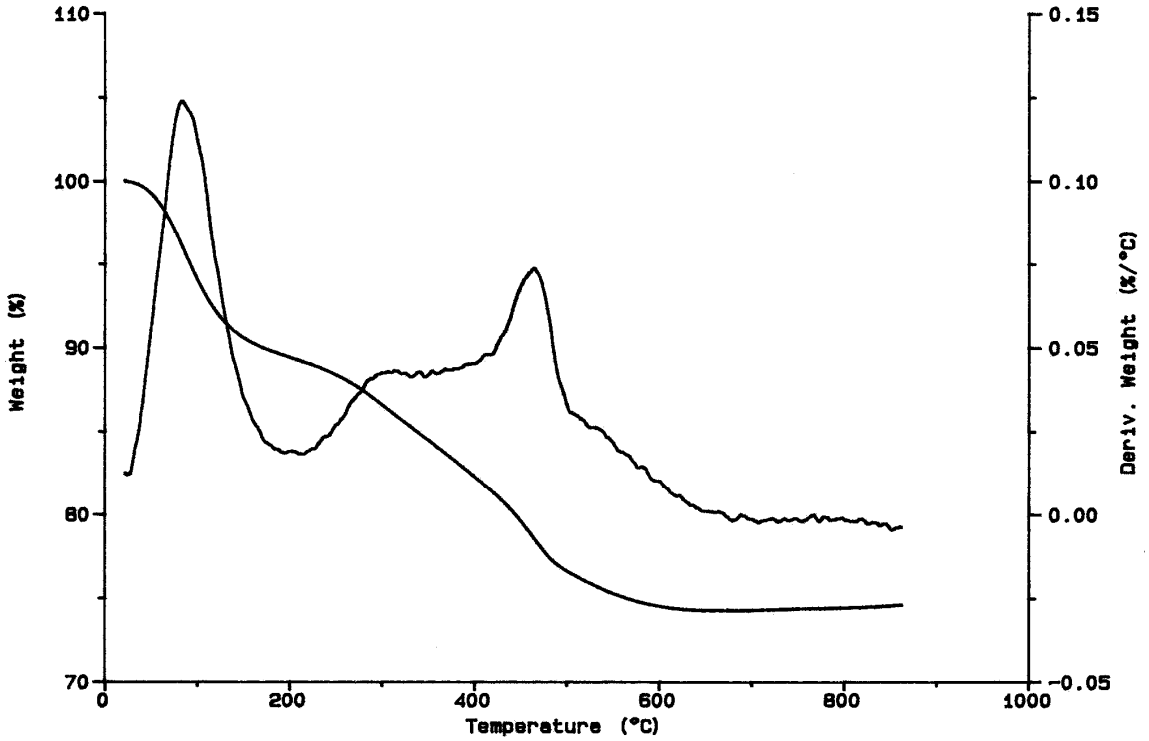

Figure 33: TGA Pattern of Mg-Saturated Clay Fraction (<2µm) Specimen from the Haplustand (10-30 cm) before Soil Mineral Dispersion.

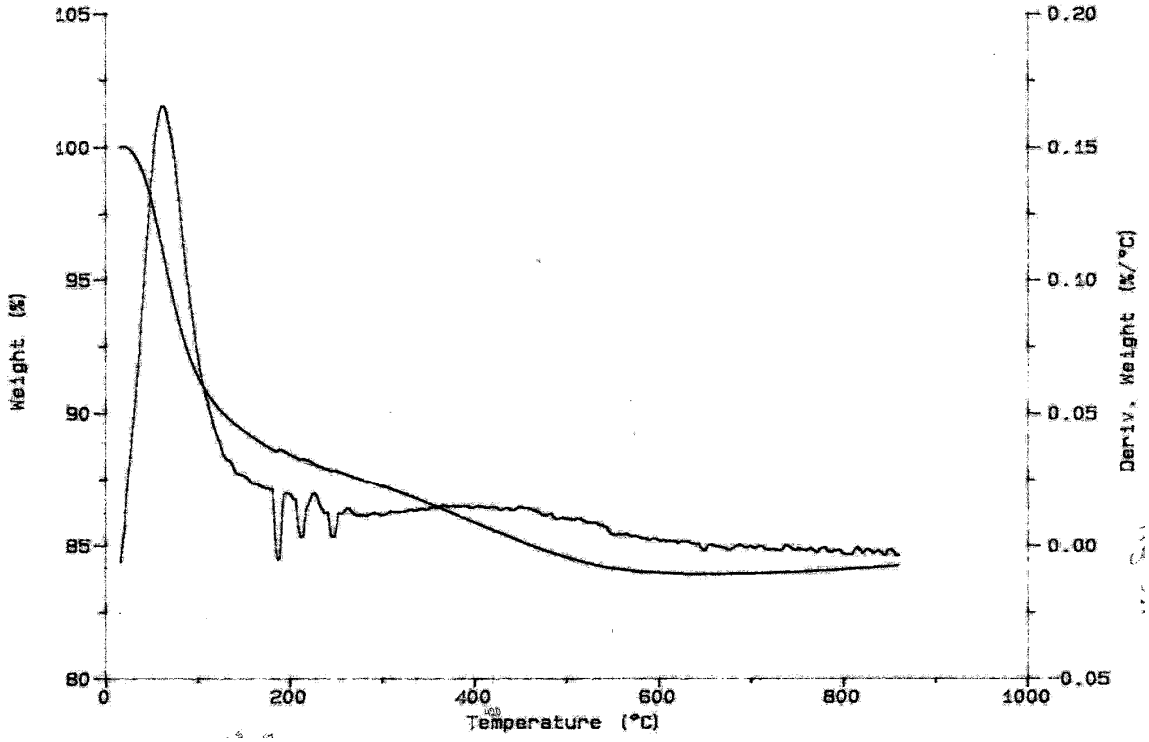

Figure 34: TGA Pattern of Mg-Saturated Clay Fraction (<2µm) Specimen from the Melanudand (20-40 cm) after Soil Mineral Dispersion.

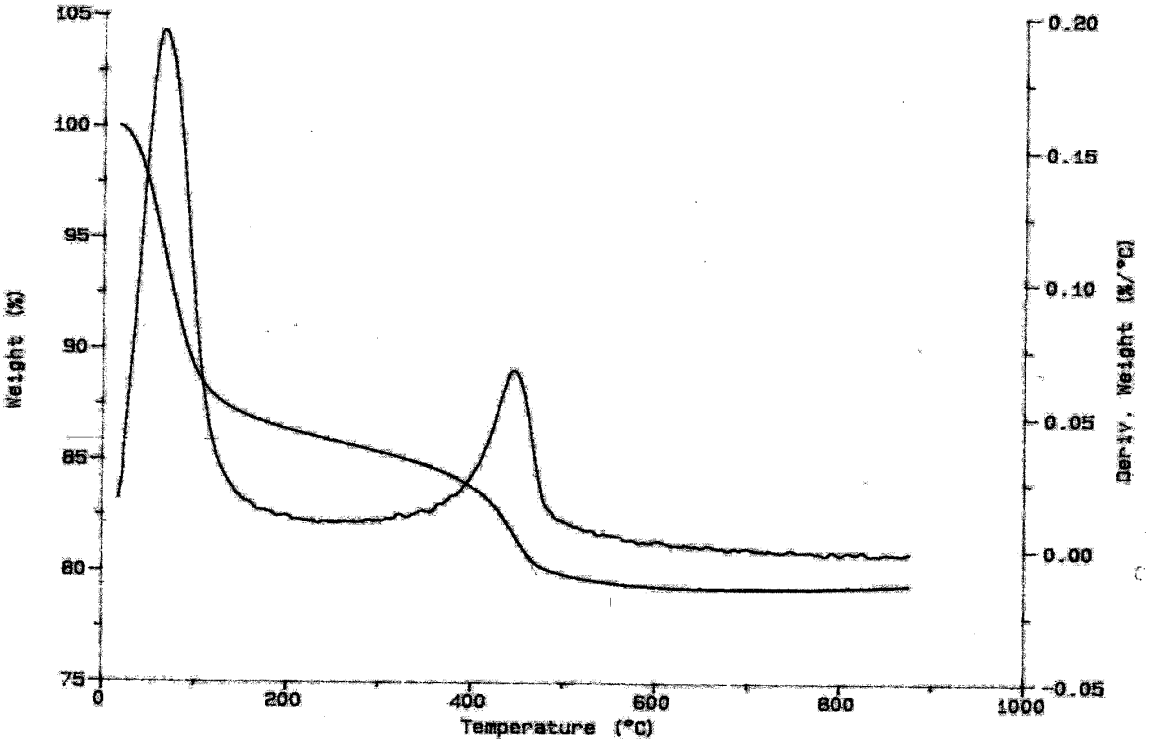

Figure 35: TGA Pattern of Mg-Saturated Clay Fraction (<2µm) Specimen from the Haplustand (10-30 cm) after Soil Mineral Dispersion.

After the combination of both pretreatments, soil mineral dispersion and amorphous mineral dissolution, the TG patterns for both the Melanudand and the Haplustand (Figures 34 to 37) consistently indicated two weight losses. The first one was at 100 ^{o}C, which could be attributable to dehydration of 2:1 layer silicates (Karathanasis and Hajek, 1982). The other one was between 400 and 600 ^{o}C, and could be associated with dehydration of 1:1 layer silicates such as kaolinite or halloysite (Jackson, 1975). Nonetheless, the presence of 'hydroxide' water in the amorphous minerals associated with those soils and the lack of standards to compare with did not allow use of these TG patterns for quantification purposes.

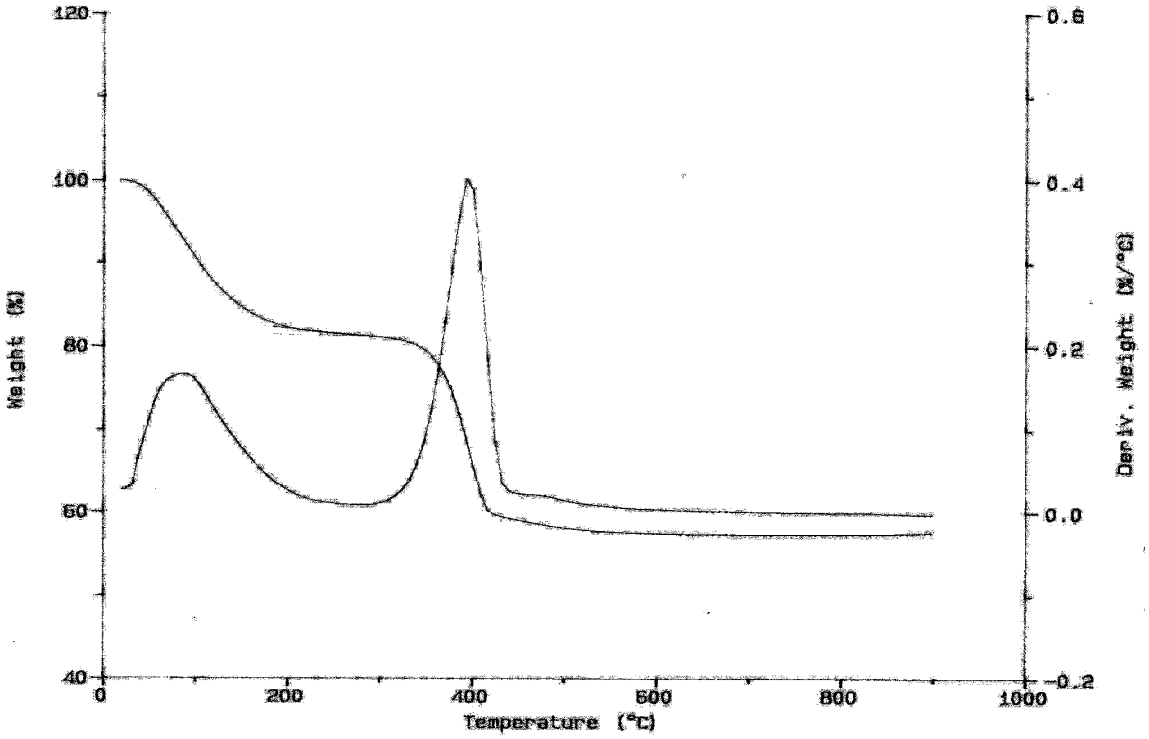

Figure 36: TGA Pattern of Mg-Saturated Clay Fraction (<2µm) Specimen from the Melanudand (20-40 cm) after Amorphous Material Dissolution.

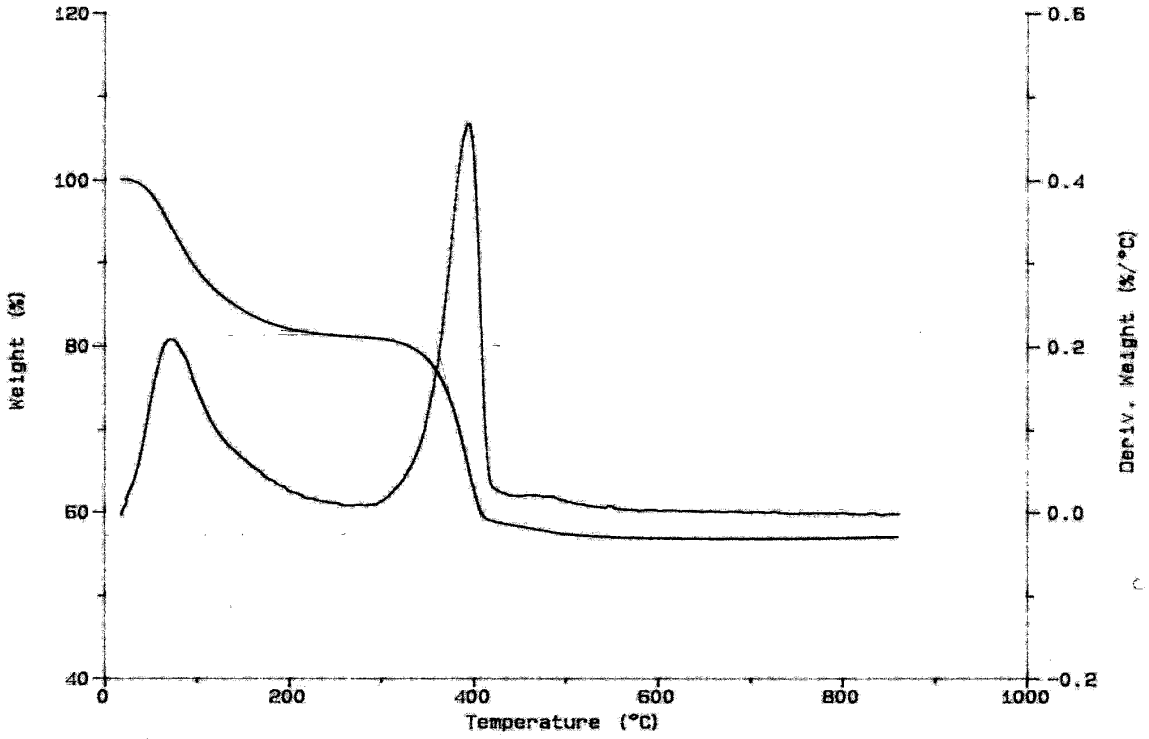

Figure 37: TGA Pattern of Mg-Saturated Clay Fraction (<2µm) Specimen from the Haplustand (10-30 cm) after Amorphous Material Dissolution.

The mineralogical compositions for both subsurface Andisols, reported in Table 4, are values obtained after the XRD analysis, Fe determination in the free-Fe oxides fraction, and Si and Al quantification in the poorly crystalline aluminosilicate fraction.

Texture Analysis

Particle size distribution analysis indicated a loam textural class for both the Haplustand and the Melanudand. Detailed particle-size distributions for each soil are presented in Table 5. These results were expected since the Ecuadorian Andisols have been previously characterized as medium in textural class, i.e., loam, fine loamy sand, or sandy loam (Mejia, 1997). There was no difference in particle size distribution between surface and subsurface for both Andisols. This contrasts somewhat with the results of

Zehetner (2003), who found differences in particle size distribution through the profile of some Andisols of northern Ecuador.

Table 5: Particle-Size Distribution of the Haplustand and Melanudand Soil Samples

Soil	Soil treatment	Sand	Silt	Clay	Textural Class
		g/kg			
Melanudand (0-20 cm)	0 ton lime/ha	361	454	185	Loam
	3 ton lime/ha	361	454	185	Loam
	6 ton lime/ha	354	467	179	Loam
	12 ton lime/ha	361	460	179	Loam
	18 ton lime/ha	368	460	172	Loam
Melanudand (20-40 cm)	0 ton lime/ha	368	460	172	Loam
	3 ton lime/ha	361	454	185	Loam
	6 ton lime/ha	361	467	172	Loam
	12 ton lime/ha	361	460	179	Loam
	18 ton lime/ha	369	460	171	Loam
Haplustand (0-10 cm)	Control	333	425	242	Loam
	N	338	425	237	Loam
	NPK	338	430	232	Loam
	NPKSMg	353	430	217	Loam
	NPKSMgCa	355	415	230	Loam
Haplustand (10-30 cm)	Control	328	420	252	Loam
	N	328	430	242	Loam
	NPK	338	430	232	Loam
	NPKSMg	358	425	217	Loam
	NPKSMgCa	340	425	235	Loam

Preliminary Soil Fertility Evaluation of the Ecuadorian Andisols

Organic Carbon Content

Both the Haplustand and the Melanudand possessed dark color (10 YR 4/2, 2.5 YR 2.5/1 respectively), which would be associated with the presence of higher amounts of organic carbon. However, Smith (1984) has pointed out that the darkness of some Hawaiian surface soils and subsoils showing moist values of 3 or less seems to be related partly with iron rather than carbon.

There was no major difference in the content of organic matter in the Haplustand with depth, i.e., the surface soil averaged 4.1 percent soil organic matter (Table 6), only moderately higher than the 3.4 percent of the subsurface soil (Table 7). These values were lower than those observed for the Melanudand, and could be explained by the lower annual supply of plant residues associated with the oil palm management practices, and the isohyperthermic (24.3 ^{o}C) temperature regime. The Melanudand averaged 10.3 and 8.7 percent in the surface and subsurface soil respectively (Tables 8 and 9). Differences in climate are the likely major factor in the soil organic matter differences between the two soils, due to the fact that the coastal plain environment favors a greater rate of organic matter decomposition. Additionally, some geographical variation in the amount of volcanic ash deposition, and consequent differences in the degree of interaction between organic matter and poorly crystalline aluminosilicates, could explain some differences in soil organic matter content between these Andisols.

As was expected, total nitrogen content was directly related to the soil organic matter content. The Haplustand surface soil was slightly higher in total nitrogen content

as compared to the subsurface soil. In contrast, the Melanudand exhibited no particular difference in total nitrogen content between surface and subsurface soil samples.

Table 6: Some Chemical Properties of the Haplustand (0-10 cm depth)

Soil Treatment	pH (H_2O)	pH (NaF)	Al+H ($cmol_c/kg$)	Total Nitrogen (g/kg)	Organic Matter (g/kg)	S (ppm)
Control	6.5 a*	9.3 a	-	3.2 a	37.2 a	2.6 b
N	4.4 c	9.3 a	1.7	3.0 a	39.7 a	7.6 b
NPK	4.5 c	9.2 a	1.4	3.0 a	41.6 a	3.9 b
NPKSMg	4.6 c	9.3 a	1.6	3.2 a	44.8 a	28.7 a
NPKSMgCa	5.8 b	9.4 a	0.2	2.8 a	40.1 a	32.9 a

Table 7: Some Chemical Properties of the Haplustand (10-30 cm depth)

Soil Treatment	pH (H_2O)	pH (NaF)	Al+H ($cmol_c/kg$)	Total Nitrogen (g/kg)	Organic Matter (g/kg)	S (ppm)
Control	6.5 a*	9.3 a	-	2.7 a	29.8 a	3.5 c
N	5.6 c	9.3 a	-	2.7 a	39.2 a	3.9 c
NPK	5.5 c	9.4 a	0.3	2.1 a	29.2 a	3.2 bc
NPKSMg	5.5 c	9.5 a	0.5	2.8 a	35.6 a	27.2 ab
NPKSMgCa	5.8 b	9.4 a	-	2.3 a	35.3 a	34.0 a

Table 8: Some Chemical Properties of the Melanudand (0-20 cm depth)

Soil Treatment	pH (H_2O)	pH (NaF)	Al+H ($cmol_c/kg$)	Total Nitrogen (g/kg)	Organic Matter (g/kg)	S (ppm)
0 ton lime/ha	5.5 d*	9.8 a	2.05 a	4.3 a	104.7 a	18.73ab
3 ton lime/ha	5.6 d	10.1 a	1.33 b	4.5 a	111.8 a	25.10a
6 ton lime/ha	5.8 c	10.2 a	0.65 c	5.1 a	103.0 a	19.69ab
12 ton lime/ha	6.5 b	10.5 a	0.29 d	4.9 a	102.7 a	18.26b
18 ton lime/ha	6.9 a	10.5 a	0.29 d	4.8 a	92.8 a	13.96b

Table 9: Some Chemical Properties of the Melanudand (20-40 cm depth)

Soil Treatment	pH (H_2O)	pH (NaF)	Al+H ($cmol_c/kg$)	Total Nitrogen (g/kg)	Organic Matter (g/kg)	S (ppm)
0 ton lime/ha	5.4 c*	10.0	1.80 a	5.3 a	89.5 ab	29.07a
3 ton lime/ha	5.5 c	10.1	1.51 ab	5.5 a	84.5 ab	25.89a
6 ton lime/ha	5.8 bc	10.2	0.94 bc	3.5 a	87.6 ab	23.03a
12 ton lime/ha	6.0 b	10.4	0.57 cd	4.6 a	95.6 a	24.62a
18 ton lime/ha	6.4 a	10.4	0.32 d	4.2 a	78.7 b	19.53a

* Mean values for a given column, followed by the same letter, are not significantly different at the 95 % level of confidence.

pH

A large hydroxyl (OH^-) release upon reaction with sodium fluoride (NaF) is one of the chemical features associated with Andisols (Wada, 1985). That reaction was evident for the studied soils. The pH values in NaF solution were greater than 9 for both the Haplustand and the Melanudand (Tables 6 through 9). According to Wada (1985), the pH in NaF is higher in soils containing allophane than in those not containing allophane and imogolite. That is supported by Smith (1984) who found Andisols formed in thicker deposits of ash, but lacking allophane in the surface horizon, which did not react to NaF. A boundary pH in NaF of 9.7 was established by Mizota, et al. (1982). The high reactivity of Al and Fe bound with humus is reflected in the high pH in NaF, so high pH values in NaF are also features common to Andisols containing a large amount of humus (Wada, 1985). The Melanudand gave a slightly higher pH value in NaF than that found for the Haplustand. This result would imply that the former soil contains higher amounts of allophane and imogolite as well as humus materials, which is supported by its greater organic carbon content.

Both the Haplustand and the Melanudand gave acidic pH values in H_2O. However, the former soil was less acid than the latter one. That result could be explained by the greater amount of organic matter associated with the Melanudand. According to Tan (1984), most of the acidity in Andisols is the result of the organic fraction since allophane is generally considered weakly acidic in nature. Wada (1980) and Henmi and Wada (1976) point out that in allophone the Al occurring in tetrahedral sheets is coordinating two oxygen atoms, one OH^- and one H_2O molecule .The water molecule is suspected of behaving as a Bronsted acid and, depending on pH, may dissociate its proton, a very weak reaction.

The pH in H_2O response to fertilizer treatment in the Haplustand is shown in Figures 38 and 39 (Tables 6 and 7). There were significant differences among the control, nitrogen fertilizer treatments without Ca, (+N, +NPK, and +NPKSMg), and that with Ca (+NPKSMgCa). The nitrogen fertilizer treatments dramatically decreased soil pH in H_2O, which was slightly increased with the last treatment, due to the $CaCO_3$ addition. The effect of nitrogen fertilization on pH was greater in the surface soil than in the subsurface soil. The exchangeable acidity associated with the Haplustand was lower than that observed for the Melanudand, even at lower pH values, which is related to the higher amount of organic matter present in the Melanudand, and the high reactivity of the Al adsorbed to that humus.

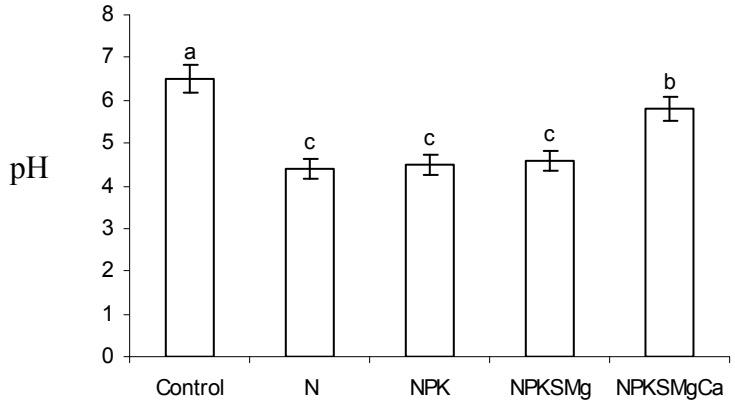

Figure 38: pH Response of the Surface (0-10 cm) Haplustand to Fertilizer Treatment. Mean pH values followed by the same letter are not significantly different at the 95 % level of confidence.

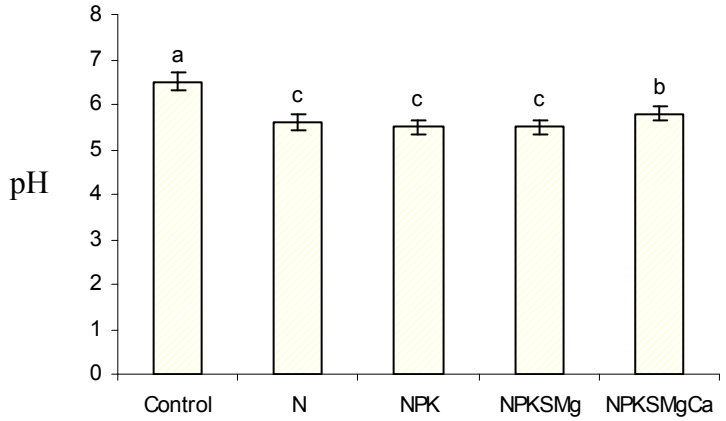

Figure 39: pH Response of the Subsurface (10-30 cm) Haplustand to Fertilizer Treatment. Mean pH values followed by the same letter are not significantly different at the 95 % level of confidence.

The surface and subsurface Melanudand, in the unlimed control, exhibited pH in H_2O values of 5.5 and 5.4, respectively, reflecting its acidic character (Tables 8 and 9). There was a greater increase in pH and a greater decrease in exchangeable acidity in the surface soils, compared to the subsurface soils, with lime application. These results were expected because the liming effect is observed mainly in the surface horizon, where the

lime was applied and incorporated. A significant increase in pH was noticed after application of 6 or more tons of lime/ha (Figures 40 and 41). The highest pH value reached after application of 18 ton lime/ha was not greater than 6.9 in the surface soil. These results clearly illustrate the soils' pH buffer capacity, which is consistent with the fact that variable charge soils are weakly buffered at pHo but highly buffered on either side of pHo. This behavior is because the hydroxyl ions formed by the hydrolysis of the carbonate ion create charge by deprotonation of surface hydroxyls, and consequently do not raise soil solution pH. In short, there is resistance to an increase in soil pH (Uehara and Gillman, 1981). The buffering at a low soil pH has been explained by the release of complexed aluminum via its protonation, or the presence of soil organic matter with its low negative log acid dissociation constant (pKa) for carboxyl groups (Lumbanraja and Evangelou, 1991).

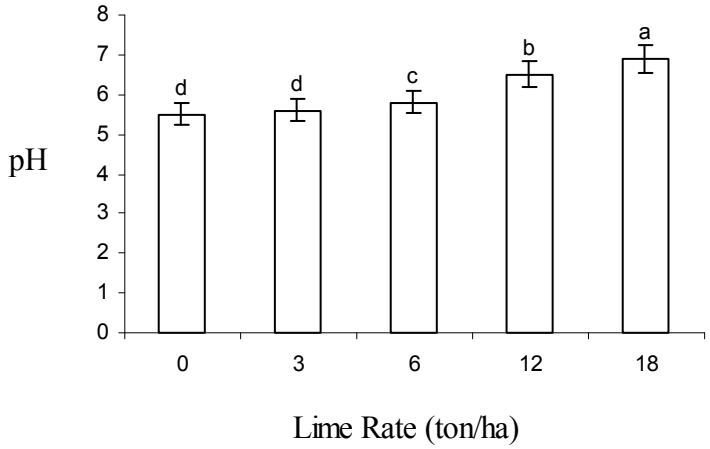

Figure 40: pH Response to Liming of the Surface (0-20 cm) Melanudand. Mean pH values followed by the same letter are not significantly different at the 95 % level of confidence.

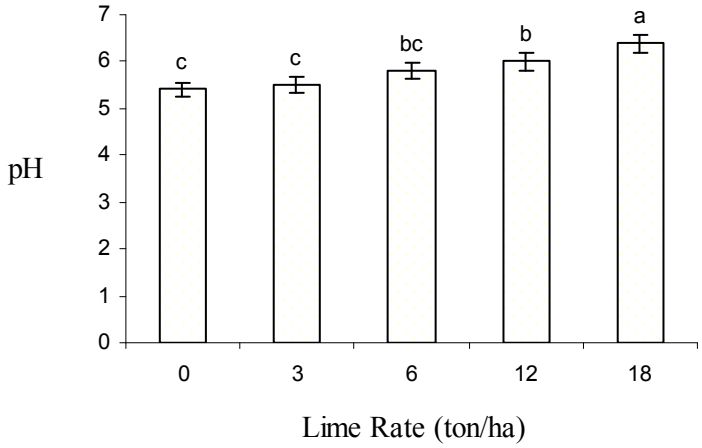

Figure 41: pH Response to Liming of the Subsurface (20-40 cm) Melanudand. Mean pH values followed by the same letter are not significantly different at the 95 % level of confidence.

Macrocations (K, Ca, Mg) and CEC in the Haplustand

The exchangeable nutrient cation status of the Haplustand is shown in Tables 10 to 15. This was evaluated using the extracting solutions most common in the region, i.e. Olsen at pH 8.5, ammonium acetate at pH 7.0, and unbuffered barium chloride. There was a positive response in extractable K to the three fertilizer treatments where K was applied, for every method used on the surface and subsurface Haplustand (Figures 42 and 43). Significant differences in extractable K among the three K fertilizer treatments were detected by each extraction method used on the surface Haplustand. On the other hand, significant differences in exchangeable K among the three K fertilizer treatments were detected just by ammonium acetate and barium chloride extraction of the subsurface soil. These results imply lower sensitivity of the Olsen extraction in assessing exchangeable K, probably due to the higher hydrated radius of Na. Additionally, the amount of exchangeable K was much higher with ammonium acetate extraction than with Olsen or barium chloride extraction. The inability of Ba^{2+} to displace as much K^{+} as NH_4^{+} is

believed to be due to barium's high (negative) heat of hydration relative to that of K^+ (Bohn et al. 1985).

Table 10: Extractable Nutrients in the Haplustand (0-10 cm depth) using the Olsen Solution

Soil treatment	K	Ca	Mg	Zn	Cu	Fe	Mn	P
	($cmol_c$ / kg soil)			(ppm)				
Control	0.20c*	10.95a	1.11b	8.02 a	15.72a	235 cb	1.98 b	36.31 c
N	0.17 c	2.68 b	0.23c	5.15 b	10.70b	340 a	17.06 a	60.62 b
NPK	1.13ab	3.02 b	0.21c	7.06ab	10.70b	326 a	13.62ab	86.60 a
NPKSMg	0.84 b	3.48 b	0.94b	7.19ab	10.47b	255 b	10.22ab	67.02ab
NPKSMgCa	1.33 a	11.01a	1.80a	5.49ab	10.03b	177 c	4.97 b	69.22ab

Table 11: Extractable Nutrients in the Haplustand (10-30 cm depth) using the Olsen Solution

Soil treatment	K	Ca	Mg	Zn	Cu	Fe	Mn	P
	($cmol_c$ / kg soil)			(ppm)				
Control	0.33b*	11.70a	1.20a	8.06 a	15.03 a	237 a	2.41 b	36.12 b
N	0.19b	8.07 b	0.65b	4.66 b	11.51 b	254 a	6.61 a	35.60 b
NPK	1.15a	8.17 b	0.48b	5.73ab	11.86 b	249 a	8.13 a	49.18 ab
NPKSMg	1.02a	8.38 b	1.45a	6.60ab	12.80ab	215 a	7.69 a	37.92 ab
NPKSMgCa	1.28a	10.72a	1.37a	5.83ab	11.93 b	221 a	5.98ab	56.20 a

Table 12: Extractable Cations and CEC of the Haplustand (0-10 cm depth) using 1N Ammonium Acetate Solution

Soil treatment	K	Ca	Mg	Na	∑ Bases	CEC	Base Sat.
	($cmol_c$ / kg soil)						(%)
Control	0.33 c*	10.14 a	1.28 b	0.02 b	11.78 b	31.20 a	37.70 b
N	0.26 c	2.46 b	0.25 c	0.14 a	3.11 d	30.92 a	10.26 d
NPK	1.99 ab	3.11 b	0.37 c	0.11 ab	5.58 cd	30.67 a	18.28 dc
NPKSMg	1.58 b	4.04 b	1.20 b	0.10 ab	6.91 c	29.52 a	23.25 c
NPKSMgCa	2.19 a	11.68 a	1.89 a	0.08 ab	15.84 a	30.66 a	51.71 a

Table 13: Extractable Cations and CEC of the Haplustand (10-30 cm depth) using 1N Ammonium Acetate Solution

Soil treatment	K	Ca	Mg	Na	∑ Bases	CEC	Base Sat.
			($cmol_c$ / kg soil)				(%)
Control	0.50 c*	11.62 a	1.31 b	0.24 a	13.67 a	30.03 a	45.48 a
N	0.31 c	8.30 b	0.70 c	0.17 ab	9.48 b	30.41 a	31.10 b
NPK	2.12 ab	7.67 b	0.48 c	0.11 bc	10.38 b	32.19 a	32.26 b
NPKSMg	1.75 b	7.13 b	1.44 b	0.09 bc	10.41 b	30.66 a	34.01 b
NPKSMgCa	2.43 a	10.70 a	1.76 a	0.07 c	14.96 a	30.16 a	49.65 a

Table 14: Extractable Cations and CEC of the Haplustand (0-10 cm depth) using the Barium Chloride Solution

Soil treatment	K	Ca	Mg	Na	∑ Bases	CEC	Base Sat.
			($cmol_c$ / kg soil)				(%)
Control	0.14 c*	10.16 a	1.01 b	0.14 a	11.45 b	12.82 a	89.43 b
N	0.19 c	2.32 b	0.22 c	0.22 a	2.96 d	9.01 b	38.02 d
NPK	1.27 ab	2.72 b	0.22 c	0.07 a	4.28 cd	7.39 b	57.70 c
NPKSMg	0.96 b	3.27 b	0.95 b	0.14 a	5.31 c	7.67 b	68.99 c
NPKSMgCa	1.42 a	10.57 a	1.82 a	0.05 a	13.85 a	13.66 a	101.88 a

Table 15: Extractable Cations and CEC of the Haplustand (10-30 cm depth) using the Barium Chloride Solution

Soil treatment	K	Ca	Mg	Na	∑ Bases	CEC	Base Sat.
			($cmol_c$ / kg soil)				(%)
Control	0.30 c*	10.92 a	1.14 a	0.17 a	12.52 a	13.67 a	91.72 a
N	0.17 c	8.01 b	0.62 b	0.13 ab	8.92 b	10.37 b	85.47 a
NPK	1.23 ab	7.71 b	0.44 b	0.11 ab	9.49 b	11.07 b	85.69 a
NPKSMg	1.03 b	7.25 b	1.28 a	0.06 b	9.61 b	12.19 ab	81.90 a
NPKSMgCa	1.36 a	10.16 a	1.32 a	0.06 b	12.90 a	13.50 a	95.84 a

* Mean values for a given column, followed by the same letter, are not significantly different at the 95 % level of confidence.

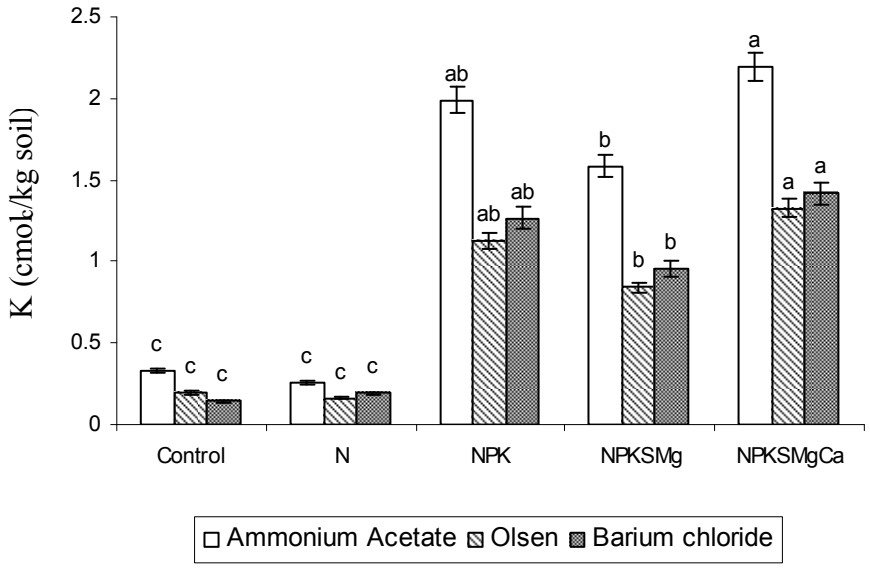

Figure 42: Extractable Potassium Response to Fertilizer Treatments in the Surface Haplustand. Mean extractable K values, for a given extraction method, followed by the same letter are not significantly different at the 95 % level of confidence.

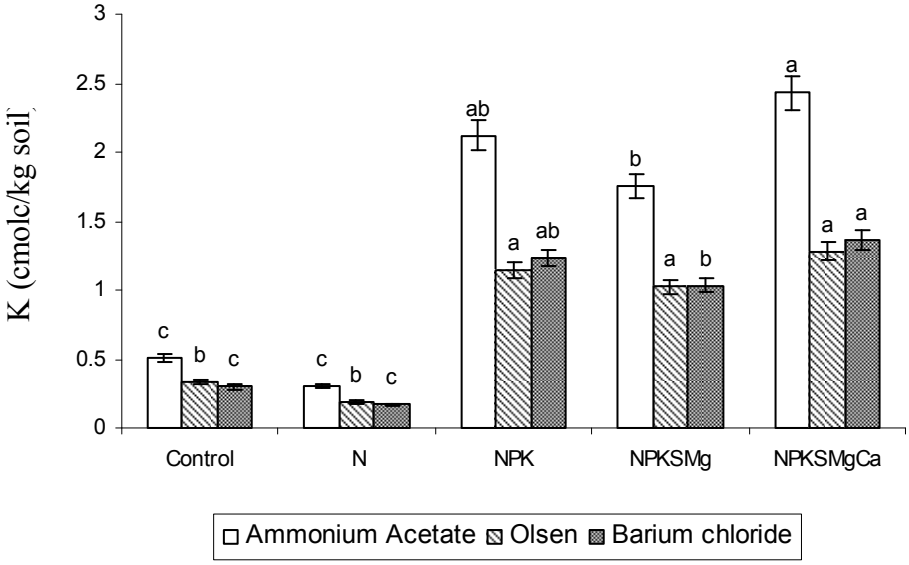

Figure 43: Extractable Potassium Response to Fertilizer Treatments in the Subsurface Haplustand. Mean extractable K values, for a given extraction method, followed by the same letter are not significantly different at the 95 % level of confidence.

In the surface and subsurface Haplustand, there were clearly two levels of extractable Ca among the fertilizer treatments (Figures 44 and 45). The higher was found in the control and +NPKSMgCa treatments, and the lower was in the nitrogen fertilizer treatments without Ca (+N, +NPK, +NPKSMg). This trend was consistent with every extraction solution used. These results were expected due to nitrogen fertilizer effects on pH, because of nitrification. In contrast to what was observed for the extractable K, there was no particular difference in the amount of extractable Ca found by the three extraction methods used. However, a higher amount of extractable Ca was found in the subsurface soil (Figure 46). This could be the result of greater leaching of Ca than K in this soil.

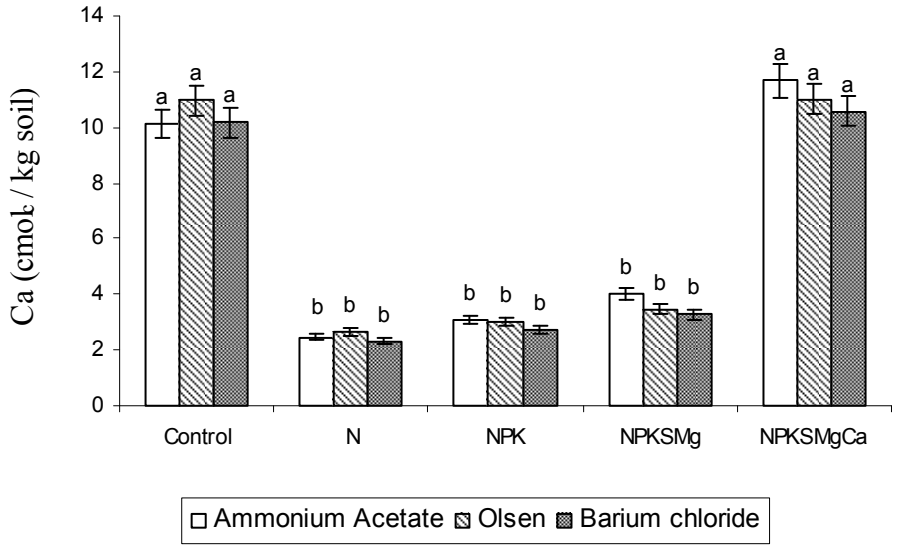

Figure 44: Extractable Calcium Response to Fertilizer Treatments in the Surface Haplustand. Mean extractable Ca values, for a given extraction method, followed by the same letter are not significantly different at the 95 % level of confidence.

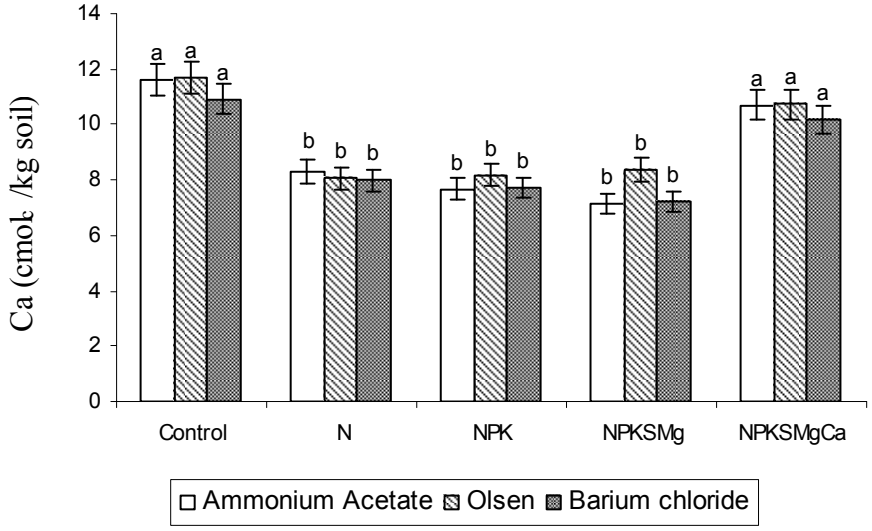

Figure 45: Extractable Calcium Response to Fertilizer Treatments in the Subsurface Haplustand. Mean extractable Ca values, for a given extraction method, followed by the same letter are not significantly different at the 95 % level of confidence.

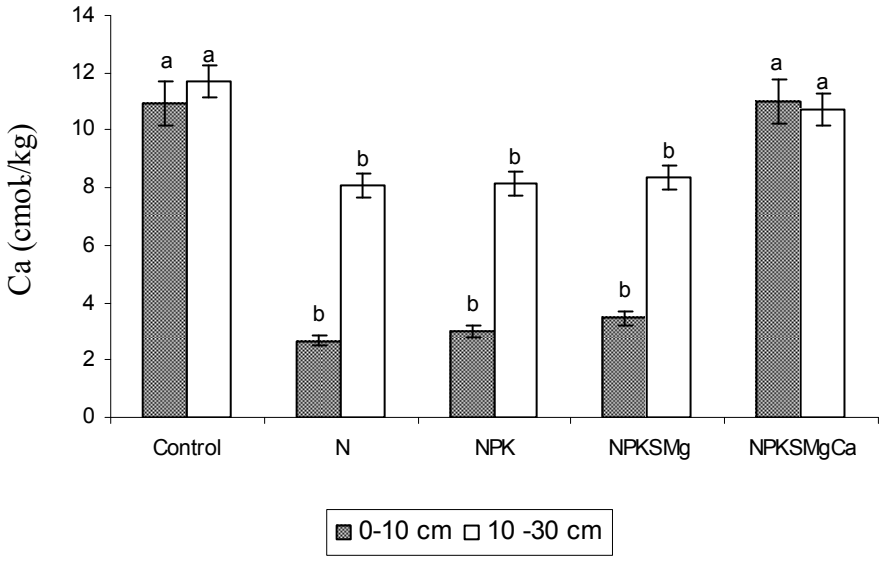

Figure 46: Extractable Calcium (Olsen Method) Response to Fertilizer Treatments and Soil Depth in the Haplustand. Mean extractable Ca values, for a given soil depth increment, followed by the same letter are not significantly different at the 95 % level of confidence.

The extractable Mg behaved in a way similar to the extractable Ca, i.e., a decrease in exchangeable Mg with nitrogen fertilizer application and a positive response to Mg fertilizer application (Figures 47 and 48). Additionally, Ca amendment in the last treatment seemed to be responsible for a significant increase in extractable Mg. This trend was consistent across the three extracting solutions, and there was no great difference among them in the amount of Mg extracted. These results were expected due to the fact that soil Mg behaves similarly to soil Ca. Beckett (1964a) assumed that Ca^{2+} and Mg^{2+} were held with equal attraction by the soil's exchange surfaces. Consequently, the acidification process associated with nitrogen fertilization is thought responsible for Mg leaching as well. Figure 49 shows the distribution of the extractable Mg with soil depth for the Haplustand, and, as was expected, the subsurface soil exhibited greater amounts of extractable Mg in every fertilizer treatment, with the exception of the last one, (+NPKSMgCa). This suggests that the increase in extractable Ca and the greater soil pH resulting from $CaCO_3$ application was responsible for higher CEC, and Mg leaching was reduced.

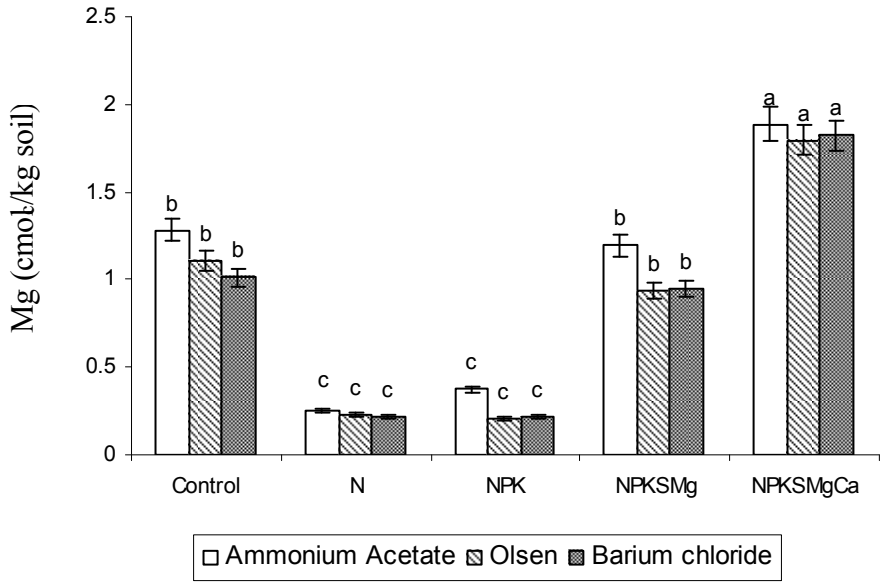

Figure 47: Extractable Magnesium Response to Fertilizer Treatments in the Surface Haplustand. Mean extractable Mg values, for a given extraction method, followed by the same letter are not significantly different at the 95 % level of confidence.

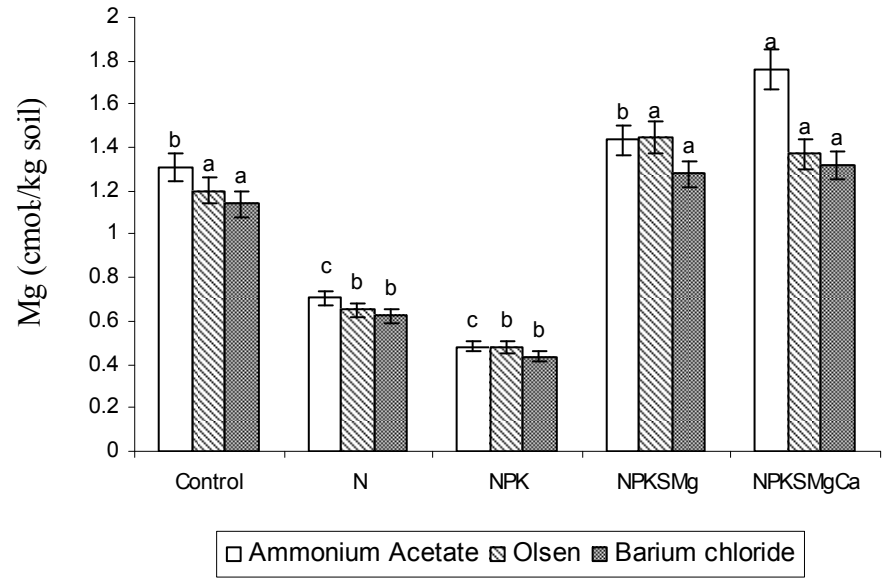

Figure 48: Extractable Magnesium Response to Fertilizer Treatments in the Subsurface Haplustand. Mean extractable Mg values, for a given extraction method, followed by the same letter are not significantly different at the 95 % level of confidence.

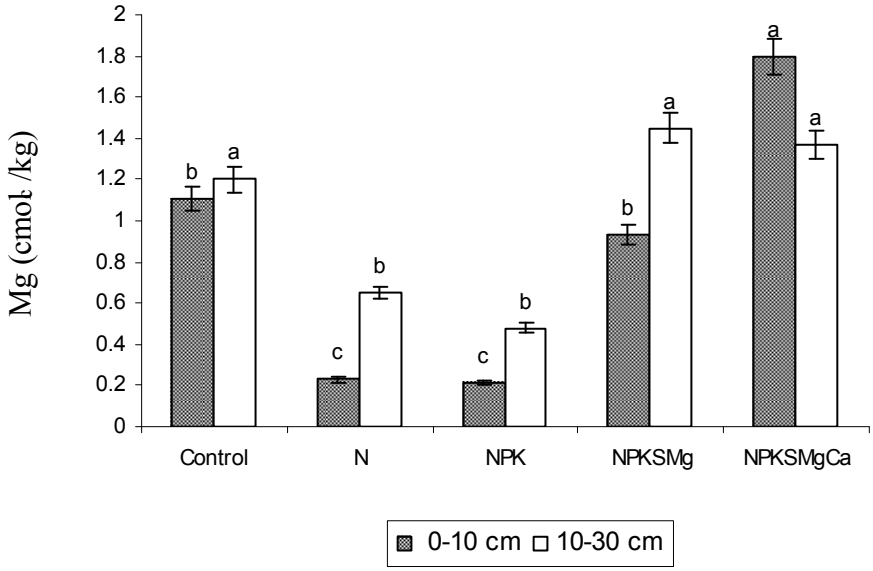

Figure 49: Extractable Magnesium (Olsen Method) Response to Fertilizer Treatments and Soil Depth in the Haplustand. Mean extractable Mg values, for a given soil depth increment, followed by the same letter are not significantly different at the 95 % level of confidence.

The amount of K, Ca and Mg found in the saturated paste extracts of the surface and subsurface Haplustand is given in Tables 16 and 17. The concentration trends observed for all of these nutrients in the saturated paste extracts was the same as that found for these nutrients' exchangeable fraction in all of the fertilizer treatments. However, their quantities were generally much lower than those of the corresponding exchangeable fractions. These results are supported by the fact that the pool of each nutrient that would be represented by the exchangeable fraction is expected to be much larger than the solution pool. Additionally, the amount of K, Ca, and Mg determined from the saturated paste was clearly higher in the surface soil than in the subsurface soil, which implies greater readily available nutrient levels at the surface. That behavior could be also observed in Figures 50 and 51, which show the response of potential partition coefficients, calculated with the saturated paste and barium chloride extractable nutrients,

to represent the soil solution and exchangeable nutrient pools, respectively. Of particular interest is the fact that the potential partition coefficients for the surface Haplustand, principally for K, decreased with the +NPKSMg and +NPKSMgCa fertilizer treatments. That decline was very dramatic for the last treatment, which implies that the K is strongly held by the exchange sites, even after the increase in surface charge generated by higher pH. The amount of readily available macronutrient cations is lower, causing the partition coefficients to decrease in magnitude. Those results are supported by some oil palm leaf tissue data (Figure 52), where K and Mg concentrations are low for the last three fertilizer treatments, despite their application. In contrast, a different trend for the partition coefficients was observed in the subsurface Haplustand. These results could be strongly related to soil pH changes, which were less drastic in the subsurface soil than in the surface soil.

Table 16: Saturation Paste Extract Composition of the Haplustand (0-10 cm depth)

Soil Treatment	**EC**	**K**	**Ca**	**Mg**	**Na**	**Cl^-**	**HCO_3^-**	**CO_3^{-}**	**SO_4^{-2}**
	(dS/m)				**($cmol_c$/liter)**				
Control	0.10 c*	0.06 c	0.54 c	0.11b	0.07b	0.38b	1.96 a	0	0.41b
N	0.97 b	0.28 c	5.45 b	1.06b	0.31 a	0.25b	2.07 a	0	0.05b
NPK	1.61ab	38.08a	5.52 b	0.95b	0.30 a	7.81a	1.96 a	0	0.07b
NPKSMg	1.47ab	19.84b	5.47 b	4.06a	0.32 a	6.31a	2.19 a	0	0.45b
NPKSMgCa	1.87 a	2.65 c	11.77a	4.20a	0.23ab	8.94a	1.72 a	0	1.37a

Table 17: Saturation Paste Extract Composition of the Haplustand (10-30 cm depth)

Soil Treatment	EC	K	Ca	Mg	Na	Cl^-	HCO_3^-	$CO_3^=$	SO_4^{-2}
	(dS/m)				($cmol_c$/liter)				
Control	0.10c*	0.07b	0.46 c	0.11b	0.05 b	0.50b	2.30 a	0	0.34b
N	0.39bc	0.07b	2.80bc	0.44b	0.19ab	0.44b	1.61ab	0	0.12b
NPK	0.72 b	1.38a	3.65 b	0.47b	0.27 a	3.56a	1.61ab	0	0.07b
NPKSMg	0.78ab	1.35a	4.08 b	1.32a	0.22 a	3.38a	0.92 b	0	0.60b
NPKSMgCa	1.15 a	1.71a	7.26 a	1.84a	0.22 a	4.94a	1.73ab	0	1.67a

* Mean values for a given column, followed by the same letter, are not significantly different at the 95 % level of confidence.

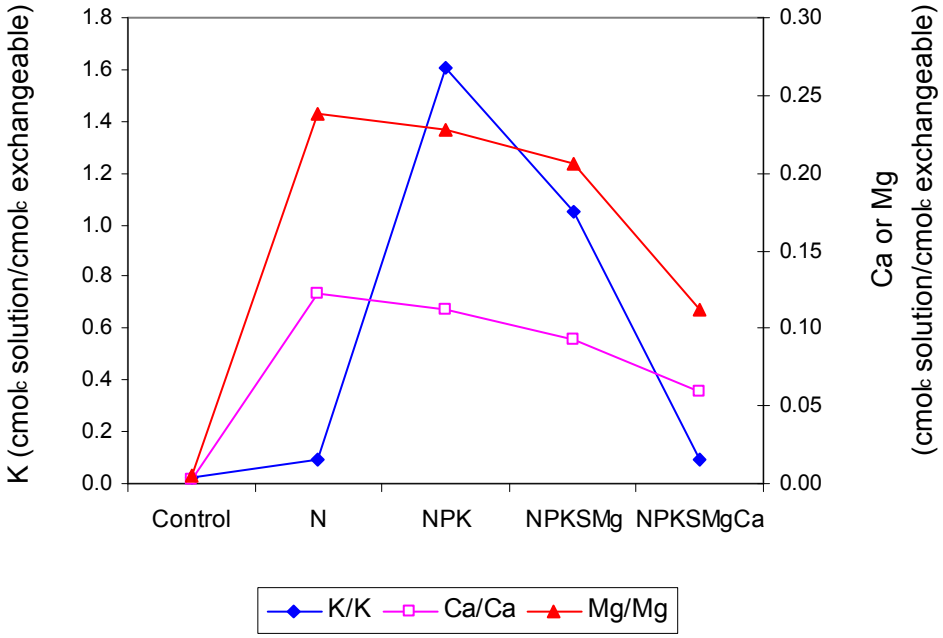

Figure 50: Potential Partition Coefficients for the Surface Haplustand.

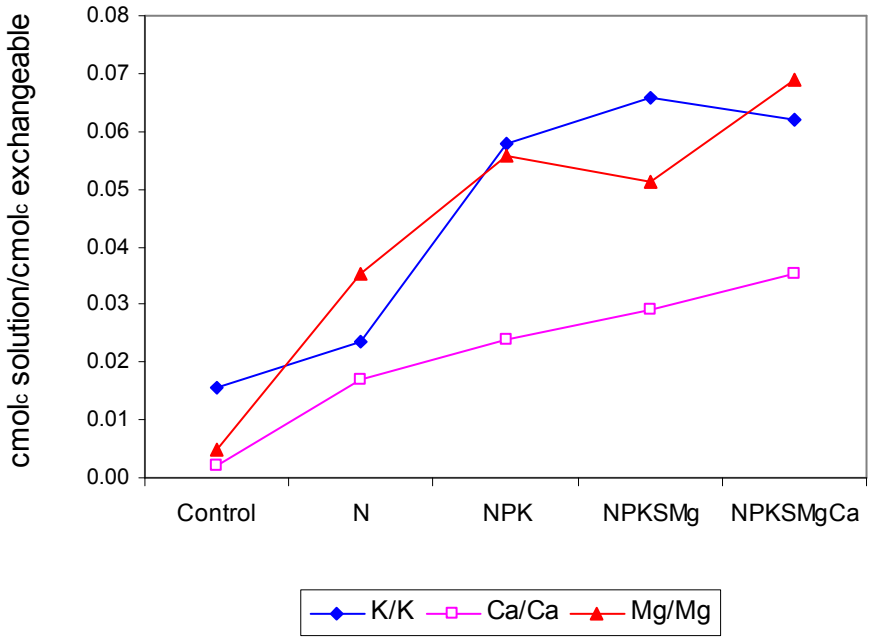

Figure 51: Potential Partition Coefficients for the Subsurface Haplustand.

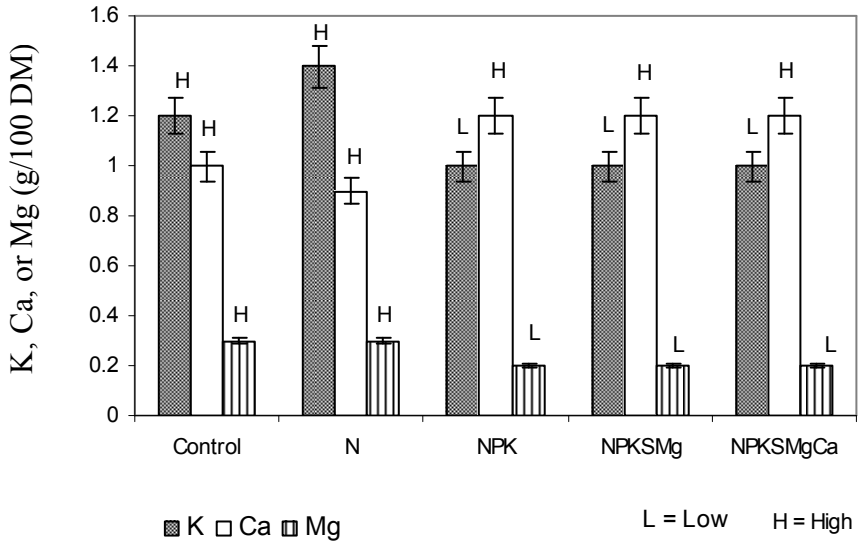

Figure 52: Oil Palm Leaf K, Ca, and Mg Response to Fertilizer Treatments in 2001. The sufficiency of the oil palm leaf levels are according to Jones (1991).

There was no significant difference in soil CEC due to fertilizer amendment of the Haplustand, as determined by the ammonium acetate method. This result was the same

for both surface and subsurface soil samples (Tables 12 and 13). In contrast, significant differences in CEC, due to the fertilizer treatments, were found with the barium chloride method (Tables 14 and 15). Additionally, the CEC found with neutral, normal ammonium acetate was much higher than that determined by barium chloride (Figures 53 and 54). That outcome is supported by Gillman et al. (1982), who worked with non-calcareous and non-saline Australian soils and found differences between methods for CEC, especially for soils that have variable charge characteristics, even though effects on exchangeable cation assessment were found to be much smaller. Those authors pointed out that washing with alcohol, which is part of ammonium acetate method, gave higher CEC values. Low values might have been expected, since ionic strength would be reduced to very low levels during the alcohol wash, causing a reduction in negative charge on variable charge surfaces. The explanation for the converse outcome has been given by Grove et al. (1982), who pointed out that the alcohol wash would preserve the diffuse double layer in a compressed condition similar to that when no wash is used, so that mutual neutralization of positive and negative charges sites are suppressed, and the measured CEC is significantly greater. Additionally, these authors attributed part of the larger CEC values found with buffered ammonium acetate to acetate adsorption by soil surfaces, which was also pointed out by El-Swaify and Sayegh (1975).

The pH response to fertilizer treatments was clearly related to CEC differences found by the barium chloride method (Figure 55). The surface soil exhibited a linear relationship ($r^2 = 0.78$) between CEC and pH. Those results are supported by the fact that Andisols are dominated by pH-dependent surface charge minerals, and consequently the

surface negative charge will increase as a result of higher soil pH. That suggests the use of an unbuffered approach for a precise assessment of CEC in these kinds of soils.

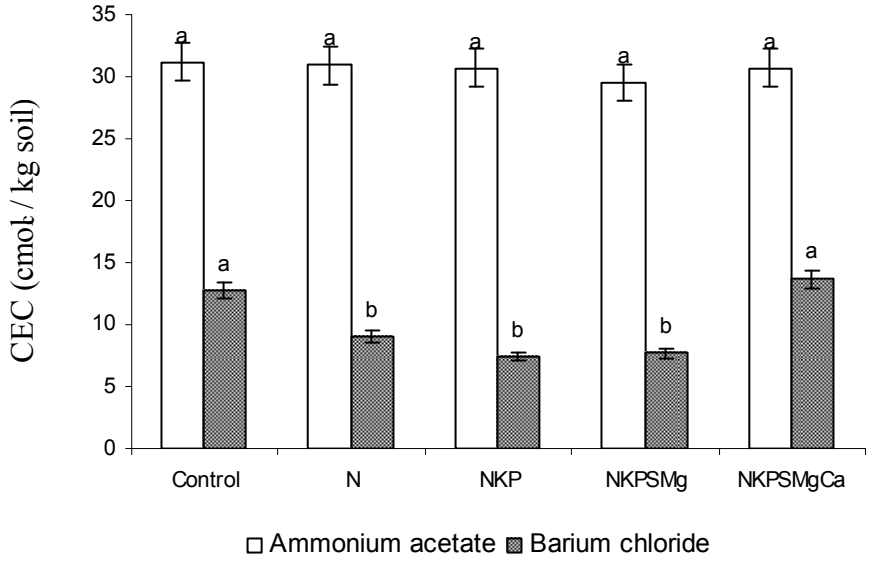

Figure 53: CEC Response of the Surface Haplustand to Fertilizer Treatment and Method of Determination. Mean CEC values, for a given method of determination, followed by the same letter are not significantly different at the 95 % level of confidence.

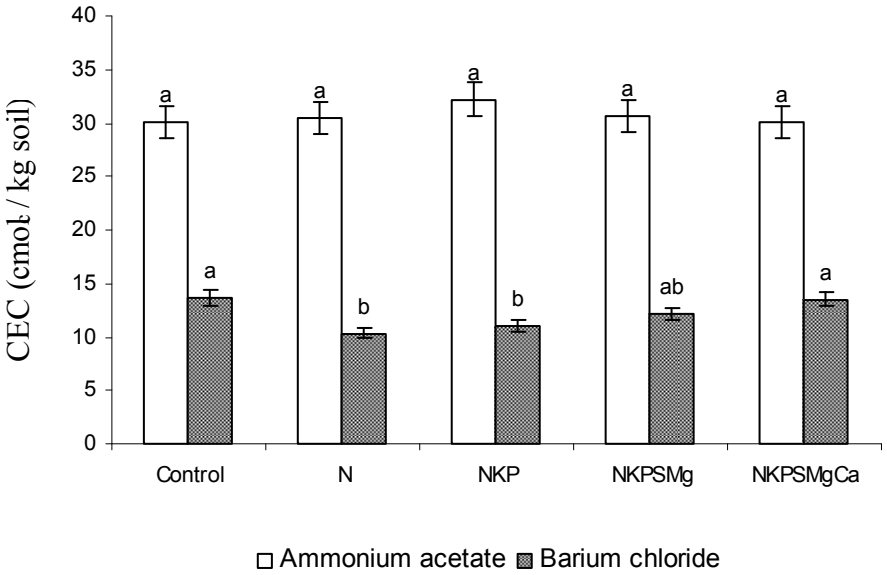

Figure 54: CEC Response of the Subsurface Haplustand to Fertilizer Treatment and Method of Determination. Mean CEC values, for a given method of determination, followed by the same letter are not significantly different at the 95 % level of confidence.

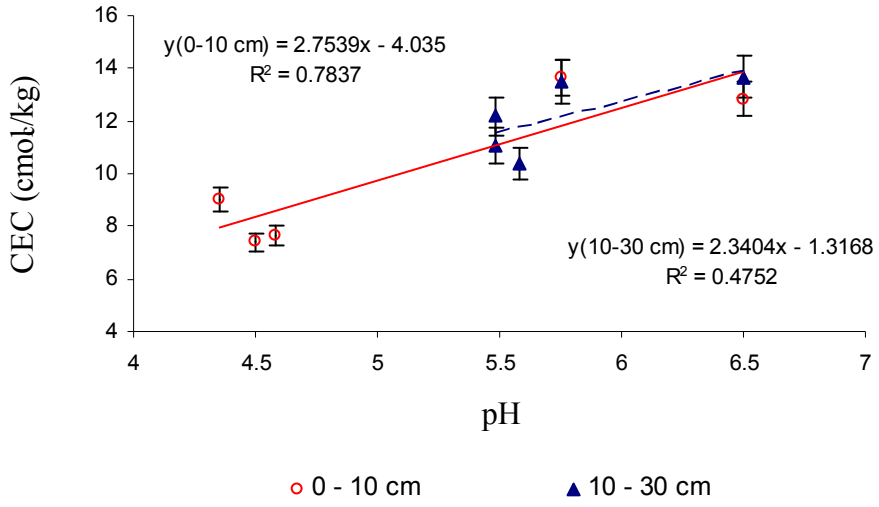

Figure 55: Linear Relationship between CEC and pH at Different Depths in the Haplustand.

Macrocations (K, Ca, Mg) and CEC in the Melanudand

The exchangeable nutrient cation status of the Melanudand, which was assessed using different extraction solutions, is shown in Tables 18 to 23. There was no significant difference ($\alpha = 0.05$) in extractable K in the surface soil due to liming treatments, though there was a trend for decreased K as the lime rate increased. Those results were consistently observed with every method used (Figure 56). However, it was evident that the amount of exchangeable K determined by the ammonium acetate method was higher than that extracted by Olsen or barium chloride. This was expected since NH_4^+ has a smaller hydrated radius than either Ba^{2+} or Na^+. On the other hand, even though the subsurface soil exhibited lower concentrations of extractable K than did the surface soil, there were significant reductions in extractable K with increasing lime rates using either Olsen or barium chloride methods (Figure 57), but not with ammonium acetate

extraction. These results suggest that the ammonium acetate method might overestimate exchangeable K in this soil.

Table 18: Extractable Nutrients in the Melanudand (0-20 cm depth) using the Olsen Solution

Soil Treatment	K	Ca	Mg	Zn	Cu	Fe	Mn	P
	($cmol_c$ / kg soil)			(ppm)				
0 ton lime/ha	0.26a*	3.30c	0.34b	3.93a	12.95a	472 a	4.56a	45.86a
3 ton lime/ha	0.23a	4.25bc	0.31b	3.59ab	12.81a	439 a	3.37ab	37.34ab
6 ton lime/ha	0.24a	6.55b	0.44b	3.39b	12.59a	446 a	3.29ab	35.7ab
12 ton lime/ha	0.20a	12.98a	0.68a	3.07b	11.13ab	255 b	1.88b	31.81ab
18 ton lime/ha	0.18a	14.92a	0.67a	2.53c	10.07b	172 b	1.62b	22.75b

Table 19: Extractable Nutrients in the Melanudand (20-40 cm depth) using the Olsen Solution

Soil Treatment	K	Ca	Mg	Zn	Cu	Fe	Mn	P
	($cmol_c$ / kg soil)			(ppm)				
0 ton lime/ha	0.17a*	2.80b	0.22b	3.36ab	14.17a	519 a	3.69ab	32.07ab
3 ton lime/ha	0.15ab	3.40b	0.20b	3.50a	14.31a	479 a	3.94a	39.23a
6 ton lime/ha	0.15ab	4.83b	0.31b	2.40b	12.86ab	490 a	2.38abc	25.70ab
12 ton lime/ha	0.13 b	8.67a	0.44a	2.76ab	12.12b	395 b	2.17bc	27.12ab
18 ton lime/ha	0.14ab	9.91a	0.53a	2.73ab	12.83ab	391 b	1.87c	19.85b

Table 20: Exchangeable Cations and CEC of the Melanudand (0-20 cm depth) using 1N Ammonium Acetate Solution

Soil Treatment	K	Ca	Mg	Na	∑ Bases	CEC	Base Sat.
	($cmol_c$ / kg soil)						(%)
0 ton lime/ha	0.36a*	2.69c	0.35b	0.02a	3.42c	30.37a	11.27c
3 ton lime/ha	0.33a	3.88bc	0.35b	0.03a	4.59bc	31.72a	14.57bc
6 ton lime/ha	0.33a	6.39b	0.51b	0.02a	7.25b	30.19a	24.18b
12 ton lime/ha	0.28a	12.63a	0.86a	0.03a	13.81a	30.54a	45.29a
18 ton lime/ha	0.26a	15.01a	1.00a	0.06a	16.33a	31.55a	51.54a

Table 21: Exchangeable Cations and CEC of the Melanudand (20-40 cm depth) using 1N Ammonium Acetate Solution

Soil treatment	K	Ca	Mg	Na	∑ Bases	CEC	Base Sat.
			($cmol_c$ / kg soil)				(%)
0 ton lime/ha	0.22a*	2.41b	0.21b	0.05ab	2.89b	30.20a	9.74b
3 ton lime/ha	0.20a	2.95b	0.22b	0.10a	3.46b	30.70a	11.45b
6 ton lime/ha	0.19a	4.35b	0.31b	0.02b	4.88b	30.37a	16.19b
12 ton lime/ha	0.18a	8.13a	0.51a	0.04ab	8.85a	30.53a	29.05a
18 ton lime/ha	0.19a	9.42a	0.61a	0.02b	10.24a	29.69a	34.47a

Table 22: Exchangeable Cations and CEC of the Melanudand (0-20 cm depth) using the Barium Chloride Solution

Soil treatment	K	Ca	Mg	Na	∑ Bases	CEC	Base Sat.
			($cmol_c$ / kg soil)				(%)
0 ton lime/ha	0.24 a*	3.17 c	0.36 bc	0.06 a	3.83 c	6.74 c	56.39 c
3 ton lime/ha	0.19 a	4.10 bc	0.33 c	0.07 a	4.69 c	7.22 bc	64.19 bc
6 ton lime/ha	0.19 a	6.42 b	0.47 b	0.04 a	7.12 b	9.85 b	74.02 b
12 ton lime/ha	0.17 a	12.44 a	0.80 a	0.10 a	13.51 a	14.04 a	96.27 a
18 ton lime/ha	0.13 a	14.82 a	0.85 a	0.09 a	15.90 a	16.09 a	98.50 a

Table 23: Exchangeable Cations and CEC of the Melanudand (20-40 cm depth) using the Barium Chloride Solution

Soil treatment	K	Ca	Mg	Na	∑ Bases	CEC	Base Sat.
			($cmol_c$ / kg soil)				(%)
0 ton lime/ha	0.12 a*	2.77 b	0.21 c	0.05 a	3.16 b	6.56 b	47.46 c
3 ton lime/ha	0.11 ab	3.16 b	0.22 c	0.06 a	3.54 b	6.47 b	54.32 bc
6 ton lime/ha	0.11 ab	4.70 b	0.31 b	0.08 a	5.20 b	7.63 b	67.56 b
12 ton lime/ha	0.09 b	8.14 a	0.44 a	0.05 a	8.73 a	10.15 a	85.55 a
18 ton lime/ha	0.09 b	9.16 a	0.51 a	0.20 a	9.96 a	11.36 a	87.68 a

* Mean values for a given column, followed by the same letter, are not significantly different at the 95 % level of confidence.

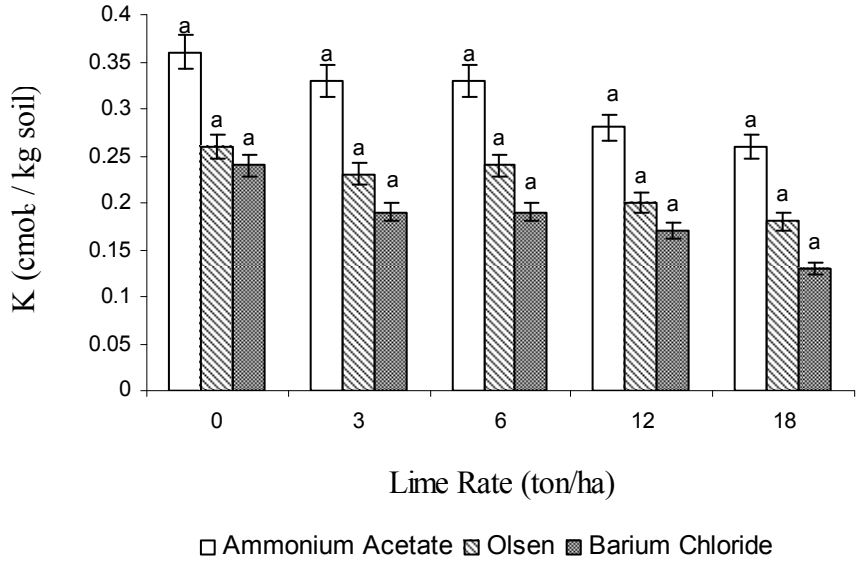

Figure 56: Extractable Potassium Response to Liming in the Surface Melanudand. Mean K values, for a given method of determination, followed by the same letter are not significantly different at the 95 % level of confidence.

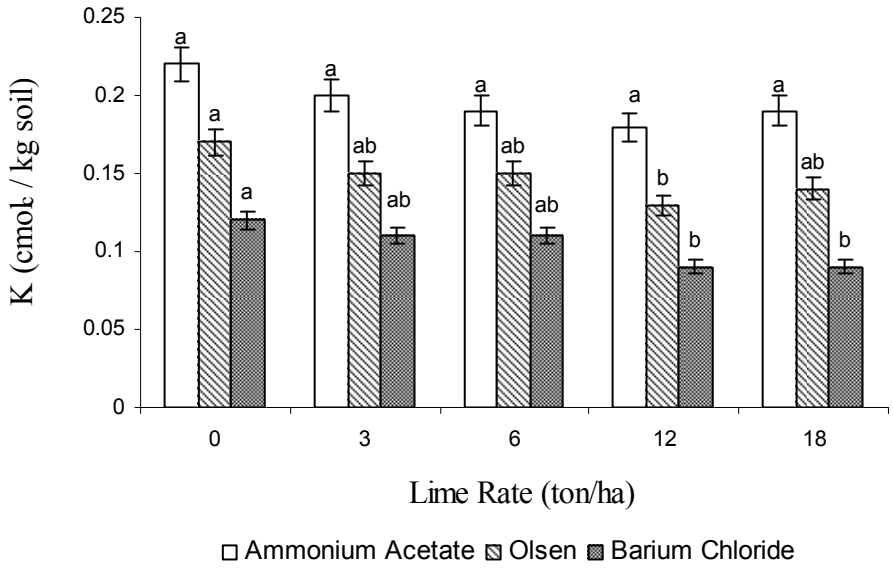

Figure 57: Extractable Potassium Response to Liming in the Subsurface Melanudand. Mean K values, for a given method of determination, followed by the same letter are not significantly different at the 95 % level of confidence.

There were significant differences in extractable Ca in the surface soil, due to lime rate (Figure 58). The expected positive response to liming was consistently found by every extraction method. In contrast to K, the amount of Ca extracted was not different among the three extracting solutions used. The subsurface soil was lower in extractable Ca, which suggests that the Ca leaching associated with this soil was not great (Figure 59). On the other hand, the effect of lime rate on extractable Ca in the deeper soil became significant, at the 12 ton/ha rate. These results were expected, as the lime was applied to the surface soil. Nevertheless, higher Ca concentrations in soil solution after heavy lime applications, along with leaching, have caused positive changes in the exchangeable Ca status of the subsurface soil.

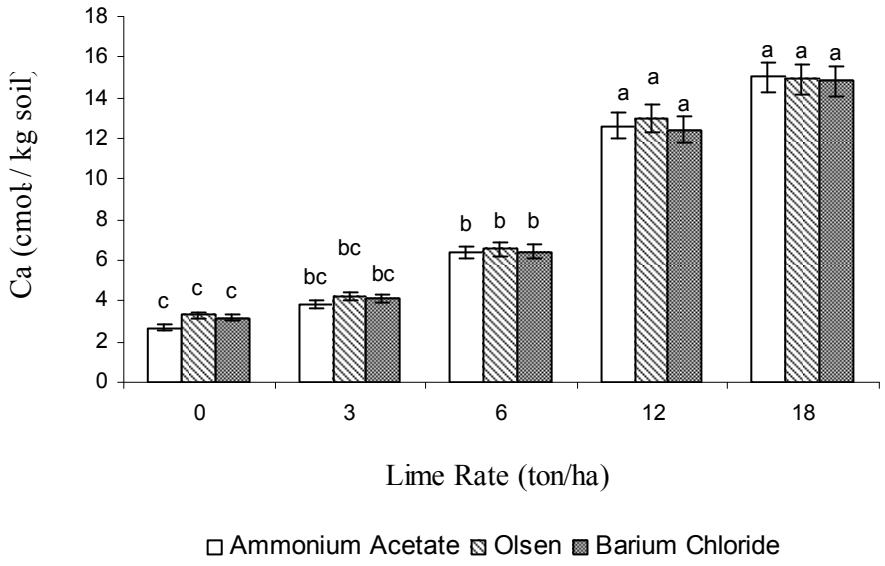

Figure 58: Extractable Calcium Response to Liming in the Surface Melanudand. Mean Ca values, for a given method of determination, followed by the same letter are not significantly different at the 95 % level of confidence.

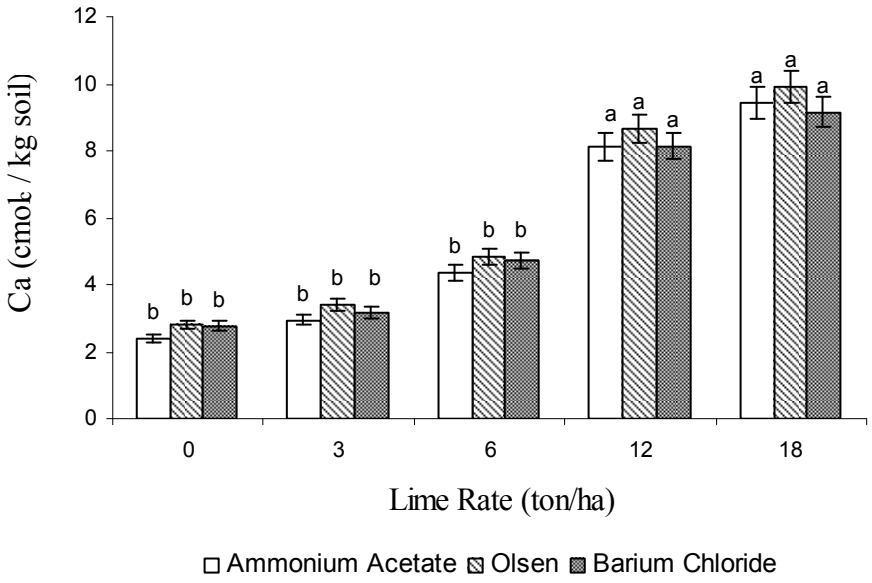

Figure 59: Extractable Calcium Response to Liming in the Subsurface Melanudand. Mean Ca values, for a given method of determination, followed by the same letter are not significantly different at the 95 % level of confidence.

According Curtin and Smillie (1983), liming reduces soil solution Mg, K, and Na due to the reduction in the fractional saturation of the cation exchange complex by these cations as a result of the lime-induced increase in CEC. Additionally, Grove et al. (1981) pointed out that lime application to acid topsoils dominated by constant surface potential colloids reduces exchangeable Mg at pH values higher than 5.1 due to a fixation mechanism, which mainly is described by the adsorption and possible solid diffusion of soluble Mg into newly precipitated and amorphous-hydroxy Al polymers created when acid soils are limed. In contrast to what was found by these authors, this liming experiment resulted in a significant increase in exchangeable Mg in the surface and subsurface soils as the lime rate increased (Figures 60 and 61). These results could be explained by the presence of dolomite impurities in the calcitic lime used.

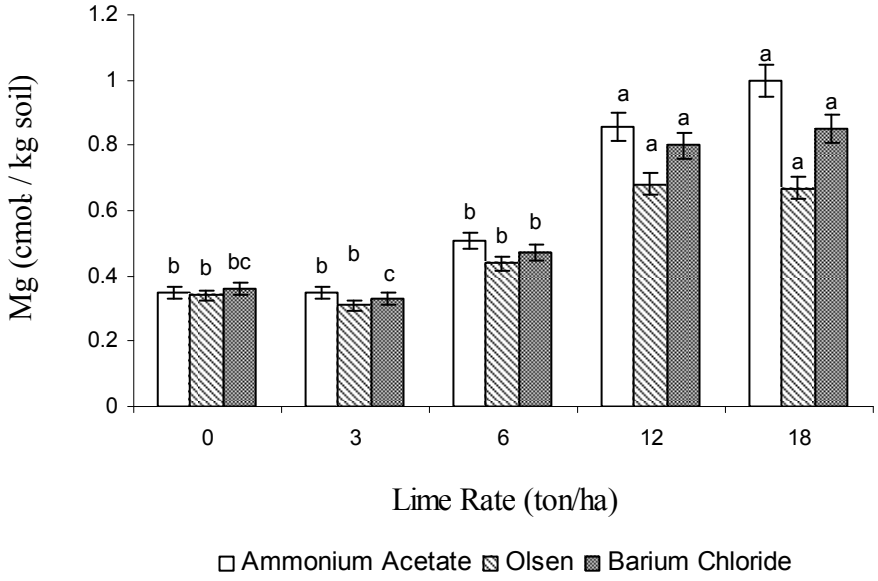

Figure 60: Extractable Magnesium Response to Liming in the Surface Melanudand. Mean Mg values, for a given method of determination, followed by the same letter are not significantly different at the 95 % level of confidence.

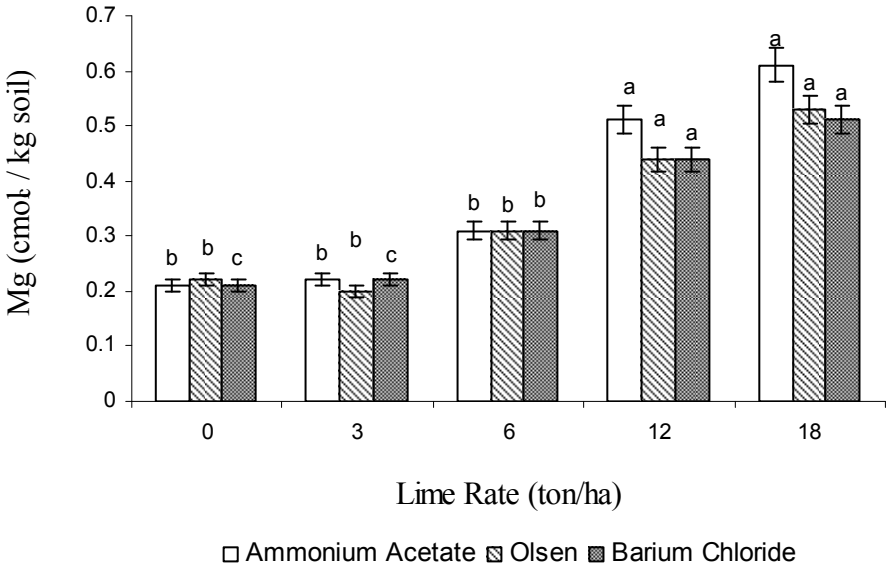

Figure 61: Extractable Magnesium Response to Liming in the Subsurface Melanudand. Mean Mg values, for a given method of determination, followed by the same letter are not significantly different at the 95 % level of confidence.

The trend for greater exchangeable Mg with lime rate was consistently found with each extraction method used, and there was no particular difference among them in the amount of Mg extracted. The extractable Mg found in the surface soil was higher than that found in subsurface soil, at all lime rates, similar to the behavior observed for Ca.

The amounts of K, Ca and Mg found in saturated paste extracts of the surface and subsurface Melanudand are presented in Tables 24 and 25. The trend in nutrient cation concentrations in the saturated paste with lime rate was the same as that previously found for the exchangeable fraction, though the concentration of the cations in the saturated paste was much less than that of the corresponding exchangeable fraction. The pool of each nutrient found in the exchangeable fraction is usually bigger than that found in the solution. Additionally, there was no great difference between the surface and the subsurface soil in their saturated paste concentrations of K, Ca, and Mg, which implies that readily available nutrient concentrations at each lime rate were nearly homogeneous, up to a depth of 40 cm, in this soil. That behavior is further illustrated by the potential partition coefficients (Figures 62 and 63), calculated using the saturated paste and barium chloride extracts as soil solution and exchangeable concentrations, respectively. Higher lime rates resulted in lower K and Mg partition coefficients in the surface soil. These results imply that Ca in the surface soil, which increased with lime rate, is more strongly held on the exchange sites. Consequently, even after the increase in surface charge generated by higher soil pH, the readily available K and Mg are reduced, given that their partition coefficients generally decrease in magnitude. In the subsurface soil, there was no great variation in the partition coefficients.

Table 24: Saturation Paste Extract Composition of the Melanudand (0-20 cm depth)

Soil treatment	EC	K	Ca	Mg	Na	Cl^-	HCO_3^-	$CO_3^=$	SO_4^{-2}
	(dS/m)				($cmol_c$/liter)				
0 ton lime/ha	0.12b*	0.28a	0.41d	0.15a	0.19a	0.42b	1.99a	0	0.38a
3 ton lime/ha	0.14ab	0.26a	0.48cd	0.15a	0.20a	0.75ab	1.69a	0	0.33a
6 ton lime/ha	0.17a	0.27a	0.62c	0.19a	0.19a	0.92a	1.99a	0	0.40a
12 ton lime/ha	0.16a	0.20a	0.94b	0.20a	0.20a	0.67ab	1.99a	0	0.42a
18 ton lime/ha	0.15ab	0.17a	1.16a	0.19a	0.16a	0.67ab	2.99a	0	0.55a

Table 25: Saturation Paste Extract Composition of the Melanudand (20-40 cm depth)

Soil treatment	EC	K	Ca	Mg	Na	Cl^-	HCO_3^-	$CO_3^=$	$SO_4^=$
	(dS/m)				($cmol_c$/liter)				
0 ton lime/ha	0.12c*	0.21a	0.38c	0.11a	0.40a	0.67a	2.07a	0	0.28a
3 ton lime/ha	0.16ab	0.19a	0.61bc	0.13b	0.26a	0.75a	1.38b	0	0.50a
6 ton lime/ha	0.14abc	0.20a	0.56bc	0.16ab	0.18a	0.42a	1.84ab	0	0.43a
12 ton lime/ha	0.17a	0.16a	0.97a	0.19a	0.19a	0.58a	2.07a	0	0.28a
18 ton lime/ha	0.13bc	0.17a	0.72ab	0.18a	0.19a	0.42a	1.76ab	0	0.36a

* Mean values for a given column, followed by the same letter, are not significantly different at the 95 % level of confidence.

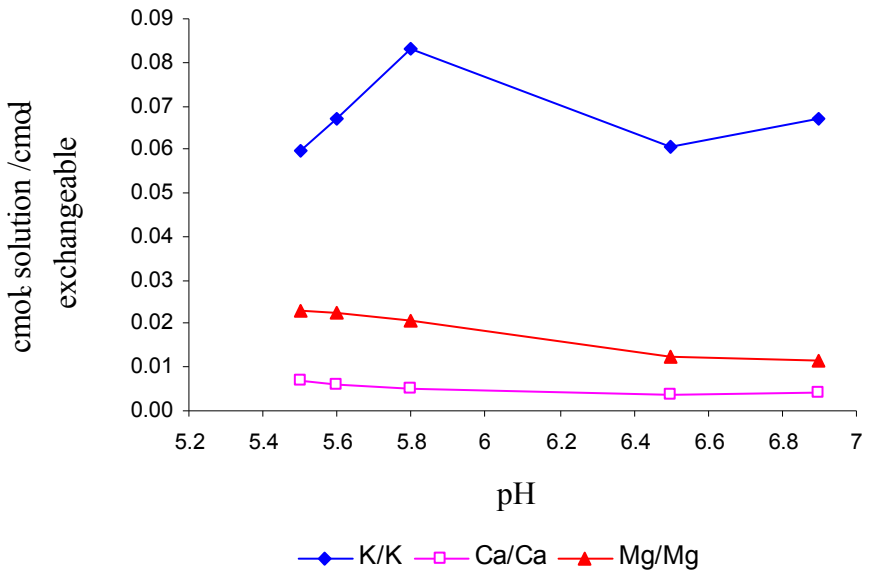

Figure 62: Potential Partition Coefficients in the Surface Melanudand.

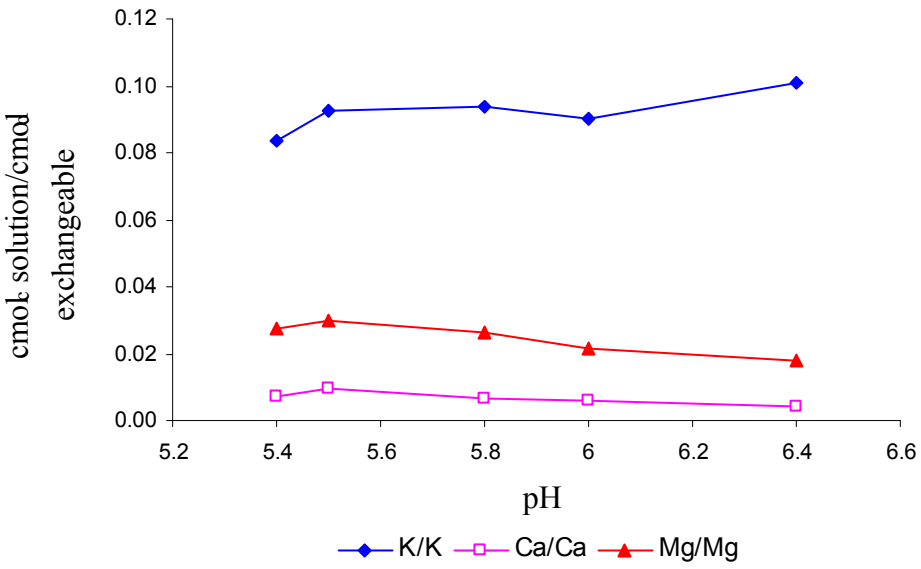

Figure 63: Potential Partition Coefficients in the Subsurface Melanudand.

There was no significant change in CEC determined by the ammonium acetate method due to lime rate. The same trend was observed in both surface and subsurface soil (Tables 20 and 21). Additionally, CEC values found by the buffered ammonium acetate

method were much higher than those determined by the unbuffered barium chloride method (Figures 64 and 65). Also, significant differences in CEC due to lime rate were found with the barium chloride method (Tables 22 and 23). Figure 64 illustrates the significant increase in CEC with nearly all lime rates for the surface soil. In contrast, 12 ton lime/ha were necessary to cause a significant CEC increase in the subsurface soil, because the lime application was made to the surface. Nevertheless, higher lime rates were associated with some CEC increase at deeper depths in this soil. The pH response to liming was linearly related to CEC values determined by the barium chloride method (Figure 66). The surface soil's CEC response exhibited greater slope (6.7 $cmol_c$/kg / unit pH) and less variation ($r^2 = 0.983$) than did the subsurface soil. The results are supported by the fact that this Andisol is dominated by constant surface potential colloids, and surface negative charge will increase as a result of higher soil pH. This suggests the need for an unbuffered approach to the precise assessment of CEC in this kind of soil. A better relationship between pH and CEC was found for the Melanudand rather than for the Haplustand, which could be explained by the greater amount of organic matter present in the former soil and the important role of organic matter as a constant surface potential colloid and the greater spread in soil pH values among the treatments (due to the fact that this was a liming study).

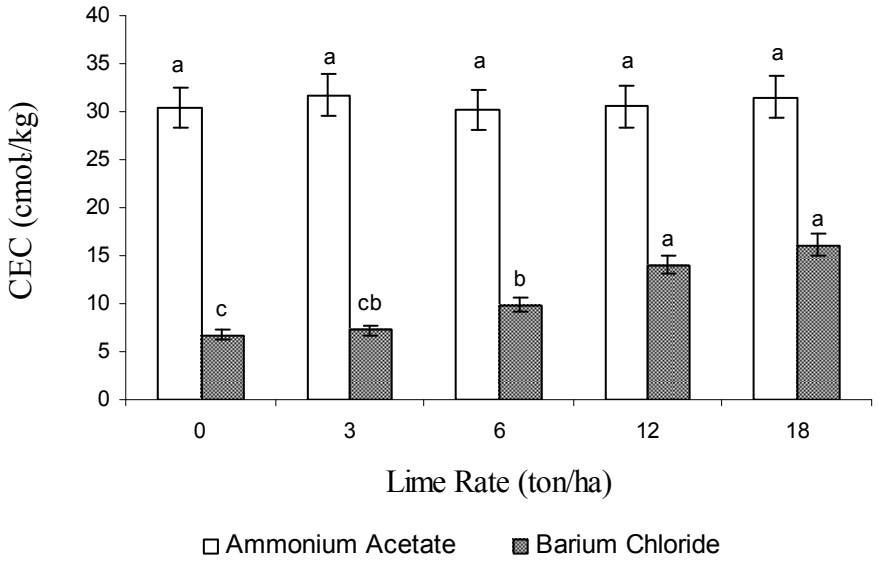

Figure 64: CEC Response to Lime Rate in the Surface Melanudand. Mean CEC values, for a given method of determination, followed by the same letter are not significantly different at the 95 % level of confidence.

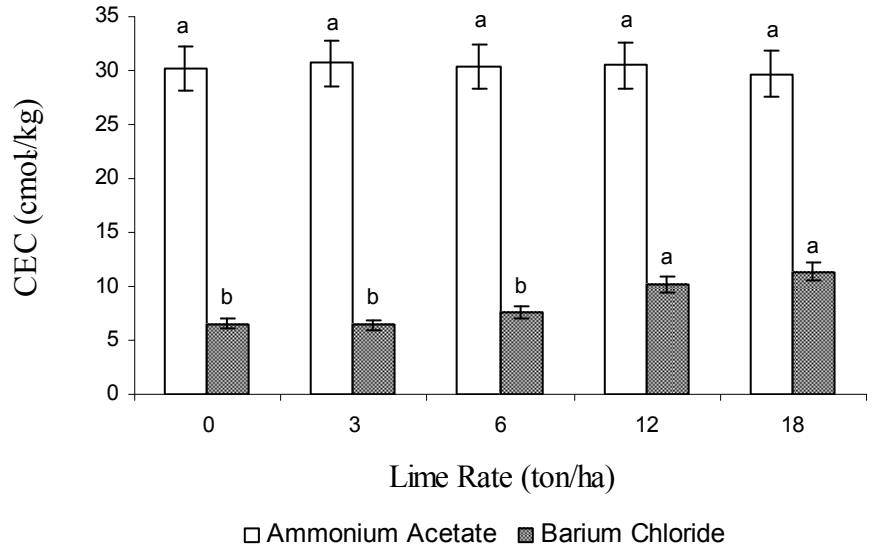

Figure 65: CEC Response to Lime Rate in the Subsurface Melanudand. Mean CEC values, for a given method of determination, followed by the same letter are not significantly different at the 95 % level of confidence.

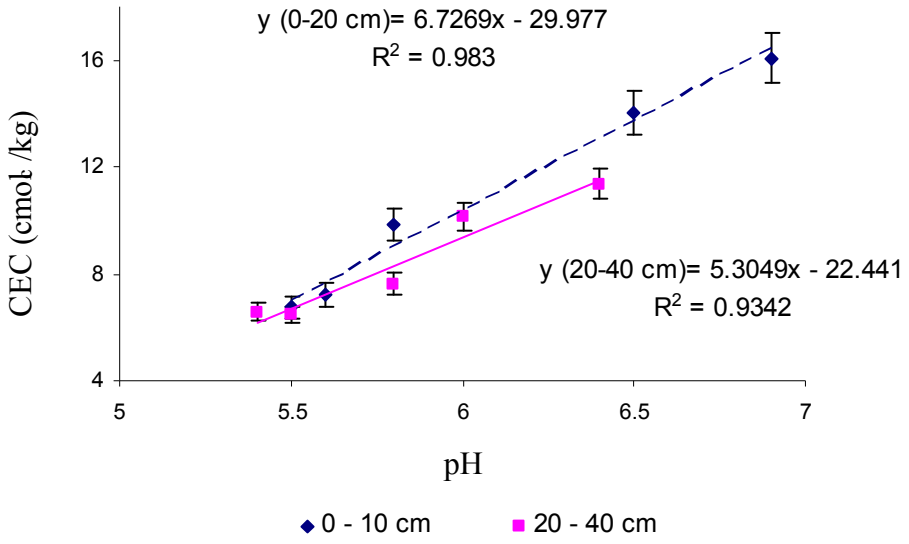

Figure 66: Linear Relationship between CEC and pH at Different Depths in the Melanudand.

Specific Surface

The specific surface determined for the surface and subsurface soil samples is given in Appendix C. The Melanudand possessed the highest specific surface, for both the surface and subsurface soil samples, followed by the Haplustand, and finally by, the Typic Paleudalf. The Melanudand had higher soil organic matter content, which is related to greater specific surface. Also, amorphous clay minerals, which were characteristic constituents of the Haplustand and the Melanudand, would be associated with higher specific surface, as compared to the nonexpanding layer silicates, such as kaolinite and some micas, present in the Typic Paleudalf.

Figure 67 illustrates the effect of drying on the measured specific surface for surface soil samples. As was expected, drying was detrimental to specific surface. Similar results have been reported by Kanehiro and Sherman (1956). The decline in specific surface with drying was greater for the surface Melanudand, even though it had the

higher silica-sesquioxide ratio. These results suggest that the observed decrease in specific surface could be related to shrinkage and cementation by both the amorphous minerals and soil organic matter. Additionally, it was observed that the higher the drying temperature, the greater the decrease in specific surface, except for the Typic Paleudalf, which did not show any change between 45 and 110 ^{o}C.

The specific surface of moist subsurface soil samples (Figure 68) was higher than that found with the surface soils. This could be explained by the greater gravimetric water content associated with the deeper horizons. After drying, the subsurface soil samples for both Andisols gave specific surface values similar to those of their surface soils. In contrast, the dry Typic Paleudalf subsurface sample exhibited greater specific surface than that of the dry surface soil, which could be explained by the dramatic increase in kaolinite (33 % in the upper horizon and 71 % in the lower-Appendix A) and clay content (16 % in the surface and 63 % in the subsurface). Additionally, the specific surface for the moist subsurface Typic Paleudalf was not significantly different from that observed with dry soil. These results suggest that kaolinitic soils do not loose specific surface with drying, in the absence of organic matter. On the other hand, specific surface values for the subsurface Andisols were more sensitive to drying at 45 ^{o}C than those of the corresponding surface soils. Nevertheless, it is possible that the lower soil organic matter concentrations associated with deeper horizons increase the sensitivity of the EGME method for specific surface. Cihacek and Bremner (1979) found that specific surface values obtained by the EGME procedure on Ca-saturated soils with and without organic matter removal, were significantly positively correlated.

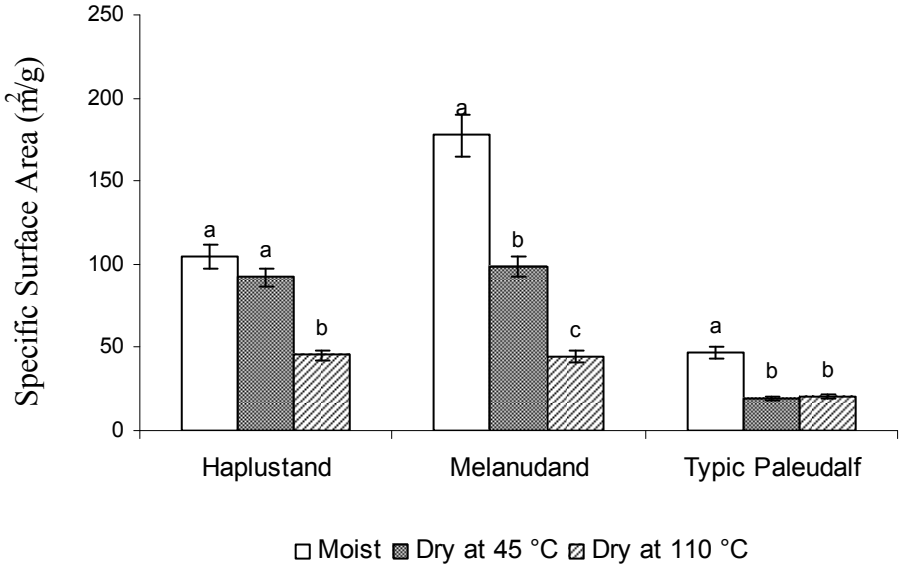

Figure 67: Drying Effect on Specific Surface of Surface Soils.

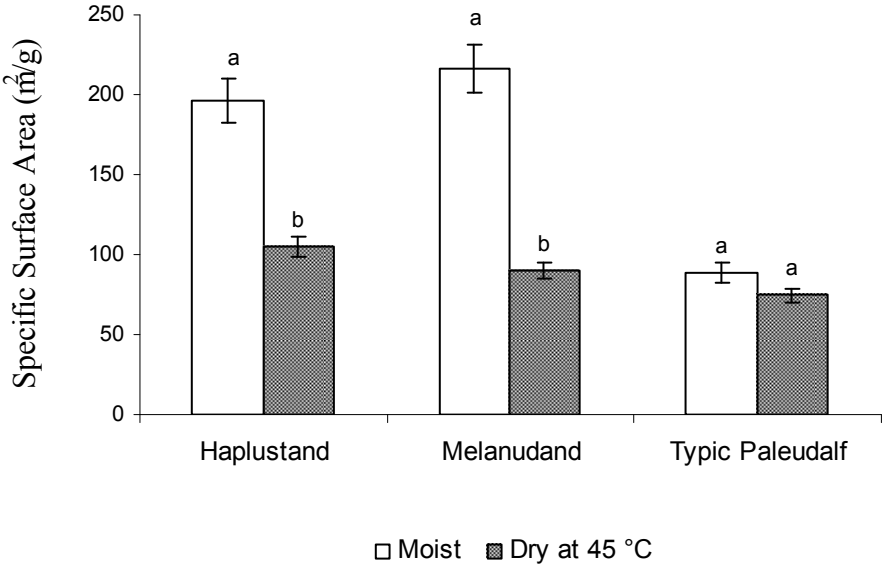

Figure 68: Drying Effect on Specific Surface of Subsurface Soils.

Electrochemical Properties

Standardization of the "Charge Fingerprint" Method

According to the "Charge Fingerprint" method described by Gillman (1984) and used mainly in Oxisols' characterization, the soil surface charge is determined by the sum of exchangeable Ca^{2+}, Al^{3+} and Cl^{-} using a 1 M NH_4NO_3 extraction after the soil has been saturated with Ca^{2+} and then equilibrated with a 0.002 M $CaCl_2$ solution. In this research, two and twenty four-hour periods of NH_4NO_3 equilibration, with shaking, were tested. As one can see in Table 26 and Figures 69 through 71, after a two-hour equilibration period there were no extractable cations, i.e. $Ca^{2+}$and Al^{3+}, at pH values $\geq$ 5 in the Haplustand and at pH values $\geq$ 6 in the Melanudand and Typic Paleudalf. The initial increase in extractable calcium with soil pH was expected because the studied soils are dominated by constant surface potential colloids. However, the expected greater CEC was not observed at greater pH values. This suggested that even as the negative surface charge increased at higher soil pH values, the 1 M NH_4NO_3 solution with two hours of equilibration was not strong enough to extract Ca strongly held by the soil.

On the other hand, exchangeable chloride decreased as the soil pH increased, as expected, due to the fact that AEC in soil systems dominated by constant surface-potential colloids decreases at greater soil pH values. This is driven by deprotonation reactions. Additionally, exchangeable chloride values were coincident at both extraction times for the Haplustand and the Melanudand, while the Typic Paleudalf presented greater exchangeable chloride or higher AEC after the longer equilibration time. Those results suggest that Andisols had greater chloride, or lower nitrate affinity.

Table 26: Soil pH Effect on Surface Charge after a 1 M NH_4NO_3 Equilibration/Extraction Time of Two Hours for Selected Calcium Saturated Surface Soils

Soil	pH ($CaCl_2$)	Ca^{2+} ex.	Al^{3+} ex.	Cl^- ex.	At soil pH ($CaCl_2$)	
					σ^-	σ^+
		$cmol_c\ kg^{-1}$				
Haplustand (0-10cm)	3.39	2.33	2.72	0.95	-5.06	0.95
	4.03	4.53	1.13	0.42	-5.66	0.42
	5.06	0.00	0.02	0.17	-0.02	0.17
	5.90	0.00	0.00	0.09	0.00	0.09
	6.69	0.00	0.00	0.08	0.00	0.08
	7.54	0.02	0.00	0.06	0.00	0.06
Melanudand (0-20cm)	3.46	0.96	2.33	0.64	-3.30	0.64
	4.09	1.51	1.38	0.25	-2.89	0.25
	4.95	3.62	0.33	0.09	-3.95	0.09
	5.73	0.00	0.00	0.05	0.00	0.05
	6.42	0.00	0.00	0.04	0.00	0.04
	6.92	0.00	0.00	0.04	0.00	0.04
Typic Paleudalf (0-18 cm)	3.52	0.97	1.00	0.12	-1.97	0.12
	4.39	3.26	0.12	0.14	-3.38	0.14
	5.28	4.21	0.01	0.09	-4.22	0.09
	6.30	0.00	0.00	0.06	0.00	0.06
	7.04	0.00	0.00	0.06	0.00	0.06
	7.38	0.00	0.00	0.05	0.00	0.05

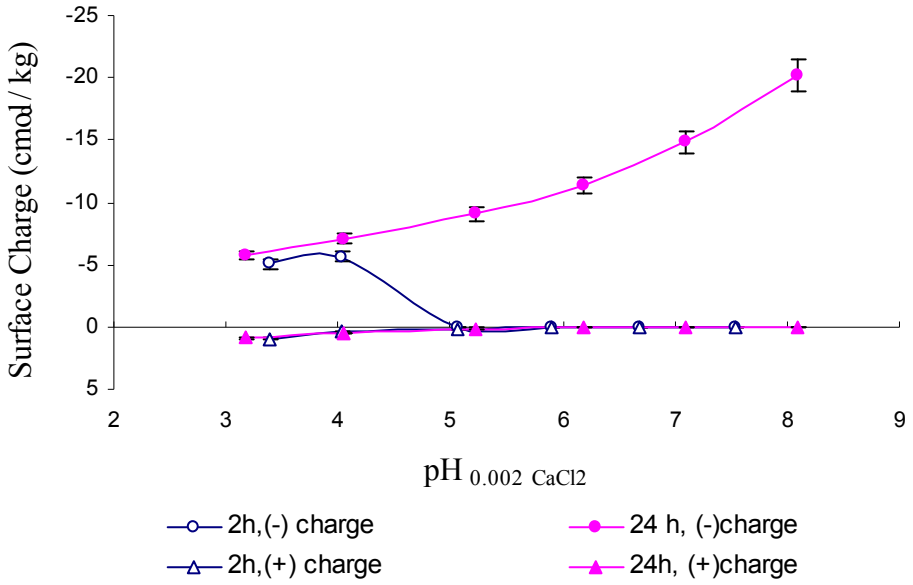

Figure 69: Soil pH effect on Surface Charge for Two NH_4NO_3 Extraction Times on the Calcium Saturated Surface Haplustand.

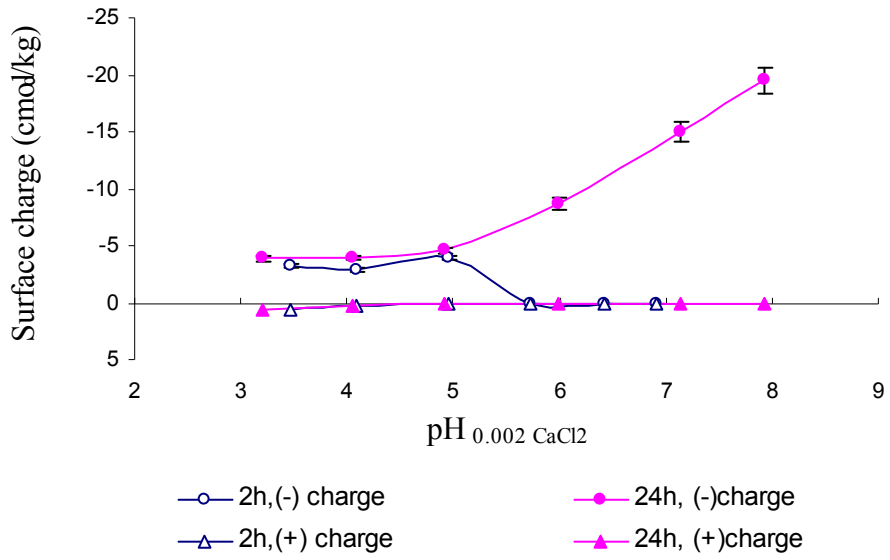

Figure 70: Soil pH effect on Surface Charge for Two NH_4NO_3 Extraction Times on the Calcium Saturated Surface Melanudand.

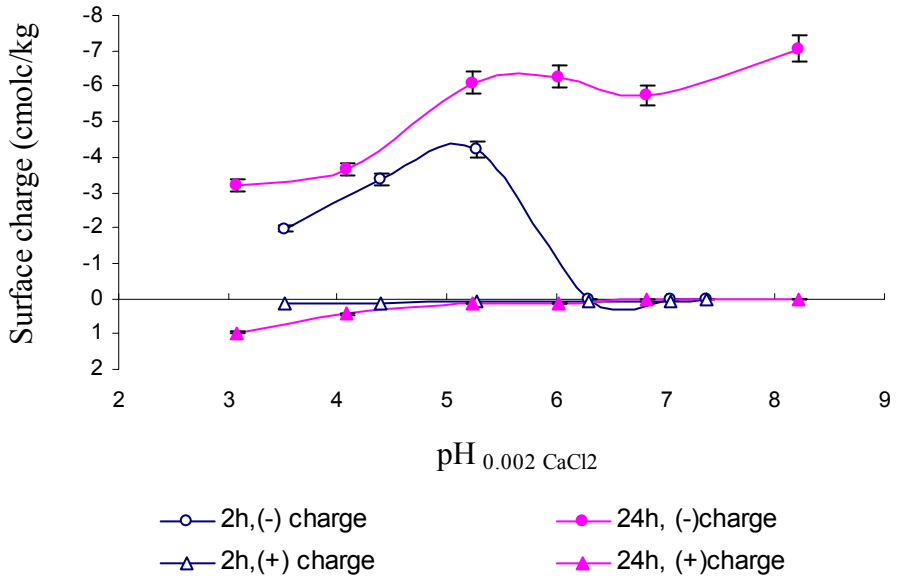

Figure 71: Soil pH effect on Surface Charge for Two NH_4NO_3 Extraction Times on the Calcium Saturated Surface Typic Paleudalf.

Measurements of the negative surface charge response to changes in soil pH using a NH_4NO_3 equilibration period of twenty-four hours, presented in Table 27, were more consistent with what would be expected for soil systems dominated by constant surface-potential colloids, i.e., greater CEC as the pH increases. The Haplustand and the Melanudand charge behavior, illustrated in Figures 69 and 70, indicated a dramatic and continuous increase in CEC with pH values beyond 5. However, the charge buffering capacity was greater above pH 5 for the Melanudand. The rise in CEC with pH for the Typic Paleudalf gave a different response pattern, reaching a plateau between pH 5 and 7. Additionally, the amount of CEC with greater pH was larger for both Andisols than for the Typic Paleudalf, which would suggest that the amorphous minerals and soil organic matter in these soils had greater pH dependent-charge potential than did those in the Typic Paleudalf. However, the AEC values for the Haplustand and Typic Paleudalf were very similar, and greater than that of the Melanudand. In summary, these results imply that a twenty four-hour period of shaking was necessary for completion of the exchange reactions, especially for Ca, though not as much for chloride, which are involved in the determination of surface charge properties by this method.

Table 27: Soil pH Effect on Surface Charge after a 1 M NH_4NO_3 Equilibration/Extraction Time of Twenty-Four Hours for Selected Calcium Saturated Surface Soils

Soil	pH ($CaCl_2$)	Ca^{2+} ex.	Al^{3+} ex.	Cl^- ex.	At soil pH ($CaCl_2$)	
					σ^-	σ^+
		$cmol_c\ kg^{-1}$				
Haplustand (0 -10cm)	3.18	2.17	3.56	0.87	-5.73	0.87
	4.04	6.12	1.00	0.49	-7.11	0.49
	5.23	8.95	0.13	0.11	-9.08	0.11
	6.18	11.23	0.10	0.04	-11.33	0.04
	7.09	14.82	0.03	0.04	-14.84	0.04
	8.10	20.06	0.12	0.00	-20.18	0.00
Melanudand (0 -20cm)	3.21	1.22	2.69	0.53	-3.91	0.53
	4.05	2.12	1.84	0.20	-3.96	0.20
	4.92	4.11	0.51	0.03	-4.62	0.03
	5.98	8.61	0.05	0.00	-8.67	0.00
	7.13	14.72	0.22	0.00	-14.94	0.00
	7.92	19.29	0.22	0.01	-19.51	0.01
Typic Paleudalf (0 -18 cm)	3.08	1.25	1.96	0.96	-3.21	0.96
	4.08	3.19	0.45	0.43	-3.64	0.43
	5.24	6.02	0.07	0.14	-6.09	0.14
	6.03	6.21	0.05	0.13	-6.26	0.13
	6.83	5.70	0.05	0.05	-5.74	0.05
	8.22	7.02	0.04	0.03	-7.06	0.03

The "Charge Fingerprint" method uses 1 M NH_4NO_3 solution as the Ca^{2+}, Al^{3+} and Cl^- exchangeable solution. However, 1 M $Mg(NO_3)_2$ solution was also used in this study in order to evaluate a divalent cation as part of the extracting solution. Table 28 presents charge data obtained with 1 M $Mg(NO_3)_2$ solution after a twenty four-hour equilibration period. The surface charge response to changes in pH determined by the 1 M NH_4NO_3 and 1 M $Mg(NO_3)_2$ solutions were similar in magnitude and pattern for every soil (Figures 72, 73 and 74), except at the two highest soil pH values for the Haplustand (Figure 74), where the $Mg(NO_3)_2$ solution extracted less Ca. The results suggest that Ca is held more strongly than Mg by the Haplustand at these pH values. These results also suggest that 1 M NH_4NO_3 solution is a reasonable solution to use to assess surface charge

in the studied soils. There are clogging difficulties with the atomic absorption spectrophotometer when $Mg(NO_3)_2$ is the background solution.

Table 28: Soil pH Effect on Surface Charge after a 1 M $Mg(NO_3)_2$ Equilibration/Extraction Time of Twenty-Four Hours for Selected Calcium Saturated Surface Soils

Soil	pH ($CaCl_2$)	Ca^{2+} ex.	Al^{3+} ex.	Cl^- ex.	At soil pH ($CaCl_2$)	
					σ^-	σ^+
		$cmol_c\ kg^{-1}$				
Haplustand (0 -10cm)	3.25	2.02	3.36	0.87	5.38	0.87
	4.05	5.87	1.32	0.42	7.19	0.42
	5.30	8.60	0.29	0.15	8.89	0.15
	6.23	10.66	0.15	0.04	10.81	0.04
	7.12	9.43	0.24	0.02	9.67	0.02
	8.16	11.59	0.24	0.03	11.83	0.03
Melanudand (0 -20cm)	3.27	0.95	3.23	0.54	4.17	0.54
	3.99	1.45	2.30	0.36	3.76	0.36
	5.12	4.03	1.17	0.10	5.20	0.10
	6.12	8.13	0.20	0.05	8.33	0.05
	6.90	15.35	0.05	0.04	15.40	0.04
	7.74	15.62	0.23	0.10	15.85	0.10
Typic Paleudalf (0 -18 cm)	3.04	1.00	1.62	0.18	2.62	0.18
	4.48	3.63	0.28	0.13	3.92	0.13
	5.00	4.28	0.54	0.08	4.82	0.08
	6.13	5.09	0.20	0.05	5.29	0.05
	7.54	5.03	0.40	0.06	5.43	0.06
	8.32	6.41	0.28	0.02	6.69	0.02

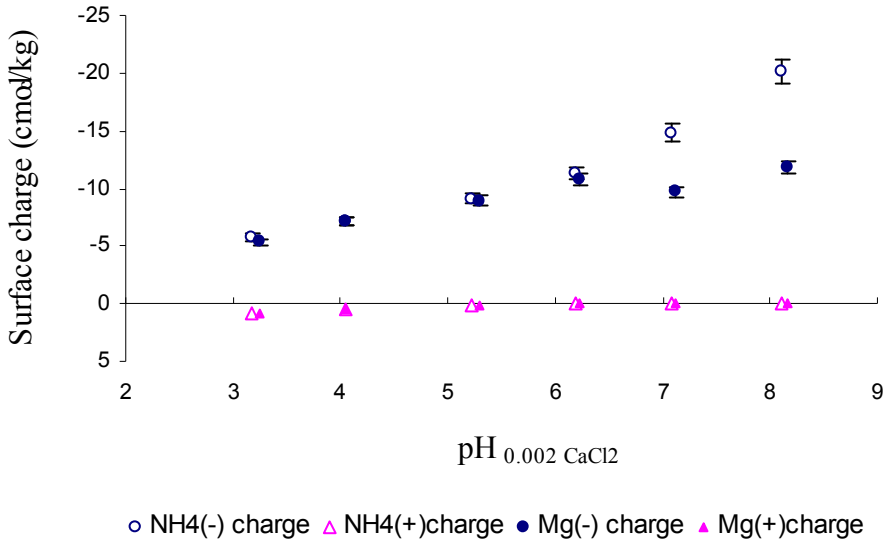

Figure 72: Soil pH Effect on Surface Charge of Calcium Saturated Surface Haplustand after Equilibration with 1 M NH_4NO_3 and 1 M $Mg(NO_3)_2$ Solutions.

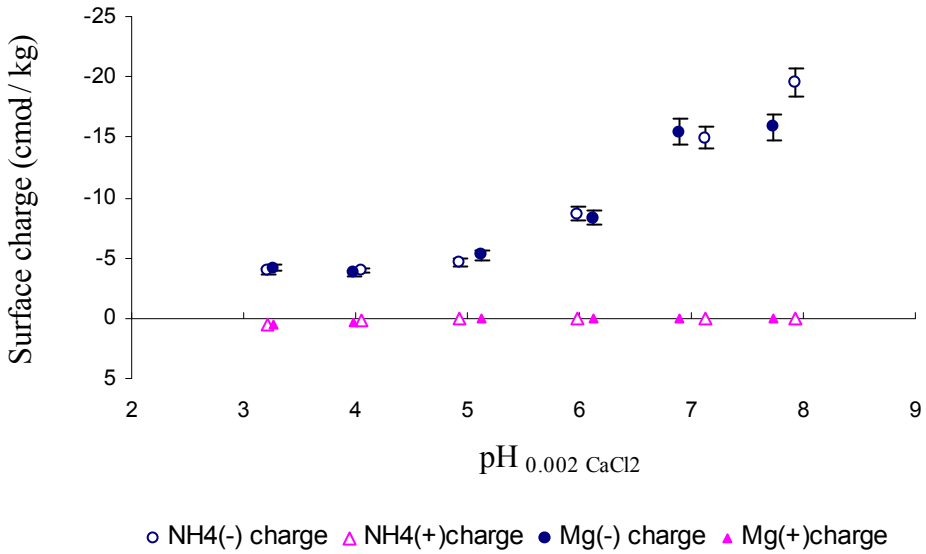

Figure 73: Soil pH Effect on Surface Charge of Calcium Saturated Surface Melanudand after Equilibration with 1 M NH_4NO_3 and 1 M $Mg(NO_3)_2$ Solutions.

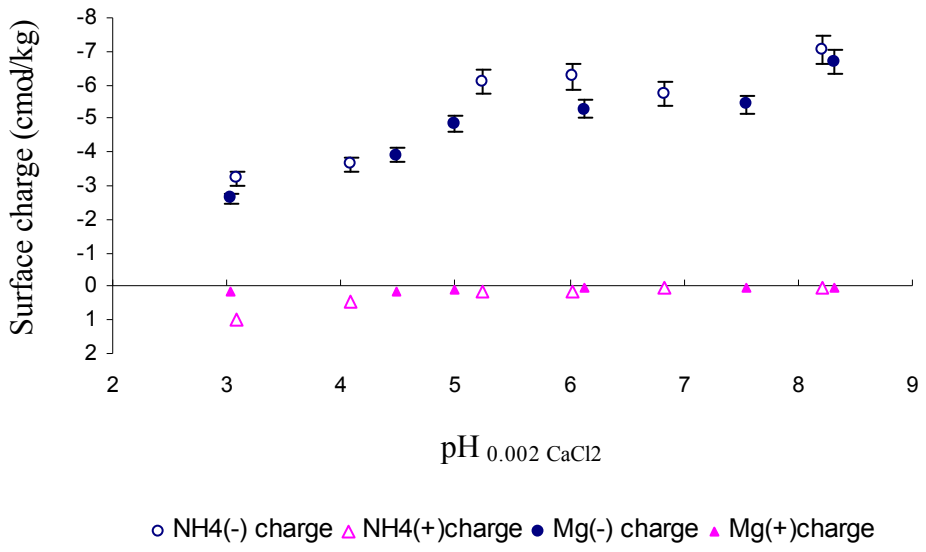

Figure 74: Soil pH Effect on Surface Charge of Calcium Saturated Surface Typic Paleudalf after Equilibration with 1 M NH_4NO_3 and 1 M $Mg(NO_3)_2$ Solutions.

Soil Electrochemical Properties after Calcium Saturation

The "Charge Fingerprint" method was standardized for the studied soils using a twenty four-hour equilibration period and 1 M NH_4NO_3 as the exchanging/extracting solution. It was assumed that this equilibration period was adequate for the exchange of Ca^{+2} by NH_4^+, which is supported by research results reported by other authors (Lumbanraja and Evangelou, 1994; Eick et al., 1990).

The same selected surface samples used for the standardization, and their respective subsurface samples, were analyzed. Table 29 illustrates the effect of soil pH on surface charge in the subsurface soil samples. The surface charge development with pH for the Ca saturated surface and subsurface soil samples was similar in the Haplustand and the Melanudand (Figures 75 and 76), which suggests that the constant surface-potential charge behavior was pretty consistent to a 30 and 40 cm depth, respectively. The Typic Paleudalf contrasted sharply with the two Andisols (Figure 77). While the

negative surface charge of the surface soil increased with greater soil pH, the negative surface charge of the subsurface soil decreased slightly as pH values rose to 6, followed by an increase at pH 7 and 8. The colloidal composition of the Paleudalf's surface horizon was quite different from that of the subsurface one (Appendix A). The surface horizon had lower kaolinite and greater organic matter than the subsurface, which implies that organic matter is responsible for increases in surface negative charge at lower soil pH values due to its lower pKa value, as compared to that of kaolinite. The greater amount of negative charge at low pH in the subsurface soil might indicate greater permanent negative charge in this soil layer. Nevertheless, very large differences in extractable aluminum at lower soil pH values between the surface and subsurface Typic Paleudalf suggest that the possible dissolution of kaolinite, caused by low pH, could also be associated with the contrasting behavior of the subsurface Typic Paleudalf.

Table 29: Soil pH Effect on Surface Charge after a 1 M NH_4NO_3 Equilibration/Extraction Time of Twenty-Four Hours for Selected Calcium Saturated Subsurface Soils

Soil	pH ($CaCl_2$)	Ca^{2+}ex.	Al^{3+} ex.	Cl^- ex.	At soil pH ($CaCl_2$)	
					σ^-	σ^+
		$cmol_c\ kg^{-1}$				
Haplustand	3.15	2.94	3.96	0.96	-6.91	0.96
	4.21	7.90	0.54	0.29	-8.44	0.29
(10-30cm)	5.09	9.84	0.08	0.13	-9.92	0.13
	6.06	11.48	0.12	0.07	-11.60	0.07
	7.01	15.23	0.10	0.02	-15.33	0.02
	8.10	20.64	0.17	0.03	-20.81	0.03
Melanudand	3.30	1.20	3.12	0.63	-4.32	0.63
	4.20	2.13	1.54	0.14	-3.67	0.14
(20-40cm)	5.09	3.80	0.34	0.02	-4.14	0.02
	5.99	6.84	0.08	0.00	-6.92	0.00
	7.00	13.97	0.08	0.00	-14.06	0.01
	8.22	18.49	0.12	0.00	-18.61	0.00
Typic Paleudalf	2.89	2.27	6.82	1.12	-9.09	1.12
	4.05	4.44	3.73	0.70	-8.17	0.70
(100-138 cm)	5.01	6.35	1.00	0.43	-7.35	0.43
	5.88	7.06	0.02	0.24	-7.08	0.24
	7.35	8.03	0.12	0.10	-8.15	0.10
	8.26	9.96	0.10	0.07	-10.07	0.07

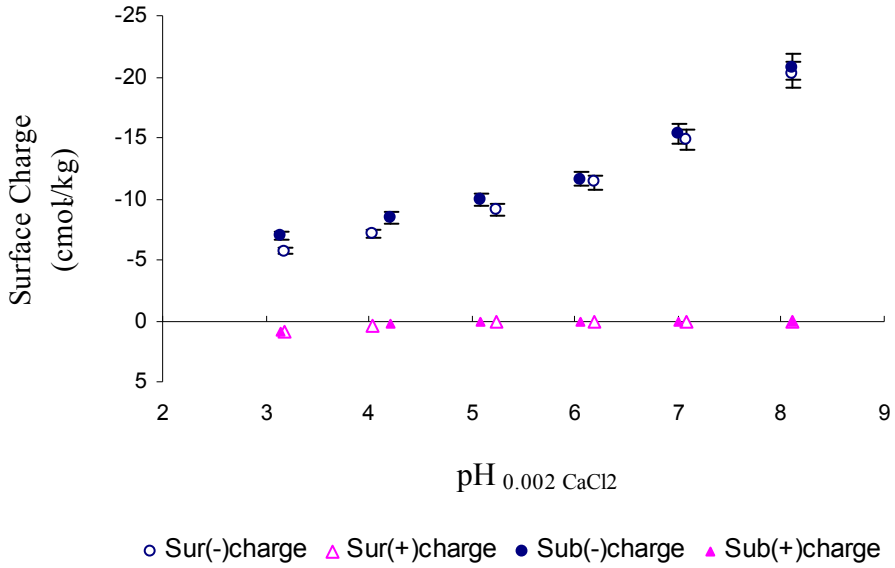

Figure 75: Soil pH Effect on Surface Charge of the Calcium Saturated Surface and Subsurface Haplustand.

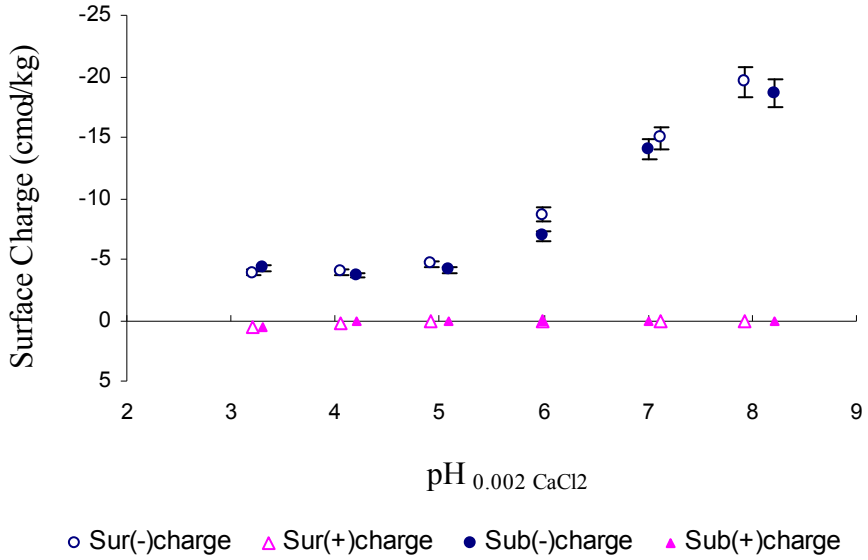

Figure 76: Soil pH Effect on Surface Charge of the Calcium Saturated Surface and Subsurface Melanudand.

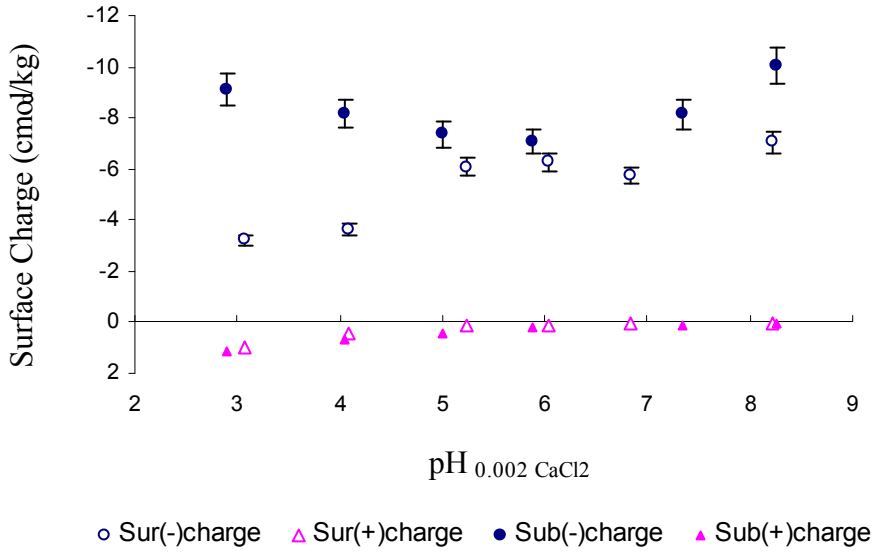

Figure 77: Soil pH Effect on Surface Charge of the Calcium Saturated Surface and Subsurface Typic Paleudalf.

The development of positive charge in both the surface and subsurface of every studied soil was much less than that of the negative charge. Those results could be explained by the high organic matter content present in both Andisols and the Typic

Paleudalf surface. Organic anions released by organic matter decomposition are adsorbed by positive charge sites, consequently reducing the measured AEC for the soil (Fox, 1982). Additionally, the lack of positive charge development in these Andisols could be related to their relatively high SiO_2/Al_2O_3 ratio, as Wada (1985) has reported for some Japanese Andisols. The mineralogy results suggest a low content of allophane and imogolite in the amorphous fraction of these two Andisols. The degree of development of negative and positive charge, across a range in pH and electrolyte concentration, for Andisols and weathered pumices depends on the kind of major ion-exchange materials (Wada, 1985). Wada (1985) found that only Andisols containing allophane and imogolite with a SiO_2/Al_2O_3 ratio of about 1 exhibited positive charge comparable with negative charge at field pH values, and positive charge was not found in soils containing Al-humus complexes unless the soil also contained allophane and imogolite.

The data used for determination of the pHo in selected Ca saturated surface and subsurface soil samples is given in Tables 30 and 31. As one can see in Figures 78 through 83, the quadratic equation was used to determine the pHo value, i.e., the point where $pH_{0.05} - pH_{0.002}$ was zero. There was no great difference in the pHo values for the surface and subsurface soil samples in both the Haplustand and the Melanudand. In contrast, the pHo found for the Typic Paleudalf subsurface was greater than that for the surface. These latter results imply that a higher pHo is associated with kaolinite than those found where organic matter and/or amorphous minerals dominate the colloid fraction. Gillman (1985) found that iron and aluminum oxides, which have high point of zero charge, tend to increase overall pHo, where as organic matter, with a low point of zero charge, would have the opposite effect. Additionally, the lower pHo values observed

for the studied soils are associated with a lack of positive surface charge development (Gillman and Sumpter, 1986b).

The PZNC could not be determined for all the studied soils because it was associated with values lower than the lowest soil pH used in this study. Consequently, for all of the soils the PZNC was less than the pHo (Table 32). The PZNC should be less than the pHo if the sign of the permanent charge is negative (Uehara and Gillman, 1980). The negative permanent surface charge associated with subsurface soil samples at the soil's field pH (Table 32) was highest for the Typic Paleudalf, and lowest for the Melanudand, which could be explained by the greater presence of organic matter in the latter soil. On the other hand, the Haplustand exhibited the highest net negative variable surface charge, which was expected since the greater the difference between the soil pH and pHo, the greater the negative surface charge development.

Table 30: pHo Determination Data for Selected Calcium Saturated Surface Soil Samples

Soil	$pH_{0.002}$	$pH_{0.05}$	$pH_{0.05} - pH_{0.002}$
Haplustand (0-10cm)	3.18	3.22	0.04
	4.07	3.84	-0.23
	5.15	4.66	-0.49
	6.15	5.54	-0.61
	7.04	6.37	-0.67
	8.07	7.33	-0.74
Melanudand (0-20cm)	3.22	3.27	0.05
	4.09	3.98	-0.11
	4.91	4.46	-0.45
	5.93	5.40	-0.54
	7.05	6.45	-0.60
	7.83	7.14	-0.70
Typic Paleudalf (0-18 cm)	3.10	3.06	-0.04
	4.03	3.79	-0.25
	5.00	4.61	-0.39
	5.96	5.62	-0.34
	6.78	6.34	-0.44
	8.13	7.53	-0.60

Table 31: pHo Determination Data for Selected Calcium Saturated Subsurface Soil Samples

Soil	$pH_{0.002}$	$pH_{0.05}$	$pH_{0.05} - pH_{0.002}$
Haplustand (10-30cm)	3.16	3.23	0.08
	4.2	3.92	-0.28
	5.11	4.65	-0.47
	6.1	5.58	-0.53
	6.96	6.35	-0.61
	8.07	7.35	-0.72
Melanudand (20-40cm)	3.31	3.33	0.03
	4.18	4.00	-0.19
	5.04	4.53	-0.52
	5.98	5.37	-0.61
	6.90	6.26	-0.64
	8.06	7.30	-0.77
Typic Paleudalf (100-138 cm)	2.93	3.00	0.06
	4.00	3.71	-0.29
	4.89	4.52	-0.37
	5.95	5.73	-0.22
	7.14	6.56	-0.58
	8.32	7.55	-0.77

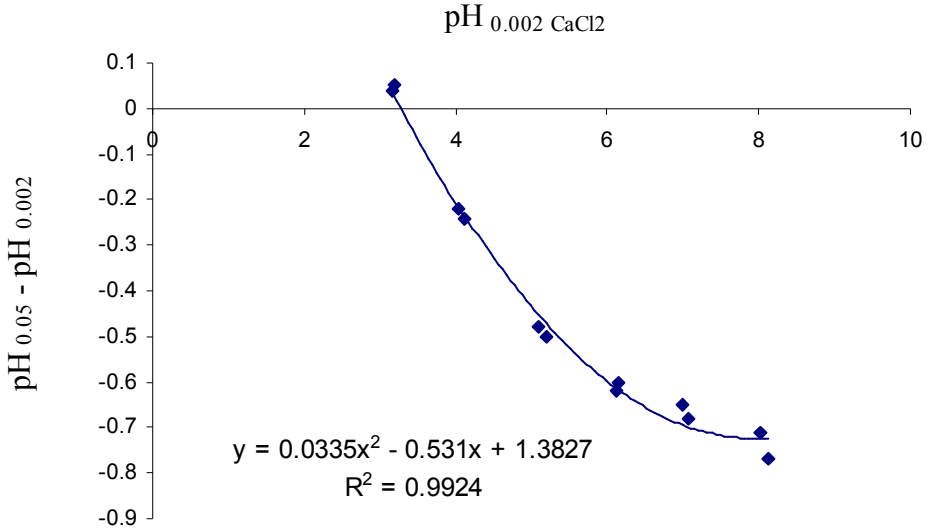

Figure 78: pHo Determination for the Calcium Saturated Surface Haplustand.

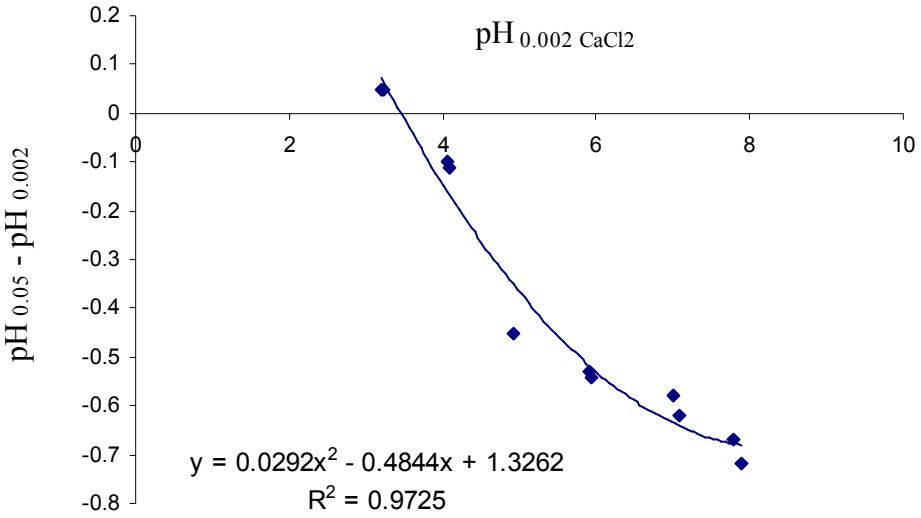

Figure 79: pHo Determination for the Calcium Saturated Surface Melanudand.

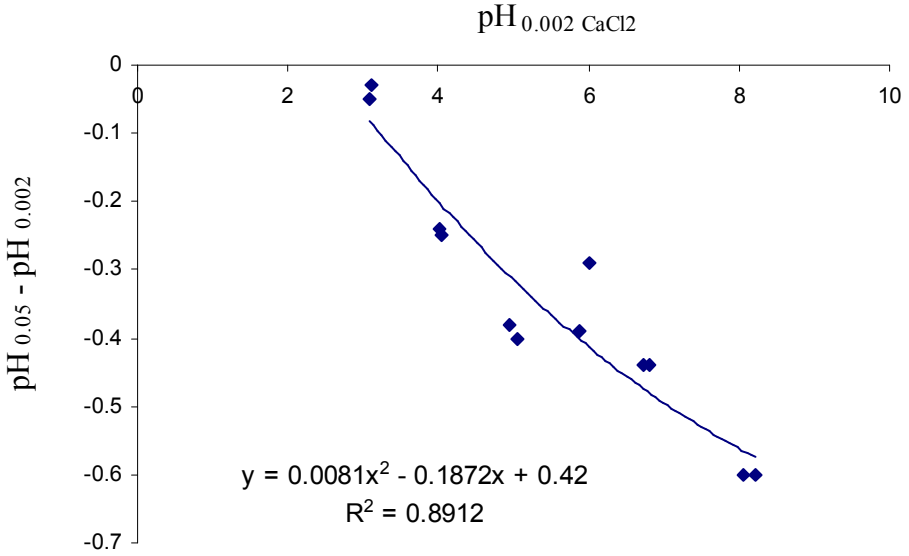

Figure 80: pHo Determination for the Calcium Saturated Surface Typic Paleudalf.

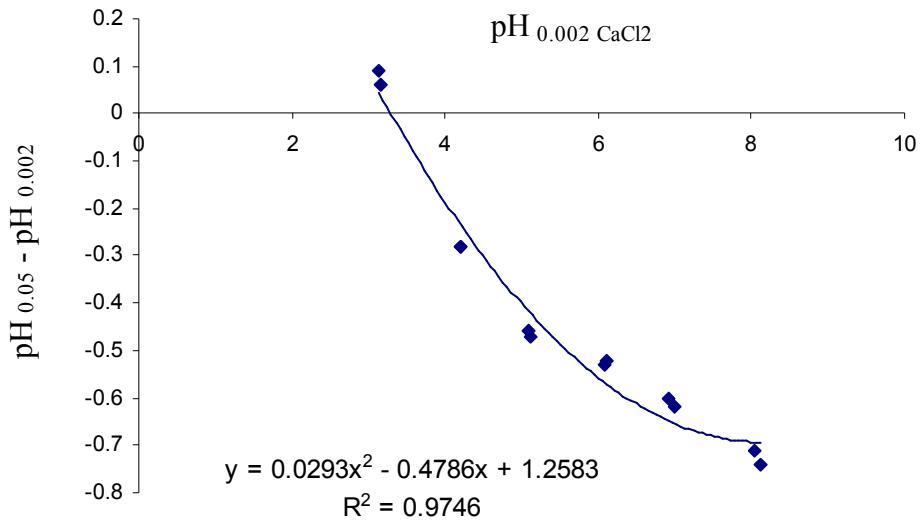

Figure 81: pHo Determination for the Calcium Saturated Subsurface Haplustand.

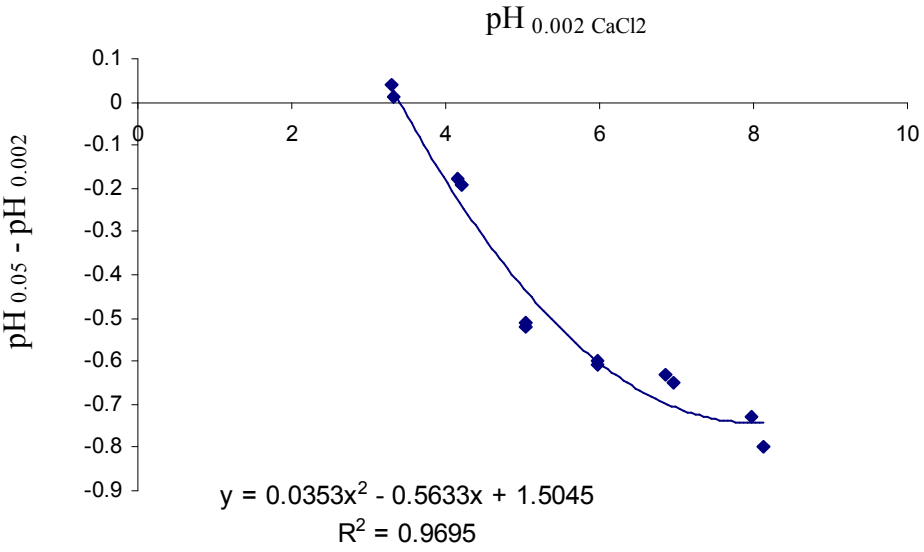

Figure 82: pHo Determination for the Calcium Saturated Subsurface Melanudand.

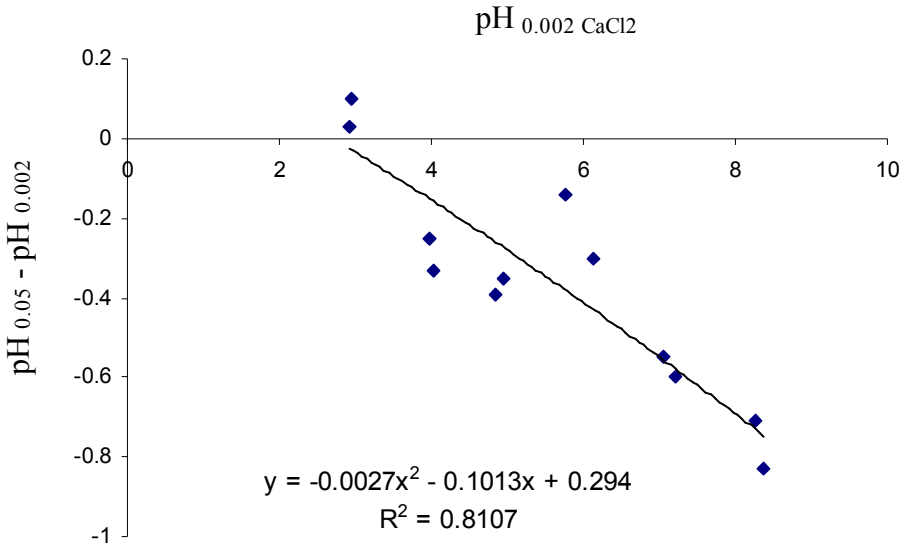

Figure 83: pHo Determination for the Calcium Saturated Subsurface Typic Paleudalf.

Table 32: Surface Charge Properties of Selected Calcium Saturated Soil Samples

Soil	PZNC	pH-$CaCl_2$	pHo		At soil pH ($CaCl_2$)		
				σ_p	σ^-	σ^+	Net σ_v
				cmolc kg-1			
Surface Haplustand	< 3.18	5.69	3.28	-4.77	11.21	0.20	-6.24
Subsurface Haplustand	< 3.15	6.19	3.29	-6.06	12.92	0.07	-6.79
Surface Melanudand	< 3.21	4.90	3.46	-2.94	5.92	0.07	-2.91
Subsurface Melanudand	< 3.30	5.04	3.39	-2.66	5.69	0.07	-2.96
Surface Typic Paleudalf	< 2.52	6.57	2.52	-1.96	5.93	0.08	-3.89
Subsurface Typic Paleudalf	< 2.89	5.75	4.92	-6.92	7.22	0.23	-0.07

Soil Electrochemical Properties after Potassium Saturation

The effect of divalent versus monovalent cation saturation in the measurement of charge characteristics was examined by repeating the standardized "Charge Fingerprint" method, i.e., twenty four-hour period of equilibration and 1 M NH_4NO_3 as the exchanging/extracting solution, on the same selected surface and subsurface samples, but using KCl as the saturating electrolyte. Tables 35 and 36 contain data illustrating the effect of soil pH on surface charge development in the surface and subsurface soil

samples, respectively. As soil pH increased, the development of negative surface charge was evident in every soil. In contrast, decreasing soil pH did not promote significant increases in positive surface charge. As illustrated in Figures 84 and 85, there was no particular difference in the amount of surface charge developed by K saturated surface and subsurface soil samples, either for the Haplustand or the Melanudand. This suggests that the amount of constant surface potential was consistent to a 30 or 40 cm depth in the two Andisols. In contrast, Figure 86 illustrates the great difference in negative surface charge between the surface and the subsurface Typic Paleudalf, though the pattern of charge development with pH was the same for both soil horizons. These results suggest that the amount of permanent charge in the subsurface horizon was greater than that in the surface. This conclusion is further supported by measured differences in colloidal composition between these horizons. However, dissolution of the solid phase primarily kaolinite, might be another factor causing the contrasting behavior between the Typic Paleudalf horizons.

The development of positive charge in both surface and subsurface layers was much less than that observed for negative charge. These results reinforce the patterns in surface charge behavior observed with the Ca-saturated soil samples.

Table 33: Soil pH Effect on Surface Charge after a 1 M NH_4NO_3 Equilibration/Extraction Time of Twenty-Four Hours for Selected Potassium Saturated Surface Soils

Soil	pH (KCl)	K^+ ex.	Al^{3+} ex.	Cl^- ex.	At soil pH (KCl)	
					σ^-	σ^+
		$cmol_c\ kg^{-1}$				
Haplustand (0-10cm)	3.06	0.95	3.56	1.27	-4.52	1.27
	4.02	1.88	1.08	0.39	-2.96	0.39
	5.07	3.49	0.23	0.03	-3.72	0.03
	6.13	5.91	0.00	0.00	-5.91	0.00
	7.06	9.67	0.00	0.08	-9.67	0.08
	7.94	13.70	0.00	0.12	-13.70	0.12
Melanudand (0-20cm)	3.14	0.14	3.44	0.82	-3.59	0.82
	3.95	0.33	2.22	0.08	-2.55	0.08
	5.07	1.56	1.22	0.04	-2.78	0.04
	6.12	5.29	0.11	0.03	-5.43	0.03
	7.29	10.71	0.00	0.03	-10.71	0.04
	8.13	13.57	0.00	0.00	-13.57	0.00
Typic Paleudalf (0-18 cm)	2.97	0.36	2.13	0.35	-2.50	0.35
	3.97	0.86	0.94	0.09	-1.80	0.09
	5.15	1.53	0.05	0.00	-1.59	0.00
	6.28	2.15	0.00	0.00	-2.15	0.00
	7.16	2.74	0.00	0.00	-2.74	0.00
	7.99	3.40	0.00	0.00	-3.40	0.00

Table 34: Soil pH Effect on Surface Charge after a 1 M NH_4NO_3 Equilibration/Extraction Time of Twenty-Four Hours for Selected Potassium Saturated Subsurface Soils

Soil	pH (KCl)	K^+ ex.	Al^{3+} ex.	Cl^- ex.	At soil pH (KCl)	
					σ^-	σ^+
		$cmol_c\ kg^{-1}$				
Haplustand (0-10cm)	3.16	1.39	4.22	1.16	-5.60	1.16
	4.11	2.74	1.08	0.26	-3.82	0.26
	5.19	4.34	0.03	0.07	-4.37	0.07
	6.16	6.56	0.00	0.00	-6.56	0.00
	7.26	9.26	0.00	0.00	-9.26	0.00
	8.20	13.19	0.00	0.00	-13.19	0.00
Melanudand (0-20cm)	3.18	0.58	3.50	0.88	-4.08	0.88
	4.02	1.86	2.06	0.10	-3.91	0.10
	4.96	1.79	1.32	0.00	-3.11	0.00
	6.08	3.76	0.39	0.00	-4.14	0.00
	7.08	8.69	0.00	0.00	-8.69	0.00
	8.08	15.22	0.00	0.00	-15.22	0.00
Typic Paleudalf (0-18 cm)	3.17	3.34	5.55	0.88	-8.90	0.88
	4.13	4.76	4.40	0.35	-9.16	0.35
	5.05	6.65	1.92	0.11	-8.57	0.11
	5.96	9.55	0.10	0.00	-9.65	0.00
	7.10	10.06	0.01	0.00	-10.08	0.00
	8.47	11.43	0.00	0.00	-11.45	0.00

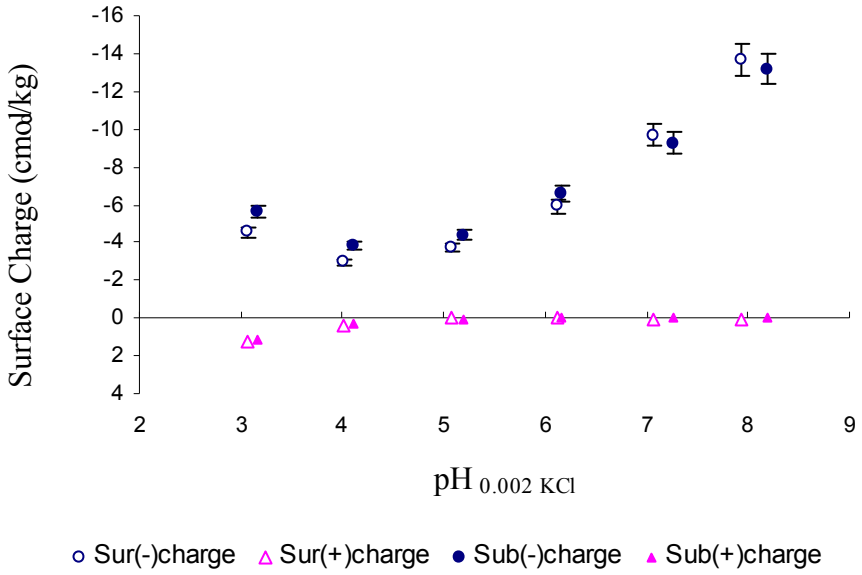

Figure 84: Soil pH Effect on Surface Charge of the Potassium Saturated Surface and Subsurface Haplustand.

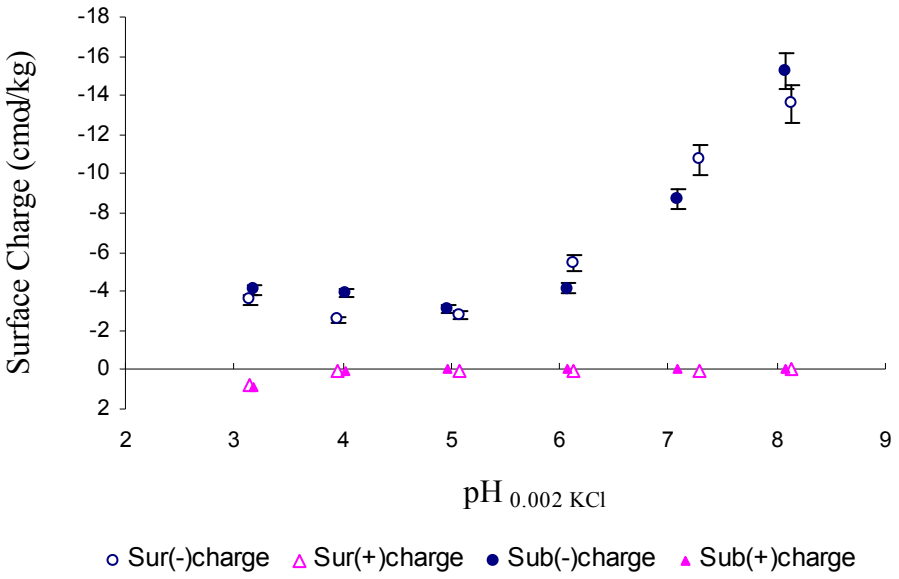

Figure 85: Soil pH Effect on Surface Charge of the Potassium Saturated Surface and Subsurface Melanudand.

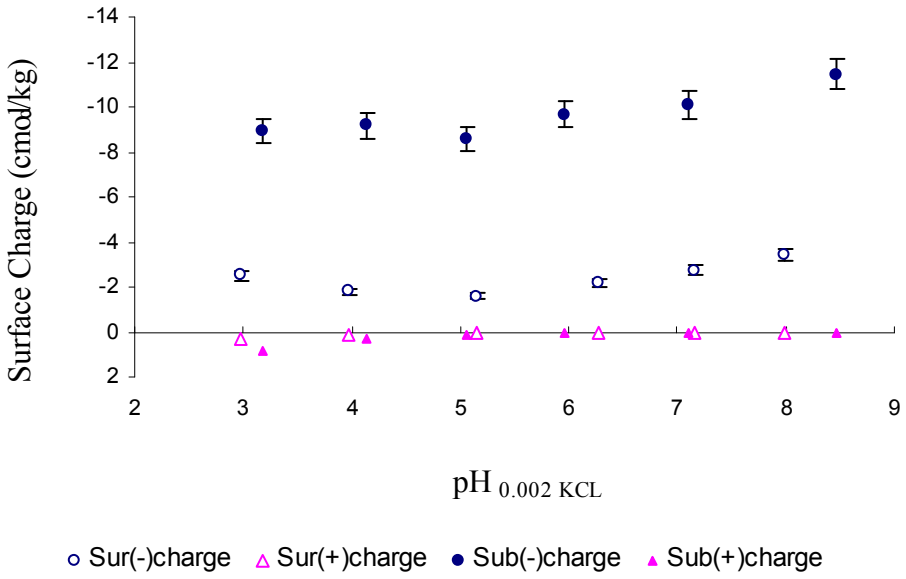

Figure 86: Soil pH Effect on Surface Charge of the Potassium Saturated Surface and Subsurface Typic Paleudalf.

The data used for determination of the pHo in selected K saturated surface and subsurface soil samples is given in Tables 37 and 38. As one can see in Figures 87 through 92, the quadratic equation was used to determine the pHo value. There was no difference in the pHo values between the surface and subsurface soil samples for each of the studied soils.

The PZNC could not be determined for all the studied soils because it was associated with values lower than the lowest soil pH used in this study. Values of PZNC below pH 3.0 were not pursued, because of the possible alteration of colloid surfaces through dissolution at such a low pH. However, it was clear that the PZNC was less than pHo for every studied soil (Table 37). The PZNC should be less than pHo if the sign of the permanent charge is negative (Uehara and Gillman, 1980). The negative permanent surface charge associated with subsurface soil samples at the soil's field pH was higher than that of the surface layer for every soil, and especially for the Typic Paleudalf. This soil had the lowest organic matter content in its subsurface horizon. Additionally, the greatest net negative variable surface charge was exhibited by the Haplustand, even though the greater difference between soil pH and pHo was found in the surface Typic Paleudalf. The results suggest soil organic matter and amorphous minerals were both important to the development of negative surface charge.

Table 35: pHo Determination Data for Selected Potassium Saturated Surface Soil Samples

Soil	$pH_{0.002}$	$pH_{0.05}$	$pH_{0.05} - pH_{0.002}$
Haplustand (0-10cm)	3.07	3.11	0.05
	4.02	3.88	-0.14
	5.02	4.62	-0.40
	6.10	5.45	-0.65
	7.04	6.44	-0.61
	7.94	7.46	-0.48
Melanudand (0-20cm)	3.16	3.13	-0.03
	3.96	3.86	-0.10
	5.08	4.47	-0.62
	6.11	5.53	-0.58
	7.25	6.79	-0.46
	8.02	7.53	-0.49
Typic Paleudalf (0-18 cm)	3.08	3.02	-0.05
	4.01	3.73	-0.28
	5.12	4.79	-0.34
	6.25	5.63	-0.62
	7.09	6.56	-0.53
	7.88	7.42	-0.47

Table 36: pHo Determination Data for Selected Potassium Saturated Subsurface Soil Samples

Soil	$pH_{0.002}$	$pH_{0.05}$	$pH_{0.05} - pH_{0.002}$
Haplustand (0-10cm)	3.17	3.13	-0.04
	4.09	3.87	-0.22
	5.15	4.70	-0.45
	6.10	5.27	-0.83
	7.16	6.26	-0.90
	8.10	7.28	-0.82
Melanudand (0-20cm)	3.17	3.21	0.05
	4.01	3.94	-0.07
	4.97	4.40	-0.57
	6.04	5.07	-0.97
	7.02	6.34	-0.68
	7.99	7.42	-0.57
Typic Paleudalf (0-18 cm)	3.15	3.11	-0.05
	4.04	3.60	-0.44
	5.00	4.09	-0.92
	6.09	5.51	-0.59
	7.09	6.61	-0.48
	8.16	7.44	-0.72

Table 37: Surface Charge Properties of Selected Potassium Saturated Soil Samples

Soil	PZNC	pH-KCl	pHo		At soil pH (KCl)		
				σ_p	σ^-	σ^+	Net σ_v
				$cmol_c\ kg^{-1}$			
Surface Haplustand	< 3.06	6.52	3.33	-2.20	7.61	0.00	-5.42
Subsurface Haplustand	< 3.16	6.68	3.22	-2.92	7.99	0.00	-5.07
Surface Melanudand	< 3.14	5.59	3.20	-1.73	5.17	0.00	-3.44
Subsurface Melanudand	< 3.18	5.65	3.45	-3.42	3.75	0.00	-0.33
Surface Paleudalf	< 2.97	7.34	2.89	-0.95	2.79	0.00	-1.84
Subsurface Paleudalf	< 3.17	5.01	2.77	-7.00	9.44	0.11	-2.33

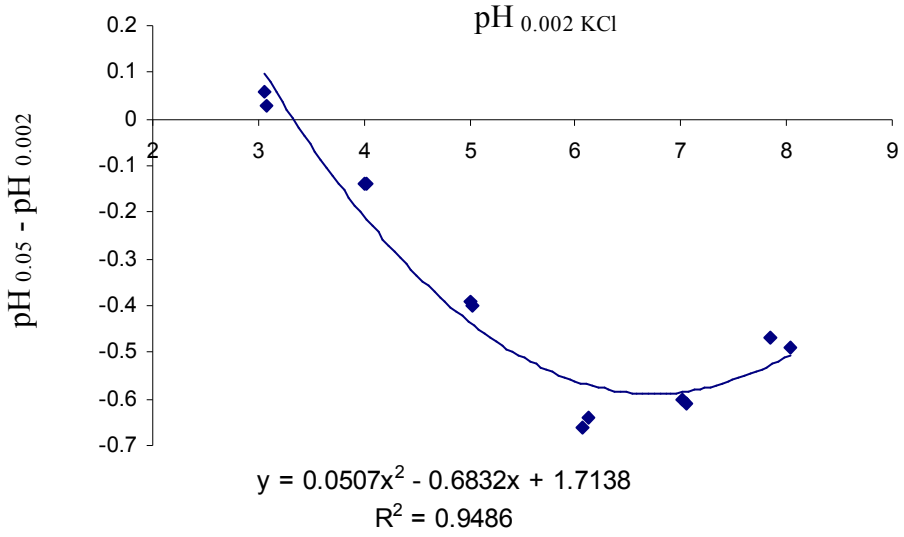

Figure 87: pHo Determination for the Potassium Saturated Surface Haplustand.

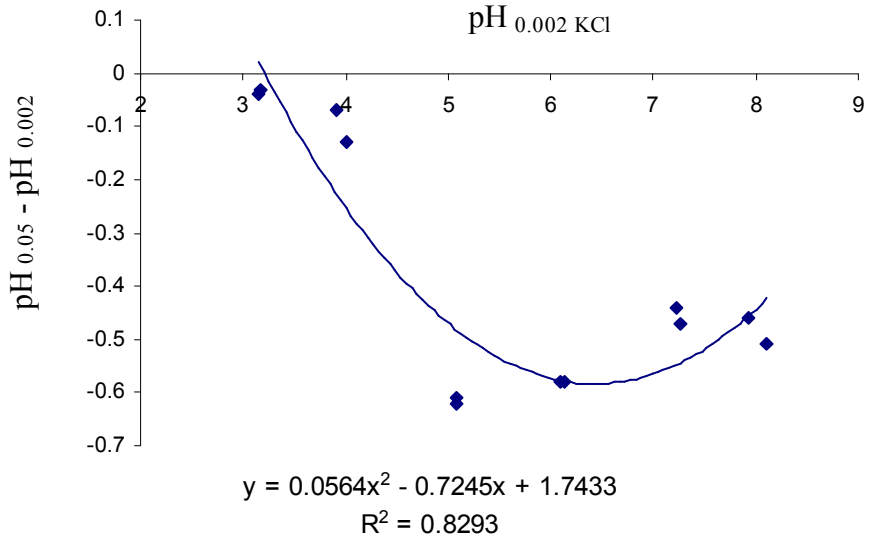

Figure 88: pHo Determination for the Potassium Saturated Surface Melanudand.

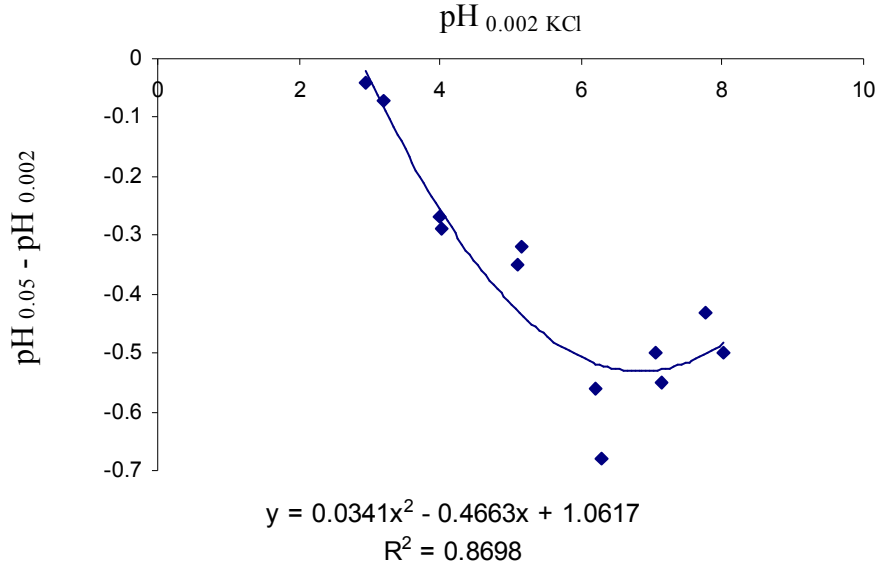

Figure 89: pHo Determination for the Potassium Saturated Surface Typic Paleudalf.

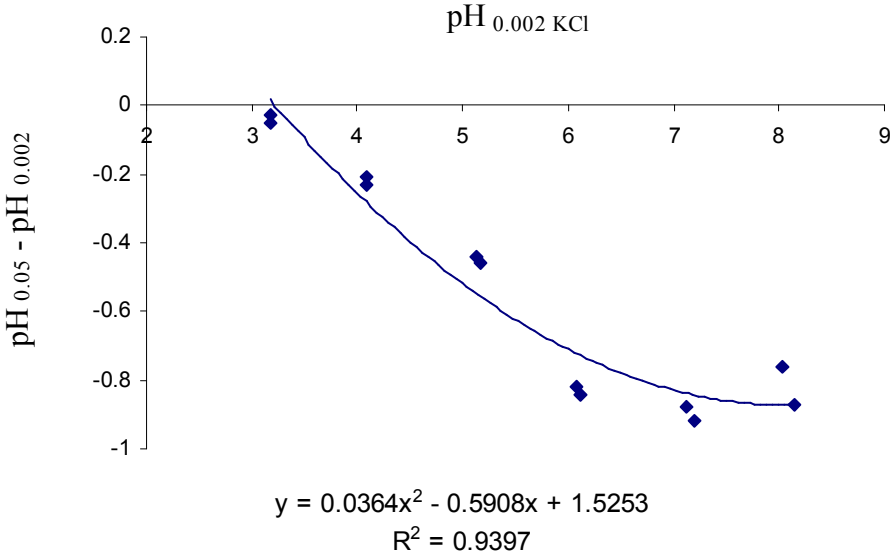

Figure 90: pHo Determination for the Potassium Saturated Subsurface Haplustand.

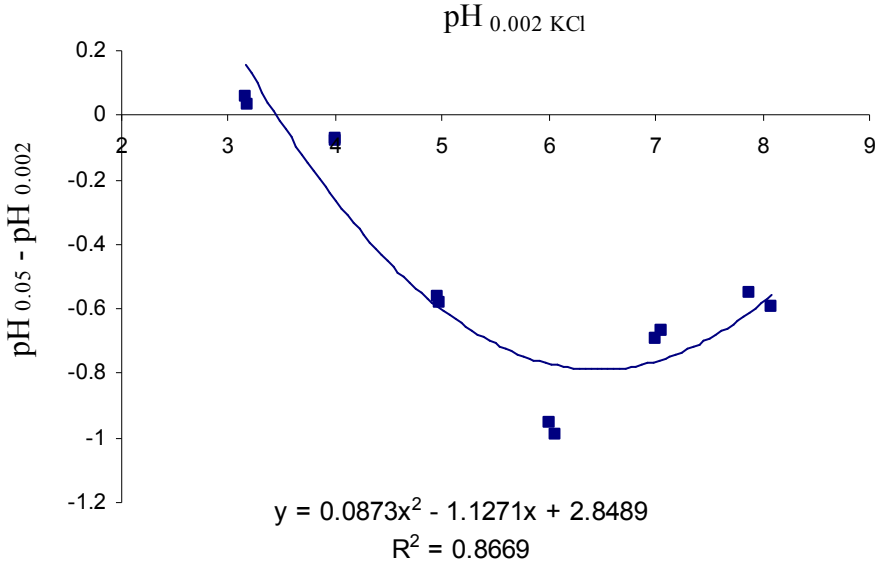

Figure 91: pHo Determination for the Potassium Saturated Subsurface Melanudand.

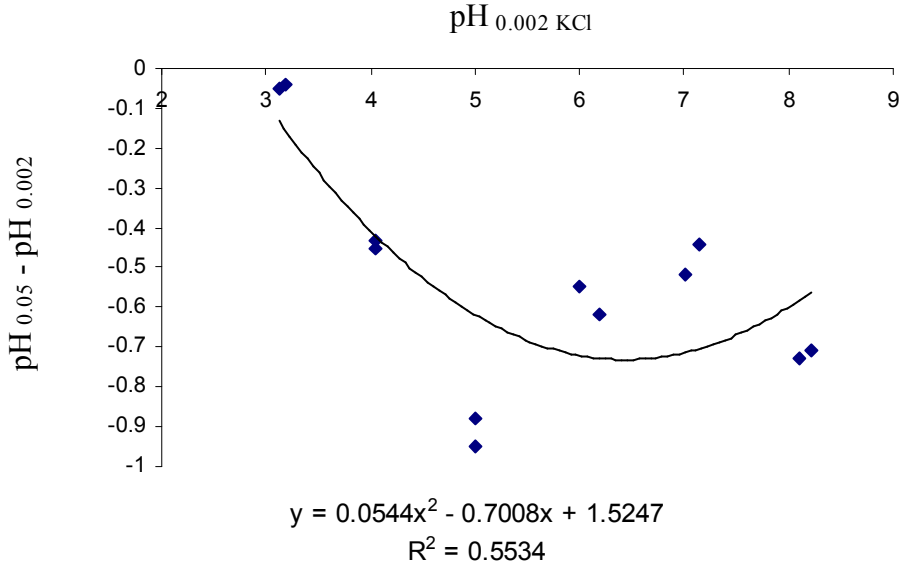

Figure 92: pHo Determination for the Potassium Saturated Subsurface Typic Paleudalf.

The Ca saturated surface and subsurface Haplustand developed more negative surface charge as soil pH values rose above 4 than did the respective K saturated soils

(Figures 93 and 94). Similar results were observed for the surface and subsurface Melanudand (Figures 95 and 96), though for this soil charge development diverged as soil pH values rose above 5. The results suggest that Ca^{2+} was preferred over K^{+} for both Andisols, regardless of depth. This was likely due to greater affinity between soil organic matter and Ca^{2+}. In contrast, the Typic Paleudalf exhibited differences in surface negative charge development after K or Ca saturation, depending upon whether the surface or subsurface soil horizon was being examined. The negative surface charge found subsequent to Ca saturation was higher than that for K saturation in the surface soil (Figure 97), but the opposite was true in the subsurface soil (Figure 98). The results imply preference for Ca over K in the surface horizon, and the opposite preference in the subsurface horizon.

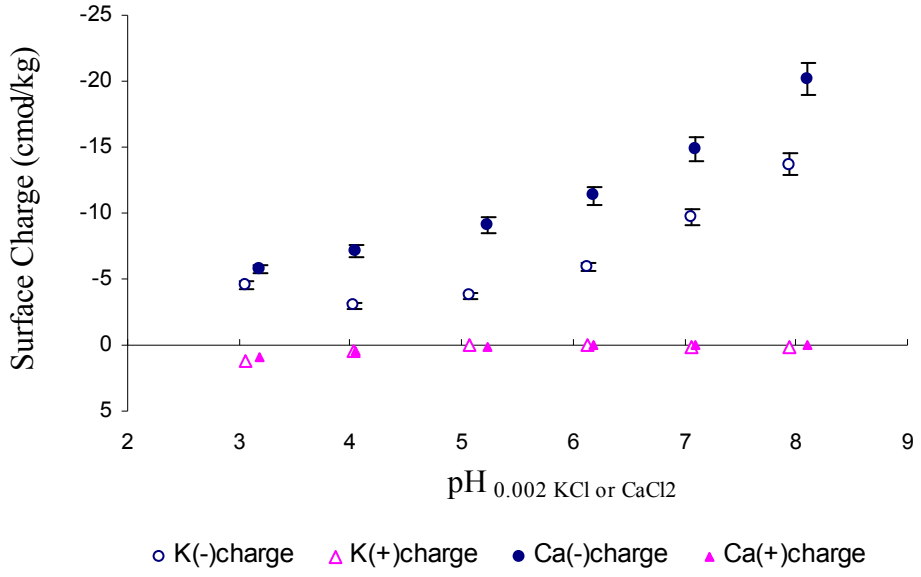

Figure 93: Soil pH Effect on Surface Charge in the Calcium and Potassium Saturated Surface Haplustand.

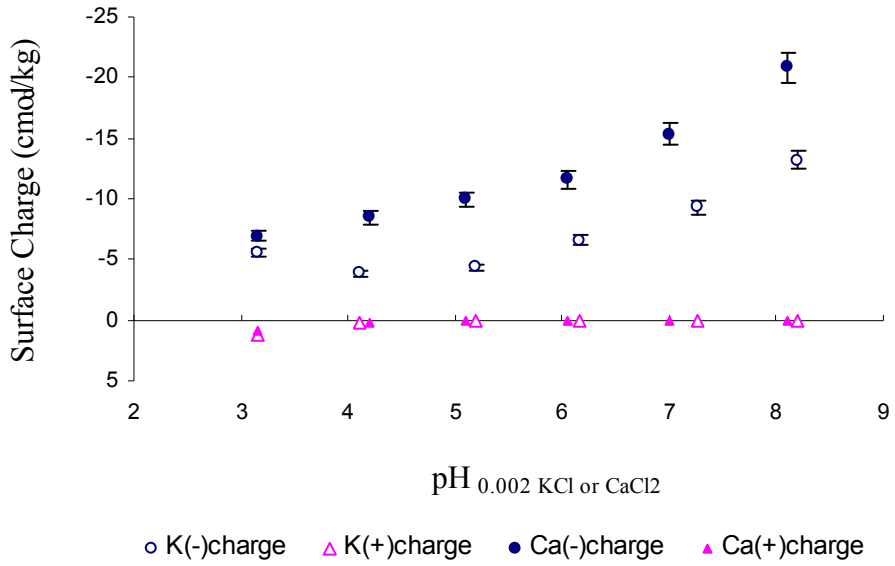

Figure 94: Soil pH Effect on Surface Charge in the Calcium and Potassium Saturated Subsurface Haplustand.

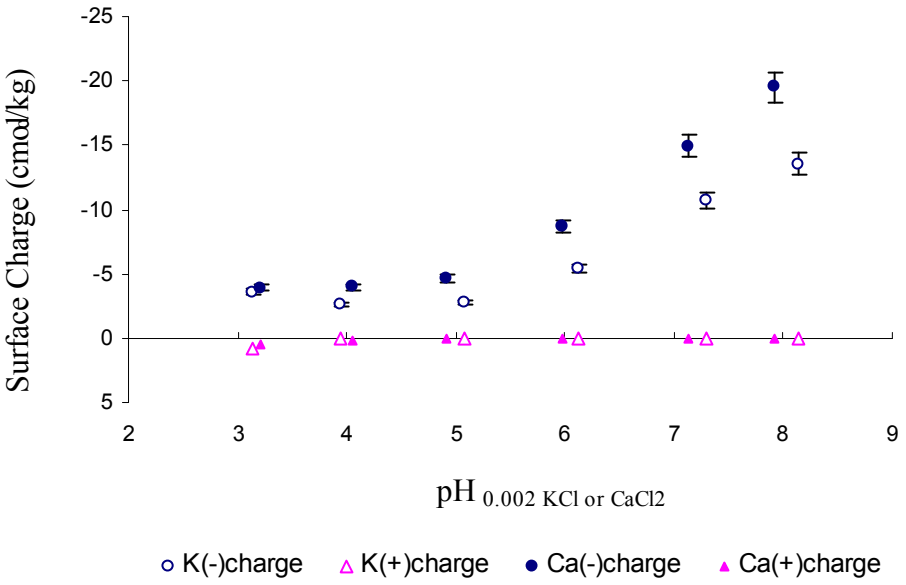

Figure 95: Soil pH Effect on Surface Charge in the Calcium and Potassium Saturated Surface Melanudand.

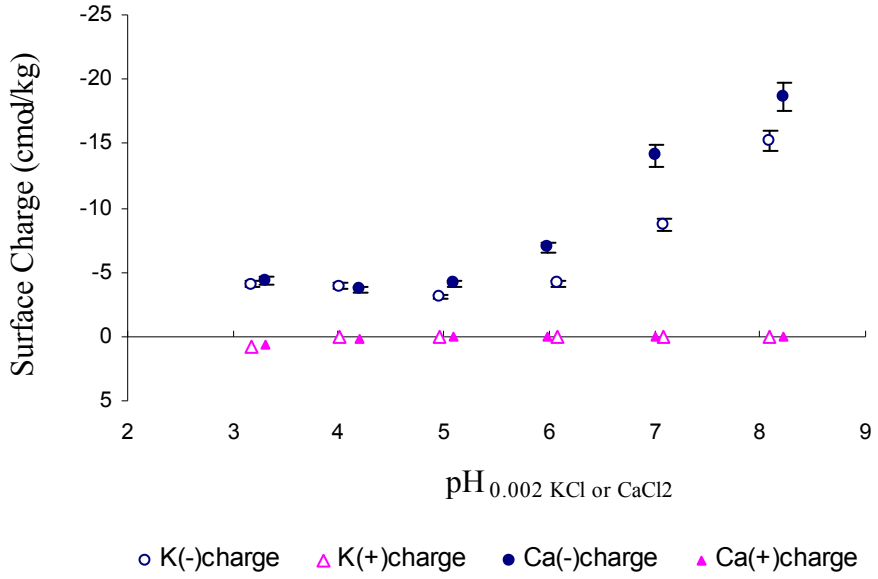

Figure 96: Soil pH Effect on Surface Charge in the Calcium and Potassium Saturated Subsurface Melanudand.

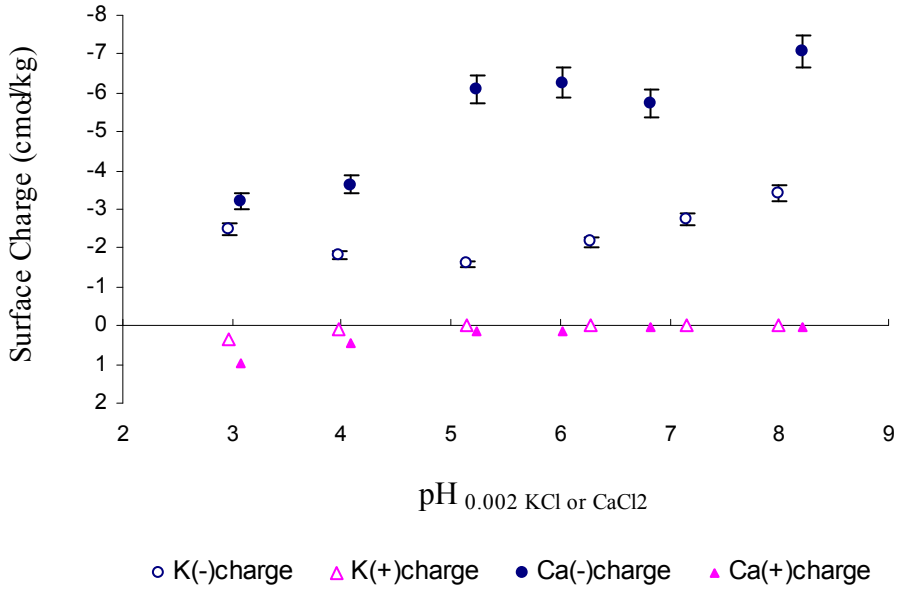

Figure 97: Soil pH Effect on Surface Charge in the Calcium and Potassium Saturated Surface Typic Paleudalf.

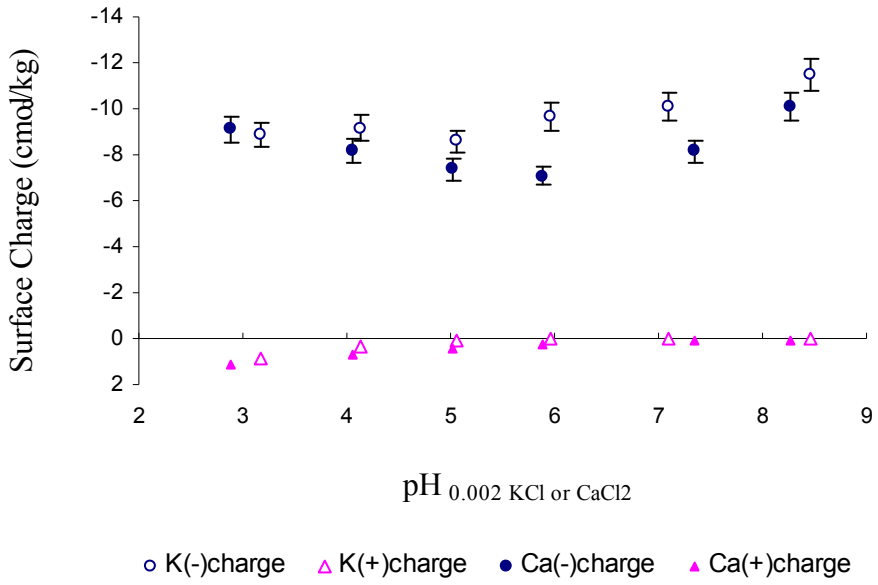

Figure 98: Soil pH Effect on Surface Charge in the Calcium and Potassium Saturated Subsurface Typic Paleudalf.

There was a difference in soil solution pH (pH 0.002 M $CaCl_2$ or KCl) after K and Ca saturation of all the studied soils (Tables 34 and 39). K-saturated samples exhibited higher soil pH values than those of Ca-saturated ones, except for the subsurface Typic Paleudalf. The divalent cation was a better potential determining ion than the monovalent one for the studied Andisols, and developed greater negative surface charge and lower soil solution pH, which suggests low-affinity specific adsorption of Ca^{2+} by these soils. Low-affinity specific adsorption of a cation would induce additional negative charge in constant surface potential colloids by proton desorption (Uehara and Gillman, 1981). Additionally, Evangelou and Karathanasis (1986) indicated that organic matter had lower affinity for the monovalent cation (low Kg). That supports the finding of greater Ca affinity in soils with an abundance of soil organic matter. In contrast, Ca adsorption would not be favored in soils dominated by kaolinite or HIV as is that of the subsurface Typic Paleudalf, where K^+ was preferred over Ca^{2+}.

There was no great difference in the pHo values determined after Ca or K saturation for all the studied soils except for the subsurface Typic Paleudalf. The organic matter and amorphous minerals present in the Andisols have similar pHo values. In contrast, kaolinitic colloids caused the higher pHo that was observed using Ca saturation of the subsurface Typic Paleudalf. Additionally, the pHo for both of the studied Andisols, located in the very acid range, was also observed by Uehara and Gillman (1981), who reported a pHo of 3.5 for a Haplustand. There was not a large difference in pHo values between the two Andisols, contrary to what was expected since the amorphous mineral fraction for each Andisol exhibited differences in their SiO_2/Al_2O_3 ratios (Table 4). That result could be explained either by the presence of similar proportions of each of the variable charge components or that organic matter dominated the constant surface potential colloid suites of both soils. Organic molecules would be adsorbed onto the amorphous minerals, modifying the protonation/deprotonation reactions (Gillman, 1985).

The surface negative charge at soil solution pH (0.002 M $CaCl_2$ and/or KCl) was higher for the Haplustand than for the Melanudand (Tables 34 and 39); even though the organic mater content was lower in the former Andisol. Those results could be explained by the fact that the difference between soil solution pH and pHo was higher for the Haplustand, and this is the major factor governing the magnitude of surface charge (Uehara and Gillman, 1981). That also would explain the higher buffer capacity exhibited by the Melanudand, which did not reach a soil pH greater than 6.9 after an application of 18 ton lime/ha (Table 18).

There was a difference in the permanent negative charge calculated at soil solution pH due to the Ca and K saturation of the Andisols (Tables 34 and 39). Greater

permanent negative charge was found in the Ca saturated samples, especially for the Haplustand. Those results suggest that the interaction between Ca and the colloids is stronger than that of a low affinity specific adsorption reaction in these Andisols. There may be a type of inner-sphere complex, as suggested by Charlet and Sposito (1989), working with some Oxisols. Another explanation, given by Gillman and Fox (1980), suggests that the presence of too much Ca would cause charge reversal when Ca is adsorbed into Stern layer, and would mean that even though surface charge density was greatly increased, the capacity to retain indifferent nutrient cations such as NH_4^+ and K^+ would be reduced. That would also explain why concentrated super phosphate would have a more beneficial amendment effect than single super phosphate, owing to the lower calcium/phosphate ratio of the former. Field experiments have shown that the CEC of a hydrandept and a gibbsihumox were significantly increased, and losses of Ca, Mg, and K reduced, by the application of triple super phosphate.

Quantity-Intensity Relationships

Potassium Quantity-Intensity in the Haplustand

Fertilization treatments applied to the surface Haplustand caused dramatic changes in the soil's potassium quantity-intensity relationships (Figure 99). The control and +N treatments exhibited similar sized labile pools for K, which were lower than that of the rest of the treatments. This was expected since those former treatments did not include any potassium fertilization. Also, it was evident that there were differences in slope with every fertilizer treatment except between +NPK and +NPKSMg. The steep slope of the control plot indicated that K on the exchange complex of this soil was being held with the greatest affinity. When the soil was nitrogen fertilized, the potassium buffer

capacity decreased. Fertilizer K addition further decreased the soil's potassium buffer capacity. When $CaCO_3$ was added, the buffer capacity increased. The results imply that lower soil pH values, related to nitrogen fertilization, could be modifying the potential potassium buffering capacity in this soil. However, there was a large difference in potential potassium buffer capacity between the control and the +NPKSMgCa treatments even though, both of them exhibited similar soil pH values and exchangeable calcium values (Figure 100). In contrast, there was no significant difference in the potential potassium buffer capacity of the +N and +NPKSMgCa treated soils, despite differences in soil pH and exchangeable potassium. Those results suggest not only a close relationship among pH, calcium availability, and the potential potassium buffer capacity, but also the dominant effect of Ca^{2+} on the exchange sites. The net CEC due to calcium adsorption, associated with lower K activities, was positive for both the control and the +N treatments (Figures 101 and 102) which implies that calcium adsorption was dominating, independently of soil pH. When potassium was applied at lower soil pH, Ca (+NPK treatment and Mg) desorption occurred and net negative CEC values were generally observed (Figures 103 and 104). However, when $CaCO_3$ was added, net CEC values were positive at higher K equilibrium values (Figure 105). Exchangeable K and its saturation of the soil's CEC, varied most between treatments that did, or did not receive fertilizer K (Figure 106).

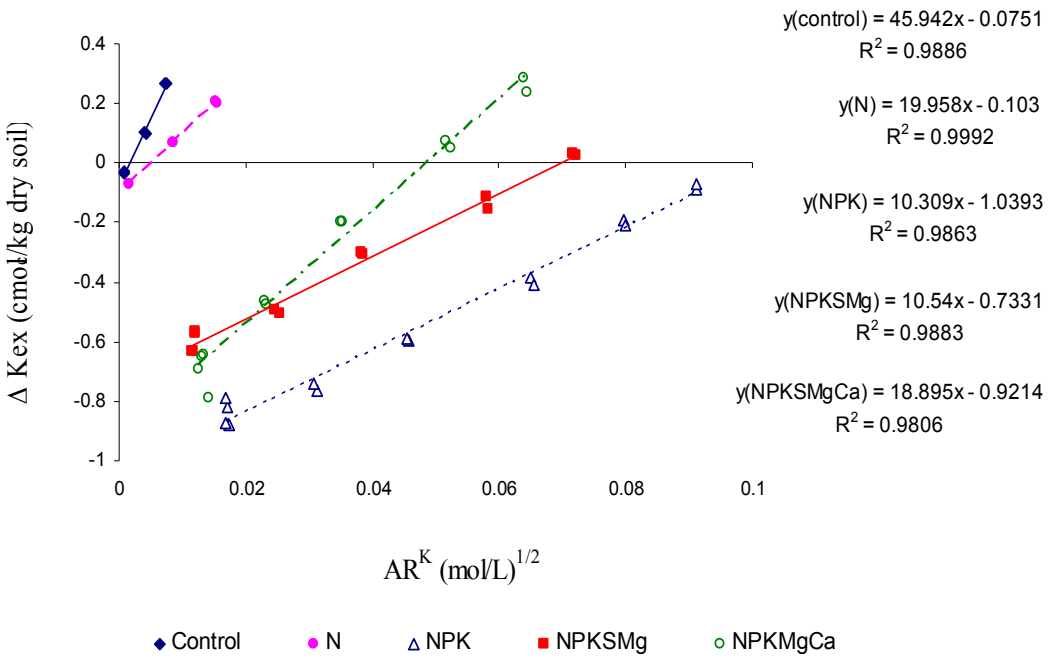

Figure 99: Quantity-Intensity Plot for the Surface Haplustand after Fertilization.

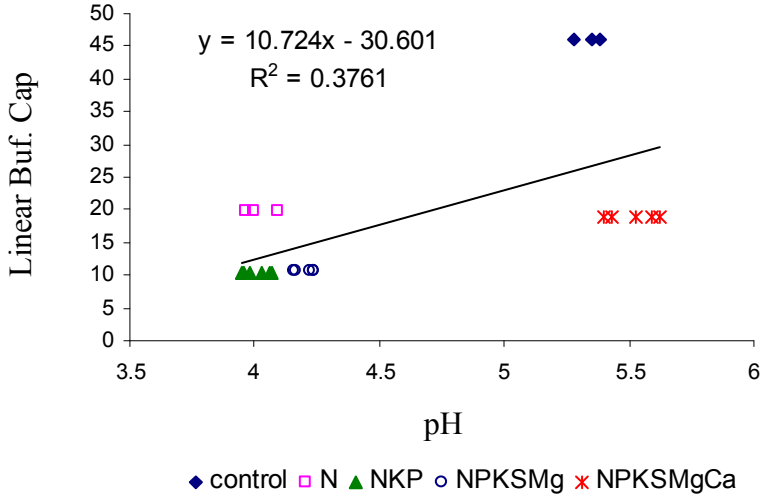

Figure 100: Quantity-Intensity Slope vs. pH for the Surface Haplustand.

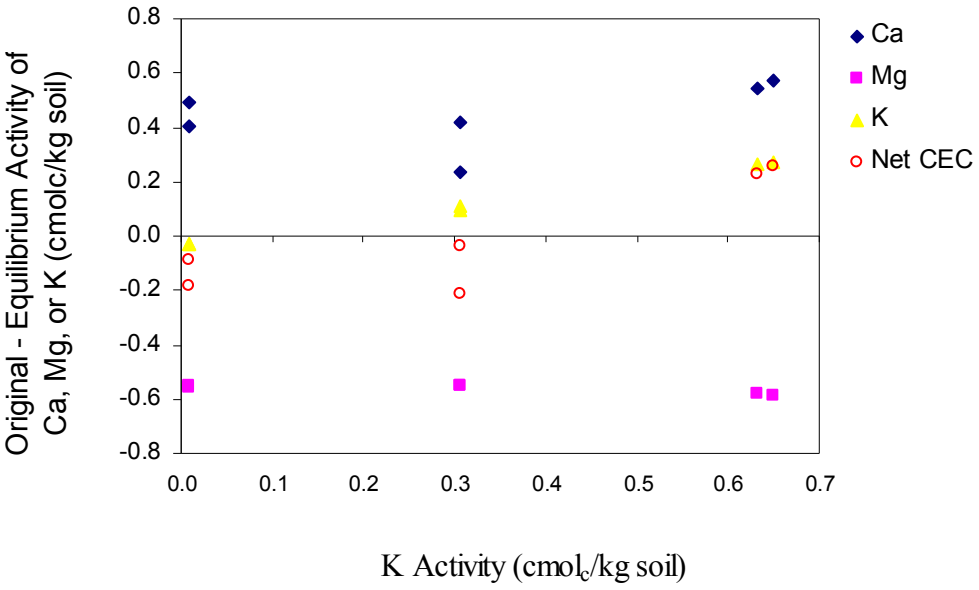

Figure 101: Change in Net CEC and Exchangeable Ca, Mg, and K vs. K Activity for the Surface Haplustand (Control Treatment).

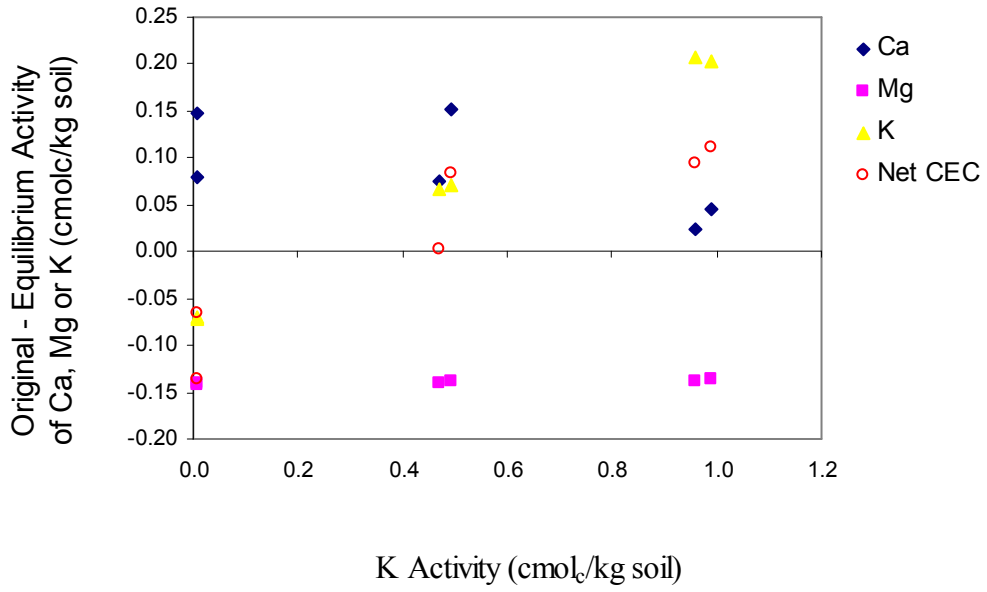

Figure 102: Change in Net CEC and Exchangeable Ca, Mg, and K vs. K Activity for the Surface Haplustand (+N Treatment).

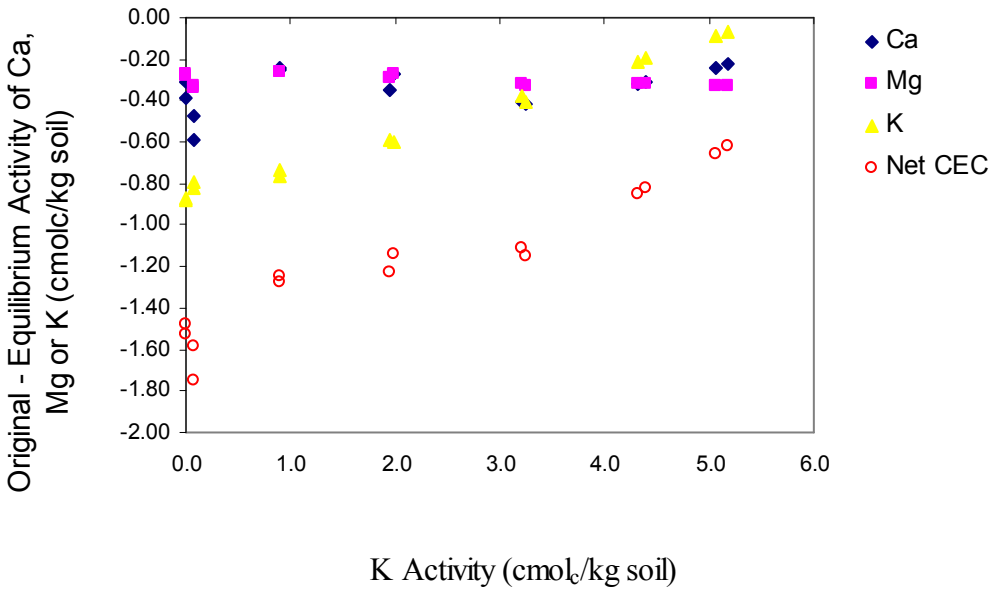

Figure 103: Change in Net CEC and Exchangeable Ca, Mg, and K vs. K Activity for the Surface Haplustand (+NPK Treatment).

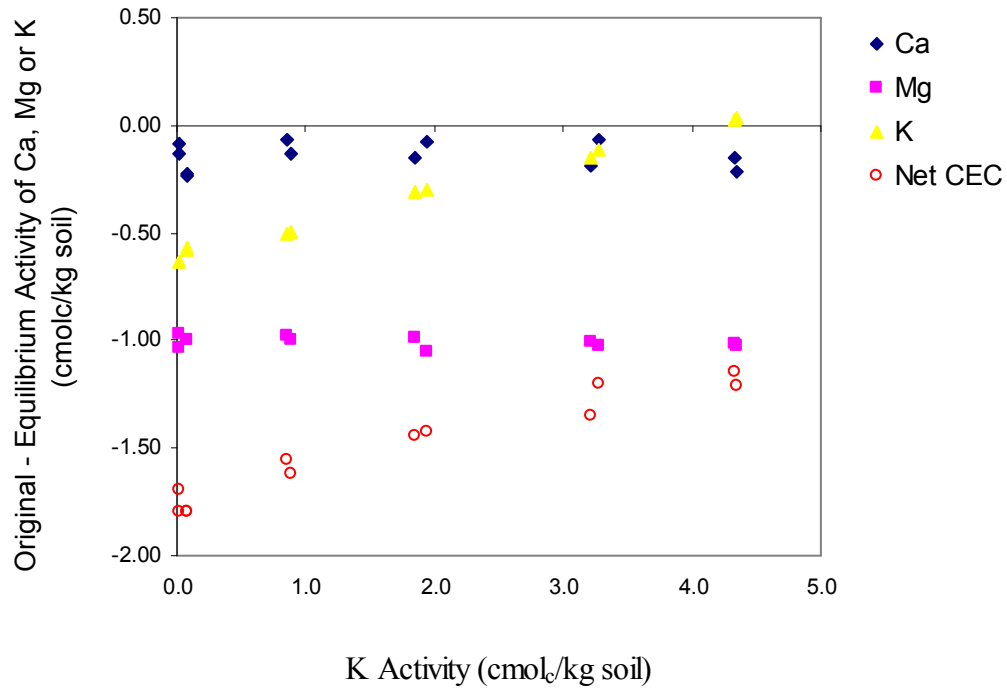

Figure 104: Change in Net CEC and Exchangeable Ca, Mg, and K vs. K Activity for the Surface Haplustand (+NPKSMg Treatment).

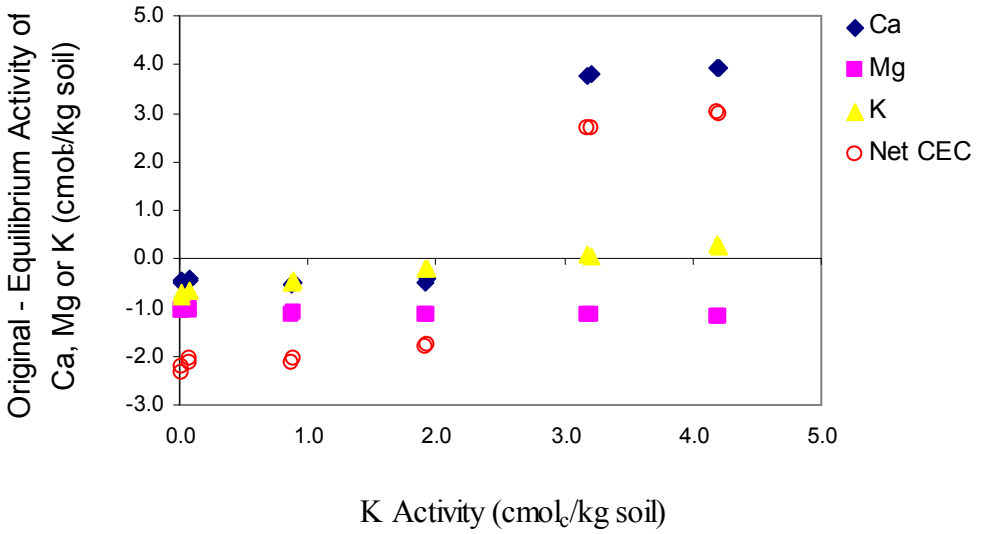

Figure 105: Change in Net CEC and Exchangeable Ca, Mg, and K vs. K Activity for the Surface Haplustand (+NPKSMgCa Treatment).

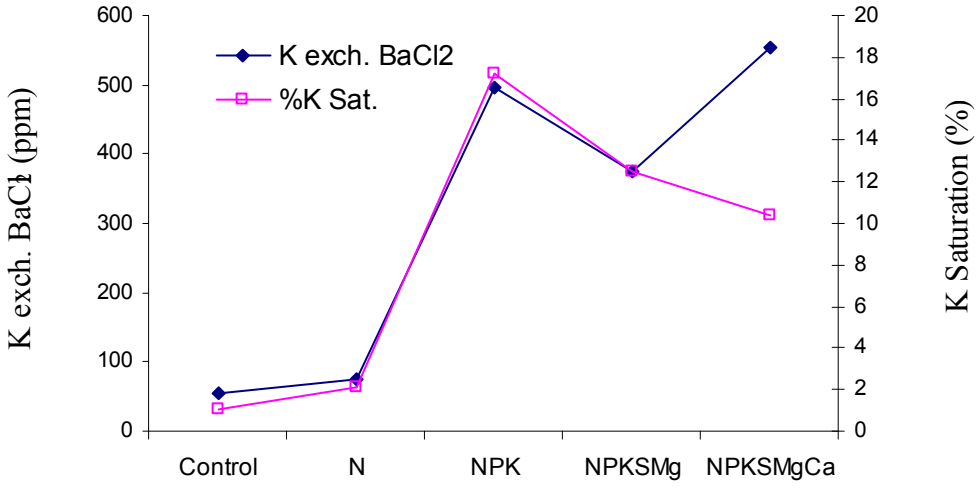

Figure 106: Exchangeable K and K Saturation of the Fertilizer Treated Surface Haplustand.

The Gapon coefficients, given in Appendix D were calculated from K, Ca, and Mg concentrations determined by the quantity-intensity procedure, plus the exchangeable Ca and Mg in the soil as determined by extraction with 1 M $BaCl_2$, which was the method

that more consistently found changes due to fertilizer treatment. There were greater differences in Q/I relationships due to the fertilizer treatments for the surface horizon than for the subsurface horizon. The highest and the lowest Gapon coefficient values were associated with +N and +NPKSMgCa treatments respectively, which indicates that even though K is being held on the exchange complex of the soil with similar affinity for both of those treatments, i.e., similar slope in the quantity-intensity curves, the amount of K in soil solution is higher in the latter one, and supported by its greater labile K pool (exchangeable K). This appears to be directed related to the low leaf yellowing and largest oil palm yield observed for this treatment in the field trial. In addition, the equilibrium Gapon coefficients (at ΔKex = 0) shown in Figure 107 further suggest that the control and +N treatments have lower soil solution K availability.

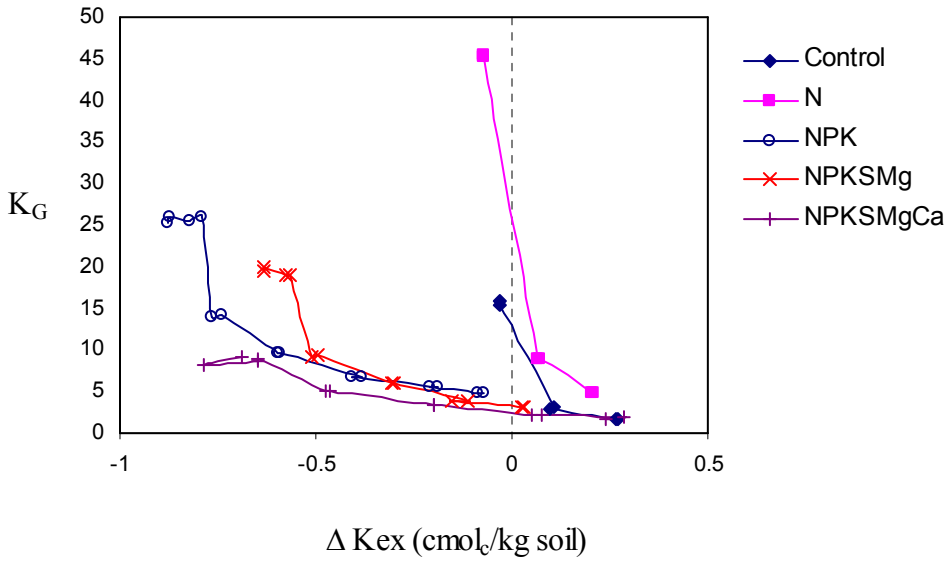

Figure 107: Gapon Coefficients (K_G) vs. ΔK ex for the Surface Haplustand

The Q/I relationships for the subsurface Haplustand were also influenced by fertilization (Figure 108; Appendix D). As was observed in the surface soil, both the

control and +N treatments exhibited similarly small labile pools for K, considerably lower than that of the other treatments. Also, the most steeply sloping relationship occurred in the control. When the soil was nitrogen fertilized, the potential potassium buffer capacity decreased, following a trend similar to that observed in the surface soil. However, the magnitude of the potential K buffer capacity was much higher for the subsoil samples than for the respective surface ones. That could be due to the subsurface soil receiving a considerable amount of macrocations, especially Ca, associated with dramatic changes in surface soil pH and the leaching process. As a result, subsurface soils exhibited greater CEC, across all the fertilizer treatments, which suggest that potassium would be held on the exchange complex with higher affinity. There was a poor relationship between pH and the potential K buffer capacities observed in the subsurface soil (Figure 109). Even between those treatments exhibiting similar soil pH and exchangeable Ca values, there were significant differences in potential K buffer capacity, which were more related to the size of the labile pool of potassium. That behavior was more clearly observed after calculation of the Gapon coefficients (Appendix D). The highest equilibrium coefficient was exhibited by the +N treatment (Figure 110), i.e., the lowest available potassium, which also has the lowest labile pool of potassium. On the other hand, it is important to point out that even though the three treatments receiving K fertilizer have similar Gapon coefficients, only the +NPKSMgCa treatment had Mg and K activities high enough to cause net negative CEC values, due to Ca desorption, to be observed at lower potassium activity levels. That behavior is illustrated in Figures 111 through 115.

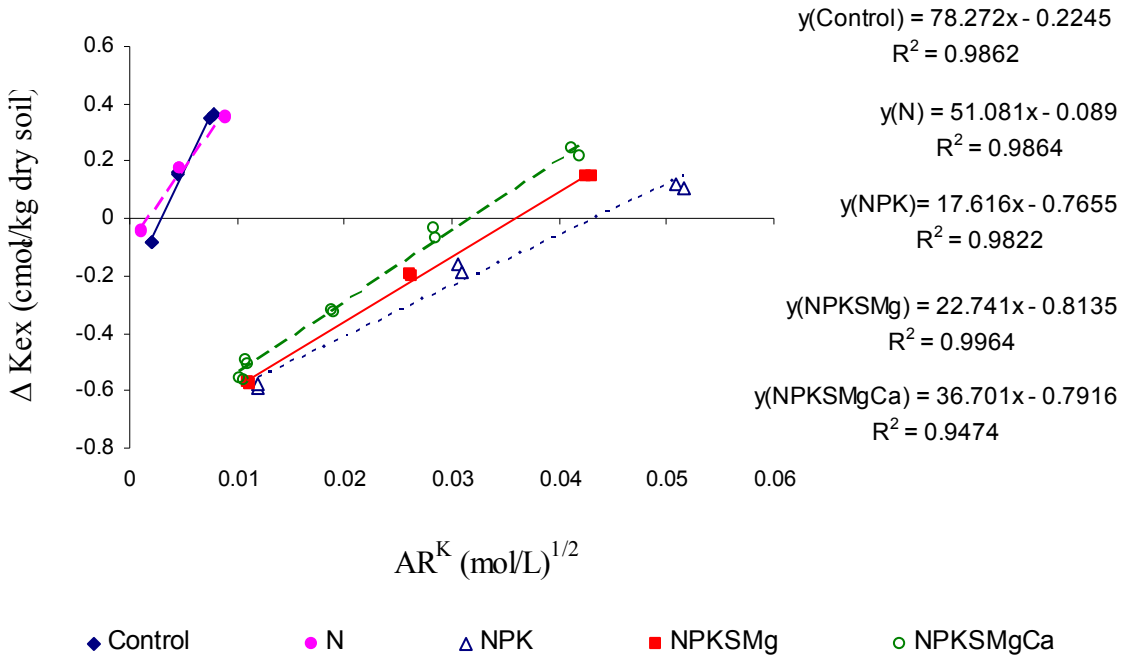

Figure 108: Quantity-Intensity Plot for the Subsurface Haplustand after Fertilization.

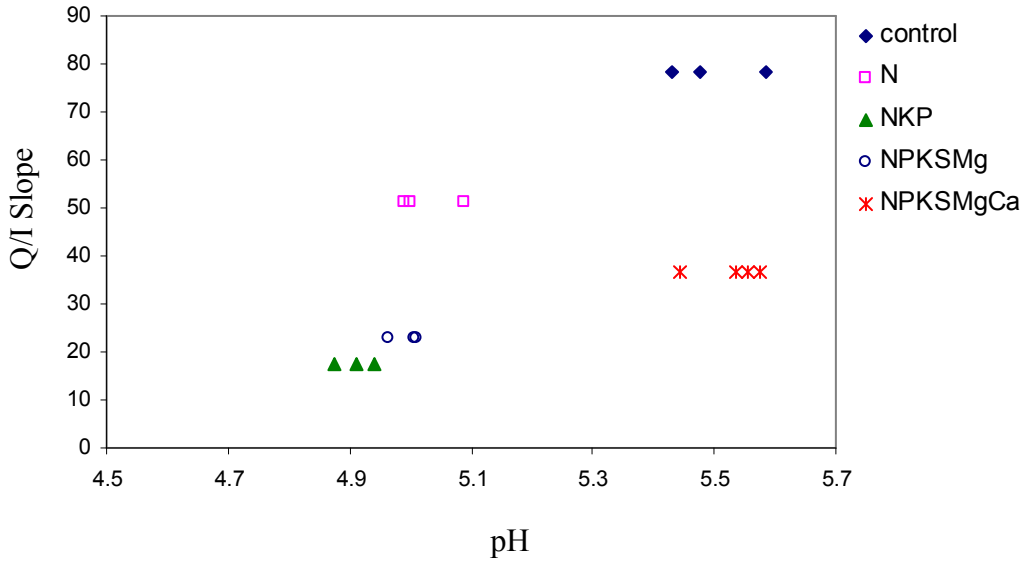

Figure 109: Quantity-Intensity Slope vs. pH for the Subsurface Haplustand.

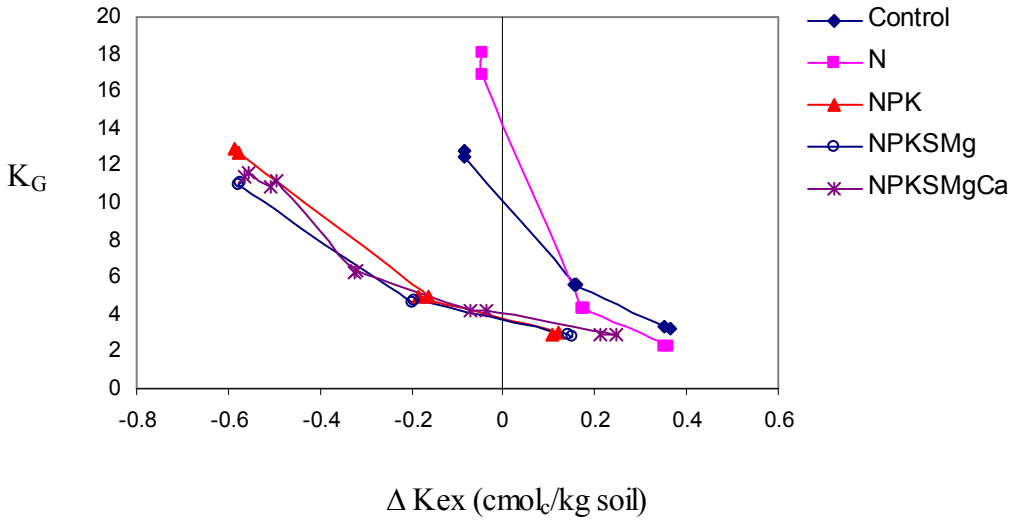

Figure 110: Gapon Coefficients (K_G) vs. ΔK ex for the Subsurface Haplustand.

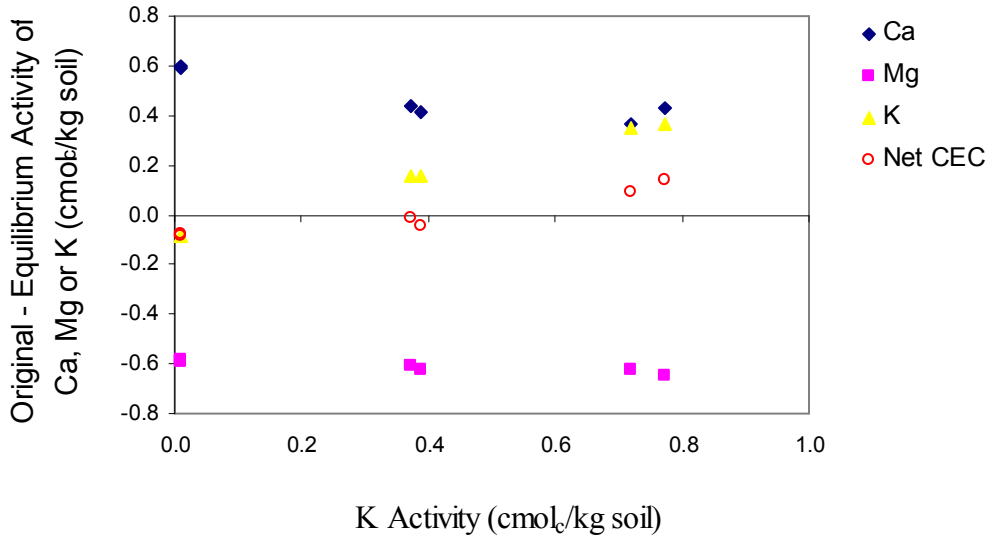

Figure 111: Change in Net CEC and exchangeable Ca, Mg, and K vs. K Activity for the Subsurface Haplustand (Control Treatment).

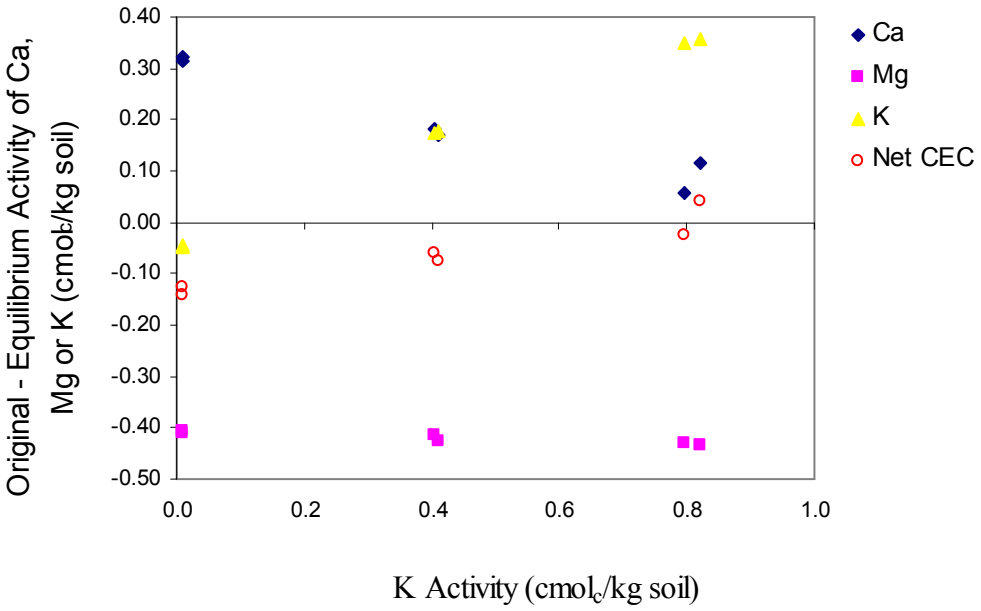

Figure 112: Change in Net CEC and exchangeable Ca, Mg, and K vs. K Activity for the Subsurface Haplustand (+N Treatment).

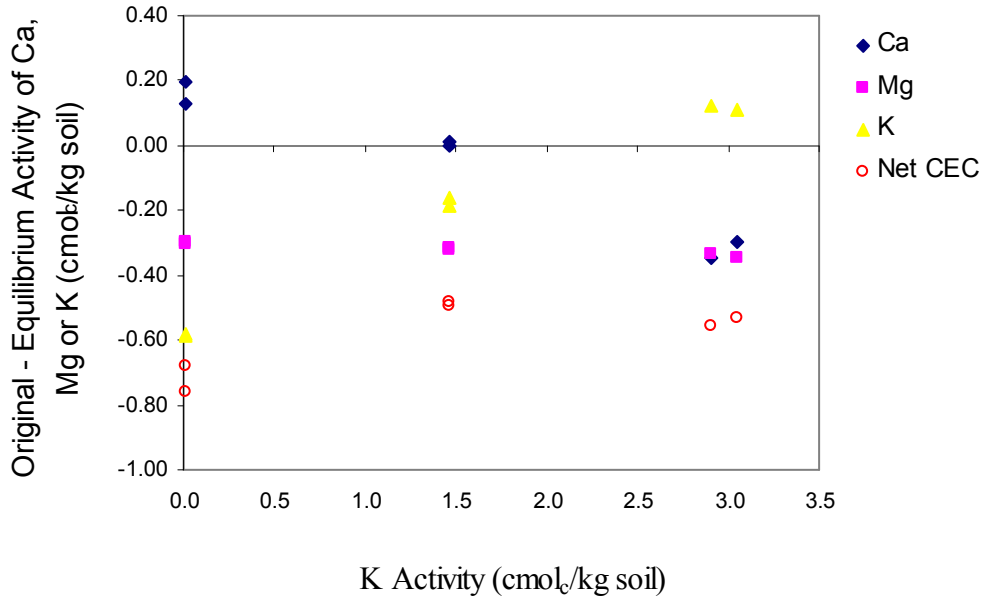

Figure 113: Change in Net CEC and exchangeable Ca, Mg, and K vs. K Activity for the Subsurface Haplustand (+NPK Treatment).

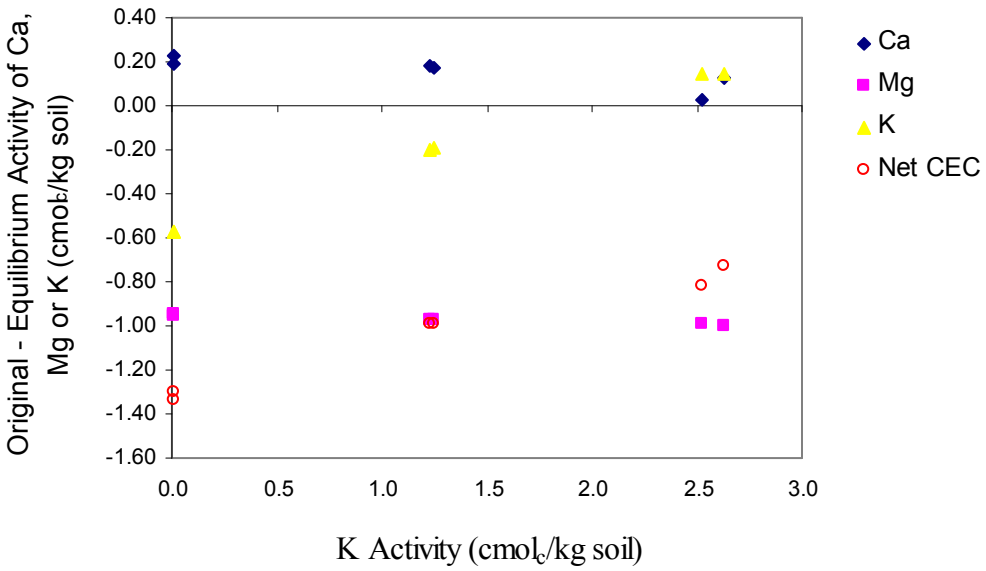

Figure 114: Change in Net CEC and exchangeable Ca, Mg, and K vs. K Activity for the Subsurface Haplustand (+NPKSMg Treatment).

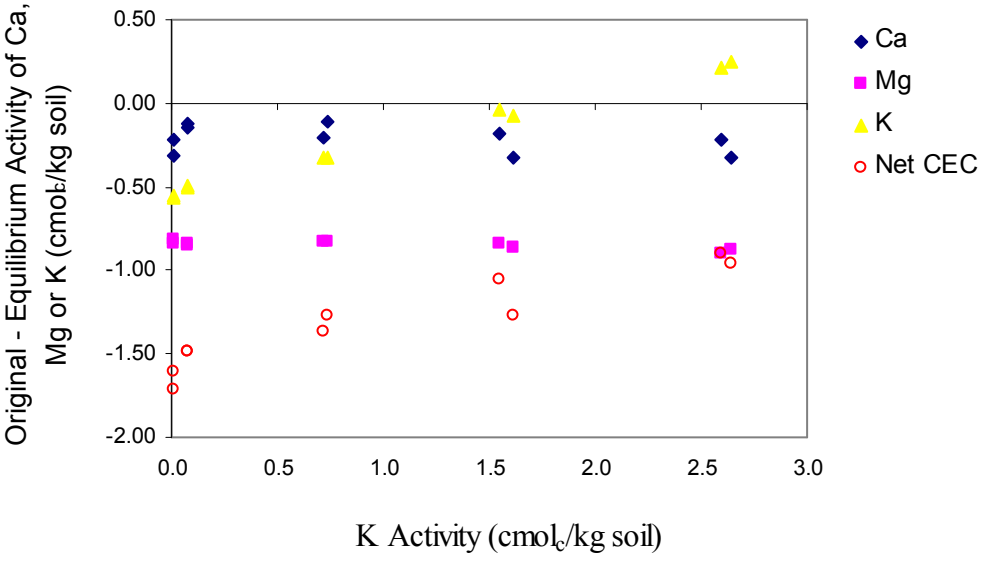

Figure 115: Change in Net CEC and exchangeable Ca, Mg, and K vs. K Activity for the Subsurface Haplustand (+NPKSMgCa Treatment).

Potassium Quantity-Intensity in the Melanudand

The surface of the Melanudand exhibited differences in its potassium quantity-intensity relationship, i.e., its potassium buffer capacity, labile K, and equilibrium activity ratio with liming (Figure 116; Appendix D). As the lime rate increased the labile pool of K decreased, even though the exchangeable potassium extracted by $BaCl_2$ did not change significantly ($\alpha = 0.05$). This was expected since greater crop yield and nutrient removal was associated with higher lime rates (Appendix E). Also, it was evident that there was a difference in slope for every lime rate. The most steeply sloping curve was found at the highest lime rate, which indicates that K on the exchange complex of the soil is being held with greater affinity, perhaps as a result of greater CEC. As the lime rate decreased lower soil pH values and lower exchangeable Ca were observed, and the potential potassium buffer capacity decreased. The results imply that under these conditions, with the same native level of potassium due to the fact that no potassium fertilizer had been applied, soil pH would be one of the factors determining the potential potassium buffering capacity in this soil. There was a high positive correlation ($r^2 = 0.778$) between soil pH and the potential potassium buffer capacity (Figure 117). A close relationship among pH, calcium availability, CEC, and potential potassium buffer capacity was evident. The Gapon coefficients (Appendix D) were calculated from K, Ca, and Mg solution concentrations determined with the quantity/intensity method and the exchangeable Ca and Mg in the soil as determined by extraction with 1 M $BaCl_2$, which was the most consistent method for determining changes in exchangeable cations due to liming. In contrast to what was expected, the highest Gapon coefficient value was associated with the control plot. As the lime rate increased, the Gapon coefficient

decreased (Figure 118). Those results could be explained after disproportionation of the Gapon coefficient calculation. An increase in exchangeable Ca and Mg, or a decrease in exchangeable K, as a result of liming, was related to lower K_G values (Figure 119; r^2 = 0.8046). In a similar way, the soil solution concentrations determined with the quantity/intensity method showed that the increase in solution Ca and Mg or the decrease in K with lime rate was associated with lower K_G values (Figure 120). However, there was no significant relationship between the Gapon coefficient and the exchangeable K/soil solution K ratio (Figure 121; r^2 = 0.1496), but at lower lime rates (0, 3, and 6 ton lime/ha) the soil solution K was higher, and there was a lower exchangeable K/soil solution K ratio, which is consistent with the pH trend observed in the slopes of the quantity/intensity relationships.

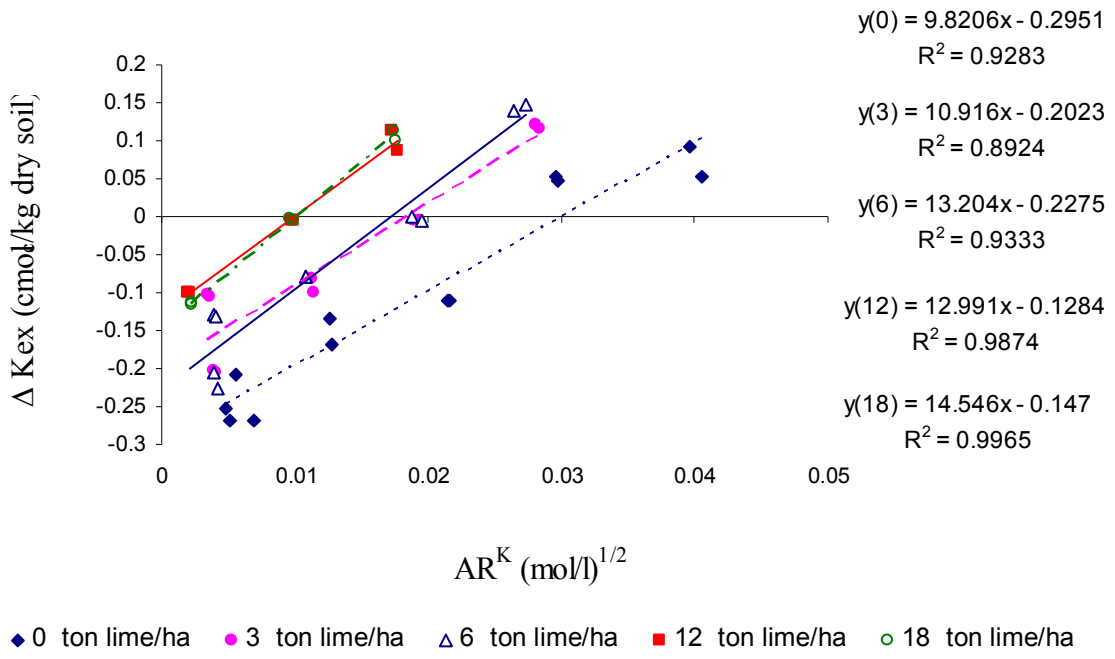

Figure 116: Quantity-Intensity Plot for the Surface Melanudand after Liming.

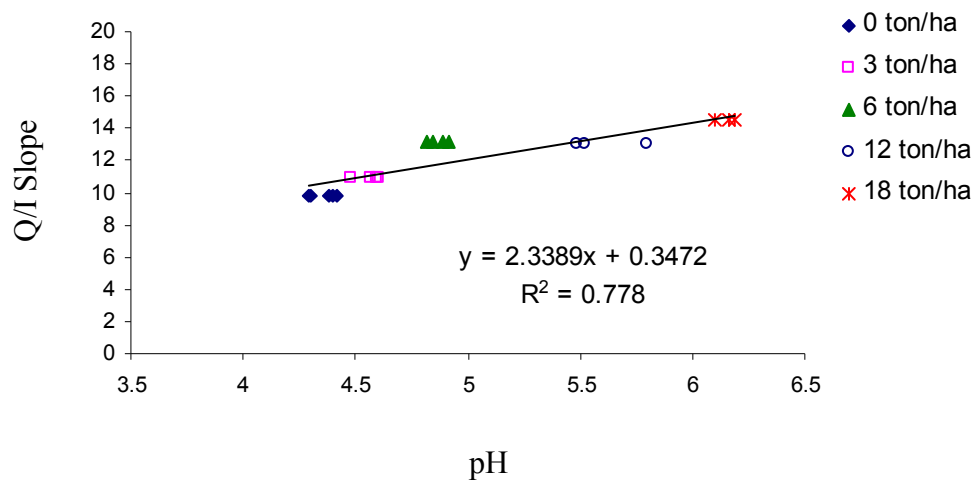

Figure 117: Quantity-Intensity Slope vs. pH for the Surface Melanudand.

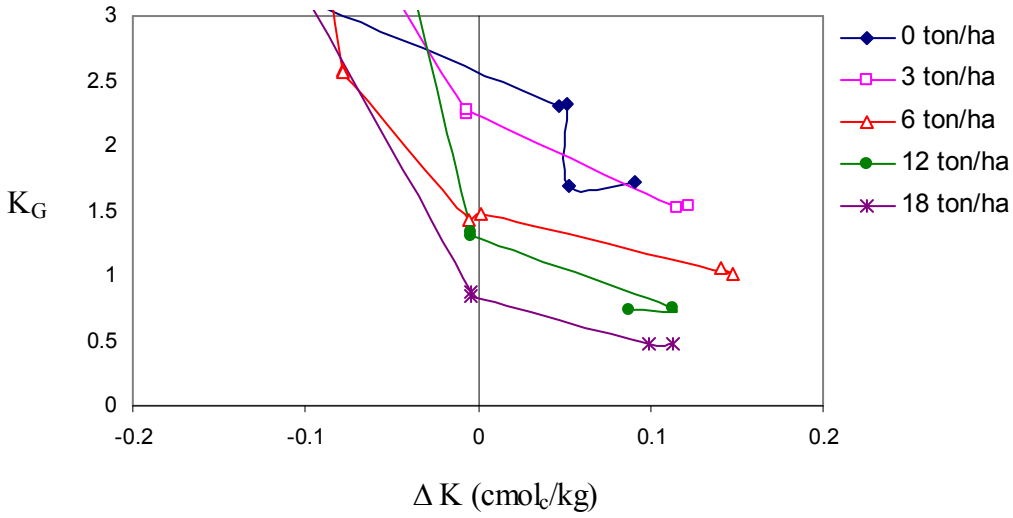

Figure 118: Gapon Coefficients (K_G) vs. ΔK ex for the Surface Melanudand.

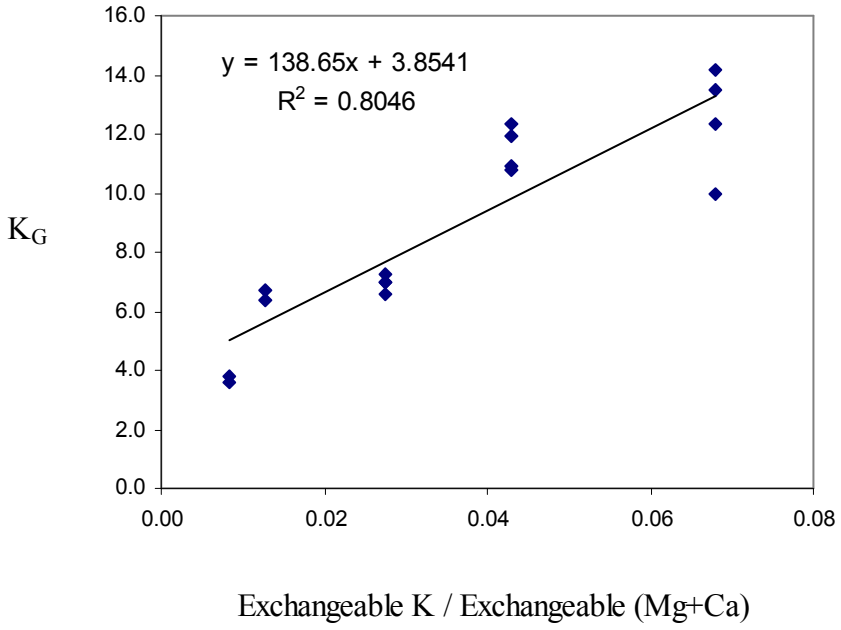

Figure 119: Gapon Coefficient Response to Exchangeable Cation Ratio in the Surface Melanudand.

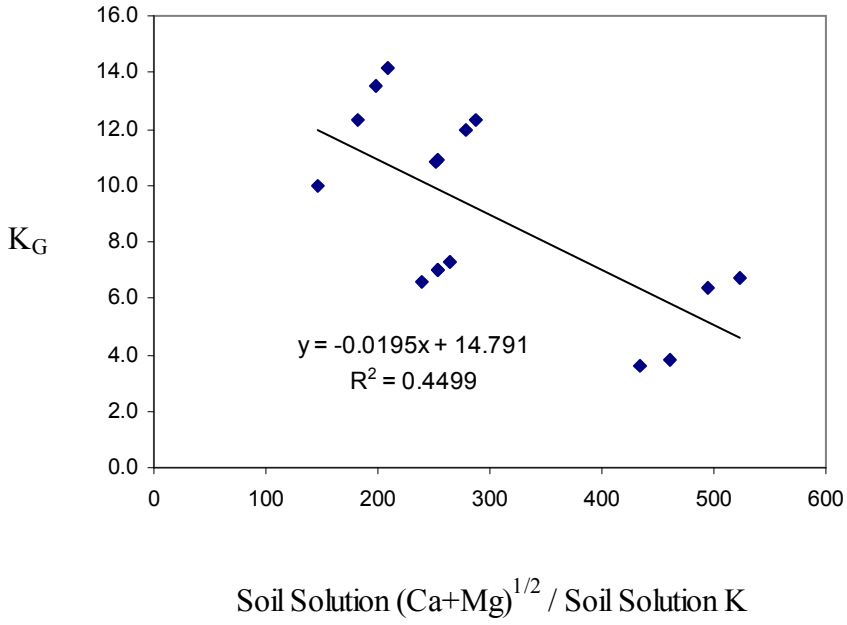

Figure 120: Gapon Coefficient Response to Soil Solution Cation Ratio in the Surface Melanudand.

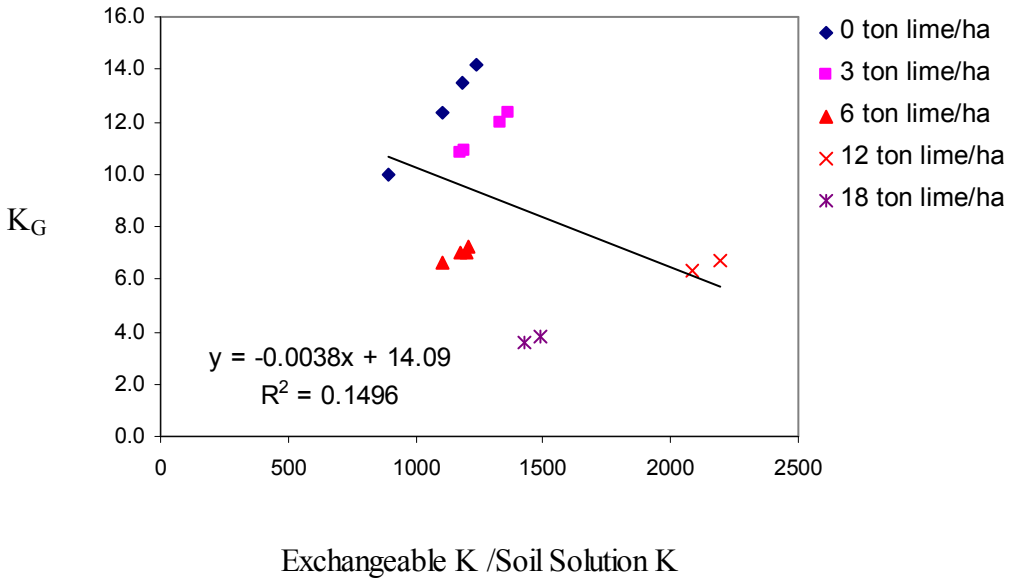

Figure 121: Gapon Coefficient Response to Exchangeable K /Soil Solution K Ratio for the Surface Melanudand.

The subsurface Melanudand also exhibited changes in its potassium quantity-intensity relation with liming (Figure 122; Appendix D). Similar to the surface soil, the labile pool for K tended to decrease as the lime rate increased. However, the magnitude was lower for the subsurface soil, so that the equilibrium potassium activity was easily reached using lower solution K concentration additions. Also, there were still differences in slope at each lime rate, although these values were similar to those observed for the surface soil. The most steeply sloping relationship was associated with the highest lime rate, indicating that the effect of liming, in subsurface horizons, would be greatest at the highest lime rates. Consequently, the K on the exchange complex of the soil would be held with greatest affinity as a result of higher pH and greater CEC. As the lime rate decreased, giving lower soil pH and exchangeable Ca, the potential potassium buffer capacity decreased (Figure 123). There was a high positive correlation (r^2 = 0.7613)

between the subsurface soil pH and the potential potassium buffer capacity. Higher Gapon coefficients were observed for the subsurface horizon (Appendix D), as expected, due to lower exchangeable Ca and Mg as compared to the surface soil. However, the trend for increasing the Gapon coefficients, as the lime rate increased, was the same as that observed for the surface soil. These results can be explained, after disproportionation of the Gapon coefficient calculation, as one can see in Figures 124 through 126. Increases in exchangeable Ca and Mg, relative to exchangeable K, as a result of liming, were most strongly and positively related to lower Gapon coefficients values ($r^2 = 0.8951$). The soil solution concentration ratios determined in the quantity/intensity method indicated that the increase in solution Ca and Mg, relative to K was moderately related to lower K_G values (Figure 125; $r^2 = 0.3434$). However, there was no significant relationship between K_G and the exchangeable K/soil solution K ratio (Figure 126; $r^2 = 0.1024$), but it was observed that the solution K was higher at lower lime rates (0, 3 ton lime/ha). This resulted in a lower exchangeable K/soil solution K ratio, which is consistent with the trend in the slopes of the quantity/intensity curves. In contrast to the surface horizon, the highest lime rate for the subsurface soil exhibited a exchangeable K/soil solution K ratio more comparable to the lowest lime rate, likely due to the low K content of this treatment.

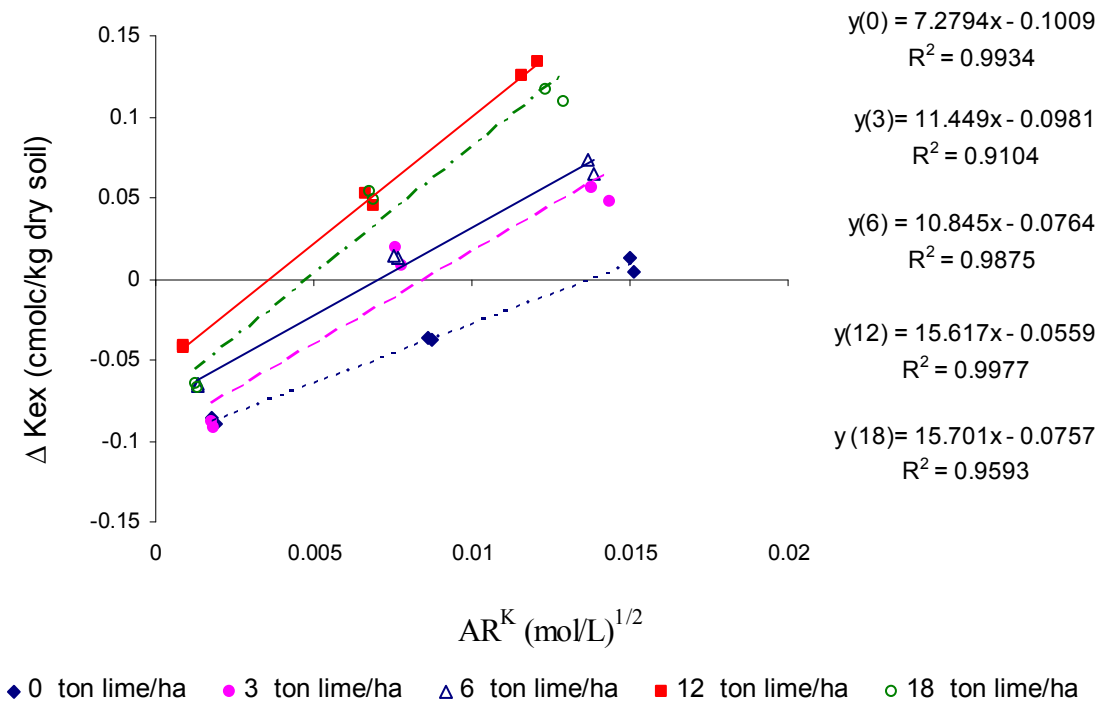

Figure 122: Quantity-Intensity Plot for the Subsurface Melanudand after Liming.

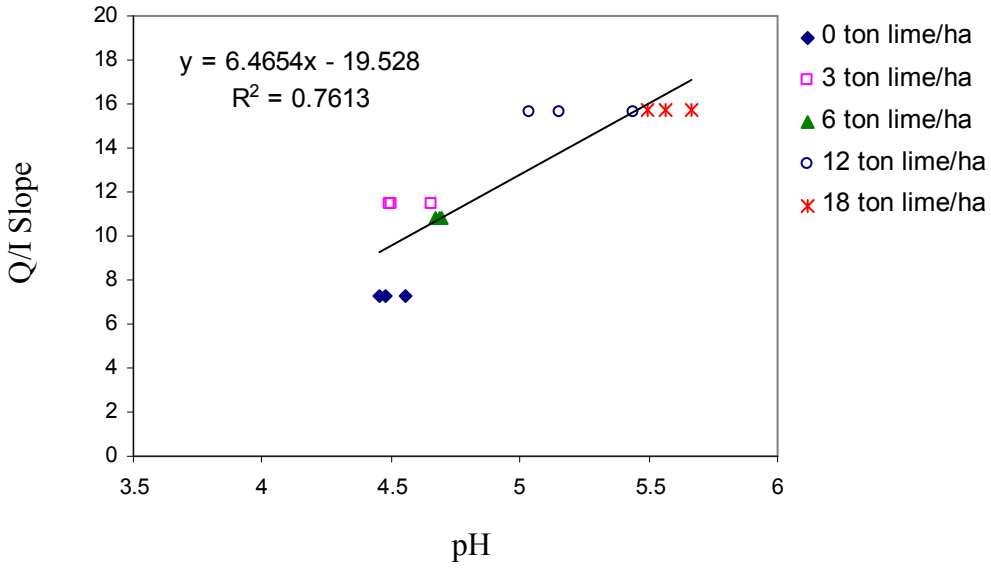

Figure 123: Quantity-Intensity Slope vs. pH for the Subsurface Melanudand.

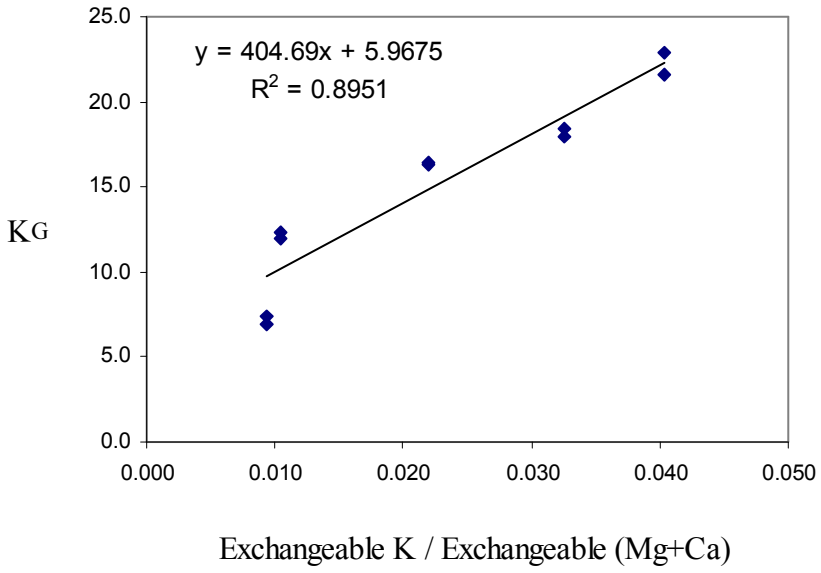

Figure 124: Gapon Coefficient Response to Exchangeable Cation Ratio in the Subsurface Melanudand.

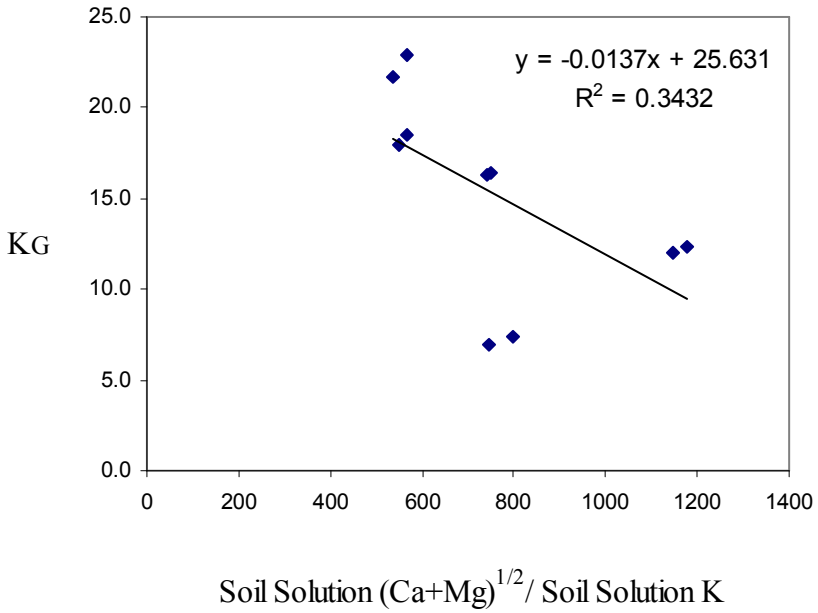

Figure 125: Gapon Coefficient Response to Soil Solution Cation Ratio in the Subsurface Melanudand.

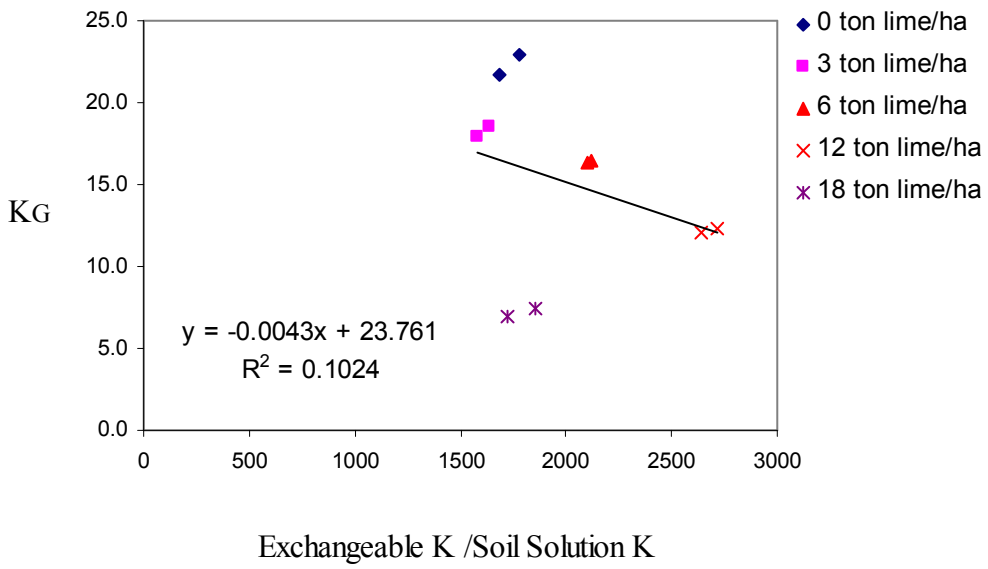

Figure 126: Gapon Coefficient Response to Exchangeable K / Soil Solution K Ratio for the Subsurface Melanudand.

CONCLUSIONS

The mineralogical analysis of both of the Ecuadorian Andisols indicated the presence of enough quantifiable crystalline minerals and there was a different mineral composition for each soil. The Haplustand possessed smectite and interstratified vermiculite-mica. In contrast, the Melanudand was dominated by HIV. Nevertheless, both of the Andisols contained kaolinite and/or metahalloysite, mica, feldspars and quartz. Additionally, the poorly crystalline aluminosilicate fraction of the Haplustand exhibited a lower silica/sesquioxide ratio than that of the Melanudand, which clearly suggests that these Andisols have been subjected to different degrees of weathering, driven by differences in climate and/or parent materials.

The chemical analysis also illustrated significant differences in the studied Andisols. One of the major distinguishing chemical properties was the organic matter content, which was higher for the Melanudand than for the Haplustand. This was directly related to differences in climate and crop management at the highland and coastal plain locations. Another dissimilar chemical property was the soil pH. The Haplustand exhibited a higher soil pH in the unfertilized control, but its lower pH buffer capacity was reflected in its considerable decrease in pH after nitrogen fertilizer application. On the other hand, the pH buffer capacity of the Melanudand was remarkable due to the fact that the soil pH was not greater than 6.9 even after a series of 18 ton lime/ha applications. Also, higher exchangeable soil acidity was found in the unlimed Melanudand, consistent with its lower soil pH, high organic matter content, and a predominance of HIV. Finally, the basic nutrient cation status for both Andisols was clearly correlated with soil pH. The Haplustand exhibited greater CEC and base saturation, especially calcium and

magnesium, compared to the Melanudand. Each Andisol did not exhibit any particular difference in CEC and base status, either in surface or subsurface soil samples, unless those soils were subjected to fertilization or liming practices.

Nitrogen fertilization of the Haplustand was responsible for decreasing soil pH, with consequently lower CEC and base saturation. That effect was greater in the surface horizon, so that higher base saturation, especially with calcium, was observed in the subsurface horizon as a result of the associated leaching process. On the other hand, if N fertilization is accompanied by calcium carbonate application (+NPKSMgCa) the decline in soil pH was controlled, and a greater CEC was observed.

Liming of the Melanudand was responsible for increasing soil CEC and calcium saturation, even though a greater soil pH change was not observed. The greater liming effect was observed in the surface horizon. Nevertheless, higher lime rates (12 to 18 ton/ha) also caused changes in CEC and calcium saturation in the subsurface horizon.

Extraction solutions used to assess bio-available basic nutrient cations in these Andisols, i.e., ammonium acetate pH 7, barium chloride, and Olsen pH 8.5, were consistent in extracting calcium and magnesium. In contrast, determinations of exchangeable potassium depend upon choice of the extraction solutions. The Olsen pH 8.5 method was less able to detect differences due to fertilizer treatments in the subsurface Haplustand, whereas ammonium acetate pH 7 was less sensitive to lime rate effects on the Melanudand. Consequently, the barium chloride extraction was the better method for both of these soils.

The specific surface was highest for the Melanudand, followed by the Haplustand, and finally by the Typic Paleudalf. Also, the greater drying effect on specific surface

assessment was observed for both Andisols and the surface Typic Paleudalf, which suggests that the decreased specific surface after drying was due not only to shrinkage and cementation of the amorphous minerals, but also to dehydration of soil organic matter.

The determination of CEC by the barium chloride and ammonium acetate pH 7 methods confirms the observations of previous workers that the value obtained is markedly dependent upon solution conditions, such as pH, ionic strength, and valence of the counterion, especially when the soil possesses variable charge characteristics. Consequently, an unbuffered approach should be used to attempt to reproduce field conditions and to estimate the capacity of a soil to retain cations on its exchange complex.

The study soils are dominated by constant surface potential behavior, which is directly related to their soil organic matter, terminal edges of minerals like kaolinite, HIV, iron and aluminum oxides, and amorphous aluminosilicates, in the case of the Andisols. The "Charge Fingerprint Method" found that there was significant development of negative surface charge with increasing soil pH in every studied soil. The increase in surface negative charge was greater for the Andisols than for the Typic Paleudalf, which is related to the higher specific surface of the Andisols. However, the charge buffering versus pH relationship was not the same for both Andisols. Additionally, there was a greater difference between soil pH and pHo in these soils, such that the Haplustand, with the higher soil pH, has the greater variable negative surface charge component. On the other hand, even though the difference between soil pH and pHo for the Haplustand was lower than that of the surface Typic Paleudalf, the former

soil exhibited greater negative charge development, suggesting that the difference between pH and pHo was not a good basis for comparisons between soils dominated by constant surface potential behavior, but with different mineralogical composition. In addition, the pHo for both surface and subsurface Andisols and the surface Typic Paleudalf was more acidic than that determined for the subsurface Typic Paleudalf, which suggest the dominant role of soil organic matter as a constant surface potential component. The organic matter in the Andisols exhibited a pHo similar to that of the amorphous minerals in the Andisols.

Additionally, the marked increase in CEC and consequent enhanced retention of exchangeable "bases" with increasing pH observed for both surface and subsurface layers in the Haplustand and Melanudand, and for the surface Typic Paleudalf, was more marked for calcium than for potassium. In contrast, potassium was preferred to calcium in the subsurface Typic Paleudalf, whose clay fraction was dominated by kaolinite. That cation preference was also observed in the different soil pH measurements in either $CaCl_2$ or KCl solution.

On the other hand, the development of positive surface charge in the studied soils was not greatly affected by changes in pH, which was supported by the fact than the positive charge was lower in Andisols, with their high soil organic matter content, high silica/aluminum ratio for the poorly crystalline fraction and with the presence of some negative charged crystalline minerals.

The PZNC for all of the studied soils was lower than their pHo, suggesting that the permanent charge associated with these soils was negative. However, the greater permanent negative charge was associated with the subsurface Typic Paleudalf, which

was dominated by kaolinite and HIV. Also, greater permanent negative charge was found with calcium saturation, suggesting that calcium was held more strongly than suggested by the low-affinity specific adsorption model.

The quantity-intensity data presented in this study for both Andisols showed that the release of potassium to the soil solution was influenced by the presence of competing cations, such as calcium and magnesium, and their close relationship with changes in soil pH that are directly affected by soil fertilizer and/or lime application. The potential potassium buffer capacity for the Haplustand decreased with nitrogen fertilization, and was greater with calcitic lime application. Nevertheless, the greater the labile potassium pool, the greater the potassium in soil solution, even in fertilizer treatments with similar potential potassium buffer capacity, which suggests that Gapon coefficient analysis is able to predict potassium availability in cases where the slope of quantity –intensity curves does not allow further interpretation. On the other hand, the potential potassium buffer capacity for the Melanudand was lower than that for the Haplustand, and increased after liming, partly as a result of a decline in the labile potassium pool. Finally, the exchangeable potassium assessed by barium chloride extraction was of similar magnitude to that for labile exchangeable K obtained from the quantity-intensity method, which suggests that the former method could be used to assess potassium bioavailability in these Ecuadorian Andisols.

In short, this study demonstrates the dynamic nature of soils dominated by different constant surface potential colloids, where fertilizer and/or lime application would bring about changes not only in the soil pH, but also in the surface charge with consequent effects on soil nutrient cation release characteristics.

APPENDICES

APPENDIX A

Physical-Chemical and Mineralogical Characteristics of the Typic-Paleudalf

Selected Physical Properties ‡

Horizon	Depth (cm)	Particle-size distribution			
		Sand (%)	Silt (%)	Clay (%)	Texture
Ap	0-18	21.2	63.3	15.5	sil
Bt4	100-138	22.1	15.3	62.6	c

Selected Chemical Properties ‡

Horizon	pH	Ca^{2+}	Mg^{2+}	K^{+}	Na^{+}	ExAl	AEC	CEC	O.M.	Base Sat	P
		($cmol_c$/kg soil)						*	(%)		(mg/kg)
Ap	5.9	3.95	0.56	0.37	0.18	0.03	-	51.5	2.23	63.5	6.0
Bt4	4.9	2.00	2.80	0.28	0.13	3.10	0.39	21.8	0.12	38.2	0.5

* CEC = $cmol_c$/ kg clay

Mineralogical Composition of Clay (<2 µm) Fraction ‡

Horizon	Kaolinite	HIV	Mica	Quartz	Goethite
			(%)		
Ap	33	37	16	11	3
Bt4	71	19	10	Nd*	Nd

*None detected

Extractable Iron Oxides Distribution ‡

Horizon	CBD Fe_2O_3 (%)	NH4-oxalate Fe_2O_3 (%)	Crystalline Fe_2O_3 (%)	Gibbsite (%)	Fe_2O_3 (%) + % Gib.) / %C *
Ap	1.38	0.14	1.24	-	0.09
Bt4	7.48	0.11	7.37	-	0.12

*(% Fe_2O_3 + % Gibbsite) / %Clay $\geq$ 0.2 (oxidic mineralogy criterion)

‡ Source of data: Mubiru (1992)

APPENDIX B

Pedon Descriptions for Ecuadorian Andisols

Pedon Description for the Melanudand ‡

SOIL:	NSD*
CLASSIFICATION €:	Isomesic (11 °C), Udic, Melanudand (formerly classified as an Entic-Dystrandept)
LOCATION:	0°20'15'' S Lat, 78°33'45''W Long; el., 3,050 m INIAP Exp. Stn, at Mejia, Ecuador
PARENT MATERIAL:	Andesitic volcanic ash
VEGETATION:	Corn-peas-barley
LANDSCAPE:	Upland
DRAINAGE:	Drained
MOISTURE WHEN SAMPLED:	Moist
SLOPE:	3 %
PEDON DESCRIPTION:	
A11	0-17 cm; black (2.5YR 2.5/1) silt loam; weak granular structure; many fine roots; clear, smooth boundary.
A12	17-55 cm; black (2.5 YR 2.5/2) silt loam, weak granular structure; many fine roots; clear, smooth boundary.
A13	55-87 cm; black (2.5 YR 3/1) loam, few roots, strong granular structure; clear, smooth boundary.
D	87-112 cm; black (2.5 YR 2.5/2) loam, few roots; strong granular structure; 36 percent pomes fragments (0.5 to 2.0 cm in diameter), clear boundary.
A14	112-140 cm; black (2.5 YR 3/1) sandy clay loam; strong granular structure; unknown boundary.

‡ Unpublished description taken from the Soil Department of the "Santa Catalina" Experimental Station of the National Agricultural Research Institute of Ecuador (INIAP)

* No series designated

€ Reclassified by Dr. A. D. Karathanasis (Agronomy Department, University of Kentucky) according to Keys to Soil Taxonomy (1998).

Pedon Description for the Haplustand ‡

SOIL:	NSD*
CLASSIFICATION €:	Isohyperthermic (24.3 °C), Ustic (2,021 mm), Haplustand (formerly classified as an Eutrandept)
LOCATION:	1°06' S Lat, 79 °21' W Long; el., 120 m; INIAP Exp. Stn, at Quevedo - Ecuador
PARENT MATERIAL:	Andesitic volcanic ash
VEGETATION:	Oil palm
LANDSCAPE:	Upland
DRAINAGE:	Well-drained
SLOPE:	0-2 %
PEDON DESCRIPTION:	
Ap	0-20 cm; dark yellowish brown (10YR 4/2 silt loam; weak sub-angular blocky structure to weak fine granular structure; friable; many fine roots; medium acid; clear, smooth boundary.
Bw1	20-70 cm; yellowish brown (10 YR 5/3) silt loam; moderate fine sub-angular blocky structure, friable; many fine roots; medium acid; clear, smooth boundary.
2Bw2	70-80 cm; yellowish brown (10 YR 5/4) loam; weak fine sub-angular blocky structure; friable; few fine roots; medium acid; clear, smooth boundary.
2Bt1	80-130 cm; strong brown (7.5 YR 4/2) clay loam; moderate medium to coarse sub-angular blocky structure; medium acid.
2Bt2	130 + cm; Reddish brown (5 YR 4/4) clay; common medium distinct black mottles (10 YR 2/1); strong angular structure; medium acid.

‡ Source of description: Mite (1972)

* No series designated

€ Reclassified by Dr. A. D. Karathanasis (Agronomy Department, University of Kentucky) according to Keys to Soil Taxonomy (1998)

APPENDIX C

Data for the Specific Surface Experiment

Specific Surface of the Surface Soils

Sample	Gravimetric Water Content (%)	Specific Surface* (m^2/g)		
		Dry Samples at 45°C	Dry Samples at 110°C	Wet Samples
Haplustand (0-10 cm)	21.5	92.2	45.5	105.0
Melanudand (0-20 cm)	27.2	98.2	44.5	177.4
Typic Paleudalf (0-18 cm)	9.1	19.0	20.6	46.7

* Means of duplicate samples

Specific Surface of the Subsurface Soils

Sample	Gravimetric Water Content (%)	Specific Surface* (m^2/g)	
		Wet Samples	Dry Samples at 45°C
Haplustand (10-30 cm)	28.2	196.7	104.4
Melanudand (20-40 cm)	29.8	215.8	89.9
Typic Paleudalf (100 -138cm)	11.5	88.4	74.9

* Means of duplicate samples

APPENDIX D

Potassium Quantity – Intensity Relationships

Gapon Coefficients for the Haplustand

Fertilizer Treatment	K_G $(mol/L)^{-1/2}$	
	Surface (0-10 cm)	Subsurface (10-30 cm)
Control	15.85	12.77
Control	15.32	12.46
N	45.55	18.08
N	45.24	16.90
NPK	25.29	12.86
NPK	26.04	12.73
NPKSMg	19.45	11.11
NPKSMg	20.03	10.93
NPKSMgCa	9.14	11.35
NPKSMgCa	8.12	11.65

Quantity-Intensity Data for the Surface Haplustand

Sample	[K] initial	pH	EC	[Ca] eq.	[Mg] eq.	[K] eq.	Delta K	AR^K
	(ppm)		(dS/m)	(mol/L)	(mol/L)	(mol/L)	(cmol/kg)	$(mol/L)^{1/2}$
Control	0	5.16	0.004	0.00126	0.00022	0.00003	-0.02922	0.00080
Control	0	5.39	0.004	0.00130	0.00022	0.00003	-0.03167	0.00082
Control	12	5.38	0.004	0.00138	0.00022	0.00016	0.10702	0.00409
Control	12	5.39	0.004	0.00131	0.00022	0.00017	0.09852	0.00436
Control	24	5.35	0.005	0.00140	0.00023	0.00029	0.26780	0.00722
Control	24	5.35	0.004	0.00139	0.00023	0.00029	0.26923	0.00736
N	0	4.15	0.004	0.00139	0.00006	0.00006	-0.07091	0.00166
N	0	4.04	0.004	0.00142	0.00006	0.00006	-0.07100	0.00167
N	18	3.98	0.005	0.00151	0.00006	0.00033	0.06742	0.00845
N	18	4.01	0.005	0.00148	0.00005	0.00033	0.07008	0.00855
N	36	3.97	0.005	0.00156	0.00006	0.00061	0.20721	0.01536
N	36	3.96	0.005	0.00156	0.00005	0.00062	0.20295	0.01561
NPK	0	4.07	0.005	0.00158	0.00011	0.00070	-0.87841	0.01725
NPK	0	4.07	0.005	0.00160	0.00010	0.00068	-0.87141	0.01674
NPK	33	4.08	0.006	0.00167	0.00010	0.00131	-0.76388	0.03128
NPK	33	4.06	0.006	0.00167	0.00010	0.00128	-0.73822	0.03073
NPK	66	4.04	0.007	0.00177	0.00010	0.00196	-0.59772	0.04577
NPK	66	4.02	0.007	0.00180	0.00011	0.00196	-0.59173	0.04533
NPK	99	3.98	0.007	0.00177	0.00013	0.00280	-0.38150	0.06506
NPK	99	3.98	0.007	0.00177	0.00013	0.00282	-0.41038	0.06547
NPK	132	3.96	0.008	0.00181	0.00012	0.00346	-0.18904	0.07971
NPK	132	3.94	0.008	0.00182	0.00012	0.00348	-0.20961	0.07998
NPK	165	3.97	0.009	0.00184	0.00013	0.00400	-0.08753	0.09122
NPK	165	3.95	0.009	0.00183	0.00012	0.00398	-0.06933	0.09118
NPKSMg	0	4.24	0.005	0.00151	0.00041	0.00051	-0.63413	0.01181
NPKSMg	0	4.28	0.005	0.00149	0.00037	0.00049	-0.63067	0.01147
NPKSMg	33	4.23	0.006	0.00160	0.00040	0.00112	-0.50780	0.02527
NPKSMg	33	4.24	0.006	0.00163	0.00040	0.00110	-0.49358	0.02468
NPKSMg	66	4.22	0.007	0.00173	0.00040	0.00175	-0.30575	0.03846
NPKSMg	66	4.23	0.007	0.00169	0.00041	0.00174	-0.30135	0.03835
NPKSMg	99	4.17	0.007	0.00164	0.00039	0.00259	-0.11028	0.05810
NPKSMg	99	4.15	0.007	0.00169	0.00039	0.00262	-0.15299	0.05817
NPKSMg	132	4.18	0.008	0.00178	0.00039	0.00330	0.03280	0.07163
NPKSMg	132	4.15	0.008	0.00175	0.00039	0.00330	0.02605	0.07221
NPKSMgCa	0	5.34	0.005	0.00164	0.00044	0.00057	-0.69102	0.01266
NPKSMgCa	0	5.69	0.005	0.00165	0.00043	0.00064	-0.78684	0.01426
NPKSMgCa	33	5.58	0.006	0.00179	0.00045	0.00109	-0.47463	0.02319
NPKSMgCa	33	5.66	0.006	0.00176	0.00044	0.00107	-0.46286	0.02302
NPKSMgCa	66	5.51	0.007	0.00183	0.00044	0.00166	-0.19959	0.03525
NPKSMgCa	66	5.68	0.007	0.00186	0.00045	0.00166	-0.19713	0.03496
NPKSMgCa	99	5.39	0.007	0.00182	0.00045	0.00246	0.05119	0.05236
NPKSMgCa	99	5.47	0.008	0.00185	0.00045	0.00245	0.07409	0.05158
NPKSMgCa	132	5.53	0.008	0.00194	0.00046	0.00309	0.28549	0.06388
NPKSMgCa	132	5.52	0.008	0.00195	0.00047	0.00313	0.23882	0.06445

Quantity-Intensity Data for the Subsurface Haplustand

Sample	K initial	pH	EC	[Ca] eq.	[Mg] eq.	[K] eq.	Delta K	AR^K
	(ppm)		(dS/m)	(mol/L)	(mol/L)	(mol/L)	(cmol/kg)	$(mol/L)^{1/2}$
Control	0	5.64	0.004	0.00122	0.000233	0.00007	-0.08510	0.00196
Control	0	5.53	0.004	0.00121	0.000234	0.00008	-0.08592	0.00201
Control	14	5.49	0.004	0.00133	0.00024	0.00018	0.15807	0.00451
Control	14	5.46	0.004	0.00132	0.000243	0.00017	0.15532	0.00447
Control	28	5.46	0.004	0.00140	0.000257	0.00030	0.35171	0.00746
Control	28	5.40	0.004	0.00139	0.000248	0.00031	0.36493	0.00777
N	0	5.09	0.004	0.00132	0.000163	0.00004	-0.04331	0.00110
N	0	5.09	0.004	0.00133	0.000162	0.00004	-0.04765	0.00118
N	15	5.01	0.004	0.00143	0.000165	0.00019	0.17244	0.00467
N	15	4.99	0.004	0.00144	0.000166	0.00018	0.17754	0.00463
N	30	5.00	0.005	0.00150	0.000171	0.00036	0.35858	0.00896
N	30	4.98	0.005	0.00152	0.000174	0.00036	0.34956	0.00886
NPK	0	4.95	0.004	0.00140	0.000116	0.00046	-0.58765	0.01184
NPK	0	4.93	0.004	0.00137	0.000117	0.00046	-0.57828	0.01196
NPK	49	4.88	0.006	0.00161	0.000125	0.00126	-0.16174	0.03048
NPK	49	4.87	0.006	0.00160	0.000123	0.00127	-0.18413	0.03095
NPK	98	4.90	0.007	0.00181	0.000133	0.00222	0.11990	0.05096
NPK	98	4.92	0.007	0.00178	0.000131	0.00223	0.10773	0.05164
NPKSMg	0	5.02	0.004	0.00138	0.000373	0.00045	-0.57259	0.01097
NPKSMg	0	5.00	0.004	0.00136	0.000372	0.00046	-0.57666	0.01115
NPKSMg	43	5.00	0.006	0.00154	0.000387	0.00114	-0.19933	0.02621
NPKSMg	43	5.01	0.006	0.00154	0.000382	0.00113	-0.19194	0.02602
NPKSMg	86	4.97	0.007	0.00168	0.000399	0.00191	0.14406	0.04244
NPKSMg	86	4.96	0.007	0.00164	0.000386	0.00191	0.14876	0.04298
NPKMgCa	0	5.71	0.005	0.00154	0.000323	0.00045	-0.56241	0.01054
NPKMgCa	0	5.69	0.005	0.00158	0.00033	0.00044	-0.55530	0.01026
NPKMgCa	0	5.49	0.005	0.00135	0.000329	0.00045	-0.50626	0.01105
NPKMgCa	0	5.41	0.005	0.00136	0.000317	0.00043	-0.49443	0.01072
NPKMgCa	27	5.55	0.005	0.00162	0.000326	0.00083	-0.32549	0.01904
NPKMgCa	27	5.52	0.005	0.00166	0.000333	0.00083	-0.31957	0.01885
NPKMgCa	54	5.47	0.006	0.00174	0.000333	0.00129	-0.07021	0.02850
NPKMgCa	54	5.42	0.006	0.00169	0.000333	0.00126	-0.03716	0.02833
NPKMgCa	81	5.66	0.007	0.00170	0.000338	0.00184	0.24523	0.04122
NPKMgCa	81	5.45	0.007	0.00166	0.000351	0.00186	0.21344	0.04196

Gapon Coefficients for the Melanudand

Lime Rate (ton/ha)	K_G (mol/L)$^{-1/2}$ Surface (0-20 cm)	K_G (mol/L)$^{-1/2}$ Subsurface (20-40 cm)
0	13.49	21.65
0	14.17	22.88
3	10.80	17.95
3	10.90	18.48
6	6.61	16.28
6	7.26	16.46
12	6.36	12.02
12	6.71	12.34
18	3.82	6.93
18	3.61	7.43

Quantity-Intensity Data for the Surface Melanudand

Sample	K initial (ppm)	pH	EC (dS/m)	[Ca] eq. (mol/L)	[Mg] eq. (mol/L)	[K] eq. (mol/L)	Delta K (cmol/kg)	AR^K $(mol/L)^{1/2}$
0 ton lime/ha	0	4.38	0.004	0.00149	0.00012	0.00020	-0.26756	0.00509
0 ton lime/ha	0	4.47	0.005	0.00152	0.00012	0.00019	-0.25177	0.00484
0 ton lime/ha	17	4.40	0.005	0.00158	0.00012	0.00052	-0.16804	0.01281
0 ton lime/ha	17	4.43	0.005	0.00145	0.00011	0.00049	-0.13461	0.01256
0 ton lime/ha	34	4.39	0.005	0.00156	0.00011	0.00088	-0.11084	0.02165
0 ton lime/ha	34	4.40	0.005	0.00158	0.00011	0.00088	-0.11088	0.02152
0 ton lime/ha	51	4.29	0.006	0.00163	0.00012	0.00123	0.04717	0.02966
0 ton lime/ha	51	4.30	0.006	0.00163	0.00012	0.00123	0.05150	0.02961
0 ton lime/ha	68	4.29	0.006	0.00157	0.00014	0.00167	0.05226	0.04060
0 ton lime/ha	68	4.31	0.006	0.00160	0.00014	0.00164	0.09141	0.03969
3 ton lime/ha	0	4.60	0.004	0.00153	0.00012	0.00016	-0.20641	0.00401
3 ton lime/ha	0	4.62	0.004	0.00152	0.00012	0.00016	-0.20369	0.00397
3 ton lime/ha	17	4.60	0.005	0.00159	0.00012	0.00047	-0.10124	0.01146
3 ton lime/ha	17	4.59	0.005	0.00157	0.00012	0.00046	-0.08262	0.01121
3 ton lime/ha	34	4.60	0.005	0.00162	0.00012	0.00080	-0.00653	0.01932
3 ton lime/ha	34	4.61	0.005	0.00169	0.00012	0.00080	-0.00651	0.01897
3 ton lime/ha	51	4.46	0.006	0.00162	0.00014	0.00118	0.11558	0.02832
3 ton lime/ha	51	4.50	0.006	0.00163	0.00014	0.00117	0.12228	0.02807
6 ton lime/ha	0	4.87	0.004	0.00155	0.00016	0.00017	-0.22505	0.00421
6 ton lime/ha	0	4.92	0.004	0.00156	0.00015	0.00016	-0.20534	0.00383
6 ton lime/ha	17	4.91	0.005	0.00164	0.00016	0.00045	-0.07813	0.01079
6 ton lime/ha	17	4.92	0.005	0.00162	0.00016	0.00045	-0.07792	0.01083
6 ton lime/ha	34	4.88	0.005	0.00154	0.00016	0.00080	-0.00468	0.01951
6 ton lime/ha	34	4.89	0.005	0.00165	0.00016	0.00079	0.00128	0.01881
6 ton lime/ha	51	4.79	0.006	0.00163	0.00018	0.00115	0.14733	0.02740
6 ton lime/ha	51	4.84	0.006	0.00179	0.00018	0.00116	0.14061	0.02638
12 ton lime/ha	0	5.42	0.004	0.00146	0.00018	0.00008	-0.10120	0.00204
12 ton lime/ha	0	5.62	0.004	0.00146	0.00018	0.00008	-0.10116	0.00193
12 ton lime/ha	17	5.42	0.005	0.00151	0.00017	0.00039	-0.00396	0.00972
12 ton lime/ha	17	5.55	0.004	0.00145	0.00017	0.00039	-0.00456	0.00990
12 ton lime/ha	34	5.84	0.005	0.00154	0.00017	0.00071	0.11315	0.01726
12 ton lime/ha	34	5.76	0.005	0.00154	0.00018	0.00073	0.08748	0.01766
18 ton lime/ha	0	6.21	0.004	0.00145	0.00017	0.00009	-0.11325	0.00219
18 ton lime/ha	0	6.12	0.004	0.00140	0.00017	0.00009	-0.11705	0.00232
18 ton lime/ha	17	6.07	0.004	0.00157	0.00016	0.00039	-0.00391	0.00956
18 ton lime/ha	17	6.13	0.005	0.00146	0.00017	0.00039	-0.00398	0.00987
18 ton lime/ha	34	6.17	0.005	0.00152	0.00018	0.00072	0.09870	0.01751
18 ton lime/ha	34	6.20	0.005	0.00150	0.00017	0.00071	0.11350	0.01740

Quantity-Intensity Data for Subsurface Melanudand

Sample	K initial	pH	EC	[Ca] eq.	[Mg] eq.	[K] eq.	Delta K	AR^K
	(ppm)		(dS/m)	(mol/L)	(mol/L)	(mol/L)	(cmol/kg)	$(mol/L)^{1/2}$
0 ton lime/ha	0	4.59	0.004	0.00139	0.00007	0.00007	-0.08987	0.00188
0 ton lime/ha	0	4.52	0.004	0.00140	0.00006	0.00007	-0.08619	0.00177
0 ton lime/ha	13	4.48	0.004	0.00143	0.00006	0.00033	-0.03796	0.00872
0 ton lime/ha	13	4.48	0.004	0.00146	0.00006	0.00033	-0.03631	0.00862
0 ton lime/ha	26	4.46	0.005	0.00145	0.00006	0.00058	0.01274	0.01500
0 ton lime/ha	26	4.45	0.005	0.00146	0.00007	0.00059	0.00379	0.01510
3 ton lime/ha	0	4.52	0.004	0.00142	0.00005	0.00007	-0.09167	0.00183
3 ton lime/ha	0	4.49	0.004	0.00140	0.00005	0.00007	-0.08873	0.00178
3 ton lime/ha	13	4.80	0.004	0.00142	0.00007	0.00029	0.01944	0.00757
3 ton lime/ha	13	4.52	0.004	0.00146	0.00005	0.00030	0.00781	0.00776
3 ton lime/ha	26	4.49	0.004	0.00147	0.00005	0.00055	0.04719	0.01434
3 ton lime/ha	26	4.50	0.004	0.00154	0.00005	0.00055	0.05613	0.01378
6 ton lime/ha	0	4.68	0.004	0.00142	0.00008	0.00005	-0.06536	0.00136
6 ton lime/ha	0	4.71	0.004	0.00144	0.00008	0.00005	-0.06570	0.00135
6 ton lime/ha	13	4.68	0.004	0.00144	0.00008	0.00030	0.01281	0.00764
6 ton lime/ha	13	4.70	0.004	0.00146	0.00008	0.00029	0.01450	0.00755
6 ton lime/ha	26	4.66	0.005	0.00147	0.00008	0.00053	0.07290	0.01366
6 ton lime/ha	26	4.69	0.005	0.00151	0.00004	0.00054	0.06490	0.01383
12 ton lime/ha	0	5.01	0.004	0.00141	0.00012	0.00003	-0.04255	0.00088
12 ton lime/ha	0	5.06	0.004	0.00140	0.00012	0.00003	-0.04116	0.00086
12 ton lime/ha	13	5.14	0.004	0.00146	0.00011	0.00027	0.04481	0.00688
12 ton lime/ha	13	5.16	0.004	0.00148	0.00012	0.00026	0.05210	0.00663
12 ton lime/ha	26	5.47	0.005	0.00152	0.00012	0.00048	0.13359	0.01209
12 ton lime/ha	26	5.41	0.005	0.00169	0.00012	0.00049	0.12568	0.01159
18 ton lime/ha	0	5.52	0.004	0.00138	0.00013	0.00005	-0.06670	0.00135
18 ton lime/ha	0	5.47	0.004	0.00138	0.00013	0.00005	-0.06437	0.00126
18 ton lime/ha	13	5.41	0.004	0.00142	0.00013	0.00027	0.04852	0.00688
18 ton lime/ha	13	5.72	0.004	0.00140	0.00013	0.00026	0.05383	0.00676
18 ton lime/ha	26	5.54	0.005	0.00144	0.00013	0.00051	0.10921	0.01289
18 ton lime/ha	26	5.79	0.004	0.00150	0.00014	0.00049	0.11681	0.01235

APPENDIX E

Data for the Ecuadorian Andisol Field Experiments

Data for the Melanudand Field Liming Experiment

Yield Response to Lime Rate for Peas (2001) and Barley (1999)

Lime rate (ton/ha)	Peas yield (ton/ha)	Barley yield (ton/ha)
0	*0.74 bc ŧ	*1.72 de ŧ
1.5	0.53 dc	1.04 f
3.0	0.51 d	1.24 ef
4.5	0.78 ab	2.02 cd
6	0.84 ab	1.98 cd
9	0.98 a	2.47 bc
12	0.92 ab	2.82 ab
15	0.97 ab	3.07 ab
18	0.90 ab	3.33 a

* Mean of three replications
ŧ Means within a column followed by the same letter are not significant different at the 95 % level of confidence.

Yield Response to Liming Frequency for Peas (2001) and Barley (1999)

Liming frequency	Peas yield (ton/ha)	Barley yield (ton/ha)
1X (1986)	* 0.64 c ŧ	* 1.82 b ŧ
2X (1992)	0.77 b	2.06 b
3X (1993)	0.99 a	2.69 a

*Mean of three replications
ŧ Means within a column followed by the same letter are not significant different at the 95 % level of confidence.

Data for the Haplustand Field Fertilizer Experiment

Oil Palm Yield Response to Fertilizer Treatment

Fertilizer treatment	Yield response in 2000 (ton/ha)	Yield response in 2001 (ton/ha)
Control	* 25.15 b ŧ	* 19.96 c ŧ
N	25.34 b	20.93 bc
NPK	27.69 ab	23.36 ab
NPKSMg	27.41 ab	24.68 a
NPKSMgCa	28.13 a	25.88 a

*Mean of four replications
ŧ Means within a column followed by the same letter are not significant different at the 95 % level of confidence.

Oil Palm Yield Response to Irrigation

Treatment	Yield response in 2000 (ton/ha)	Yield response in 2001 (ton/ha)
Irrigation	* 27.35 a ŧ	* 23.92 a ŧ
Rain fed	26.14 a	22.00 b

*Mean of four replications
ŧ Means within a column followed by the same letter are not significant different at the 95 % level of confidence.

Oil Palm Leaf K, Ca, and Mg Response to Fertilizer Treatments (1999, 2000, and 2001)

Fertilizer treatment	K (g/kg)			Ca (g/kg)			Mg (g/kg)		
	1999	2000	2001	1999	2000	2001	1999	2000	2001
Control	15.8M*	10.8L	12M	8.2H	14.7H	10.0H	1.9L	2.9M	3.0M
+N	14.7M	10.0L	14M	9.7H	10.7H	9.0H	1.9L	2.1M	3.0M
+NPK	11.5M	9.0L	10M	10.0H	12.0H	12.0H	1.8L	2.0M	2.0L
+NPKSMg	17.4M	8.3L	10M	8.8H	15.2H	12.0H	2.0L	2.2M	2.0L
+NPKSMgCa	12.9M	8.6L	10L	9.5H	12.3H	12.0H	2.0L	2.0M	2.0L

* L = Low, M = Medium, and H = High. The sufficiency of the oil palm leaf levels are according to Jones (1991).

REFERENCES

Adams, F. 1966. Calcium deficiency as a casual agent of ammonium phosphate injury to cotton seedlings. Proc. Soil Sci. Soc. Am. 30:485-488.

Adams, F. 1971. Ion concentrations and activities in soil solutions. Proc. Soil Sci. Soc. Am. 35:420-426.

Barnhisel, R. I., and P. M. Bertsch. 1989. Chlorites and hydroxy-interlayered clays. pp. 729-788. In J.B. Dixon and S.B. Weed, Ed. Minerals in Soil Environments. SSSA, Madison, WI.

Beckett, P. H. T. 1964a. Studies on soil potassium: I. Confirmation of the ratio law: Measurement of potassium potential. J. Soil Sci. 15:1-8.

Beckett, P. H. T. 1964b. Studies on soil potassium: II. The "Immediate" Q/I relations of labile potassium in the soil. J. Soil Sci. 15:9-23.

Beckett, P. H. T., and M. H. M. Nafady. 1967. Studies on soil potassium: VII. Potassium-calcium exchange equilibria in soils: The location of non-specific (Gapon) and specific exchange sites. J. Soil Sci. 18:263-281.

Bennett, A. C., and F. Adams. 1970. Calcium deficiency and ammonia toxicity as separate causal factors of $(NH_4)_2HPO_4$-injury to seedlings. Proc. Soil Sci. Soc. Am. 34:255-259.

Bettany, J. R., and E. H. Halstead. 1972. An automated procedure for the nephelometric determination of sulfate in soil extracts. Can. J. Soil Sci. 52:127-129.

Birch, J. A., I. R. Devine, and M. R. J. Holmes. 1966. Field experiments on the magnesium requirements of cereals, potatoes, and sugar beet in relation to nitrogen and potassium application. J. Sci. Food Agr. 17:76-81.

Birrel, K. S., and M. Gradwell. 1956. Ion-exchange phenomena in some soils containing amorphous mineral constituents. J. Soil Sci. 7:130-143.

Bohn, H. L., B. L. McNeal, and G. A. O'Conner. 1985. Soil Chemistry. 2nd. ed. Wiley, New York.

Borchardt, G. 1989. Smectites. pp. 675-727. In J. B. Dixon and S. B. Weed, Ed. Minerals in Soil Environments. SSSA, Madison, WI.

Bouyoucos, G. J. 1962. Hydrometer method improved for making particle size analyses of soils. Agron. J. 54:464-465.

Bremner, J. M. 1960. Determination of nitrogen in soil by the Kjeldahl method. J. Agric. Sci. 55:11-33.

Bremner, J. M., and G. A. Breitenbeck. 1983. A simple method for determination of ammonium in semimicro-Kjeldahl analysis of soils and plant materials using a block digester. Commun. Soil Sci. Plant Anal. 14:905-914.

Carolus, R. T. 1938. Effect of certain ions, used singly and in combination, on the growth and potassium, calcium, and magnesium adsorption of the bean plant. Plant Physiol. 13: 349-363.

Carter, D. L., M. M. Mortland, and W. D. Kemper. 1986. Specific surface. pp. 413-423. In Methods of Soil Analysis. Part 1. Physical and Mineralogical Methods. Agronomy Monograph No. 9. (2nd Edition). Am. Soc. Agron., Madison, WI.

Chapman, H. D. 1965. Cation-exchange capacity. pp. 894-901. In C.A. Black et al., Ed. Methods of Soil Analysis. Chemical and Microbiological Properties. Agronomy Monograph No. 9. Am. Soc. Of Agron., Madison, WI.

Charlet, L., and G. Sposito. 1989. Bivalent ion adsorption by an Oxisol. Soil Sci. Am. J. 53:691-695.

Cihacek, L. J., and J. M. Bremner. 1979. A simplified ethylene glycol monoethyl ether procedure for assessment of soil surface area. Soil Sci. Soc. Am. J. 43:821-822.

Colmet-Daage, F. 1969. Nature of the Clay of some volcanic ash soils of the Antilles, Ecuador and Nicaragua. In: Panel on Volcanic Ash Soils in Latin America. Turrialba. Costa Rica. B.2.1 – B.2.11.

Curtin, D., and G. W. Smillie. 1983. Soil solution composition as affected by liming and incubation. Soil Sci. Soc. Am. J. 47:701-707.

Dixon, J. B., and T. R McKee. 1974. Spherical halloysite formation in a volcanic soil of Mexico. Tr. Mezhdunar. Kongr. Pochvovedov. 7:115-124.

Egawa, T., Y. Watanabe, and A. Sato. 1959. A study on cation exchange capacity of allophane. Proc. Clay Sci., Jap. 1:260-272 (in Japanese, with English abstract).

Eick, M. J., A. Bar-Tar, D. L. Sparks, and S. Feigenbaum. 1990. Analyses of adsorption kinetics using a stirred-flow chamber: II. Potassium-calcium exchange on clay minerals. Soil Sci. Soc. Am. J. 54:1978-1982.

El-Swaify, S. A., and A. H. Sayegh. 1975. Charge characteristics of an Oxisol and an Inceptisol from Hawaii. Soil Sci. 120:49-56. In Grove, J. H., C. S. Fowler, and M. E. Sumner. 1982. Determination of the charge character of selected acid soils. Soil Sci. Soc. Am. J. 46:32-38.

Elzam, D. E., and T. K. Hodges. 1967. Calcium inhibition of potassium adsorption in corn roots. Plant Physiol. 42:1483-1488.

Espinosa, J. 1987. Suelos Volcánicos en el Ecuador. INPOFOS, Quito. pp. 1-23.

Espinosa, J. 1992. Phosphorus Diagnosis and Recommendations in Volcanic Ash Soils. Proceedings of the Trop. Soils. Honolulu (US). pp. 109-115.

Espinoza, W., R. G. Gast, and R. S. Adams. 1975. Charge characteristics and nitrate retention by two Andepts from South-Central Chile. Proc. Soil Sci. Soc. Am. 39:842-846.

Evangelou, V. P. 1986. The influence of anions on potassium quantity-intensity relationships. Soil Sci. Soc. Am. J. 50:1182-1188.

Evangelou, V. P. 1998. Environmental soil and water chemistry. Principles and Applications. John Willey & Sons, Inc., New York (US).

Evangelou, V. P., and A. D. Karathanasis. 1986. Evaluation of potassium quantity-intensity relationships by a computer model employing the Gapon equation. Soil Sci. Soc. Am. J. 50:58-62.

Evangelou, V. P., A. D. Karathanasis, and R. L. Blevins. 1986. Effect of soil organic matter accumulation on potassium and ammonium quantity-intensity relationships. Soil Sci. Soc. Am. J. 50:378-382.

Evangelou, V. P., J. Wang, and E. Phillips. 1994. New developments and perspectives on soil potassium quantity/intensity relationships. Adv. Agronomy 52:173-227.

Fieldes, M., and G. G. C. Claridge. 1975. In J. E. Gieseking, Ed. Inorganic Components. Soil components. Volume 2. Springer-Verlag, Berlin and New York. pp. 351-393.

Fox, R. C. 1982. Some highly weathered soils of Puerto Rico. III. Chemical properties. Geoderma. 27: 139 - 176.

Galindo, G. G., and F. T. Bingham. 1977. Homovalent and heterovalent cation exchange equilibria in soils with variable surface charge. Soil Sci. Soc. Am. J. 41:883-886.

Gillman, G. P. 1979. A proposed method for the measurement of exchange properties of highly weathered soils. Aust. J. Soil Res. 17:129-139.

Gillman, G. P. 1984. Using variable charge characteristics to understand the exchangeable cation status of oxic soils. Aust. J. Soil Res. 22:71-80.

Gillman, G. P. 1985. Influence of organic matter and phosphate content on the point of zero charge of variable charge components in oxidic soils. Aust. J. Soil Res. 23: 643-646.

Gillman, G. P., and D. J. Abel. 1986. A summary of surface charge characteristics of the major soils of the Tully-Innisfail area, north Queensland. CSIRO Aust. Div. Soils, Div. rep. No. 85 CSIRO. Melbourne.

Gillman, G. P, and L. C. Bell. 1976. Surface charge characteristics of six weathered soils from tropical North Queensland. Aust. J. Soil Res. 14:351-360.

Gillman, G. P, and L. C. Bell. 1978. Soil solution studies on weathered soils from tropical north Queensland. Aust. J. Soil Res. 16:67-77.

Gillman, G. P, and R. L. Fox. 1980. Increasing in the cation exchange capacity of variable charge soils in following super phosphate application. Soil Sci. Soc. Am. J. 44:934-938.

Gillman, G. P., and G. G. Murtha. 1983. Effects of sample handling on some chemical properties of soils from high rainfall coastal North Queensland. Aust. J. Soil Res. 21:67-72.

Gillman, G. P, and E. A. Sumpter. 1986a. Modification to the compulsive exchange method for measuring exchange characteristics of soils. Aust. J. Soil Res. 24:61-66.

Gillman, G. P, and E. A. Sumpter. 1986b. Surface charge characteristics and lime requirements of soils derived from basaltic, granitic, and metamorphic rocks in high-rainfall tropical Queensland. Aust. J. Soil Res. 24:173-192.

Gillman, G. P, and M. E. Sumner. 1987. Surface charge characteristics and soil solution composition of four soils from the Southern piedmont in Georgia. Soil Sci. Soc. Am. J. 51:589-594.

Gillman, G. P., and G. Uehara. 1980. Charge characteristics of soils with variable and permanent charge minerals: II. Experimental. Soil Sci. Soc. Am. J. 44:252-255.

Gillman, G. P., J. O. Skjemstad, and R. C. Bruce. 1982. A comparison of methods used in Queensland for determining cation exchange properties. Commonwealth Scientific and Industrial Research Organization (CSIRO). Australia. Division of Soils Technical Paper 44:1-18.

Gonzales-Batista, A., J. M. Hernandez-Moreno, E. Fernandez-Caldas, and A. J. Herbillon. 1982. Influence of silica content on the surface characteristics of allophanic clays. Clays Clay Min. 30:103-110.

Griffin, R. A., and J. J. Jurinak. 1973. Estimation of activity coefficients from the electrical conductivity of natural aquatic systems and soil extracts. Soil Sci. 116:26-30.

Grove, J. H., C. S. Fowler, and M. E. Sumner. 1982. Determination of the charge character of selected acid soils. Soil Sci. Soc. Am. J. 46:32-38.

Grove, J. H., M. E. Sumner, and J. K. Syers. 1981. Effect of lime on exchangeable magnesium in variable surface charge soils. Soil Sci. Soc. Am. J. 45:497-500.

Harada, T., and K. Kutsuna. 1955. Nat. Inst. Agric. Sci., Japan. Bull. B5:1-26. In Ishizuka, Y., and C.A. Black, Eds., Soil derived from volcanic ash in Japan. Centro Internacional de Mejoramiento de Maiz y Trigo, Mexico City, 1977.

Havlin, J. L., J. D. Beaton, S. L. Tisdale, and W. L. Nelson. 1999. Soil fertility and fertilizers. An introduction to nutrient management. 6 th ed. Prentice Hall. pp. 196-244.

Haynes, R. J. 1980. Ion exchange properties of roots and ionic interactions within the root apoplasm: Their role in ion accumulation by plants. Bot. Rev. 46:75-99.

Hendershot, W.H., and M. Duquette. 1986. A simple barium chloride method for determining cation exchange capacity and exchangeable cations. Soil Sci. Soc. Am. J. 50:605-608.

Henmi, T., and K. Wada. 1976. Morphology and composition of allophone. Am. Mineral.61:379-390.

Higashi, T., and K. Wada. 1977. Size fractionation, dissolution analysis, and infrared spectroscopy of humus complexes in Ando soils. J. Soil Sci. 28:653-663.

Hingston, F., J. R. J. Atkinson, A. M. Posner, and J. P. Quirk. 1967. Specific adsorption of anions. Nature 215:1459-1461.

Howard, D. D., and F. Adams. 1965. Calcium requirement for penetration of subsoils by primary cotton roots. Soil Sci. Soc. Amer. Proc. 29:558-562.

Hunsaker, V. E., and P. F. Pratt. 1971. Calcium-magnesium exchange equilibria in soils. Proc. Soil Sci. Soc. Am. 35:151-152.

Jackson, M. L. 1975. Soil chemical analysis. Advanced course. 2nd ed. M.L.Jackson. Madison, WI.

Jackson, M. L., C. H. Lim, and L. W. Zelazny. 1986. Chapter 6. Oxides, Hydroxides, and Aluminosilicates. pp. 113-131. In Methods of Soil Analysis. Part 1. Physical and Mineralogical Methods. (2 nd. Edition). Klute, A., Ed. Agronomy 9. American Society of Agronomy, Inc., Soil Science Society of America, Inc. Madison, WI.

Jones, B. 1991. Plant Analysis Handbook. Micro-Macro Publishing, Georgia.

Kamata, H. 1978. Studies on soil classification and land utilization in Kanagawa Prefecture- On land classification for paddy and upland field. Bull. Agr. Res. Inst. of Kanagawa Pref.119: 1-118.

Kanehiro, Y., and G. D. Sherman. 1956. Effect of dehydration-rehydration on cation exchange capacity of Hawaiian soils. Soil Sci. Soc. Amer. Proc. 20:341-344.

Kanno, I. 1956. A pedological investigation of Japanese volcanic ash soils, Kyushu Agric. Expt. Sta. Bull. 4:81-84.

Karathanasis, A. D., and B. F. Hajek. 1982. Revised methods for quantitative determinations of minerals in soil clays. Soil Sci. Soc. Am. J. 46:419-425.

Karathanasis, A. D., and W. G. Harris. 1994. Quantitative thermal analysis of soil materials. pp. 360-410. In Quantitative methods in soil mineralogy. SSSA Miscellaneous Publication. Madison, WI.

Kato, Y. 1970. A model for amorphous matters of humic soils in Japan. A preliminary report. Pedologist 14:16-21. In Wada, K. 1985. The distinctive properties of Ansodols. Advances in soil science, volume 2. Springer-Verlag New York, Inc., New York (US). pp. 174-229.

Key, J. L., L. T. Kurtz, and B. B. Tucker. 1962. Influence of ratio of exchangeable calcium-magnesium on yield and composition of soybeans and corn. Soil Sci. 93:265-270.

Keys to Soil Taxonomy. 1998. Soil Management Support Services. Technical Monograph No. 19. USDA, AID.

Khasawneh, F. E. 1971. Solution ion activity and plant growth. Soil Sci. Soc. Amer. Proc.35:426-436.

Kobo, K., and Y. Ohba. 1964. Volcanic Ash soils in Japan. pp. 29-33. Ministry of Agric. And For., Japan.

Le Roux, J., and M. E. Summer. 1967. Studies on the soil solution of various Natal soils. Geoderma 1:125-130.

Lumbanraja, J., and V. P. Evangelou. 1991. Acidification and liming influence on surface charge behavior of Kentucky subsoils. Soil Sci. Soc. Am. J. 54:26-34.

Lumbanraja, J., and V. P. Evangelou. 1992. Potassium quantity-intensity relationships in the presence and absence of the NH4 for three Kentucky soils. Soil Sci. 154:366-376.

Lumbanraja, J., and V. P. Evangelou. 1994. Adsorption-desorption of potassium and ammonium at low cation concentrations in three Kentucky subsoils. Soil Sci. 157:269-278.

Lund, Z. F. 1970. The effect of calcium and its relation to several cations in soybean root growth. Proc. Soil Sci. Soc. Amer. 34:456-459.

Maas, E. V. 1969. Calcium uptake by excised maize roots and interactions with alkali cations. Plant Physiol. 44:985-989.

Maeda, T., H. Takenaka, and B. P. Warkentin. 1984. Physical properties of allophane soils. pp.122-146. In K.H. Tan, Ed. Andosols. Benchmark Papers in Soil Science Series. Van Nostrand Reinhold Company Inc., New York.

Martin, J. P., and A. L. Page. 1969. Influence of exchangeable Ca and Mg and of percentage base saturation on growth of citrus plant. Soil Sci. 107:39-46.

Matsue, N., and K. Wada. 1985. A new equilibration method for cation-exchange capacity measurement. Soil Sci. Soc. Am. J. 49:574-578.

Matthews, B. C., and P. H. T. Beckett. 1962. A new procedure for studying the release and fixation of K ions on soil. J. Agric. Sci. 58:59-64.

McLean, E. O. 1965. Aluminum. pp. 978-999. In. C.A. Black, Ed. Methods of Soil analysis. Part 2. Agron. Monogr. 9. ASA, Madison, WI.

Mehra, O. P., and M. L. Jackson. 1960. Iron oxide removal from soils and clays by a dithionite-citrate system buffered with sodium carbonate. Clays Clay Miner. 7:317-327.

Mejia, V. 1997. Reconocimiento General de los Suelos del Ecuador en base a su Capacidad – Fertilidad. Quito. p. 41.

Menzies, N. W., and G. P. Gillman. 1997. Chemical characterization of soils of a tropical humid forest zone: a methodology. Soil Sci. Soc. Am. J. 61:1355-1363.

Mite, F. 1972. Evaluación de Tres Métodos de Análisis de Fósforo en Suelos de Quevedo en Base a las Respuestas de Plantas Cultivadas en Macetas. (In Spanish, with English abstract). B. S thesis. Universidad de Guayaquil, Ecuador.

Mite, F., M. Carrillo, and J. Espinosa. 1999. Fertilizer Use Efficiency in Oil Palm is Increased under Irrigation in Ecuador. Better Crops International, Vol. 13, No.1, pp. 30-32.

Mizota, C., M. A. Carrasco, and K. Wada. 1982. Clay mineralogy and some chemical properties of Ap horizons of Ando soils used for paddy rice in Japan. Geoderma, 27:225-237.

Mubiru, D. N., 1992. Mineralogical and P-sorption characteristics of some highly weathered soils in South-Central Kentucky. M.S. Thesis. University of Kentucky, Lexington. p. 245.

Nakai, M., and N. Yoshinaga. 1980. Fibrous goethite in some soils from Japan and Scotland. Geoderma 24:143-158.

Nelson, D. W., and L. E. Sommers. 1972. A simple digestion procedure for estimation of total nitrogen in soils and sediments. J. Environ. Qual. 1:423-425.

Okamura, Y., and K. Wada. 1983. Electric charge characteristics of Ando (B) and Red-Yellow B soils and weathered pumices. J. Soil Sci. 34:287-295.

Olsen, S. R., C. V. Cole, F. S. Watanabe, and L. A. Dean. 1954. Estimation of available phosphorous in soils by extraction with sodium bicarbonate. USDA Circ. 939. USDA, Washington, DC.

Omar, M. A., and T. El Kobbia. 1966. Some observations in the interrelationships of potassium and magnesium. Soil Sci. 101:437-440.

Ranst, E., S. R. Utami, and J. Shamshuddin. 2002. Andisols on Volcanic Ash from Java Island, Indonesia: Physico - Chemical Properties and Classification. Soil Sci. 167:68-79.

Rasnake, M., and G. W. Thomas. 1976. Potassium status of some alluvial soil in Kentucky. Soil Sci. Soc. Am. J. 40:883-886.

Risenauer, H. M., L. M. Walsh, and R. G. Hoeft. 1973. pp. 173-200. In L. M Walsh and J. D. Beaton (ed.) Soil Testing and Plant Analysis. SSSA, Madison, WI.

SAS Institute. 1999. Software Version 8 (TS MO). SAS Institute Inc., Carry, NC.

Schalscha, E. B., P. F. Pratt, and L. De Andrade. 1975. Potassium-calcium exchange equilibria in volcanic ash soils. Proc. Soil Sci. Soc. Am. 39:1069-1072.

Schofield, R. K. 1947. A ratio law governing the equilibrium of cations in solution. Int. Congr. Pure Appl. Chem. Proc. 11th (London) 3:257-261.

Sheen, R. T., H. L. Kahler, and E. M. Ross. 1935. Turbidimetric determination of sulfate in water. Ind. Eng. Chem., Anal. Ed. 7:262.

Singh, U., and G. Uehara. 1986. Electrochemistry of the double-layer: Principles and applications to soils. pp. 1-38. In D.L Sparks, Ed. Soil Physical Chemistry. CRC Press, Boca Raton, FL.

Shoji, S., M. Nanzyo, and R. A. Dahlgren. 1993. Volcanic ash soils: Genesis, properties and utilization. Dev. Soil Sci. 21. Elsevier, Amsterdam, The Netherlands.

Shoji, S. 1983. Mineralogical properties of volcanic ash soils. In: N. Yoshinaga (ed.). Volcanic ash soil- Genesis, Properties, Classification. pp. 31-72. Hakuyusha, Tokyo. p. 204 .

Sixth International Soil Classification Workshop. 1984. Tour guide. Part 1. Chile and Part 2 . Ecuador. Soil Management Support Services, Washington, DC.

Smith, G. D. 1984. A preliminary proposal for reclassification of Andepts and some andic subgroups. pp. 122-146. In K.H. Tan, Ed. Andosols. Benchmark Papers in Soil Science Series. Van Nostrand Reinhold Company Inc., New York.

Smith, P. F., W. Reuther, A. W. Specht, and G. Henciar. 1954. Effect of differential nitrogen, potassium and magnesium supply to young Valencia orange trees in sand culture on mineral composition especially of leaves and fibrous roots. Plant Physiol. 29:349-355.

Soil Conservation Service. 1967. Soil survey of Metcalfe County, Kentucky. U. S. Govt. Print. Office. Washington, DC.

Soil Survey Staff. 1975. Soil Taxonomy. A Basic System for Making and Interpreting Soil Surveys. Dept. Agr. Handbook No. 436. Washington, DC.

Sparks, D. L. 1995. Environmental Soil Chemistry. Academic Press, California (US). p. 267.

Sposito, G. 1981. The thermodynamics of soil solutions. Clarendon Press, Oxford, London.

Sposito, G. 1984. The Surface Chemistry of Soils. Oxford University Press, London.

Sposito, G. 1989. The Chemistry of Soils. Oxford University Press, New York (US). p. 277.

Standard Methods for the Examination of Water and Wastewater. 1989. 17 th Edition. 4500-C1 E. Automated Ferricyanide Method. Published by APHA-AWWA-WPCF.

Stout, W. L., and Barker, D. E. 1981. Effects of adsorption of potassium and magnesium in soils on magnesium uptake by corn. Soil Sci. Soc. Am. J. 45:996-997.

Tan, K. H. 1984. Andosols. Van Nostrand Reinhold Company. p. 418.

Tan, K. H., and J.Van Schuylenborgh. 1961. On the Classification and Genesis of Soil Developed over Acid Volcanic Materials under Humid Tropical Conditions. II, Netherlands Jour. Agric. Sci. 9:41-54.

Taylor, N. H. 1964. The classification of volcanic ash soils in New Zealand. Meeting on the classification and correlation of soils from volcanic ash. Tokyo, Japan. Food and Agric. Org. United Nations. World Soil Resources Rept. 14:101-110.

Taylor, N. H., and J. E. Cox. 1956. The soil pattern of New Zealand. New Zealand Soil Bureau. Lower Hutt. New Zealand. Publ. 113.

Tessens, E., and J. Shamshuddin. 1983. Quantitative relationship between mineralogy and properties of tropical soils. University Pertanian Malaysia Monograph.

Theng, B. K. G., M. Russell, G. J. Churchman, and R. L. Parfitt. 1982. Surface properties of allophane, halloysite, and imogolite. Clays Clay Min. 30:143-149.

Thorp, J., and G. D. Smith. 1949. Higher categories of soil classification: order, suborder, and great soil groups. Soil Sci. 67:117-126.

Tokashiki, Y., and K. Wada. 1975. Weathering implications of the mineralogy of clay fractions of two Ando soils, Kyushu. Geoderma 14:47-62.

Uehara, G., and G. P. Gillman. 1980. Charge characteristics of soils with variable and permanent charge minerals: I. Theory. Soil Sci. Soc. Am. J. 44:250-252.

Uehara, G., and G. P. Gillman. 1981. The mineralogy, Chemistry, and Physics of Tropical Soils with Variable Charge Clays. Westview Tropical Agriculture Series, No. 4. Westview Press, Colorado (US).

U. S. Salinity Laboratory Staff. 1954. L. A. Richards (ed.) Diagnosis and improvement of saline and alkali soils. U. S. Dept. of Agriculture Handbook no. 60. USDA, Washington, DC.

Van Raij, B., and M. Peech. 1972. Electrochemical properties of some Oxisols and Alfisols. Soil Sci. Soc. Am. J. 36:587-593.

Vlamis, J. 1949. Growth of lettuce and barley as influenced by degree of calcium saturation of soil. Soil Sci. 64:453-466.

Wada, K. 1977. Allophane and Imogolite. pp. 603-638. In J.B. Dixon and S.B. Weed, Eds. Minerals in Soil Environments. Soil Sci. Soc. Am. Madison, Wisconsin.

Wada, K. 1980. Mineralogical characteristics of Andisols. pp. 87-107. In: B.K.G. Theng, Ed., Soils with Variable Charge. New Zealand Society of Soil Science, lower Hutt.

Wada, K. 1985. The distinctive properties of Andosols. Advances in Soil Science 2:174-229.

Wada, K., and S. Aomine. 1973. Soil Development on Volcanic Materials during the Quaternary. Soil Sci. 116:170-177.

Wada, K., and T. Higashi. 1976. The categories of aluminum- and iron-humus complexes in Ando soils determined by selective dissolution. J. Soil Sci. 27:357-368.

Wada, K., and Y. Kakuto. 1985a. An evaluation of the toluidine blue test for the assessment of allophane and imogolite. Kyushu University. Fukuoka, Japon. Soil Sci. Plant nutrient. 31:383-389.

Wada, K., and Y. Kakuto. 1985b. Embryonic halloysites in Ecuadorian soils derived from volcanic ash. Soil Sci. Soc. Am. J. 49:1309-1318.

Wada, K., and Y. Kakuto. 1987. Clay minerals and humus complexes in five Kenyan soils derived from volcanic ash. Japan. Geoderma 39: 307-321.

Wada, K., and Y. Okamura. 1980. Electric charge characteristics of Ando A1 and buried A1 horizon soils. J. Soil Sci. 31:307-314.

Wada, K., and Y. Tange. 1984. Interaction of methyl- and ethyl-ammonium ions and piperidium ions with soils. Soil Sci. 137:315-323.

Wada, K., H. Gondo, and S.I. Wada. 1982. An incipient form of halloysite in a Kuroboku paddy soil. Abst. 1982 MTNG., Japanese Soc. Soil Plant Nutr. 28:32. In Wada, 1985.

Wada, K., Y. Kakuto, and H. Ikawa. 1986. Clay minerals, humus complexes, and classification of four Andepts of Mauri, Hawaii. Soil Sci. Soc. Am. J. 50:1007-1013.

Wakatsuki, T., and W. G. Wielemaker. 1985. Clay mineralogy of a soil formed in peralkaline volcanic ash from the Great Rift Valley in Kenya. Soil Sci. Plant Nutr. 31:475-480.

Walker, R. G., H. M. Walker, and P. O. Ashworth. 1955. Calcium-magnesium nutrition with special reference to serpentine soils. Plant Physiol. 30:214-221.

Walkley, A., and I. A. Black. 1934. An examination of the Degtjareff method for determining soil organic matter and a proposed modification of the chromic acid titration method. Soil Sci. 37:29-38.

Walsh, T., and T. F. O'Donohoe. 1945. Magnesium deficiency in some crop plants in relation to the level of potassium nutrition. J. Agr. Sci. 35:254-263.

Wann, S. S, and G. Uehara. 1978. Surface charge manipulation of constant surface potential soil colloids. I : Relation to sorbed phosphorous. Soil Sci. Soc. Am. J. 42:565-570.

Watanabe, F. S., and S. R. Olsen. 1965. Test of an ascorbic acid method for determining phosphorus in water and NaHCO3 extracts from soil. Proc. Soil Sci. Soc. Am. 29:677-678.

Wielemaker, W.G., and T. Wakatsuki. 1984. Properties, weathering and classification of some soils formed in peralkaline volcanic ash in Kenya. Geoderma 32:21-44.

Wright, A. C. S. 1964. The "Andosols" or "Humic Allophane" soils of South America. pp. 9-22. In: World Soil Resources Report 14. FAO/UNESCO.

Yoshida, M. 1953. Jour. Sci. Soil and Manure (Japan) 23:213-215. In Ishizuka, Y., and C.A. Black, Eds., Soil derived from volcanic ash in Japan. Centro Internacional de Mejoramiento de Maiz y Trigo, Mexico City, 1977.

Yoshida, M. 1961. Jour. Sci. Soil and Manure (Japan) 31:310-313. In Ishizuka, Y., and C.A. Black, Eds., Soil derived from volcanic ash in Japan. Centro Internacional de Mejoramiento de Maiz y Trigo, Mexico City, 1977.

Zall, D. M., D. Fisher, and M. D. Garner. 1956. Photometric determination of chlorides in water. Anal. Chem. 28:16-65.

Zandstra, N. G., and A. F. MacKenzie. 1968. Potassium exchange equilibria and yield responses of oats, barley, and corn on selected Quebec soils. Proc. Soil Sci. Soc. Am. 32:76-79.

Zehetner, F., W. P. Miller, and L. T. West. 2003. Pedogenesis of volcanic ash soils in Andean Ecuador. Soil Sci. Soc. Am. J. 67:1797-1809.

VITA

Soraya Alvarado, daughter of Jorge Alvarado and Beatriz Ochoa, was born on April, 1974, at Cañar, Ecuador. She got her primary school education at "Santa Rosa de Lima" Primary School and senior education at "José Peralta" High School. She entered "Escuela Superior Politécnica de Chimborazo" University in 1991 and graduated in 1997 with a B.S honors degree in Chemistry. She was recognized as the best graduate student, 1997-98, at the Faculty of Sciences Doctorate Program at the Chemistry School.

In 1997, she was recruited as a research assistant by the National Agricultural Research Institute of Ecuador (INIAP). In 2001, she received a scholarship from the Ecuadorian Government's National Agricultural Modernization Program to carry out her graduate research program in the United States. She is now a candidate for the M.S degree in Plant and Soil Science at the University of Kentucky. She is one of the recipients of the 2003 "J. Fielding Reed PPI Fellowship" awards by the Potash & Phosphate Institute (PPI).

Upon graduation she will serve her country as a soil specialist for soil fertility purposes. The most important future career goal is to contribute significantly to the agricultural development of her native country, Ecuador, and to soil science in general.